Prebiotic-like effects of berry polyphenols on the gut microbiota: Akkermansia muciniphila and its molecular adaptation mechanisms to phenolics

Thèse

Maria Carolina Rodriguez Daza

Doctorat en microbiologie agroalimentaire
Philosophiæ doctor (Ph. D.)

Québec, Canada

Prebiotic-like effects of berry polyphenols on the gut microbiota:

Akkermansia muciniphila and its molecular adaptation mechanisms to phenolics

Thèse

Doctorat en Microbiologie agroalimentaire

Philosophiæ doctor (Ph. D.)

Maria Carolina Rodriguez Daza

Sous la direction de :

Yves Desjardins, directeur de recherche

Denis Roy, codirecteur de recherche

Résumé

Les liens entre le microbiote intestinal, la diète et les désordres métaboliques sont maintenant établis. Les polyphénols des petits fruits affectent les bactéries pathogènes dans le côlon, et stimulent les bactéries symbiotiques, particulièrement *Akkermansia muciniphila* chez l'homme et dans des modèles murins. Cette bactérie muciphile contribue à l'homéostasie intestinale et induit une réponse immunitaire et métabolique bénéfique chez l'hôte. Cependant, on comprend mal comment les polyphénols peuvent sélectivement l'affecter et l'analyse traditionnelle métagénomique obtenue d'études *in vivo* n'offre qu'une image partielle des mécanismes impliqués. Cette thèse vise à évaluer, par des approches *in vivo* et *in vitro,* comment les polyphénols modifient le microbiote intestinal, la morphologie de l'épithélium du colon, la niche écologique d'*Akkermansia,* et par extension affectent le métabolisme de souris soumises à une diète obésogène. Une attention particulière a été portée à l'effet de ces composés sur la croissance d'*A. muciniphila* et les mécanismes moléculaires qu'ils induisent chez la bactérie. Dans un premier chapitre, l'effet des poudres de fruits canneberge et de bleuets riches en polyphénols et leurs fractions fibreuses a été étudié chez des souris soumises à une diète obésogène (HFHS) pendant 8 semaines afin d'évaluer lesquels des polyphénols ou des fibres sont responsables de l'effet prébiotique observé. Cette étude a démontré que ce sont surtout les polyphénols contenus dans les poudres de canneberges et de bleuets entiers qui sont responsables de l'action prébiotique, notamment en stimulant *A. muciniphila*. En effet, la poudre de canneberge comme celle de bleuets inhibent particulièrement les pathogènes induits par la diète HFHS. En outre, l'analyse de redondance fonctionnelle a révélé que la consommation de poudre de canneberge riche en polyphénols permettait au microbiote de souris obèses de retrouver les fonctions de celui de souris maigres. Ces souris présentaient un poids et une efficacité énergétique inférieurs à celui des souris non traitées. De plus, d'autres bactéries symbiotiques étaient favorisées par les poudres de fruits entiers : *Muribaculaceae, Dubosiella newyorkensis* et *Eggerthellaceae*. Fait intéressant, les fibres de canneberge inhibaient également les pathogènes, favorisaient des bactéries dégradant les polyphénols et réduisaient les triglycérides hépatiques chez les souris obèses. Ces résultats mettent en évidence le potentiel des polyphénols, même lorsqu'ils sont associés aux fibres, à atténuer les désordres métaboliques. Le deuxième chapitre

s'intéresse à identifier les catégories de polyphénols impliquées dans l'accroissement du nombre de bactéries symbiotiques et particulièrement d'*A. muciniphila*. Les souris soumises à une diète obésogène ont été traitées avec un extrait de bleuet ou trois de leurs fractions polyphénoliques : F1, riches en anthocyanes et en acides phénoliques; F2, riche en oligomères de proanthocyanidines (PACs) ainsi qu'en flavonols; et F3 riches en polymères de PACs. Ces sous-fractions ont été administrées aux souris dans les mêmes concentrations que celles retrouvées dans l'extrait entier. Globalement, les fractions polyphénoliques ont restauré l'épaisseur de la couche de mucus, mais particulièrement les fractions riches en PACs ont significativement stimulé *A. muciniphila*, tout en améliorant la proportion de cellules caliciformes et le métabolisme du glucose chez les souris obèses. Enfin le dernier chapitre s'intéresse aux mécanismes par lesquels les polyphénols favorisent la croissance de *A. muciniphila* dans l'intestin. Des cultures d'*A. muciniphila* ont donc été effectuées dans des milieux enrichis en polyphénols afin d'évaluer les gènes impliqués dans le métabolisme cellulaire et dans la résistance aux antimicrobiens; les pompes à efflux non spécifiques, les polysaccharides capsulaires (CPS), les exopolysaccharides (EPS), les transporteurs de type ABC-2 et de resistance-nodulation-cell division (RND) ont joué un rôle crucial dans la résistance et l'adaptation de la bactérie aux polyphénols. La croissance d'*A. muciniphila* n'a pas été inhibée par l'extrait de canneberge entier ni par ses fractions polyphénoliques, mais elle a été stimulée par l'urolithine-A. Cette expérience *in vitro* a démontré que les polymères de PACs favorisent davantage les mécanismes d'adaptation antimicrobienne impliqués dans la protection des parois cellulaires et la régulation énergétique chez *Akkermansia*. Parallèlement à l'urolithine-A, les polymères de PACs ont induit la production du CPS et du EPS chez *A. muciniphila*. Ces CPS/EPS pourraient contribuer aux rôles immunomodulateur et anti-obésité d'*A. muciniphila* et par conséquent constituer des postbiotiques prometteurs. Cette thèse démontre la sélectivité des polyphénols, principalement des PACs, dans l'inhibition des pathogènes associés à l'obésité et dévoile les mécanismes moléculaires qui sous-tendent leurs effets prébiotiques sur *A. muciniphila*.

Abstract

The link between gut microbiota, diet and metabolic diseases is now established. Polyphenols from berries and other dietary sources have been shown to inhibit opportunistic pathogens and stimulate symbiotic bacteria, particularly *Akkermansia muciniphila* in humans and animals. *A. muciniphila* is a mucus-living bacterium shown to contribute to the intestinal homeostasis and to drive beneficial immune and metabolic response in the host. However, it is not yet known how polyphenols can selectively affect *A. muciniphila* from *in vivo* studies, since regular metagenomic analysis of the gut microbiota only provide a partial picture of the mechanisms involved. This thesis aims to determine, through *in vivo* and *in vitro* approaches, the prebiotic effect of polyphenols and how they affect the physiology and intestinal morphology and the ecological niche of *Akkermansia* in obesogenic diet-fed mice. Particularly, it focusses on the molecular capacity of *A. muciniphila* to induce defence mechanisms and adapt to distinct polyphenolic fractions. In the first chapter, in order to assess which constituent of berries was responsible for the prebiotic action, we compared the effect of the dietary supplementation with polyphenol-rich cranberry and blueberry fruit powders to their respective fibrous fractions (cell wall polysaccharides) of high-fat high-sucrose (HFHS) fed mice for 8-weeks. We demonstrated that the polyphenols from cranberry and blueberry fruit powders are mainly responsible for the selective prebiotic effects on *A. muciniphila* rather than their fibre-rich fractions. Both cranberry and blueberry whole fruit powders inhibited HFHS-induced pathobionts associated with obesity. A functional redundancy analysis revealed that the gut microbiota functions of obese mice were remarkably changed by polyphenol-rich whole cranberry powder, restoring it back to that observed in lean mice; that is, they presented lower body weight and energy efficiency as compared to untreated mice. Furthermore, other symbiotic bacteria were influenced by polyphenol-rich berry powders, notably *Muribaculaceae*, *Dubosiella newyorkensis*, and the polyphenol-degrading *Eggerthellaceae*; these mice presented a lower body weight and energy efficiency as compared to untreated mice. Surprisingly, cranberry fibrous fraction also inhibited pathobionts and promoted polyphenol-degrading families and reduced the hepatic triglycerides level in HFHS-fed mice. Altogether, these findings highlight the role of polyphenols associated with fibres, in attenuating obesity. The second chapter aimed to

identity which polyphenolic category was mostly responsible for the prebiotic effect and the abundance of *A. muciniphila.* HFHS-fed mice were treated with a whole blueberry extract and with the three constitutive polyphenolic fractions: F1, rich in anthocyanins and phenolic acids, F2, rich in oligomeric proanthocyanidins (PACs) and flavonols, and F3 rich polymeric PACs. These sub-fractions were administered to mice at the same concentration as encountered in the whole extract. All in all, the polyphenolic fractions restored the mucus thickness, but the PAC-rich fractions besides stimulating *A. muciniphila*, increased the proportion of goblet cells and improved the glucose homeostasis in obese mice. Finally, the third chapter looks at the mechanisms by which polyphenols promote the growth of *A. muciniphila*. Growing assays of *A. muciniphila* were carried out in polyphenols enriched media in order to assess the expression of genes involved in cell metabolism and antimicrobial resistance. Genes coding for multidrug efflux pumps, capsular polysaccharide (CPS) family, exopolysaccharides (EPS), and ABC-2 type and resistance-nodulation-cell division (RND) transporters were shown to play a crucial role in allowing the bacteria to withstand the different cranberry polyphenolic fractions and adapt to the stress they caused. *A. muciniphila* growth was not inhibited by the whole cranberry extract neither by its polyphenolic fractions, but enhanced by the phenolic metabolite urolithin-A. Moreover, we showed that the polymeric PACs were triggering most intensively the antimicrobial adaptation mechanisms involved in cell-wall protection and energy management in *A. muciniphila*. Both of these fractions up-regulated CPS and EPS in *A. muciniphila*. CPS/EPS secretion in presence of polyphenols might represent promising post-biotic products, possibly involved in the immune modulatory and anti-obesity potential by *A. muciniphila*. Altogether, this thesis demonstrates for one of the first times that berry polyphenols and their PAC-rich fractions are responsible for the prebiotic-like effect on *A. muciniphila*, and the inhibition of specific pathobionts associated with obesity and unveils the molecular mechanisms underpinning the resilience of this bacterium to phenolics.

TABLE OF CONTENT

LIST OF FIGURES

INTRODUCTION

CHAPTER I

CHAPTER II

CHAPTER III

GENERAL DISCUSSION AND CONCLUSION

LIST OF TABLES

LIST OF ABBREVIATIONS

AB/PAS Alcian Blue and periodic acid–Schiff staining

AHL N-acyl homoserine lactones

AOM Azoxymethane

ASVs Amplicon sequences variants

ATP Adenosine triphosphate

AUC area under the curve

BMI Body mass index

BW Body weght

CAZymes Carbohydrate-active enzymes

CCA Canonical Correspondence Analysis

CD Chron's disease

COG Clusters of Orthologous Groups

CPS Capsular polysaccharides

DADA2 Divisive Amplicon Denoising Algorithm 2

DIO Diet induced obesity

DP Degree of polymerization

DSS Dextran sulfate sodium

EGCG Epigallocatechin-3-gallate

EPS Exopolysaccharides

EWAT Epididymal white adipose tissues

F/B Firmicutes/Bacteroidetes ratio

FDR False discovery rate

FOS Fructo-oligasaccharides

FRI Functional redundancy

GAPDH Glyceraldehyde-3-phosphate dehydrogenase

GC Goblet cells

GI Gastrointestinal

GlcNAc N-acetylglucosamine

GLP-1 Glucagon-like peptide-1

GLUT2 Glucose transporter 2

GOS Galacto-oligosaccharides

HFD High-fat diet

HFF High-fat high-fructose

HFHS High-fat high-sucrose

HID-AB High Iron Diamine-Alcian Blue

Hprt Hypoxanthine guanine phosphoribosyl transferase

IBD Inflammatory bowel disease

ITT Insulin tolerance test

IWAT Inguinal white adipose tissue

KEGG Kyoto Encyclopedia Genes and Genomes

LDA Linear discriminant analysis

LPS Lipopolysaccharides

MaAslin Multivariate Association with Linear Models

MAGs Metagenome assembled genomes

NOD Non-obese diabetic

NOD2 Nucleotide-binding oligomerization domain 2

Ocln Occludin

OGTT Oral glucose tolerance

OUT Operational taxonomic units

PACs Proanthocyanidins

PBPs Penicillin-binding proteins

PCA Principal Component analysis

PCoA Principal coordinates analysis

PICRUSt Phylogenetic Investigation of Communities by Reconstruction of Unobserved States

Ppib Peptidylprolyl isomerase B

QIIME Quantitative Insights Into Microbial Ecology)

QS Quorum sensing

QSI Quorum sensing inhibitor

RecA DNA recombinase

RND Rsistance/nodulation/cell division

RPD Ribosomal Database Project

SCFAs Short chain fatty acids

SEM Scanning electron microscopy

SGLT1 Sodium-glucose cotransporter type 1

SHIME Simulator of Human Intestinal Microbial Ecosystem

T2D Type 2 diabetes

TEM Transmission electronic microscopy

TG Triglycerides

Th1 T helper type 1

Th17 Limphocytes T helper 17

Th2 T helper type 2

Tjp1 Tight junction protein 1

TLR Toll-like receptor

Tregs Regulatory T cells

tpiA triosephosphate isomerase enzyme

UC ulcerative colitis

USDA U.S. Department of Agriculture

VanX Vancomycin-X, D-ala D-ala dipeptidase

ZOTUs Zero-radius OTUs

To my RoDaza family: my parents Hortensia and Felipe, my brother and sister, Edgar and Mary, and to my beloved partner Diego

Acknowledgments

After five years of intense work and challenges, this Ph.D. thesis becomes a reality, which could not have been possible without the kind support of important people to whom I am greatly indebted.

I start acknowledging to my RoDaza family, especially to my mother Hortensia Daza, who taught me to thrive and persevere in my dreams, and who has been my source of reinforcement and inspiration. A very special thank you for having supported me in my determination of continuing doing research out of Colombia to somewhat contribute to improve health. Thank you RoDaza family for encouraging me throughout these last months of writing that despite the distance, a daily call was meaningful and make me feel always very close to all of you. I believe that the great sacrifices always bring great rewards, and this thesis becomes one of them.

I extend my deep gratitude to my research supervisor Dr. Yves Desjardins of the Plant Science Department, Faculty of Agriculture and Food Science at Laval University. I truly appreciate your willingness to help, guide and answer my questions. I am grateful to you for having trusted my potential and ideas and given me some autonomy to work on this project that was of great interest to me. Thank you for your dynamism to share interesting papers and generate excellent discussion about my research. Dr. Desjardins has taught me to improve my writing and present research articles as clear as possible. I would also like to thank Dr. Desjardins for the opportunity he gave me to participate in different international conferences throughout these last five years, which were important for learning and sharing outstanding knowledge.

I would especially like to thank my research co-supervisor Dr. Denis Roy, dean of the Faculty of Agriculture and Food Science at Laval University, who was always present, guiding me and supporting me throughout my Ph.D studies. Thank you for the precious advice, not only regarding to the topic of my research, but as an excellent scientist. Dr. Roy was contributory in defining the path of my research; He allowed me to integrate his Lab group, participate in other research projects and share with colleagues who are also

passionate for microbiology and molecular biology. Thank Dr. Roy for your empathy and encouraging me to always look further.

I am grateful to members of the Marette Lab at IUCPQ for the technical assistance with the animal protocols. Dr. André Marette and Dr. Geneviève Pilon, thanks for the invaluable contribution to this work. I would also like to thank Dr. Emile Levy, Dr. Marcela Roquim, Dr. Stéphanie Dudonné, Laurence Daoust, Dr. Lemia Boutkrabt, and Dr. Thibault Varin for their support in this project and their instrumental assistance with experiments.

Thanks also go out to the members of the jury for accepting to evaluate this work. I am grateful for your valuable feedback.

I would like to profoundly acknowledge the organisms that funded this work. Thanks to COLCIENCIAS (Colombia) for my Ph.D scholarship, and to Fruit D'Or, CRIBIQ, MITACS, Atrium Innovation and Diana Food Canada for the financial support to this project.

Thank you to my friends and colleagues from the Institute of Nutraceuticals and Functional Foods (INAF) for their endless support and encouraging words. Thanks to Ana Sofia Medina, Elena Pulido, Juan de Toro, Jacob Lessard, Mérilie Gagnon, Alexandre Kennang, Valentina Cattero, Briscia Tinoco and Joseph Lupien for friendship, for sharing ideas, keeping me laughing and being such great company.

To my boyfriend Dr. Diego Canizares, words cannot fully express my gratitude for your never-ending patience and constant support. Thank you for motivating me and doing this Ph.D journey much easier to walk. Thank you for being the best listener and my partner in this venture. I am looking forward to what life has for us.

Foreword

This doctoral thesis is the compilation of three scientific articles, preceded by a general overview of the subjects and concluded with a commented overview of the main findings obtained.

This thesis is focused in the prebiotic-like effects of polyphenols on symbiotic bacteria, and especially, on *Akkermansia muciniphila.* This bacterium is of a particular interest because of its proximity to the gut epithelium and its role in maintaining the host health status and immune system. The introduction provides a general outline of the gut microbiota structure and its importance for the host physiology, emphasizing the mucosa-associated microbiota, where *A. muciniphila* represents one of the key players; *Akkermansia* ecological niche and genomic repertoire are addressed. Moreover, the dynamic of the gut-microbial communities susceptible to perturbations by the host health status, diet and antimicrobials are discussed. Indeed, relevant evidence demonstrate the selectivity of dietary polyphenols to inhibit gut pathogens associated with obesity and favour health-promoting species. A large area of research on the anti-obesity and anti-diabetic activity of berry polyphenols and those from other dietary sources, has been associated with the bloom of *A. muciniphila,* but comparatively little data exist on the mechanisms underlying such effect. Accumulating evidence suggests that *A. muciniphila,* is a resilient bacterium to several factors, such as antibiotic administration. This bacterium is a dominant species in the gut after antibiotic therapies in humans and animals and is involved in improving metabolic alterations. These insights led us to hypothesize that *A. muciniphila* might express molecular mechanisms of bacterial resistance and adaptation to the antimicrobial properties of polyphenols.

Chapter I presents an article prepared and formatted for submission to the Journal of *Cell Host & Microbes.* The work was designed to unveil the prebiotic potential of cranberry and blueberry whole fruits rich in polyphenols and of their fibrous residue (rich in wall polysaccharides) in the gut microbiota of obese mice. The co-authors Dr. Yves Desjardins, Dr. Denis Roy, Dr. Emile Levy, Dr. André Marette, and Dr. Geneviève Pilon were involved in the study design. I was involved in the animal experiments together with Dr. Marcela Roquim. I carried out the histologic preparation and analysis of colon tissues. The

characterization of berry extracts and diet preparation were performed by Dr. M. Roquim and Dr. Stéphanie Dudonné. As the first author, I performed the bio-informatic analysis of the 16S rRNA gene sequences, including microbial functional profiling and multivariate analysis. I also performed the data integration, generated plots, and statistical analysis of mouse phenotypes. I was responsible for writing the manuscript, concomitantly edited by my supervisor Dr. Yves Desjardins, and revisited by all co-authors. This study reveals that polyphenol-rich whole cranberry and blueberry powders selectively stimulate *A. muciniphila* and not their fibrous fractions. Here, the functional redundancy analysis demonstrated that the polyphenols rich cranberry powder positively affected the predicted functional structure of the gut microbiota, attenuating obesity in HFHS-fed mice. In addition to *A. muciniphila,* other taxonomic biomarkers were correlated with lowering body weight and obesity-related metabolic disturbances.

The article presented in the **Chapter II** aimed to identify the polyphenolic fractions from a whole blueberry polyphenolic extract, contributing the most to prompt *A. muciniphila* and to attenuate obesity-related alterations in HFHS-fed mice. The manuscript was published in *Nature's Scientific Reports* (February 10, 2020, 10:2217, https://doi.org/10.1038/s41598-020-58863-1). The results demonstrate that the oligomeric and polymeric proanthocyanidins enriched fractions, significantly prompt *A. muciniphila* and improve its ecological niche in obese mice. In this article, I am co-first author with MSc. Laurence Daoust, since both were equally involved in the animal experiment. L. Daoust was in charge of the metabolic analytic assays. My role was to perform the bio-informatic analysis of the gut microbiota (together with Dr. Thibault Varin), perform the histo-morphological analysis of colon tissues, the molecular assays, as well as the statistical analysis. All authors importantly contributed to the interpretation and discussion of the manuscript.

Chapter III contains a manuscript prepared for being submitted to the scientific journal *Cell* in the coming months. This article uncovers compelling mechanisms underlying the selective prebiotic effect of polyphenols on *A. muciniphila.* Particularly, transcriptional response of genes related to defence and/or adaptation to antimicrobials/antibiotics were evaluated by submitting pure cultures of *Akkermansia* cells to whole cranberry extract and three derived polyphenolic fractions as applied in the previous animal experiment (Chapter

II). Molecular and physiological mechanisms induced by *A. muciniphila* when grown in polyphenols enriched culture media, contribute to maintaining a steady growth rate as compared to untreated cells. In particular, we show that membrane transporters contribute to *A. muciniphila* resistance to different cranberry polyphenolic fractions. Cranberry polymeric proanthocyanidins fractions induce the genetic expression and production of capsular and slime polysaccharides in *A. muciniphila*, that, in addition to assure cellular self-protection and physiology management, are believed to exert important physiological role in the host. Actually, the results were peer reviewed as potential matter to be patented and they remain confidential. In this work, I was responsible for the design of the experimental *in vitro* assays together with my supervisor Dr. Y. Desjardins and co-supervisor Dr. D. Roy. I carried out all the *in vitro* assays and the molecular analysis, except for the analysis of the polyphenolic extracts. I interpreted and discussed the results and wrote the manuscript. All the authors contributed to revisiting and edit the manuscript.

INTRODUCTION

1 The human intestinal microbiota

The gastrointestinal (GI) tract harbours about 10^{14} of highly metabolically active bacteria, encoding 150 times more genes than our own genome (Zhu et al., 2010). The microbiota and its encrypted genomes (including archaea and eukarya), predominantly located in the large intestine, are collectively known as the gut microbiome. In humans, the primary individual microbiota is thought to establish itself early on life. The colonization of microbial communities starts at birth and resembles the maternal vagina or skin microbiota depending on the mode of delivery (Dominguez-Bello et al., 2010). Subsequent, the dynamic of gut microbial landscape is driven by genetic factors and other environmental variables (i.e. diet, age, and the use of antibiotics) (Zhernakova et al., 2016), developing a lifelong signature with significant effects on host health.

The complexity of the gut microbiota is mainly represented by a limited number of bacterial phyla, such as *Firmicutes, Bacteroidetes* (approximately 90% of the GI microbiota), *Actinobacteria, Proteobacteria, and Verrucomicrobia* (Arumugam et al., 2011; Ley et al., 2008). Despite the high inter-individual variation, *Firmicutes* is the largest phylum in humans and rodents, with more than 250 genera (Graham et al., 2015; Ley et al., 2008). It is divided into three classes: *Clostridia* (*Clostridiales*), *Bacilli* (*Lactobacillales* and *Bacillales*) and *Erysipelotrichia (Erysipelotrichales)* (Ludwig et al., 2009). Moreover, the phylum *Bacteroidetes* includes around 20 genera, where the genus *Bacteroides* has a higher representation (Graham et al., 2015). The phylum *Actinobacteria* is less consistently detected as dominant, but represents a low percentage (5%) of the total bacteria; it includes the genus *Bifidobacterium*, widely known as a probiotic, and *Collinsella-Atopobium* group (Doré and Corthier, 2010). Finally, the phylum *Verrucomicrobia*, which includes the genera *Akkermansia* spp., is present in low proportion (3-5%) and displays a strong probiotic potential (Chang et al., 2019; Shin et al., 2019).

Three “Enterotypes” of the bacterial phyla described above have been suggested to exist in the human population. An enterotype is a functional harmonious association of several bacteria species constituting functional clusters, which are able to distinctly generate energy from fermentable

substrates available in the colon. This enterotype concept was proposed by Arumugam et al. (2011) who classified the gut microbiota of different population into three robust clusters featured by distinct genera functionally characterizing the human gut microbiome. The *Enterotype 1*, is featured by the presence of *Bacteroides (Bacteroidetes* phylum*)* and specialized in obtaining their energy from the fermentation of carbohydrates and proteins, particularly plant polysaccharides. They are more effective in the synthesis of vitamins (B8, B2, B5, Vit C) (Wu et al., 2011). The *enterotype 2* is rich in *Prevotella* and *Desulfovibrio* (*Bacteroidetes* and *Proteobacteria* phyla, respectively), particularly adapted in the degradation of mucins, the synthesis of some vitamins (B1 and B9) and glycoproteins that constitute the mucus surrounding the GI epithelium. Finally, the *enterotype 3* rich in *Ruminococcus* and *Akkermansia* (*Firmicutes* and *Verrucomicrobia* phyla)*,* besides degrading mucins (e.g. *A. muciniphila*, *Ruminococcus gnavus*, and *Ruminococcus torques*), can degrade cellulose presents in plant tissues (Arumugam et al., 2011; Costea et al., 2018; Siezen and Kleerebezem, 2011). The bacteria of this group are also rich in membrane transporters, mainly sugars, indicating a high glycolytic activity (Arumugam et al., 2011).

The characteristics of each enterotype provide an understanding on mechanisms of microbial metabolism, adaptation and depletion of bacteria under different intestinal conditions and host dietary habits. However, further studies focusing on the functional stratification of the gut microbiome have criticized the robustness of the classification of enterotypes proposed. For instance, Liang et al. (2017) stated that *Bacteroidaceae* (enterotype 1) should be integrated to the *Ruminococcaceae* (enterotype 3), revealing an ambiguous classification of the enterotype 3, as was also sustained previously by Wu et al. (2011). Moreover, a recent study similarly claimed that only two enterotypes existed after the analysis of groups of children with western-based (high-fat) and low-fat dietary habits (Nakayama et al., 2017). Using a Principal Component Analysis (PCA), the children microbiotas were then classified into two clusters characterized by high abundance of *Prevotellaceae* (denoted as P-type) and *Bacteroidaceae* (denoted as BB-type), although this latter was also significantly characterized by the bacterial families of *Bifidobacteriaceae, Ruminococcaceae* and *Lachnospiraceae.* Thus, the BB-type cluster appears to contain three microbiota subtypes. This study showed that obese children consuming a high-fat, high-protein and low-carbohydrate diet, were discriminated by a low abundance of *Prevotella.* Particularly,

many *Lachnospiraceae* and *Ruminococcaeae* species were closely associated with the fat-linked *Bacteroidaceae* community in obese children (Nakayama et al., 2017). These findings highlight that despite two major genera are discriminating the exposed enterotypes, the interactions among co-ecological species might also drive the functional-clustering or the enterotype-like stratification. For instance, the mucin-degrading specialists might improve the availability of oligosaccharides for other bacteria that do not possess the enzymes for degradation (Ouwerkerk et al., 2013).

Recent reevaluation of the enterotyte concept led to a new classification of human microbiota composition which provides an extended understanding of its involvement in functional, ecological and therapeutic context. For instance, Costea et al. (2018) proposed keeping the three enterotype clusters, now renamed ET-B (with *Bacteroides* as indicator, enterotype 1), ET-P (with *Prevotella* as indicator, enterotype 2), and ET-F (with *Firmicutes-Ruminococcus* as indicator, enterotype 3); yet the third one was shown to be inconstant or/and fused with another cluster throughout datasets of different human populations. The goal of the enterotypes-like approach is to reduce the complexity of the gut microbiota analysis within a population. The authors surmise that although species and strain-level variations might be omitted in each enterotype, there is a principal taxonomic indicator correlating best to the determined cluster.

1.1. Microbial gene richness and diversity

The first comprehensive analyse of bacterial diversity was carried by Eckburg et al. (2005) who analyzed 13,355 prokaryote rRNA gene sequences from faecal samples and mucosal biopsy of healthy volunteers. The authors showed that 11,831 bacterial 16S rRNA gene sequences were assigned to 395 bacterial phylotypes or species. The terms such as “microbiota” and “microflora” started to be used to describe the community of microbes in the human gut, and the term “metagenome” applied to describe the collective genomes of microbes, including their encrypted functions (Backhed et al., 2005). Along with the extended metagenomic analysis of the gut microbiota, the term “core microbiome” suggested by Turnbaugh et al. (2007), also arose to better define, not only the ensemble of gut microorganisms, but also their functional gut genes.

From 16S rRNA-based enumerations, it has been reported that gut bacterial phylotypes harbour more than 2-4 million genes encoding functions that have been shown to determine the host heath. Using KEGG (Kyoto Encyclopedia Genes and Genomes) pathways and COG (Clusters of Orthologous Groups) functional analysis, sequences of the gut microbiome were linked to genes involved in the metabolism of glycans, amino acids, and xenobiotics, as well as in energy metabolism, metabolism of cofactors and vitamins, among others (Gill et al., 2006). Thus, the bacterial richness and diversity assessment provide a benchmark for interpreting the predicted functional contribution and structure of a species-rich gut microbiota. The relative abundances of the different species making up the sample's richness (the number of species observed) and the evenness (defined as the frequency of the observed species) are often evaluated by using the *Shannon*-diversity index. Likewise, the *Simpson* index has been proposed as an evenness measure, which considers how well represented are the observed species in each microbiota (Koh, 2018).

Accumulating studies have shown how the diet may influence the bacterial diversity and how much it relates to the host health status (Cheng, et al., 2018; Gill et al., 2006; Ley et al., 2006; Lozupone et al., 2012; Ravussin et al., 2012; Thingholm et al., 2019). For instance, a high-fat high-sucrose (HFHS) obesogenic diet has been shown to decrease microbial diversity. Under such a diet, a number of species will overgrow leading to alteration of metabolic functions (Cotillard et al., 2013). Turnbaugh et al. (2009) compared the gut microbial diversity and metabolic functions between obese and healthy subjects. Obese individuals harboured fewer microbial phylotypes in their guts than lean individuals, presenting significant differences in taxonomic abundances and encoded functional genes. The authors demonstrated that individuals with similar taxonomic patterns belonged to similar metabolic phenotypes. 42% of enriched genes in lean individuals were attributed to *Bacteroidetes,* and 75 and 25% of obese-enriched genes were attributed to *Firmicutes* and *Actinobacteria.* In addition to obesity and Type 2 diabetes (T2D) (Cotillard et al., 2013; Le Chatelier et al., 2013; Thingholm et al., 2019; Turnbaugh et al., 2009), decreased bacterial diversity have been associated with several diseases, including colorectal cancer (Ahn et al., 2013; Liu et al., 2020), and inflammatory diseases (Alam et al., 2020; Scher et al., 2015).

Larger scale metagenomic analysis (Faith et al., 2013) also shed light into the importance of species richness and diversity, two critical characteristics conferring resilience and therefore

stability in the gut microbial ecosystem (Lozupone et al., 2012). Several studies have evidenced that species-rich microbiomes are less susceptible to pathogen invasion (Pamer, 2016; Ravi et al., 2019). Microbial phylogenetic competition, co-occurrence or co-exclusion interactions in the gut environment might also be affected by alteration in the gut bacterial diversity. For example, mucin-degrading pathobionts *Ruminococcus gnavus* and *R. torques* overgrowth in the gut microbiome, result in changes of the mucous niche and decrease of other microbial species such as *A. muciniphila* (Png et al., 2010). It is interesting to note that *A. muciniphila* might affect the host inflammatory status and indirectly impart resistance to pathogens colonization (Hanninen et al., 2018; Ottman et al., 2017; Plovier et al., 2016).

1.2 Mucosa-associated niche and colonizing bacteria

The composition and dominance of the gut microbiota differ between the mucosal and luminal intestinal compartments and is influenced by physiological, chemical, nutritional and immunological differences along the gut (Johansson et al., 2011; Johansson et al., 2008). The intestinal mucosa consists of a single layer of columnar epithelial cells covered by mucus, mainly composed of compact mesh-like network of viscous, gel-forming MUC2 mucin in the colon. Studies in mice and humans have shown that the mucus is differentiated into two separate layers with important protective and lubricating properties; namely an inner dense layer, "firmly" attached to the epithelium and a loose outer layer, which is estimated to be twice as thick as the inner one (see **Figure 1**) (Johansson et al., 2011; Ouwerkerk et al., 2013; Swidsinski et al., 2007; van der Waaij et al., 2005).

Mucin, a highly glycosylated protein, consists of primarily N-acetylgalactosamine (GalNAc), N-acetylglucosamine, fucose, galactose, sialic acid (N-acetylneuraminic acid) and traces of mannose and sulfate (Bansil and Turner, 2006). Glycan coverage of mucins is dense and contributes up to 80% of the dry weight of human mucin (Dharmani et al., 2009). Extension of the initial GalNAc generates a series of mucin core structures (Corfield, 2018). The glycosylation of the intestinal mucins is characterized by relatively large glycan chains containing more than 5 monosaccharides, terminated by sialic acids, fucose and sulfate moieties. Particularly, in the colon, the mucin glycosylation is characterized by high core of 3- or 4-based glycans, glycans with 8-9

monosaccharides, branched glycans, high sialylation, sialate O-acetylation, and high sulphation glycans (Corfield, 2018). Both the mucins and protein glycosylation have biological signification. For instance, an increased sialyltransferase activity in IBD, leads to abnormal synthesis of sialyl-Tn (Neu5Acα2-6GalNAc-) and prevents the normal extension of the colonic mucin O-glycan chains (Larsson et al., 2011). Free sialic acids are a target for scavenging by the bacterial microbiota in IBD, and the resulting dysbiosis leads to defective innate immunity and loss of commensals (Corfield, 2018). The enteric microbiota in IBD shows a decrease in gut commensals, including *Akkermansia, Clostridium IXa* and *IV groups*, *Bacteroides*, and *Bifidobacteria* and an increase in sulfate-reducing bacteria and *Escherichia coli* (Png et al., 2010). Furthermore, fucosylated glycans have been shown to be more selective and protect against bacterial glycan degradation (Corfield, 2018). The mucus layer is continuously renewed by the goblet cells (GC) and generates an antibacterial gradient from the epithelial cells out toward the lumen, explaining the lack of bacteria in the inner mucus in contact with the epithelial cells. However, anaerobic commensal microorganisms with the ability to adhere to mucus and degrade glycoprotein can colonize the outer mucus layer (Johansson et al., 2011; McGuckin et al., 2011). The glycoprotein composition of the mucin plays a key role on the bacteria ability to inhabit it. In this context, the specific antimicrobial properties of the mucus layer, the innate and acquired immunity constituents (e.g., defensins, immunoglobulins, trefoil peptides), and other factors such as oxygen concentrations and mucus viscosity, are of major importance for limiting the bacterial growth (Swidsinski et al., 2007).

Mucosa-associated bacterial species are then adapted to the glycan rich environment by the production of mucus-degrading enzymes and mucus-binding extracellular proteins (Laville et al., 2019; van Passel et al., 2011). Various members of the phyla *Bacteroidetes, Firmicutes, Actinobacteria* and *Verrucomicrobia* are able to metabolize mucins. Importantly, several studies, based on 16S RNA gene sequences, have demonstrated a marked heterogeneity in microbial composition between colon mucosa and luminal content (Hong et al., 2011; Lavelle et al., 2015; Zhang et al., 2014). *Coriobacteriaceae, Lachnospiraceae, Ruminococcaceae* and *Family XIII Incertae sedis* are enriched in the mucus gel microbiota of healthy volunteers, while *Bacteroideaceae* are higher in faecal/luminal samples (Lavelle et al., 2015). Nevertheless,

members of this last family, such as *Bacteroides thetaiotaomicron* and *Bacteroides fragilis* were shown to have mucin-degrading capabilities (Laville et al., 2019; Martens et al., 2008). Likewise, *Actinobacteria*-belonging genera, including both *Bifidobacterium bifidum* and *Bifidobacterium longum* are able to growth on mucin as sole carbon source (Kim et al., 2013; Ruas-Madiedo et al., 2008). Additionally, the phylum *Verrucomicrobia,* represented by *A. muciniphila*, is also enriched in the mucus layer due its ability to thrive on mucin (Derrien et al., 2004). The mucin-degrading capacities and biological role of *A. muciniphila* will be discussed in detail later in this chapter.

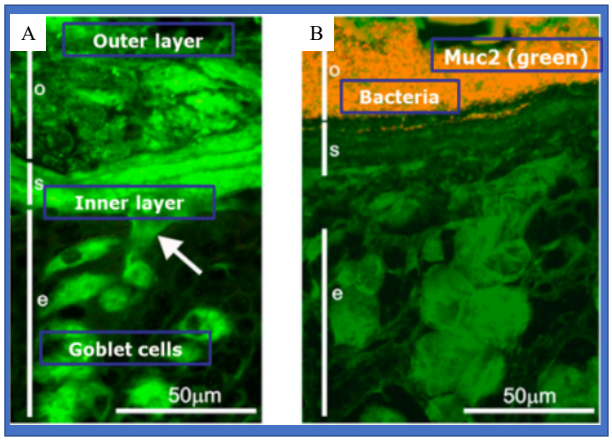

Figure 1. Structure of the colonic mucus layer

The intestinal mucosa consists of a single layer of columnar epithelial cells surrounded by two Muc2-rich mucus layers. A) An inner layer firmly attached to the epithelium and an outer layer. Immunostaining of Muc2 (green) in the distal mouse colon reveals mucus-filled goblet cells in the epithelium. Arrow indicates release of Muc2 mucin from a goblet cell. (B) FISH using a general bacterial probe visualizes the bacteria (red) in combination with staining for Muc2 (green) colonizing the outer mucus layer. The inner mucus layer (s) forms a barrier is devoid of bacteria, protecting the colonic epithelium. Image adapted from (Johansson et al., 2011).

2 Biological role of the gut microbiota: the functional redundancy concept

Identifying the compositional pattern and the functional contribution of the gut microbiota is of a particular interest, since accumulating evidence demonstrates the biological implications of the gut microbiota in the onset, maintenance or progress of different diseases (de la Cuesta-Zuluaga et al., 2018; Liu et al., 2020; Ranjan et al., 2018; Turnbaugh et al., 2009; Zeng et al., 2018; Zhang et al., 2009). This knowledge is of paramount importance to develop microbiome-based therapies,

using specific treatment, including dietary functional ingredients (prebiotics), live microbes (probiotics), or pharmaceutical interventions.

Widely studied in ecological water and soil systems, the functional redundancy (FRI) concept explains the metabolic role of the whole gut microbiota structure, beyond the pressure that might be exerted by the simple suppression or enrichment of a specific microbial phylum or species. For instance, the FRI is often evaluated in soil and environmental microbiota to examine ecosystem functions such as respiration, toxic compounds degradation and biomass production (Huang et al., 2019; Wagg et al., 2019). In analogy to the functional structure of the soil microbiota, the FRI of the gut microbiota illustrates how taxonomically different microbial communities are able to exhibit similar functions and metabolism in the host (Moya and Ferrer, 2016). In this sense, the gene content of the gut microbiota and the encrypted metabolic functions reflect the collection of microbial enzymes to utilize nutrients and their capacity to generate trophic substrates. Those microbial substrates might be cross-fed to other species occupying the same ecological niche or might be used by the host itself. An imbalance in taxonomic composition of the gut microbiota could thus affect the levels of genes (meta-transcriptomes), proteins (metaproteomes), functions (metagenomes), and metabolites (metabolomes), thereby influencing host health. For instance, fermentation of plant polysaccharides/fibres results in the generation of short-chain fatty acids (SCFAs), mainly acetate, propionate and butyrate. Consequently, changes or alterations of microbial diversity will also be reflected in the type and quantity of generated SCFAs (Koh et al., 2016), which have been demonstrated to serve as principal energy source for colonocytes and contribute to reinforce the intestinal mucosal barrier (Donohoe et al., 2011; Yan and Ajuwon, 2017).

In a context of diet-induced obesity, the dysbiotic state stems from the abundance of distinct phylotypes of the gut microbiota with analogous metabolic capacity, thus leading to a decreased functional diversity (Turnbaugh et al., 2009). Consistent with the enterotype categorization, Ferrer et al. (2013), using shotgun metaproteomic analysis, revealed that proteins/enzymes belonging to the COG category of "carbohydrate transport and metabolism" from lean individuals were linked to the *Bacteroidetes* phylum, mainly *Prevotella* (enterotype 2), while in obese subjects 90% of those proteins were linked to *Firmicutes* phylum, mainly *Ruminococcus* (Enterotype 3). These

observations illustrate that *Firmicutes* and *Bacteroidetes* phyla have redundant functions for carbohydrates degrading activity. Here, it is also worth noting that the phylum *Firmicutes* has a 10-fold higher anabolic activity for dietary carbohydrates under obesity, than the phylum *Bacteroidetes* under an eubiotic condition. Thus, despite the fact that these phyla are redundant for a particular function, the likely differences in the degradation rates of carbohydrates and in the resulting production of SCFAs, have crucial effect on host health status. A good example of such a redundance can be found in a recent study on the enterotype-based stratification of two children population with different dietary habits (Nakayama et al., 2017). In this case, through redundancy analysis, the authors claimed that the *Bacteroidaceae* (BB-type) enterotype is metabolically more active in using simple sugars, while the *Prevotellaceae* (P-type) enterotype is more active using complex carbohydrates. Thus, although both contributing to carbohydrates catabolism, the functional contrast of the two phylotypes is clearly influencing the metabolic outcome for the host.

The utility of the FRI can be twofold; a reduced FRI can help to determine whether there are prominent species conferring specific or essential role to the host, whilst an increased FRI allows to identify the species variations with a high degree of similarity in fulfilling determined functions. In the latter case, the suppression of a specific taxonomic abundance and activity may not have a major impact on the host metabolic phenotype, since its role can be substituted by another microbial phylotype, sharing similar functional and structural properties within the gut. One such example was demonstrated by Medina et al. (2019) who analyzed the gut microbiota composition and functional patterns of obesity and post-obesity-suffering subjects using shotgun DNA metagenomic sequencing. The authors showed that obese subjects presented a constant or similar metabolic phenotype, despite the variability in their gut microbiota structure and geographic origin.

As argued by Ley et al. (2006), the importance of the FRI can be also investigated by replacing the whole gut microbiota by keystone species, exerting a central role in the host system. This mono-association in germ-free mice may fulfill a number, but not the entire host phenotype as observed in mice with the conventional gut microbiota. The FRI notion, leads to rethink the influence of the gut microbiota on metabolic disturbances in the host, often confined to the codominance of *Bacteroidetes* and *Firmicutes* phyla as dysbiosis determinants (Koliada et al.,

2017; Turnbaugh et al., 2006). Other microbial phyla and specific species have also been demonstrated to play a functional role within the gut. One relevant microorganism related to the microbial functional evolution and to the capacity to interact with the host immune system is *A. muciniphila* from the *Verrucomicrobia* phylum. *A. muciniphila* 2.7 Mb genome reflects its trophic preference to exploit the mucin glycoproteins and inhabit mucin-rich specialized niche (van Passel et al., 2011). The proximity to the host epithelium suggests that the bacterium is actively involved in crosstalk with the cell surface and the immune system. Studies in gnotobiotic mice have demonstrated the functional role of *A. muciniphila* in the host metabolic and immune response (Ansaldo et al., 2019; Greig et al., 2018). Importantly, the supplementation of *A. muciniphila* cell wall protein Amuc_1100, induced the production of specific cytokines through activation of Toll-like receptor (TLR) 2 and TLR4 and strengthened the intestinal barrier function in Caco2-cell culture (Ottman et al., 2017). Another example of key species showed to positively interact with the host epithelium is *Bacteroides thetaiotaomicron*. Belonging to the phylum *Bacteroidetes* and representing 6% of the total bacteria (Eckburg et al., 2005), *B. thetaiotaomicrom*, in addition to expressing glycan-specific genes, has the molecular machinery to produce capsular polysaccharides (CPS), which were shown to largely contribute to stimulate T cells and immune response (Hsieh et al., 2020; Porter et al., 2018; Wegorzewska et al., 2019; Wrzosek et al., 2013). In this sense, *A. muciniphila* not only shares with *B. thetaiotaomicron* the ability to adhere to the mucus by glycan-specific outer membrane binding proteins, but also shares the molecular repertoire to produce CPS (van Passel et al., 2011), which might positively affect the host immune system. Moreover, because of their selective mucous niche, both species have the capacity to thrive under decreased fibre availability in the gut, shifting to host mucus polysaccharides as unique energy source.

3. Metagenomics and bioinformatic tools for studying gut microbiota dynamics

The development of culture-independent molecular techniques and bioinformatic tools, mainly based on 16S rRNA gene sequences, has provided a reliable and precise assessment of the gut microbiota. The 16S rRNA is usually chosen as a marker gene for sequencing of bacterial

communities due to its unique structure that contains both conserved and variable regions, and its presence in all known bacteria. This sequencing approach is often used to avoid the high cost of shotgun metagenomic sequencing or to avoid problems with sequencing non-microbial host DNA contamination.

Traditionally, sequence reads are clustered into operational taxonomic units (OTU) with 97% of identity to reduce sequencing errors, but this approach can still generate incorrect taxonomic units (Callahan et al., 2017). Nevertheless, bioinformatic packages have recently been released in an attempt to correct sequencing errors and establish the true biological sequences at single nucleotide resolution by generating amplicon sequences variants (ASVs) (Callahan et al., 2016). DADA2 (Divisive Amplicon Denoising Algorithm 2, ASVs assignment) uses a parametric Illumina error model based on the entire sequences run being applied to correct and collapse the sequences errors into ASVs. Thus, it builds unique errors model for each sequencing run, following a pooled-sample workflow. On the contrary, OTU pipeline (QIIME, Quantitative Insights Into Microbial Ecology) follows a denoising process sample-by-sample. This last approach, while requiring lower computational capacity, sacrifices the stability of the sequence's analysis by correcting multiple batches. Due to denoising algorithms capability of single nucleotide resolution of DADA2, it provides more strain information than OTU clustering at 97% sequences identity. Nearing et al. (2018) compared both approaches from a mock community analysis and showed that DADA2 was more sensitive to find low-abundance microorganisms. The number of different microorganisms per sample was directly affected by the choice of processing pipeline. On the one hand, DADA2 pipeline tended to find more total ASVs than OTU pipeline, but the OTU clustering exaggerated the number of unique microorganisms found within a sample, indicating that the α-diversity metrics (microbial richness and diversity) can differ between the two approaches (Edgar, 2017).

Currently, other pipelines have been published for covering the OTU-associated limitations. UNOISE2, uses another algorithm optimized for denoising Illumina amplicon reads, clustering reads in zero-radius OTUs (ZOTUs), that is, the OTUs with higher identity (>97%) (Edgar, 2016). Furthermore, using error profiles to infer putative error-free reads, Deblur offers a better taxonomic

resolution with just one bp of difference (Amir et al., 2017). Nonetheless, due to improved sequences resolution down to at single-nucleotide level, DADA2 method is rapidly becoming predominant (Callahan et al., 2017). Consequently, microorganisms might be better distinguished and thus, predicted genes annotation trend to be more precise.

To what extent might we predict the functional profile based on the presence of microbial ASVs/OTU in a community? Functional screening by shotgun metagenomics or 16S rRNA gene sequencing relies on total or partial microbial community DNA, including from uncultured members, and consequently, matches the obtained sequences to those of known functional genes in databases. Identification of genes involved in specific metabolic pathways can predict the functional capabilities of the gut microbiota, but in contrast to a transcriptional, proteomics or metabolite analyses, these remain predictions. PICRUSt (Phylogenetic Investigation of Communities by Reconstruction of Unobserved States) was the first tool developed and the most widely used for metagenome prediction (Langille et al., 2013a), but has several limitations. First, PICRUSt requires input sequences to be OTUs generated from closed-reference OTU picking against a specific, compatible version of the Greengenes database. Due to this limitation, PICRUSt's implementation is incompatible with sequence denoising methods, such as DADA2. Other packages such as Tax4Fun2 (Wemheuer et al., 2018), and Piphillin have thus been released to make up for these limitations (Narayan et al., 2020). In contrast to PICRUSt, Tax4Fun2 generates metagenome prediction based on the nearest-neighbour mapping of references 16S sequences and can be used with ASVs and SILVA database, offering the benefit of analyzing a functional redundancy index within a microbial community. Piphillin package can take as input either OTUs or ASVs. A similar tool has been shown useful for functional profile prediction from human microbiome, such as PanFP (Jun et al., 2015). Recently, an improved version of PICRUSt has been proposed (now named PICRUSt2) (Douglas et al., 2019) that insert sequences into an existing phylogenetic tree and can now be run using ASVs and OTUs. PICRUSt2 provides the identity and contribution of the taxa to each predicted function.

The predictive gut metagenome inferred from high throughput 16S rRNA gene sequencing has been shown to match specific metabolic pathways identified by other more precise methods, such as meta-transcriptomes and proteomes. For instance, in a comparative functional analysis of lean

and obese twin microbiomes, Turnbaugh et al. (2009) identified 400 obesity-related genes (enriched and depleted) from the KEGG (Kyoto Encyclopedia Genes and Genomes) pathway analysis and COGs (Clusters of Orthologous Groups) functional analysis. This functional study revealed that the gut microbiota possesses the enzymatic machinery to process the non-digestible carbohydrates. Particularly, the obesity-associated genes were predicted to be involved in carbohydrates, lipids and amino acid metabolism. Furthermore, Verberkmoes et al. (2009) through a proteomic analysis revealed that genes involved in carbohydrate metabolism and energy generation, although present in higher proportions, coincided with those predicted from metataxonomic and metagenomic data. Another relevant example of correlations between functional prediction and transcriptomic database provided insights on the microbial impact into a disease state. Using PICRUSt2, Douglas et al. (2019) found 29 associations between predicted functional pathways and ileal transcripts level of subjects with Crohn's diseases (CD). Although, these types of inferences warrant further investigations, all tools aiming to predict microbial functional profile may yield potentially useful information beyond the taxonomic composition and could be relevant targets for therapeutic strategies.

Variations in taxonomic classification of gut microbiota 16S rRNA gene sequences have also been found according to the choice of database for OTUs/ASVs annotation. The best known database classifiers are Greengenes, Ribosomal Database Project (RDP) and SILVA (DeSantis et al., 2006; Quast et al., 2013; Wang et al., 2007b). Greengenes is normally used together with QIIME pipeline, since it was first introduced in 2006 for assigning taxonomies to Archaea and Bacteria. Several studies comparing the effects of those reference databases on the identification of microbial phylotypes at different levels have reported that the highest assignment success at genus level have been obtained with SILVA, whereas Greengenes came second and RDP last (Almeida et al., 2018; Henderson et al., 2019). Likewise, other studies have reported erroneous taxonomic assignments of sequences belonging to a different family/genus, leading to incorrect conclusions (Lydon and Lipp, 2018). Hence, the genome database for OTUs/ASVs picking is also a key factor influencing the compositional and functional assessment of the gut microbiota.

Once the taxonomic composition (ASVs/OTUs) is known, the gut microbiota structure can be interpreted by calculating distance matrices (β-diversity analyses) between samples and clusters. Likewise, complex abundance distribution of specific gut taxa can be directly identified as significant feature of a specific community structure. To this effect, different ordinations-based analyses are often used. Among the most often used approaches are UniFrac and Bray-Curtis (Greenacre, 2017; Herren and McMahon, 2017). UniFrac considers the phylogenetic distance between taxonomic datasets, where a distance of zero suggests that the compared samples are identical. There are two types of UniFrac distance metrics – unweighted and weighted. Unweighted UniFrac measures the presence and absence of ASVs/OTUs, whereas weighted UniFrac besides, incorporates the abundances of ASVs/OTUs into the calculation. The Bray-Curtis distances metric calculates the dissimilarity in the samples composition, but it is not based on phylogeny; it treats all taxa as completely unrelated from each other (Beals, 1984). Applying both metrics at the same time can be advantageous (Shankar et al., 2017); when communities are composed of closely linked taxa, a smaller distance on a phylogenetic tree, will result in smaller pairwise distance between samples using the weighted UniFrac metric, relative to the Bray–Curtis metric. In this sense, if samples are unrelated, both the weighted UniFrac and Bray–Curtis distances will share similar patterns. To visually explore these taxonomic structure data, Principal coordinates analysis (PCoA) is widely used to reduce a multidimensional sample vector (for 16S data, the feature counts for a sample) to its principal components (PCs) (Christensen et al., 2018).

As discussed above, high-throughput gene sequencing enables the reconstruction of metabolic capabilities of the core microbiome. Yet, establishing the function of a specific species or phylotype within a complex and dynamic microbiota remains a challenge. Diverse bioinformatic tools, such as PICRUSt2, have been proposed for this purpose, but further investigation is needed to attribute specific function to a particular member of the gut microbiota. Other packages, such as Tax4Fun2, propose the functional redundancy index, to provide clues on the identity of keystone members bearing benefit to the host. Apart from the 16S rRNA gene sequencing, another strategy for uncovering metabolic effects associated to specific bacteria is to carry out *in vitro* fermentation experiments. With this type of experiment, the metabolome analysis can help to elucidate the role

of main substrates but eludes the contribution of the host immune system. Those profiles can then, subsequently be integrated with metagenomic data and infer statistical significance by using multivariate computational modelling. In this context, the MaAslin (Multivariate Association with Linear Models) represent a relevant tool for associating functional pathways or microbial metabolic outcomes with a sparse selection of disease status and clinical metadata (Ciocan et al., 2018; Kostic et al., 2015; Morgan et al., 2012). This tool allows to capture the effects of a parameter of interest while removing confounding variable from the data and might allow for the elucidation of the underlying interaction between the gut microbiota and the onset of several diseases. The approach based on the 16Sr RNA gene sequencing for meta-taxonomic and metagenomic data analysis of gut microbiota is presented in the **Figure 2.**

4. Gut dysbiosis: the case of diet-induced obesity

The gut microbiome structure is undoubtedly connected to dietary habits and host health status. As an extreme example, studies on mammalians and their gut microbiota revealed that both the taxonomic composition and the gene function are coupled to the diet (Muegge et al., 2011). Using PCoA plots, Muegge et al. (2011) discriminated groups of carnivores and omnivores from herbivores, while accounting for both 16S rRNA and whole bacterial community gene datasets, emphasizing the importance of diet in shaping the gut microbiota structure. Wu et al. (2011) also added evidence on the adaptation of the gut microbiota structure to dietary habits, indicating the stratification of the overall gut microbiota by enterotypes as discussed earlier. The authors analyzed the fecal microbiota of a selected cohort of 98 healthy individuals. Remarkably, the *Bacteroides* enterotype was highly associated with the intake of a western diet, including high level of animal protein, a variety of amino acids, and saturated fats; the *Prevotella* enterotype, in contrast, was associated with low values for these groups of nutrients, but with a polysaccharide-based diet, and high level for carbohydrates and simple sugars.

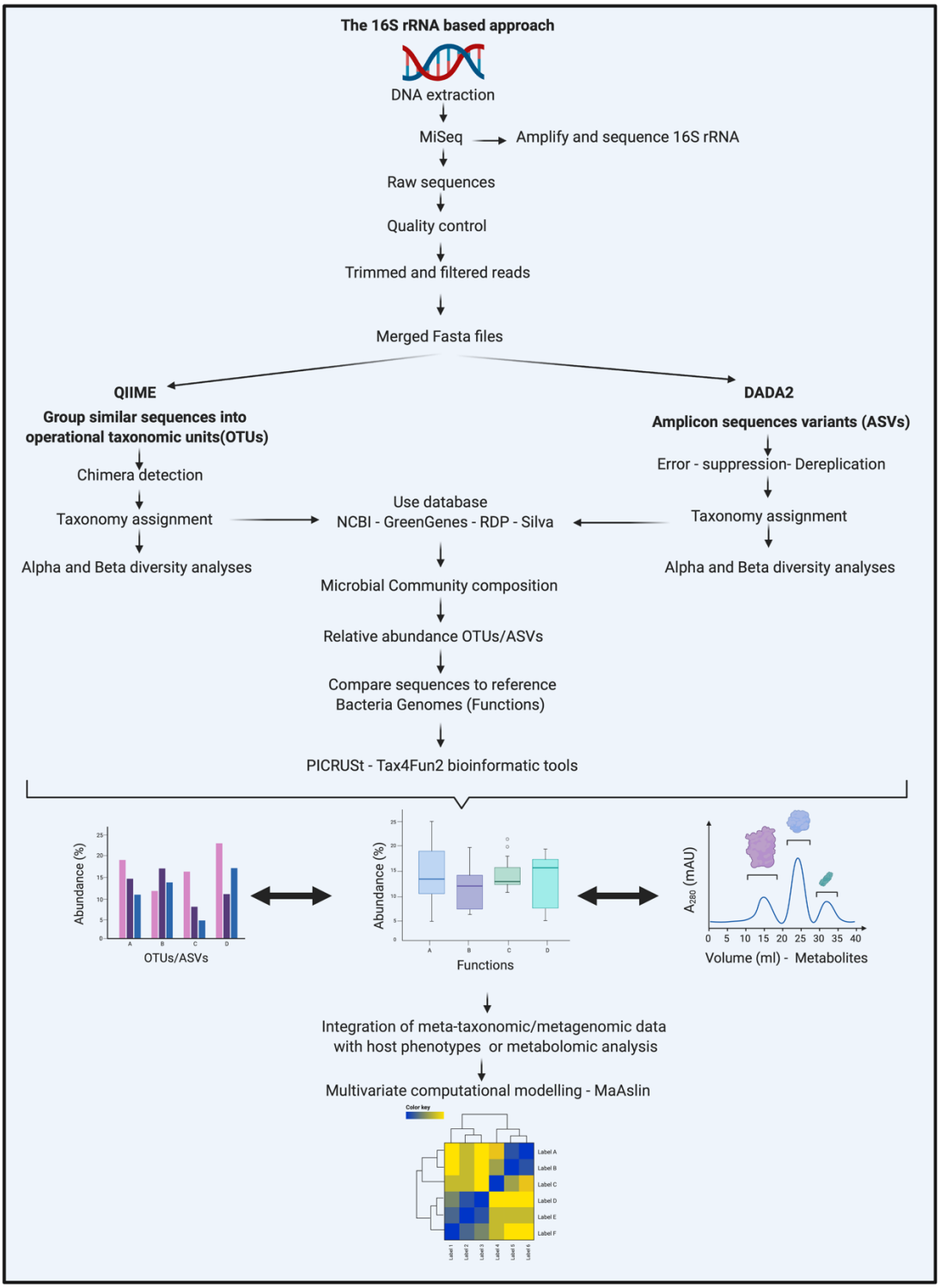

Figure 2. 16S rRNA based approach for meta-taxonomic and metagenomic data analysis of gut microbiota.

Consumption of a plant-based versus western-type diets results in distinct gut microbial community and can directly influence the risk of metabolic diseases (see **Figure 3**). For instance, David et al. (2014) revealed that a 5-days high-fat animal diet (69% total calories) and protein (30% total calories) without carbohydrates, increased β-diversity compared to baseline; on the contrary, a plant-based diet only produced a slight effect, maintaining the gut microbiota structure comparable to baseline. In this study, an animal diet caused a 2-fold higher faecal concentration of isovalerate and isobutyrate, two indicators of proteolytic activity and amino acid fermentation, and concomitantly caused a marked bacterial taxonomic shift. In contrast, the plant-based diet induced a 2-fold increase in acetate and butyrate, reflecting carbohydrate fermentation. The SCFAs are of crucial importance since they can intervene in the colonic mucosal homoeostasis, improve glycemia and insulin resistence, dyslipidemia and attenuate intestinal inflammation linked to a dysbiotic state (Donohoe et al., 2011; Slavin, 2013; Yan and Ajuwon, 2017). A dysbiotic gut microbiota is the result of an ecological unbalance of microbial communities stemming from a decreased microbial diversity and functions. Often, gut dysbiosis has been associated with the pathogenesis of IBD (Papa et al., 2012; Scher et al., 2015; Walker et al., 2011), but also to obesity (de la Cuesta-Zuluaga et al., 2018; Thingholm et al., 2019; Walters et al., 2014). For example, in a murine model of diet-induced obesity (DIO, low-fibres and HFHS) microbial diversity was lower than in mice fed a chow diet (Sonnenburg et al., 2016).

It has been more than a decade since a HFHS western diet was shown to reshape the gut microbiome potentially contributing to host adiposity (Turnbaugh et al., 2008). The first evidence of this phenomenon was provided in 2006 by the same research group, using a germ-free murine model colonized by microbes of obese donors (Turnbaugh et al., 2006). In this study, the microbes transfer resulted in a 43% higher body fat after 2-weeks of colonization compared to control mice. The role of the gut microbiota in the development of obesity was also demonstrated by inducing obesity using a HFHS-diet in a germ-free murine model. In this case, mice devoid of gut microbiota did not develop obesity (Backhed et al., 2007). The increase of *Firmicutes* phylum and the decrease of *Bacteroidetes* were suggested to cause the altered body composition in a murine model of DIO. However, the *Firmicutes/Bacteroidetes (F/B)* ratio is not a consistent parameter in obesity. More recent studies in a large sample size in humans have failed to detect a link of *F/B* ratio with body

mass index (BMI) or obesity (reviewed by Walters et al. (2014)). Similarly, some studies in rodents could not correlate weight loss with *F/B* ratio (Zhang et al., 2012; Zhang et al., 2010).

In the context of DIO, opportunistic microbes contribute to higher chronic disease risk. Particularly, HFD leads to decrease gut barrier function and cause the translocation of bacterial lipopolysaccharides (LPS), a presumed cause of chronic low-grade inflammation (Hersoug et al., 2016; Kim et al., 2012). The *Proteobacteria* phylum often increased in HFD-fed mice has been proposed to represent a microbial signature of dysbiosis (Shin et al., 2015). Families in the phylum *Proteobacteria*, such as *Enterobacteriaceae* and *Desulfovibrionaceae*, contain many pathogens that can produce LPS as an endotoxin. In Sprague Dawley rats fed a HFD, higher concentrations of plasma LPS and higher levels of gut *Enterobacteriaceae* members were observed compared to lean rats (de La Serre et al., 2010). Additionally, the genus *Roseburia* and other members of the *Lachnospiraceae* increased in subjects with IBD (Backhed et al., 2007; Beaumont et al., 2016; Turnbaugh et al., 2006). The family *Clostridiaceae* and *Lachnospiraceae* were associated with high LDL cholesterol levels, and the genus *Coprococcus* was negatively correlated with serum triglycerides (Fu et al., 2015). In a recent study, *Lachnospiraceae bacterium* and members of *Ruminococcus* and *Fusobacterium* were enriched in obese subjects (Liu et al., 2017). In other studies, the genera *Anaerotruncus* (an opportunistic pathogen) was in higher proportion in HFD-fed mice and remarkably associated with aberrant colonic crypts (Zeng et al., 2018). Other genera such as *Lactococcus, Alistipes, Oscillospira, Roseburia, Streptococcus, Ruminococcus* and *Butyricimonas* were in higher proportion in HFD-fed mice and HFD-fed mice treated with azoxymethane (AOM)-induced colonic aberrant crypts (Zeng et al., 2018). On the contrary, a reduction of *A. muciniphila, S24-7* (member of *Bacteroidetes*), *Barnesiela* (*Porphyromonadaceae*) was consistently found in metagenomic studies of DIO, albeit in some studies *Akkermansia* was unaffected by diet or obesity (Dalby et al., 2017; Ellekilde et al., 2014; Everard et al., 2013; Gurung et al., 2020; Hou et al., 2017; Ke et al., 2019; Le Chatelier et al., 2013; Rodríguez-Daza et al., 2020; Schneeberger et al., 2015).

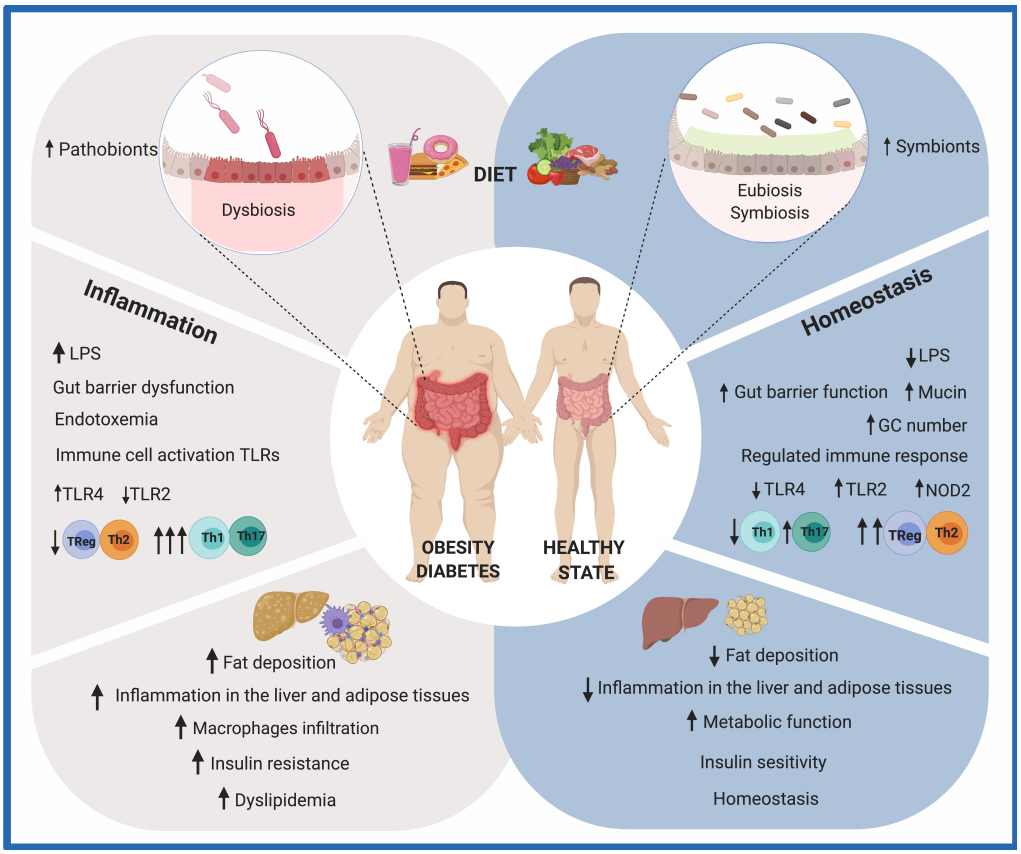

Figure 3. Effects of diet on gut health.

The consumption of a diet rich in fat and sugar (HFHS) has been shown to negatively modulate the composition and metabolic activity of the human gut microbiota. Due to the crucial role it plays in human health, imbalances in its composition and/or function (dysbiosis) are recognized as possible causes of intestinal, metabolic, and immune diseases. Particularly, HFHS leads to the translocation of bacterial lipopolysaccharides (LPS) and to chronic inflammation. A group of metabolic abnormalities, including fat deposition, insulin resistance, hyperglycemia, and dyslipidemia is exacerbated. On the other hand, a diet rich in fruits and vegetables contributes to maintaining the gut homoeostasis. Functional ingredients widely found in fruits and vegetables have been shown to increase microbial diversity and functions, maintaining the gut microbiota composition in a eubiotic state. Intestinal and immune homoeostasis is positively modulated in the host.

Studies indicate that changes in the composition of gut microbiota and functions, including lower species diversity and higher proportion of genes involved in glycolytic activity, are tightly linked with obesity and T2D. Within the encrypted metabolic function of the gut microbiota, functions encoding for membrane transporters and carbohydrate metabolism, and enrichments in LPS biosynthesis have been observed in subjects with high BMI and insulin resistance (Bodogai et al., 2018; Liu et al., 2017). Likewise, an increased proportion of pathways involved in glutathione metabolism as response to the oxidative stress, has been observed in DIO (Yassour et

al., 2016). All in all, gut microbiome contributes to the pathophysiology of obesity and is affected by changes in the diet; specific dietary ingredients may thus have potential therapeutic applications.

4.1 Intestinal barrier function in obesity

Diet-induced obesity and gut dysbiosis are often characterized by an impaired intestinal barrier function, increased LPS into blood, gut inflammation and immune response (Everard et al., 2013; Liu et al., 2017; Schneeberger et al., 2015). The mucus layer covering the gut epithelium constitutes a physical barrier against bacteria reaching the mucosal tissue. This important role was demonstrated using Muc2 knockout mice, lacking colonic mucus layer, which suffered an exacerbated inflammation with signs of colitis (Lu et al., 2011; Van der Sluis et al., 2006). Most mucin glycoproteins have a high sialic acid and sulfate content that increases the rigidity of the polymer via negative charge repulsion (Rodriguez-Pineiro et al., 2013). Histochemical analysis by Alcian blue/periodic acid-Schiff (AB-PAS), and High Iron Diamine-Alcian Blue (HID-AB) pH 2.5 staining, revealed the presence of both acid mucins, sulfomucins and sialomucins throughout the whole colon of healthy C57BL/6J mice (Liquori et al., 2012). PAS dye is specific to unsubstituted α-glycol rich neutral mucins; and AB, reveals acidic mucins, including the sulfated type or sialylated mucins (Sharma and Schumacher, 1995). In the distal colon, sulfomucins are clearly prevalent, although there are some sialomucins present; particularly, these latter are mainly located in the lower part of the colonic crypts (Liquori et al., 2012), keeping the mucin less susceptible to the attack of bacterial sialidases.

The high-fat diet profoundly affects the function of the intestinal mucus layer, and the tight junction integrity of the epithelial barrier (Kim et al., 2012). Mastrodonato et al. (2014) showed that a fat-rich diet (western-style diet) in mice alters mucin integrity with a probable shortening of glycoproteins oligosaccharide chains. In this respect, small differences in the structure or concentration of mucin may be sufficient to facilitate the microbial invasion, trigger a concomitant dysbiosis, and lead to colon diseases. In a murine model of DSS-induced colitis, the mucus layer is altered before the induction of any inflammation, indicating that mucus layer integrity prevents inflammation (Johansson et al., 2010). Similarly, HFD led to a significant increase in the ratio

sialo/sulfomucins compared to control mice (47.27 ± 9.8 vs. 21 ± 4.8 %, respectively). These alterations influence the bacterial composition and decrease microbial diversity of the intestinal mucosa (Sommer et al., 2014). In humans, the glycans of the distal colonic mucins are more acidic, containing more than 65 % sialic acid and/or sulfate residues (Robbe et al., 2004). Altered expression or glycosylation of mucins is documented in a variety of inflammatory or malignant diseases (Mastrodonato et al., 2014). CD and ulcerative colitis (UC), polyps, and colon cancer are associated with qualitative and/or quantitative changes of secreted sialomucins and sulfomucins (Earley et al., 2019).

The O-glycosylation pattern of mucins play a key role in health, by mainly triggering higher proportion of sulfated colonic mucins (Tobisawa et al., 2010). The glycans and their sialylated, sulfatated and fucosylated moieties may provide specific bacterial attachment sites, on which only certain species will adhere or will have the enzymatic machinery to adapt to each host (Johansson et al., 2011). For instance, the host sialic acids are some of the most frequently targeted carbohydrate receptors for microbes. In this regard, bacteria might modulate the mucin chain O-glycan to adapt to and forage on host sialylated glycan as nutrients for their own benefits (Wrzosek et al., 2013). Thus, bacterial sialidases and their mucosal sialoglycan targets, contribute to host–microbe interactions on every mammalian mucosal surface, possibly favouring pathobiont colonization and inflammation. Indeed, mucins are poorly sulfated in patients with UC (Raouf et al., 1992), consistent with opportunistic pathogens invasion as *Ruminococcus* species. Noteworthy, biochemical assays highlighted differences in sialylated substrate specificity between mucin-degrading bacteria, such as *Rumminococcus gnavus* and *A. muciniphila* (Tailford et al., 2015); increased mucus sialylation causes *R. gnavus* to bloom and *A. muciniphila* to disappear in IBD (Png et al., 2010). The *R. gnavus* mucin-degrading enzymatic profile appears particularly well adapted to digest mucin with short chains terminated by sialic acid, which has been found in higher proportion in IBD patients. On the contrary, *A. muciniphila* has been correlated with higher proportion of sulfated mucin and shown to attenuate inflammation in patients suffering UC (Earley et al., 2019).

The intestinal immunological regulation, the goblet cell differentiation, and mucin secretion can be influenced by the gut microbiota (Bansil and Turner, 2006; Swidsinski et al., 2007).

Deplancke and Gaskins (2001) provided some initial evidences that alteration of mucin composition affected the microbiota. The facts come from histochemical studies in which germ-free animals were compared to conventionally raised controls or inoculated with mixed microbial populations. Goblet cells of germfree rodents were fewer in number and smaller in size than those of conventionally raised mice. As a result, the mucus layer was up to twice as thick in conventionally raised than in germfree rodents, indicating greater mucus production (Johansson et al., 2015). Symbiotic bacteria can colonize the mucus layer and, at the same time promote the mucin production. For instance, *A. muciniphila* supplementation to dysbiotic aged-induced Ercc1−/Δ7 mice for 10 weeks restored the colonic mucus barrier (van der Lugt et al., 2019), as was also reported by Everard et al. (2013). Particularly, measurements of mucus thickness in PAS/AB stained colon tissues revealed that the mucus layer was significantly thicker in the mice supplemented with *A. muciniphila* compared to the control group and inflammatory markers were down regulated at the same time. The intimate contact of *A. muciniphila* with the host mucosa possibly induce responses by the host that are less susceptible to occur with further distanced commensal probiotics. Everard et al. (2013) found that *Lactobacillus plantarum* administration, for example did not change the mucus layer thickness, prevent metabolic endotoxemia, nor change the fat mass and adipose tissue metabolism. Therefore, these data suggest that *A. muciniphila* induces specific host responses compared with other putative beneficial microbes.

5. Mucin-degrading lifestyle and molecular repertoire of *Akkermansia muciniphila*

A. muciniphila is the only cultured representative of the *Akkermansiaceae* (*Verrucomicrobia* phylum) in the human gut. It is a strictly anaerobic, oval shaped Gram-negative species (**Figure 4**), accounting for 1–5% (~$1x10^9$) of the total bacterial count of the fecal microbial composition in healthy adults (Derrien et al., 2008; Derrien et al., 2004). However, further studies based on 16S rRNA gene sequencing reported that besides colonizing the colonic mucus layer, *A. muciniphila* is found in the distal ileum, ascending colon, rectum of humans with levels from 5% to 9% (Eckburg et al., 2005; Lavelle et al., 2015; Wang et al., 2005).

The strain – MucT (ATCC BAA-835) was the first purified from human GI tract using mucin, as a sole carbon and nitrogen source (Derrien et al., 2008). Nevertheless, *A. muciniphila* were shown to growth on glucose-rich media or on mucin-derived amino sugars N-acetylglucosamine (GlcNAc), and GalNAc co-supplemented with peptone, tryptone, threonine and yeast extract (Plovier et al., 2017). This alternative medium for culturing *A. muciniphila* was as efficient as the mucin medium. The ATCC BAA-835 *A. muciniphila* sequenced genome is composed of one circular chromosome of 2,664,102 bp with an average G+C content of 55.8%. The genome has a total of 88.8% predicted protein-coding sequences, from which 65% have an assigned putative function (van Passel et al., 2011).

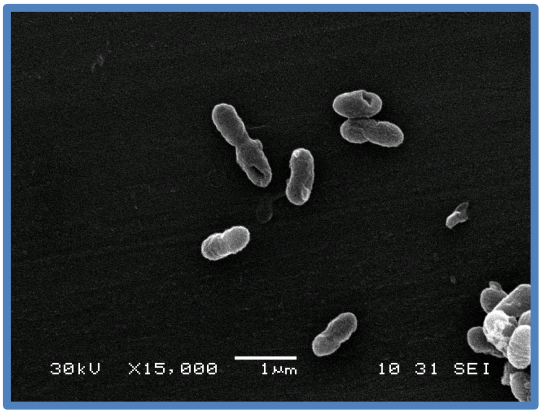

Figure 4. Scanning electron microscopy image of Akkermansia muciniphila.

Meta-genomic data suggest that, in addition to *A. muciniphila*, at least eight additional species from the same genus are colonizing the human intestine (Van den Abbeele et al., 2011). In a recent study, up to 39 *A. muciniphila* strains of differing subtypes were isolated from human faeces (Guo, Xianfeng et al., 2017; Guo et al., 2016). Three major *A. muciniphila* phylogroups across mammalian gut microbiotas were identified (defined as AmI, AmII and AmIII) by the analysis of newly *A. muciniphila* metagenome assembled genomes (MAGs), including human, mouse and pig gut microbiomes (Guo, Xianfeng et al., 2017). This allowed to stablish functional abilities linked to the *A. muciniphila* strains and the related metabolic benefits to the host. Based on KEGG databases, the predicted functional abilities of *A. muciniphila* were differently assigned among phylogroups. The AmI genomes are enriched in "phosphatidylinositol signalling system", "degradation of aromatic compounds", "two-component system", and "ABC transporters". On the

other hand, the AmII/AmIII genomes are enriched in “amino sugar and nucleotide sugar metabolism”, “glycosphingolipid biosynthesis - globo series”, “sulfur relay system”, “fructose and mannose metabolism”, etc. Interestingly, the AmI was the predominant phylogroup in all tested genomes, representing the 93% of the human population, 91% of mice and 9% of pigs (Guo, Xianfeng et al., 2017), highlighting a tight correlation of predicted functions specificity with the mammalian phenotypes or lifestyle. Noteworthy, Ranjan et al. (2018) using complementary shotgun metagenomic and meta-transcriptomic analyses from fecal samples, demonstrated that *Akkermansia* contributed to distinct biological functions, being more metabolically active than other phyla. Here, the phylum *Verrucomicrobia* was enriched for genes involved in alanine, aspartate, and glutamate metabolism [gdhA: glutamate dehydrogenase (NADP+), purB: adenylosuccinate lyase], ABC transporters [transport system ATP-binding protein] and amino sugar and nucleotide sugar metabolism [npdA: NAD-dependent deacetylase], consistent with the predicted data for aforementioned *Akkermansia* phylogroups. These findings indicate that albeit the low abundance of this phylum in the gut microbiota compared to other (3-5%), it is an active contributor to the gut physiology.

Despite of the functional diversity, the isolated *Akkermansia* strains (39 newly isolates and the ATCC BAA-835 strain) show a somewhat high proportion of genomic nucleotide identity. The complete genome provides insights into the mucin-degrading lifestyle of *A. muciniphila*. An average of 198 putative carbohydrate-active enzymes (CAZymes) genes were found to be strongly involved in mucus degradation, including glycosyl hydrolases, sialidases, proteases and sulfatases (Guo, Xianfeng et al., 2017; van Passel et al., 2011). Surprisingly, this number of CAZymes in *Akkermansia* genome exceeds that of most other microbes homologues found in the human gut microbiota, as has been reported for *Firmicutes* and *Actinobacteria* members (El Kaoutari et al., 2013). These observations underline the crucial role of *A. muciniphila* in glycan metabolism and its central position among the members of intestinal consortia in maintaining the mucosal integrity. Previous studies have demonstrated the biological implication of *A. muciniphila* in improving intestinal barrier function (Dao et al., 2016; Everard et al., 2013; Reunanen et al., 2015). As a mucin-degrading specialist bacterium, *A. muciniphila* contributes to maintaining the mucus layer integrity by the balance between mucus synthesis, secretion, and degradation. This bacterium

produces acetate, propionate, sulfate, amino-acids, cofactors, and vitamins from mucin-degradation (Derrien et al., 2004). Particularly through propionate and acetate production, *A. muciniphila* may trigger specific transcriptome responses in the intestinal epithelium improving inflammation and metabolic alterations (Derrien et al., 2011; Derrien et al., 2017; Lukovac et al., 2014). For instance, the oral administration of *A. muciniphila* reversed HFD-induced intestinal metabolic disorders, improved the mucus layer thickness, reduced LPS serum levels and associated endotoxemia (Everard et al., 2013; Shin et al., 2014). Thus, accumulating evidence has led to consider *A. muciniphila* as a next-generation probiotic bacterium (Cani and de Vos, 2017).

A whole genome assembly for an *A. muciniphila* strain isolated from stool samples of individuals under antibiotic therapy (Caputo et al., 2015), unveiled the molecular versatility of this species for the acquisition of adaptive de novo mutations, and its capacity to respond to abrupt and severe selective events. Importantly, *A. muciniphila* was found to be the dominant bacterium by up to 39% and 84% after the consumption of antibiotics (Caputo et al., 2015; Dubourg et al., 2013). The genomic capacity of microbial communities could influence the pervasive impact of antibiotics on the gut microbiota structure. Thus, the widespread colonization by *A. muciniphila* within the gut microbiota composition can be explained by its selective advantage to breakdown mucin as exclusive nutrient source, compared to the food-dependent bacterial species. Regarding to the functional adaptation and co-evolution of *Akkermansia* genome, further analysis of the COG distribution revealed that categories related to ‘‘Carbohydrate transport and metabolism’’ and ‘‘Cell envelope biogenesis, outer membrane’’ were enriched in *Akkermansia* specific genes. Additionally, several genes conferring antibiotic resistance were detected in *Akkermansia*’s genome (Caputo et al., 2015). Potential beta-lactamase genes (Amuc_0106 and Amuc_0183), as well as a gene coding for a 5-nitroimidazole antibiotic resistance protein (Amuc_1953) were encoded. The *A. muciniphila* genome contains a gene for a putative secreted antibiotic biosynthesis monooxygenase (Amuc_1805, PFAM PF03992) (van Passel et al., 2011).

Apart from the metabolic advantages, bacteria can adopt cellular morphology in response to different types of environmental stress, including cell wall damage, host immune effectors, and nutrient limitation. Supporting this observation, Dubourg et al. (2013) reported morphological changes in *A. muciniphila* cells isolated from a patient following an antibiotic treatment.

Through transmission electronic microscopy (TEM) similar oval-shaped cells were observed in *A. muciniphila* as previously described (Derrien et al., 2004), but an additional partial compartmentalization was lining the cell wall.

Besides of cell membrane alterations, the secretion of exopolysaccharides (EPS), CPS, and the expression of efflux pumps by bacteria are the main mechanisms involved in preventing surface binding-induced disruption by antimicrobials or indirect alterations to metabolism that perturb membrane physiology (Blanco et al., 2016; Cuthbertson et al., 2010; Joo et al., 2016). The whole transcriptome analysis of *A. muciniphila* exposed to oxygen revealed the up regulation of 18 genes encoding stress-related products, including ROS-mediated DNA damage, and genes involved in the capsular polysaccharide biosynthesis pathway (Amuc_2081, a family 2 glycosyl transferase) (Ouwerkerk et al., 2016). Meaningfully, a PEP-CTERM sequences and the corresponding exosortase *EpsH* (encoded by Amuc_1470), were found in 21 *A. muciniphila* proteins, forming a protein sorting system associated with exopolysaccharide expression (van Passel et al., 2011). The *EpsH* is a putative membrane protein based on its eight predicted transmembrane segments and is found within a large exopolysaccharide biosynthesis locus (Haft et al., 2006). Of note, *A. muciniphila* contains two genes involved in CPS secretion, an acyltransferase and a CPS biosynthesis protein (Amuc_2098 and Amuc_1413, respectively).

The analysis of *Akkermansia*'s genome also uncovered genes coding for the resistance/nodulation/cell division (RND) family transporters and efflux pumps (Amuc_1379, Amuc_0889), widely present in many Gram-negative bacteria, and representing another important antimicrobial resistance strategy (Delmar et al., 2014; Piddock, 2006). Bacteria use these molecular tools to remove perturbing molecules when they have already attached to or penetrated the cytoplasmic membrane. However, growing evidence indicates that multi-drug pumps, such as two-component ABC transporters, can also export polysaccharides, and its expression can be induced by endogenous metabolites (Cuthbertson et al., 2010; Liston et al., 2017; Silver et al., 2001; Stubbendieck and Straight, 2017). The ABC family utilizes ATP hydrolysis to drive the export of substrates, whereas the other families utilize the proton motive force as the energy source. Particularly, the RND superfamily is always forming part of a tripartite complex spanning across the two membranes in Gram-negative bacteria (Blanco et al., 2016). Remarkably, some RND

family efflux pumps and outer membrane lipoprotein NodT family linked to RND efflux systems (Amuc_2041 and Amuc_2043) were down regulated by *A. muciniphila* in a co-culture with *Anaerostipes caccae* (Chia et al., 2018). Altogether, these data indicate that this efflux pump plays multiple roles depending on the habitats of the bacteria, in particular if it is in symbiotic relationship with other bacterial members. The *A. muciniphila* cell wall structures, including the potential expression of EPS and CPS are interesting targets for proteomic analysis, to uncover the composition of extracellular proteins and oligosaccharides with potential biological role.

5.1 Factors influencing the *Akkermansia muciniphila* abundance in the gut

Due to the proximity to the host mucosa, *A. muciniphila* is considered a key symbiont member of the gut microbiota exerting beneficial functions. Accordingly, mono-colonized mice with *A. muciniphila* were shown to have improved intestinal tight junctions, a positive mucosal immune response and a lack of intestinal inflammation (Derrien et al., 2011; Ring et al., 2019), supporting its protective role against metabolic and intestinal diseases. For instance, a reduced abundance of *A. muciniphila* has been demonstrated in both faecal and mucosal samples of subjects with UC (Earley et al., 2019; Lavelle et al., 2015), inflammatory bowel disease (IBD) (Papa et al., 2012), atherosclerosis (Li et al., 2016), appendicitis (Swidsinski et al., 2011), obesity and T2D (Ellekilde et al., 2014; Everard et al., 2013; Gurung et al., 2020; Le Chatelier et al., 2013). The above stated examples bring us to consider the possible factors either affecting or improving the *A. muciniphila* abundance for managing its maintenance in the colon.

5.1.1 Ecological niche

The varying levels of colonic abundance of this bacterium in different diseases does not provide a clear picture of the factors affecting its colonization. However, owing to its ecological niche and its mucin degrading abilities, factors affecting mucin glycosylation and sulfation patterns, as well as factors influencing fluctuations in the mucosal pH, which is usually less acidic than the luminal pH in all the regions of the large intestine (ranging between 6.1 and 7.5), could have major impact on its presence (McDougall et al., 1993). Interestingly, a recent study using the Simulator of Human Intestinal Microbial Ecosystem (SHIME) model demonstrated that

A. muciniphila growth, in addition to being mucin-dependent is affected by the pH level (Van Herreweghen et al., 2017). Indeed, an increase of *A. muciniphila* was observed upon the addition of mucin, while a decrease was observed when the pH in the distal colon was lowered compared to a higher pH. Moreover, Earley et al. (2019) reported that a significant reduction in the proportion of sulfated mucin was observed in patients with acute UC compared to healthy controls. Importantly, in that study a positive correlation was found between *A. muciniphila* abundance and a higher proportion of sulfated mucin. These observations are consistent with the presence of sulfatase enzymes in *Akkermansia*'s genome and its ability to utilize sulfated mucin as substrate (Ottman et al., 2017). In this sense, a reduced sulfation, in addition to expose the mucin to the degradation by opportunistic pathogens and induce mucosal inflammation (Dharmani et al., 2009; Larsson et al., 2011; Theodoratou et al., 2014), provides a less hospitable niche for this symbiont. Accordingly, mucosa-associated pathobionts were shown to be co-exclusive microbes of *A. muciniphila.* Particularly, *Ruminococcus* species, which also have the ability to break down mucin, were found to dominate in IBD, UC and CD positive subjects, while *A. muciniphila* was the most abundant in healthy controls (Png et al., 2010).

5.1.2 Therapeutic drugs and age

Changes in the proportion of *A. muciniphila* have also been reported after the administration of therapeutic drugs. For instance, the antidiabetic metformin increases the fecal proportion of this bacterium, suggesting its crucial role in attenuating the metabolic outcomes in T2D (Shin et al., 2014; Wu et al., 2017), albeit the mechanism explaining the metformin effects on *A. muciniphila* remains to be elucidated. Interestingly, the pre-treatment with antibiotics (carbenicillin, metronidazole, neomycin and vancomycin) on HFD fed mice before metformin treatment, abolished the metformin activity (Shin et al., 2014), suggesting that the gut microbiota, in this case *A. muciniphila*, are mediating the antidiabetic benefits of metformin. Likewise, in a comprehensive study on the impact of the antibiotic consumption in early life on the gut microbiome structure, *A. muciniphila* was found in lower proportion in children who received antibiotic therapy, and that was highly related to a major risk to develop metabolic diseases (Karlsson et al., 2012; Korpela et al., 2016).

The fact that the colonization of the human intestinal tract by *Akkermansia* genus starts in early life and develop to levels of that observed in adults (10^8 cells/g) (Collado et al., 2007), highlights the importance of this bacterium as keystone contributing to the functional evolution of the gut microbiota. Nonetheless, *Akkermansia'*s proportion was shown to decrease in the elderly, likely due to the age-related decline of the colonic mucus thickness (Bektas et al., 2018). Conversely, a recent study characterizing the gut microbial signature in centenarian individuals, pointed out to an increase of genera of *Akkermansia, Bifidobacterium* and *Christensenella* in centenarians (99–104 years old) and semi-supercentenarians (105–109 years old), alongside a concomitant maintenance of good immunological and metabolic health (Biagi et al., 2016). In a similar way, the administration of *A. muciniphila* cells restored the protective mucus layer and attenuated inflammation in aged mice (van der Lugt et al., 2019). Altogether, these findings explain the role of *A. muciniphila* in maintaining a positive feedback loop from mucin-degrading activity, since it stimulates mucin secretion and modulates O-glycosylation and sulfation mucin profile (Earley et al., 2019; Moran et al., 2011), leading to a healthy protective mucus layer. In this respect, several studies showed that *A. muciniphila* was positively associated with the mucus thickness and intestinal barrier integrity in humans and animals (Collado et al., 2007; Everard et al., 2013; Shin et al., 2014).

5.1.3 Antibiotics

The antibiotics administered to act against pathogens, have indiscriminate effects on other symbiotic gut bacteria (Hanninen et al., 2018; Korpela et al., 2016; Modi et al., 2014). Indeed, under selective pressure by antibiotics, sensitive strains are inhibited, giving to antibiotic-resistant strains an advantage to growth. In this regard, *Akkermansia* is sensitive to some antibiotics, including penicillin, macrolides and tetracycline but is resistant to fluoroquinoles, aminoglycosides, glycopeptides, such as vancomycin and ofloxacin (Caputo et al., 2015; Dubourg et al., 2013; Guo, Xianfeng et al., 2017; Hansen et al., 2012). Surprisingly, *Akkermansia* colonized the gut microbiota of patients under a broad-spectrum antibiotic regimen by up to 84% (Dubourg et al., 2013). The genome of *Akkermansia* explains the molecular versatility of this bacterium to physiologically adapt to antibiotics, namely by modifying its cell wall properties, thereby providing antibiotic resistance. The *Akkermansia* blooms may also be explained by a reduced

competition from other microorganisms susceptible to antibiotics, and the liberation of ecological niches occupied by other bacteria.

5.1.4 Diet and xenobiotics compounds

The diet and functional ingredients are selectively influencing the gut microbiota structure. According to the enterotype concept, the functional stratification of the gut microbiome is explained by the microbe's capacity to use certain types of fermentable nutrient (Arumugam et al., 2011; Costea et al., 2018). Obesogenic diets (HFD or HFHS) have been repeatedly reported to affect the *A. muciniphila* faecal abundance and is inversely correlated with metabolic diseases (Anhê et al., 2015; Everard et al., 2013; Li et al., 2016; Roopchand et al., 2015; Schneeberger et al., 2015; Zhou et al., 2016). Nevertheless, some studies suggest that the effect of a high-fat or a high-sucrose diet on *A. muciniphila* in mouse models may be an "artefact" (Collins et al., 2016; Shan et al., 2019). Particularly, Shan et al. (2019), indicated that the high-sucrose diet contributes more than the high-fat diet to the increased abundance of *Akkermansia,* given the preference of this bacteria for sugars as nutrients. Albeit this effect warrants further investigation, that fact may also be attributable to the limited availability of carbohydrates under a high-fat diet, along to the *Akkermansia'*s capacity to switch to host glycans as selective substrate source, rather than a pathogenic mechanism of this bacterium.

Prebiotics, including fibres and polyphenols (Gibson et al., 2017), have been repeatedly reported to promote the growth of *A. muciniphila*. Several studies reported that fructo-oligosaccharides (FOS), a common prebiotic, prompted *A. muciniphila* in DIO *ob/ob* mice and Sprague-Dawley rats models (Everard et al., 2011; Reid et al., 2016). For instance, a crossover trial showed that polydextrose fibre intake for 21 days in healthy individuals increased *A. muciniphila* proportion, compared to soluble corn fibres or placebo (Hooda et al., 2012). However, another study showed that *A. muciniphila* abundance was not affected by the 8-weeks consumption of high-amylase resistant starch and wheat bran food in both healthy individuals and in patients with UC in remission (James et al., 2015). In that study, differences were found in the *A. muciniphila* relative proportion between healthy and UC subjects, being lower in the lather group (0.3-0.5% in UC vs 4.8-10% in controls). Similarly, in a HFD fed C57BL6 mouse model, a

saponin-rich aguamiel concentrate was shown to promote *A. muciniphila* faecal abundance by 5 to 9-fold and 15.3-fold in mice fed a low-dose and high-dose of saponin-rich extract respectively, as compared to controls (Leal-Diaz et al., 2016). The authors associated the *Akkermansia* bloom to an improved glucose tolerance, hepatic lipid metabolism and reduced steatosis in obese mice. Accumulating evidence also demonstrates the prebiotic-like effects of dietary polyphenols on *A. muciniphila* in clinical and animal models. Using a SHIME model, Kemperman et al. (2013) showed that a black tea or a red wine grape polyphenolic extract significantly prompted the growth of *A. muciniphila*. In humans, a pomegranate extract, rich in ellagitannins, increased *A. muciniphila* by 47-fold in subjects producers of the microbial phenolic metabolite urolithin A, compared to non-producers (Henning et al., 2017; Li et al., 2015). In C57BL6 mice, an HFD enriched with grape-polyphenols increased the growth of *A. muciniphila* (10^9/g feces) after 13-week of dietary intervention (Roopchand et al., 2015). Furthermore, a cranberry polyphenolic extract, black raspberries powder, grape polyphenols, dark sweet cherry powder, and lingonberries, also led to a dramatic faecal increase of *A. muciniphila,* which was correlated with positive metabolic outcomes in the host (Anhê et al., 2015; Collins et al., 2016; Garcia-Mazcorro et al., 2018; Heyman-Lindén et al., 2016; Pan et al., 2017; Tu et al., 2018). Likewise, polyphenolic compounds such as chlorogenic acid, caffeic acid, quercetin, resveratrol, trans-resveratrol and malvidin-3-galactoside were shown to promote *Akkermansia* in C57BL6 with dextran sulfate sodium (DSS) induced colitis, and likewise in mice with liver cancer (Cheng et al., 2018; Etxeberria et al., 2015; Zhang et al., 2017; Zhang et al., 2016). Considering that dietary polyphenols are diverse, and the impact on the host health might be variable, more studies are warranted to screen and identify the type of polyphenolic compound contributing the most in prompting the *A. muciniphila* growth and modulating the functional profile of the gut microbiota.

Given that there are many studies showing the prebiotic-like effect of a variety of phenolic compounds on the symbiont *A. muciniphila*, two relevant queries need to be answered; first, whether the *Akkermansia* bloom after polyphenols intake stems from its ability to degrade/resist those compounds within the gut microbial community, and second, whether the polyphenols boosting effects on *Akkermansia,* is an aftermath of the polyphenol-induced anti-inflammation and recovering of the intestinal mucosa-associated niche.

6. Prebiotics

"Prebiotics are substrates that are selectively utilized by host microorganisms conferring a health benefit". These *"health effects of prebiotics include benefits to the gastrointestinal tract (i.e. inhibition of pathogens, immune stimulation), cardiometabolism (i.e. reduction in blood lipid levels, effects upon insulin resistance), mental health (i.e. metabolites that influence brain function, energy and cognition) and bone (i.e. mineral bioavailability), among others"* (Gibson et al., 2017). The above statement was the last revisited concept for prebiotics, which was commonly confined to non-digestible carbohydrates (i.e inulin, fructo-oligasaccharides FOS, galacto-oligosaccharides GOS). Resistant starches and other compounds, which are not absorbed in the small intestine (Sheflin et al., 2017), and reach the colon, might be subsequently degraded by the indigenous gut microbiota, thus falling into the concept of prebiotics. According to this definition, polyphenolic compounds can be considered as prebiotics, based on accumulating evidence in promoting gut beneficial microbes, such as *A. muciniphila*, in addition to *Lactobacillus* and *Bifidobacterium* genera. Such stimulation has been linked with polyphenols therapeutic role, attenuating metabolic diseases, cancer and intestinal inflammation (Anhê et al., 2014; Henning et al., 2017; Heyman-Lindén et al., 2016; Lacombe, A. et al., 2013a; Roopchand et al., 2015). The dietary compounds fulfilling the current prebiotic concept are described in the **Figure 5.**

6.1 Fibres

Dietary fibers are subdivided into non-starch polysaccharides, oligosaccharides and resistant starch (See **Figure 5**). Insoluble fibers include cellulose, hemi-celluloses and lignin, which are major components of plant cell walls. Fermentable fibres that possess high solubility and viscosity, include β-glucan and pectins (Holscher, 2017). The biological benefits of these prebiotics involve the production of microbial metabolites SCFAs in the cecum and colon, as well as the reduction of bacterial constituents (LPS) (Canfora et al., 2015; Dewulf et al., 2013). A recent study summarized how the production of specific SCFAs can vary with a range of insoluble and soluble fine-powdered fibre sources. For instance, resistant starch may result in higher amount of butyrate, while cellulose and pectin may result in high amount of acetate (Dreher, 2017). SCFAs are tightly involved in energy homeostasis, insulin signalling, fat accumulation and immune signalling, as

reviewed elsewhere (Delzenne et al., 2015; Holscher, 2017). Among the SCFAs, butyrate is the primary energy source for colonocytes and protects against colorectal cancer and inflammation. It has been demonstrated that butyrate suppresses proinflammatory effectors in macrophages and promote the differentiation of dendritic cells (reviewed by Koh et al., 2016). Slowed glucose absorption and binding of bile acids are also possible mechanisms by which fibres may impact the gastrointestinal microbiota (Holscher, 2017).

When fermentable fibers are limited in the diet, microbes can switch to other sources, such as a dietary fat, endogenous proteins (mucus-rich glycans), likely energetically less favourable for bacteria to growth, as well as, metabolically detrimental for the host (Koh et al., 2016; Sonnenburg and Sonnenburg, 2014). A very low fiber intake in the western-diet increases the growth of opportunistic bacteria and affect the mucus barrier function, leaving the epithelium susceptible to infections. A recent study evaluated the effect of fibre supplementation in a mouse model of diet-induced and genetic obesity (Schroeder et al., 2018). The authors showed that the penetrability and growth rate of the inner colonic mucus were significantly affected by a HFD, and suggested that the defects might be a consequence of dietary composition rather than of obesity and impaired glucose metabolism (Schroeder et al., 2018). In addition, there was demonstrated that the supplements with inulin prevented the penetrability of the inner colonic mucus layer, highlighting the protective role of fibre-associated gut community (Schroeder et al., 2018). Co-supplementation of HFD with fibre might restore the levels of beneficial microbes, whose fermenting activity lead to a higher production of SCFAs, known to contribute to the intestinal homoeostasis (Donohoe et al., 2011; Yan and Ajuwon, 2017). Interestingly, dietary inulin was shown to restore microbiota richness, prevent colon epithelial atrophy, dysglycemia and adiposity, compared to insoluble cellulose fibre HFD fed mice (Zou et al., 2018). 16S gene sequencing indicated that inulin increased *Akkermansia* and *Bifidobacterium*, while decreased *Proteobacteria* in obese mice. The role of the gut microbiota in potentiating the benefits of fibres in the host was further substantiated by the propensity of inulin to improve colon morphology, glycemic response and decrease adipose depots in germ-free Swiss-Webste mice (Zou et al., 2018). High fibre intake has also been associated with increased fecal *Bacteroides, Prevotella, Lactobacillales*, *Faecalibacterium* and

Bifidobacteria groups which help to maintain a healthy microbiota (Heinritz et al., 2016; Shinohara et al., 2010; Wang et al., 2016).

The consumption of non-starch oligosaccharides, such as GOS and FOS have been shown to mainly induce *Bifidobacterium* species (Russell et al., 2011; Vulevic et al., 2013; Walton et al., 2012) and promote butyrate-producing bacteria *Roseburia* (Falony et al., 2009)*;* similar results have been induced by xylo-oligosaccharides (Lecerf et al., 2012). Moreover, inulin, in addition to modulate *Bifidobacterium* and *Lactobacillus*, were shown to decrease *Bacteroides*/*Prevotella* (Costabile et al., 2008). In a separated study, inulin type-fructans were shown to stimulate the butyrate-producing genus of *Anaerostipes* (Vandeputte et al., 2017).

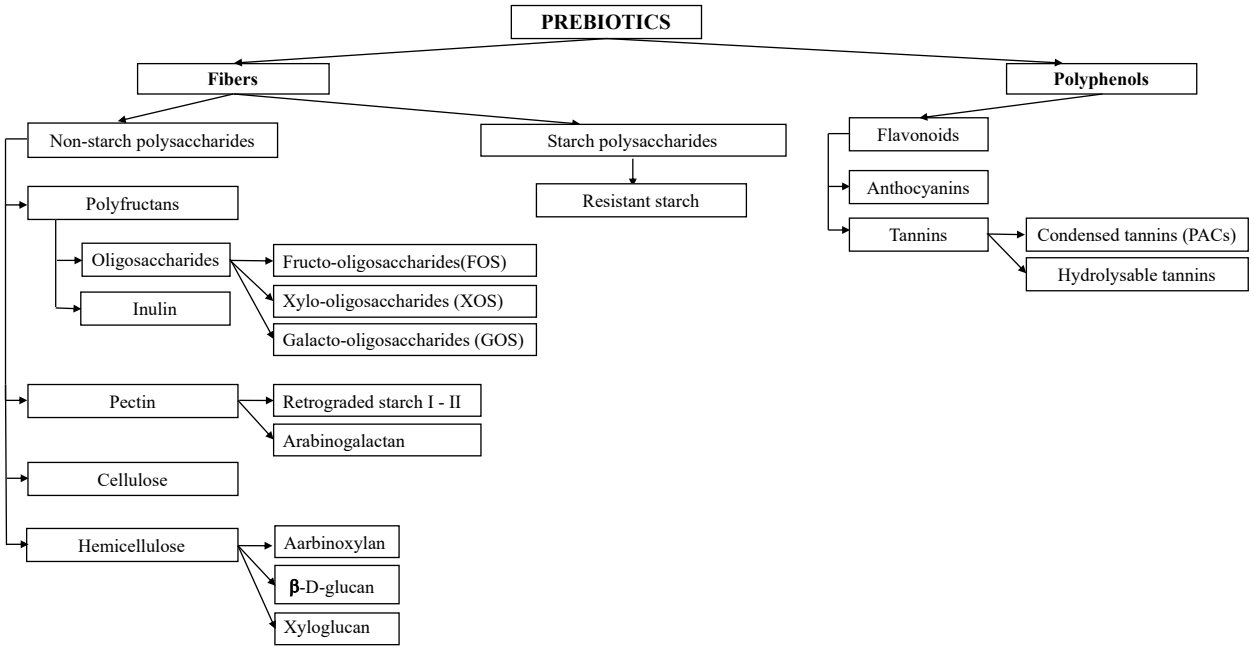

Figure 5. Dietary polysaccharides and phenolics with potential prebiotic.

Dietary polysaccharides, defined as fibres, can be divided into starches and non-starch. Polyphenols, mainly flavonoids, have been shown to exert prebiotic effects.

6.2 Phenolic compounds

Phenolics are composed by an aromatic ring with at least one hydroxyl group. Their structure can vary from one molecule to complex polymers of high molecular weight. Polyphenols are

classified in two main groups: flavonoids and non-flavonoids (Singla et al., 2019). The diversity of polyphenols and the categorization are illustrated in the **Figure 6.** Most of polyphenolic classes, mainly flavonoids, pass through the small intestine without being absorbed (Clifford, 2004; Masumoto et al., 2016) and thus reach the colon, where two-way mutual interaction arises between the polyphenols and the gut microbiota. In the colon, those compounds can directly change the composition of the gut microbiota through antimicrobial action, inhibiting pathogenic bacteria and favouring symbiotic members of the gut microbiota or can be degraded to specific metabolites by certain bacteria.

6.2.1 Non-flavonoids

Nonflavonoid compounds include phenolic acids, stilbenes, lignans and hydrolyzable tannins. Phenolic acids are subdivided in hydroxybenzoic and hydroxycinnamic acids. Representative mocules belong to the hydroxybenzoic acids are gallic, p-hydroxybenzoic, vanillic and syringic acids, while caffeic, ferulic, sinapic, and p-coumaric acids belong to hydroxycinnamic acids. Several studies have noted the biological activity of naturally occurring phenolics, including their anti-hyperlipidemic, anti-inflammatory and antimicrobial properties with a protective potential in chronic disease and obesity (Alam et al., 2016; Coman and Vodnar, 2020; Guo, X. et al., 2017; Song et al., 2016).

6.2.2 Flavonoids

Flavonoids are subclassified as anthocyanins, flavanol, flavanones, flavanols, flavonones, and isoflavones (Durazzo et al., 2019; Singla et al., 2019). Epicatechin, and catechins belong to subgroup of monomeric flavanols. Polymeric forms of catechin and epicatechin are referred as condensed tannins or proanthocyanindins (PACs) (Serrano et al., 2009). Several outstanding studies on the biochemical properties of flavonoids have highlighted their antioxidant, antimicrobial, anti-inflammatory, hepatoprotective, and anti-hyperlipidemic effects (Gonzalez-Sarrias et al., 2018; Kim, Y. et al., 2013; Lacombe, A. et al., 2013b; Lacombe et al., 2010; Ogura et al., 2016). All flavonoids share the chemical structure of diphenyl propane (C6-C3-C6).

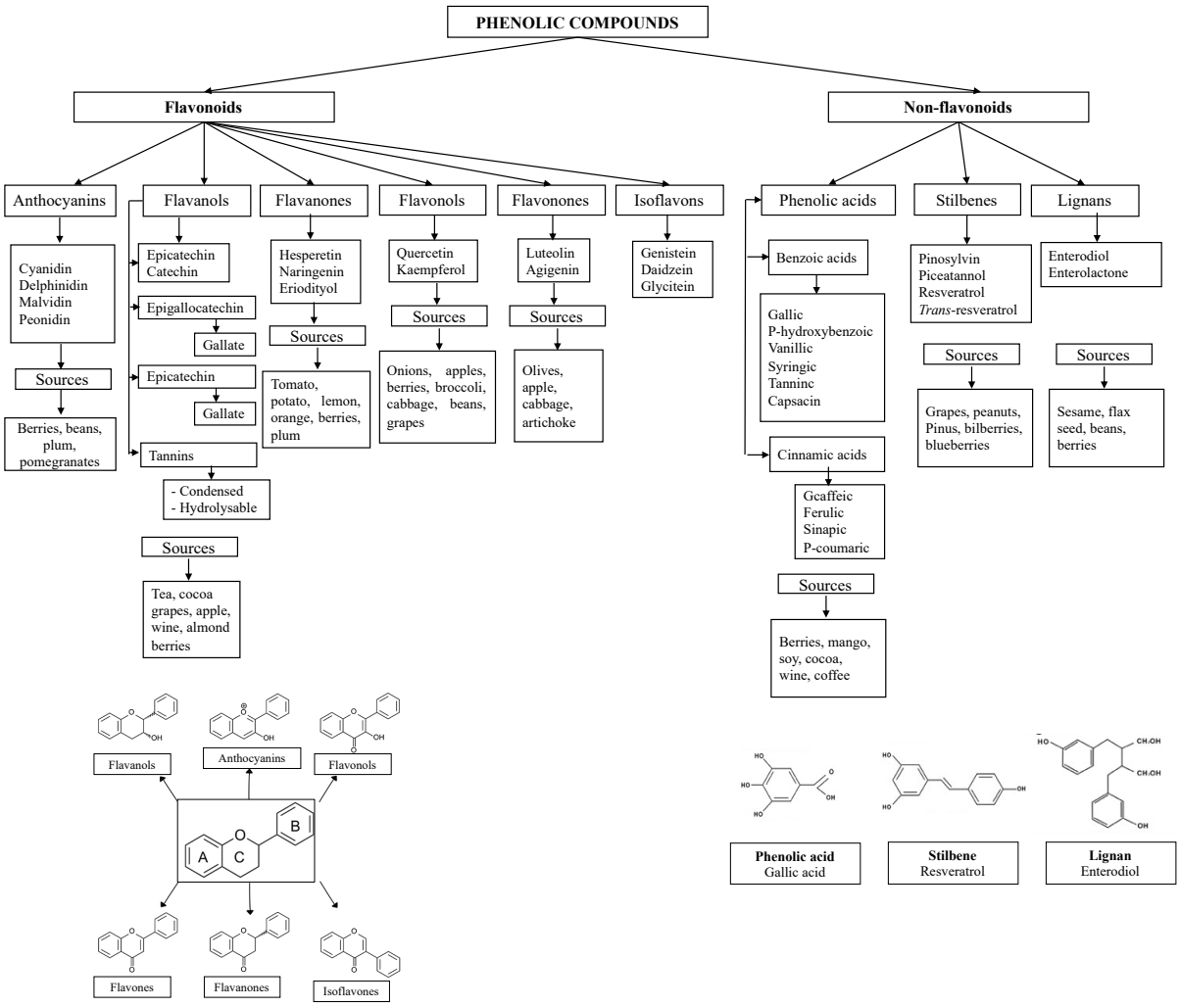

Figure 6. Classification of phenolic compounds.

7. Bioactive compounds in berries

Epidemiological studies have demonstrated that the consumption of fruits and vegetables reduce the risk of cardiovascular and metabolic diseases (Dauchet et al., 2009; Gregori et al., 2019; Yoshizaki et al., 2020). Berries are of a particular interest because of their high content in bioactive compounds such as fibres (plant cell wall polysaccharides) and polyphenols (Blaker and Olmstead, 2015; Dudonné et al., 2015; Hotchkiss et al., 2015; Vicente et al., 2007; White et al., 2010). They also contain sugar (mainly glucose and fructose), vitamins, organic acids, such as citric acid, malic acid, tartaric, oxalic and fumaric acid; and minerals in trace amounts (Nile and Park, 2014). Apart

from the botanical signification, berries, in layman terms, refer to the genera of *Rubus* (blackberries, raspberries), *Fragaria* (strawberries), *Ribes* (blackcurrant), and *Vaccinium* (blueberries, cranberries and lingonberries) (Skrovankova et al., 2015). The botanical term also refers to a number of boreal and Arctic species (Dudonné et al., 2015). This section will be mainly focused on the bioactive compounds found in the *Vaccinium* genus.

7.1 Plant cell wall polysaccharides

The North American Cranberry (*Vaccinium macrocarpon* Aiton) harbours ~65.5% of insoluble dietary fibre within the cell wall structure, including cellulose, hemicellulose and pectin (Hotchkiss et al., 2015; White et al., 2010). A GC-MS profile of cranberry pectic fraction indicates that it is composed of xyloglucan and arabinan chains, with possible xyloglucan-pectin complex covalently bound (Sun et al., 2015). Blueberry species include the Lowbush or Wild (*Vaccinium angustifolium* Aiton) and the Highbush (*Vaccinium corymbosum* L.). Blueberries biochemical characterization of cell wall polymers revealed a high content of pectin rich in xyloglucan and xylan, as well as a hemicellulose fraction rich in arabinoxylan, xylan and xyloglucan polymers (Vicente et al., 2007). Plant cell walls are known to be a potential source of active polysaccharides that possess prebiotic and antimicrobial activity (Adam et al., 2014; Coleman et al., 2019; Hotchkiss et al., 2015; Larsen et al., 2019; Licht et al., 2010). Recent work has shown that cranberry xyloglucan, characterized as arabino-xyloglucan (SSGG structure), prevented adhesion of uropathogenic *E. coli* strains to human uroepithelial cells, and to colonic epithelial cells *in vitro* (Hotchkiss et al., 2015). Furthermore, cellulosic and hemicellulosic fractions were also shown to stimulate the growth of bacterial genera such as *Enterococcus, Ruminococcus, Bacteroides* and *Roseburia,* since these bacteria have the capacity to degrade cellulose (Chassard et al., 2010; Robert and Bernalier-Donadille, 2003). In another study, rat supplemented either with 3.3% apple pectin or 7% pectin for 4-weeks, had a higher proportion of Gram-negative genera of *Anaeroplasma, Anaerostipes*, *Roseburia* and *Clostridium* cluster XIVa, while decreased *Alistipes, Parabacteroides* and *Bacteroides* in their feces. However, no changes were observed in *Lactobacillus* and *Bifidobacterium* (Licht et al., 2010).

Polyphenols can be entrapped in the cellulosic/pectin matrices (Jakobek and Matić, 2018) and the colonic fermentation of both may alter the bioactivity and taxonomic composition of the resident gut microbiota. In terms of microbial metabolism, it is noteworthy to mention that the colonic bacteria cannot access to phenolics without degrading the cell wall polysaccharides and releasing the chemical bonds to which they are attached. This is possible by the action of specialized bacteria that possess the genetic capability of hydrolyzing these compounds. For instance, since the genera of *Bacteroides*, *Eubacterium, Roseburia* and *Butyrivibrio* (*Lachnospiraceae*) have the ability to degrade xylans, while the genera of *Ruminococcus* and *Faecalibacterium* are capable of degrading hemicelluloses or pectin; these species were modulated by wheat bran (arabinoxylan-rich phenolic acid-rich polysaccharides) in *in vitro* fermenter system, resulting in the release of ferulic acid (Duncan et al., 2016). In bran and aleurone, ferulic acid is mainly convalently bound to arabinoxylans and other cell wall polysaccharides that are able to resist digestion in the upper gastrointestinal tract (Zhao et al., 2003). Further, PACs are also reported to constitute the dietary fibre fraction of foods. Extractible PACs are exclusively obtained after extracting the food with acetone, the most common solvent used for their analysis; but a considerable proportion of PACs, notably the non-extractible, remains in the residue from such extractions. For instance, Mateos-Martin et al. (2012) studied the fate and metabolism of grape dietary fibre, rich in non-extractible PACs (14.8%), in female Sprague–Dawley rats for 24 h. The grape residues obtained after the extraction with 70 % acetone was demonstrated to be a source of non-extractible PAC polymers, which are progressively depolymerised in the intestine into epicatechin monomers and dimers, and later metabolized by the gut microbiota into smaller units. Microbially derived PACs metabolites such as valerolactones, phenylvaleric acids, phenylpropionic acids, phenylacetic acids, benzoic acid, cinnamic acids and lignans were detected in urine, but they were not present in the control group. Likewise, the authors identified 4-hydroxyphenylpropionic acid and 3,4-dihydroxyphenylpropionic acid in faeces, suggesting that putatively active species remain in contact with the colonic epithelium for at least 24 h after ingestion. This study indicates that a fibre fraction, rich in non-extractible PACs, but devoid of epicatechin and extractible oligomers, generates bioavailable derivatives of epicatechin by the fermenting action of the gut microbiota.

Biological activities have been demonstrated for both phenolic compounds and the products of carbohydrate fermentation, thus, an overall synergistic effect on the host might occur between them. Interestingly, dietary fibres and polyphenols have been shown to act synergistically in processes like antiradical activity and lipid oxidation (Celik et al., 2015), as well as in lowering hepatic cholesterol levels in apolipoprotein E-deficient mice with atherosclerosis (Auclair et al., 2008).

7.2 Polyphenols

Because on their polyphenolic content, cranberry and blueberry have been widely studied for their preventive effect in cardiovascular diseases, obesity, T2D and intestinal dysbiosis (Anhê et al., 2014; Chenget al., 2018; Jiao et al., 2019; Lee et al., 2018; Rodríguez-Daza et al., 2020). Cranberry phytochemical includes three classes of flavonoids: flavonols, anthocyanidins and PACs (Dudonné et al., 2015). The anthocyanidins total content is between 25-30 mg/100 g of fruits (Dudonné et al., 2015; Neto, 2007). Among the anthocyanidins, cyanidin and peonidin glycosides are the predominant. Cranberry is also rich in quercetin, with a total flavonol content of 20-30 mg/100 g of fruit (Dudonné et al., 2015; Neto, 2007) (U.S. Department of Agriculture USDA, http://www.ars.usda.gov/nutrientdata/flav). Particularly, cranberry is well known for its antimicrobial and antiadhesive action on pathogenic bacteria associated with urinary tract infections *(i.e Escherichia coli)*, which positive effects have been attributed to the PACs content (Feliciano et al., 2014; Howell et al., 2005).

Blueberries are among the richest fruits in ascorbic acid, chlorogenic acid and anthocyanidins, and numerous studies have shown their anti-inflammatory and antioxidant role (Borges et al., 2010; Esposito et al., 2014; Huang et al., 2016; Li et al., 2017; Skrovankova et al., 2015). Among the anthocyanins, the fruit contains malvidin, delphinidin and petunidin glycosides (Dudonné et al., 2015) (USDA, http://www.ars.usda.gov/nutrientdata/flav). The total count of anthocyanins ranges from 120 to 208 mg/100 g in highbush variety, and ~70 mg/100 g in lowbush (Dudonné et al., 2015; Neto, 2007). Blueberry also contains PACs; however, cranberry appears to have a higher content. The USDA database for PACs concentration in selected food (March 2018 V. 2.1) reported that wild blueberry contains on average 255.09 mg/100 g fruits of polymeric PACs,

typically ranging from 4-10 degree of polymerization (DP), whereas cranberry is reported to be quite richer with a mean of 1004.30 mg/100g. (Agriculture., 2018) (https://www.ars.usda.gov/nutrientdata). PACs or condensed tannins vary in structure and composition characterized by oligomers or polymers of either catechin, epicatechin or galloylated catechins. For instance, it has been indicated that cranberry contains both oligomer and polymers of A-type (doubly linked by a C4–C8/C6 bond and an additional C2–O–C7 or C2–O–C5 ether bond), and B-types PACs (C4–C8 or C4–C6 bond); whereas in blueberry, only the B-type linkage has been observed (Prior et al., 2001) (**Figure 7**). MALDI-TOF MS analysis of cranberry PACs showed up to 12 DP of A-type linkage of epicatechin units and also with some epigallocatechin units (Neto et al., 2005).

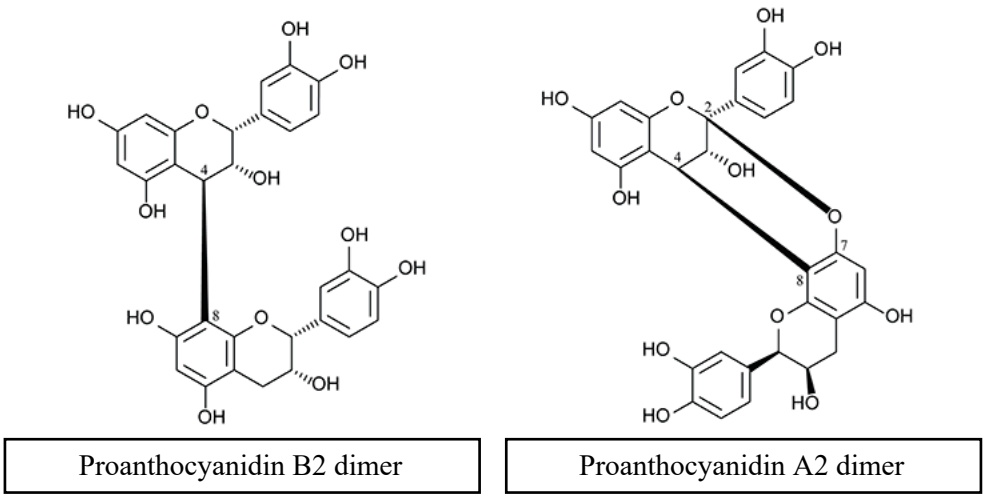

Figure 7. Chemical structures of proanthocyanidins dimers.

Many studies have reported the limited bioavailability of flavonoids, indicating that most of their bioactivity might be occurring in the large intestine (Clifford, 2004; Masumoto et al., 2016; Stoupi et al., 2010; Yi et al., 2006). Once the digesta passes through the small intestine, the transit time in the colon is thought to be more than 24 h (Cummings et al., 1978), being long enough to actively interact with the resident gut microbiota, induce metabolic and compositional changes, and enhance or reduce the generation of microbial metabolites (i.e SCFAs and phenolic metabolites). The antimicrobial properties of polyphenols have been broadly associated with the microbial modulatory effects restoring or preventing the microbiota alteration observed in several

diseases (Adewunmi et al., 2020; Côté et al., 2011; Lacombe and Wu, 2017; Marin et al., 2015; Puupponen-Pimiä et al., 2005). In the following section, the antimicrobial mechanisms of polyphenols, their implications in the gut microbial taxonomic and metabolic changes will be reviewed.

8. Antimicrobial properties of polyphenols

Important prebiotic effects and selective antimicrobial activities against gut pathogenic bacteria have been attributed to the polyphenolic fraction contained in berry fruits; particularly PACs have been widely studied (Denev et al., 2019; Lacombe and Wu, 2017; Lacombe et al., 2012). Cranberry PACs have demonstrated to affect the adhesion to uroepithelial cells (Feliciano et al., 2014; Howell et al., 2005). Specific antimicrobial activity of cranberry has been documented toward numerous groups of illness-causing pathogenic bacteria, including *Helicobacter pylori*, *Salmonella*, *S. aureus, E. coli*, and *Campylobacter* (Côté et al., 2011; Wu et al., 2008). In most of the cases, polyphenols toxicity has been linked to selective inhibition of cell wall synthesis (Firrman et al., 2016; Lacombe et al., 2013b; Lacombe et al., 2010). For instance, polyphenols can bind to bacterial cell membranes in a dose-dependent manner, thus disturbing membrane function and therefore inhibiting cell growth (Lacombe et al., 2013; Lacombe et al., 2013b). Cranberry and blueberry fractional components were shown to cause permeation of the extracellular membrane of *E. coli O157:H7* at doses of 5% v/v (Lacombe et al., 2013b; Lacombe et al., 2010). Lacombe et al. (2012) detected by scanning electron microscopy (SEM) images that blueberry juice treated cells presented blebs, while blueberry PAC treated cells had pores on the bacteria cell membrane. These results are consistent with other studies which show that berries phenolics affect membrane fluidity, change fatty acid profile, and disrupt cellular metabolism (Joshi et al., 2014; Shen et al., 2014).

Microbes stressed by exposure to polyphenols could up-regulate proteins related to defensive mechanisms, which protect cells while simultaneously down-regulated various metabolic and biosynthetic proteins involved, for example, in amino acid and protein synthesis as well as phospholipid, carbon and energy metabolism (Firrman et al., 2016). Gene expression studies demonstrated that total cranberry concentrate down regulated genes encoding outer membrane

proteins in *E. coli* O157:H7 (Wu et al., 2009). Furthermore, cranberry PACs active fractions were shown to interfere with quorum sensing inhibitor (QSI) and anti-virulence genes of *Pseudomonas aeruginosa*, and they could exert synergistic or adjuvant action with conventional antibiotics (Ulrey et al., 2014; Vadekeetil et al., 2016). Polyphenols therefore may mimic some antibiotic compounds that inhibit bacteria. Antibiotics also target the bacterial cell by destabilizing the outer membrane, increasing its permeability and affecting protein synthesis (O'Rourke et al., 2020; Walsh, 2020). For instance, vancomycin is a glycopeptide antibiotic, whose action mechanism works by inhibiting proper cell wall synthesis, specifically of gram-positive bacteria (Ge et al., 1999), and it has been shown to stimulate symbiotic bacteria in the gut. One such example is the dominance of *A. muciniphila* in the human gut during vancomycin treatment, which increase showed to be involved in the improvement of metabolic disturbance (Hansen et al., 2012; Ray and Aich, 2019; Rodrigues et al., 2017). In those studies, the phyla *Proteobacteria* and *Verrucomicrobia* were present with a high incidence in vancomycin-treated groups, but there was a loss of *Firmicutes* (Gram positive) and *Bacteroidetes* (Gram negative). Indeed, vancomycin treatments could influence the development of symptoms in diabetic-induced mice (Hansen et al., 2012; Rodrigues et al., 2017).

Metal ion-chelating properties of polyphenols is also an efficient strategy to limit pathogen colonization. Sequestering metal ions by polyphenols, lead to iron-deprivation, can decrease the activity of metalloenzymes, and inhibit oxidative phosphorylation by inhibiting heme production necessary for cytochromes (Smith et al., 2005). It has long been known that iron availability is crucial for bacterial growth, and iron deprivation can affect the pathogenic strains growth and metabolism. For instance, gallotannins from mango were shown to inhibit Gram-positive food pathogens and Gram-negative *Escherichia coli,* whereas little or no effects were observed on lactic acid bacteria, as this last group was not heme dependent. This mechanism was supported by the attenuation of the inhibitory effects of polyphenols upon the addition of iron in the growing media (Engels et al., 2009).

8.1 Effects of polyphenols on symbiotic and pathogenic bacteria: the prebiotic-like effect

Recently published reviews have extensively discussed the modulation of the intestinal microbiota by polyphenols; they have been focused on the microbial metabolism of polyphenols, the antimicrobial properties against pathogens and the influence on beneficial microorganism (Cardona et al., 2013; Duynhoven et al., 2010; Hervert-Hernández and Goñi, 2011; Ma and Chen, 2020).

Polyphenol-rich extracts have demonstrated to exert prebiotic-like effects, not only by stimulating recognized probiotics, such as strains from *Lactobacillus* spp*., Bifidobacterium* spp., but also other bacteria with important biological roles (Boto-Ordóñez et al., 2014; Chang et al., 2019; Gómez-Gallego et al., 2016). Anthocyanins have been shown to stimulate *Lactobacillus* and *Bifidobacterium* by *in vitro* and in humans (Boto-Ordóñez et al., 2014; Hidalgo et al., 2012). The fecal bacteria composition of rats whose diet consisted in PAC-rich red wine extract, shifted from a predominance of *Bacteroides, Clostridium* and *Propionibacterium* spp. to a dominance of *Lactobacillus* and *Bifidobacterium* spp. (Dolara et al., 2005). In C57BL/6J mice fed a HFHS diet, polymeric apple PACs increased the proportion of *Adlercreutzia, Roseburia, S24-7, Bacteroides, Anaerovorax* and *Akkermansia* genera, over that of the untreated HFHS-fed mice. In contrast, the proportion of *Clostridium, Lachnospiraceae, Peptococcaceae* and *Bifidobacterium* were decreased (Masumoto et al., 2016). Interestingly, in that study, the effect on the gut microbiota composition was also reflected by positive changes in lipid metabolism and body weight. Furthermore, 16S rRNA gene sequencing and qPCR of cecal and fecal samples have demonstrated that grape polyphenols, apple PACs, epigallocatechin-3-gallate (EGCG), puerarin, black raspberry polyphenols, chlorogenic acid, and A-type PACs rich cranberry extract dramatically increased the growth of *A. muciniphila,* and decreased the proportion of *Firmicutes* to *Bacteroidetes* in animal models, improving the host metabolic phenotype (Anhê et al., 2014; Masumoto et al., 2016; Roopchand et al., 2015; Sheng et al., 2018; Tu et al., 2018; Wang et al., 2019).

Overall, because of their effects on beneficial commensal bacteria, the polyphenols can be currently considered prebiotics. The prebiotic revisited concept (Gibson et al., 2017) actually

suggests polyphenols as being prebiotics, since they cause changes in the composition and activity of the gut microbiota, thus providing biological advantage for the host well-being. For instance, it has been demonstrated that flavan-3-ols polymers, are capable of influencing the metabolism of a large intestinal bacterial population, even in the presence of other nutrients, such as cell polysaccharides (Bazzocco et al., 2008).

The modulation of gut microbiota and the ensuing prevention against obesity after polyphenols intake are assumed to be mediated by the generation of bioactive metabolites or the inhibition of pathobionts (see **Figure 8**). Many opportunistic bacteria increased in the context of obesity and IBD (as discussed in the upper section of "Gut dysbiosis: the case of diet-induced obesity"), are inhibited by dietary supplementation with polyphenols. For instance, a black raspberries phenolic extract inhibited 10 bacterial genera from the phylum *Firmicutes*, and specifically *Ruminococcus,* while the abundance of *A. muciniphila* was increased 157-fold in C57BL/6J mice fed an obesogenic diet (Tu et al., 2018). Four-week oolong tea polyphenols treatment repressed gut dysbiosis in human flora-associated HFD-induced obesity mouse model; it increased the taxa of *Prevotellaceae,* and reduced *Ruminococcaceae, Lachnospiraceae* and *Veillonellaceae* (Cheng et al., 2018). In humans, red wine polyphenols improved metabolic markers and simultaneously increased the number of fecal *Bifidobacterium* and *Lactobacillus* and butyrate-producing bacteria *Faecalibacterium prausnitzii* and *Roseburia*, while inhibiting less desirable groups of bacteria such as LPS producers *E. coli* and *Enterobacter cloacae* (Moreno-Indias et al., 2016). Treating C57BL/6N HFD-induced obese mice with EGCG significantly increased the abundance of the genera *Adlercreutzia, Akkermansia, Allobaculum* and *Parabacteroides,* and significantly lowered the abundance of the genera *Mucispirillum*, *Ruminococcus, Lachnospiraceae*, *Desulfovibrionaceae* and *Anaerotruncus* (Ushiroda et al., 2019) Those changes were associated with improvement in bile acid dysregulation. Interestingly, the phylum *Firmicutes* and *Proteobacteria*, the genera of *Ruminococcus* and the class *Clostridia,* were inhibited in Winstar rats under a chow diet supplemented with grape seed PACs extract for 8-days (Casanova-Martí et al., 2017). It is possible that the effect of polyphenols on the suppression of those metabolic disorders may be a concomitant effect of the disappearance of certain pathobiont and the insensibility and resilience of *Akkermansia* to phenolics.

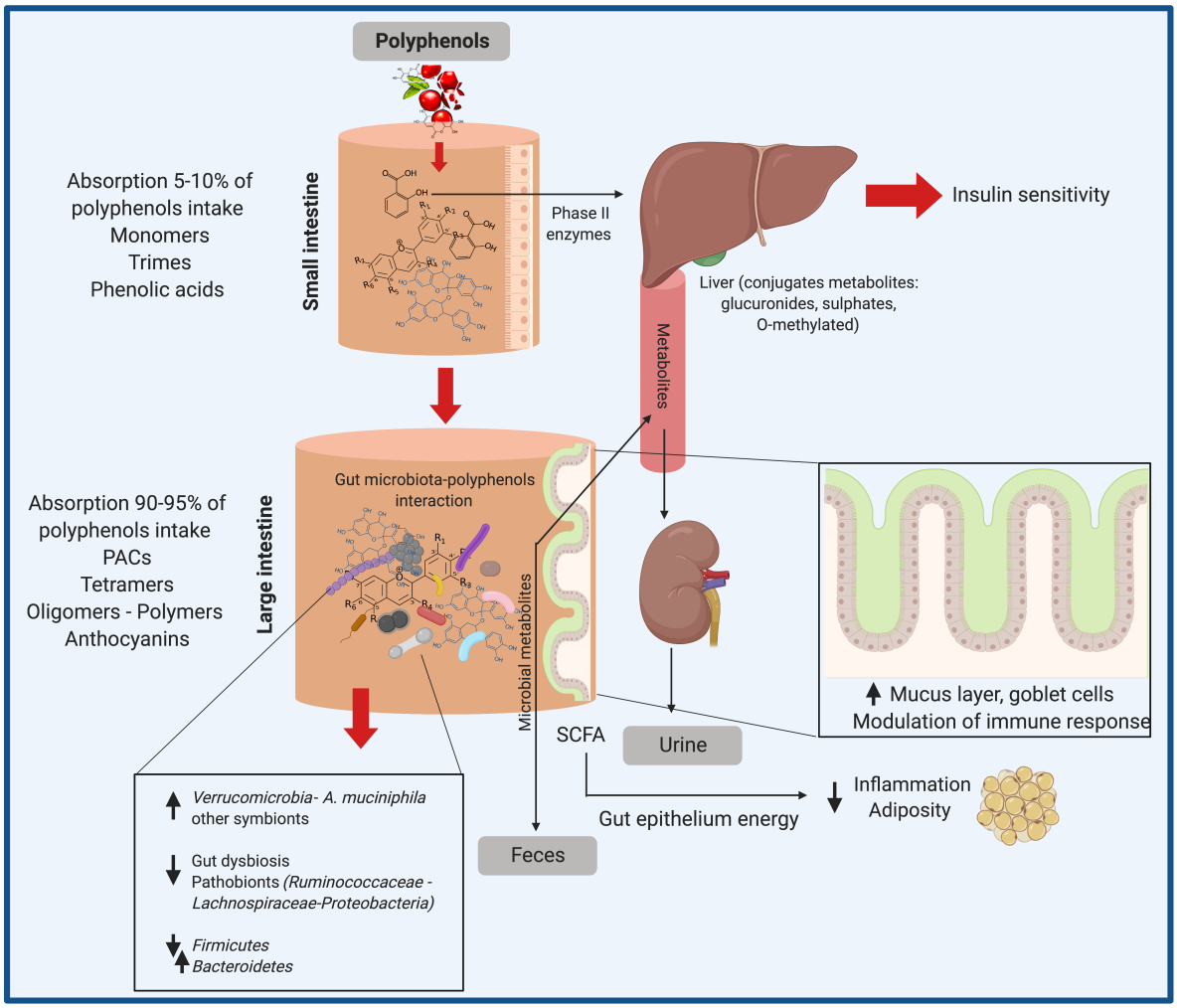

Figure 8. Overview of the effects of polyphenols and their implications on gut and host health.

Less than 5-10% of dietary polyphenols intake is estimated to be absorbed in the small intestine. Once absorbed, polyphenols undergo extensive phase II metabolism (glucuronidation, sulphatation, and methylation). Moreover, 90-95% of non-absorbed polyphenols intake reach the large intestine. In the colon, microorganisms have the ability to metabolize them or release non-extractable phenolic compounds, those intimately associated in the fibres and proteins. Microbes-polyphenols interaction leads to the generation of metabolites that can be distributed into the intestinal fluids and favour direct contact with the colonic epithelium, thus positively modulating the mucus layer thickness, mucin-secreting goblet cells and the immune system. The phenolic compounds and their microbial metabolites might also impact the gut microbiota and induce prebiotic-like effects on bacteria. Members of *Firmicutes* phylum are often reduced and the *Verrucomicrobia* phylum promoted. Opportunistic microbes are disturbed, mitigating the detrimental metabolic effects. Those changes might exert remarkable local health effects, such as reduction of inflammatory markers and adiposity, and improvement of glucose metabolism.

Most of above research supports the beneficial effect of PACs and other polyphenolic extracts on diverse antimicrobial activities, affecting the gut microbiota composition and contributing to regulating aspects of host energy balance; this includes lipid absorption and energy harvest (Anhê et al., 2014; Henning et al., 2017; Lacombe et al., 2012; Roopchand et al., 2015; Tabasco et al., 2011; Vendrame et al., 2011;Fu et al., 2015; Lukovac et al., 2014; Moreno-Indias et al., 2016; Nie and Stürzenbaum, 2019; Turnbaugh et al., 2006). Polyphenols are thus promising compounds for treating gut dysbiosis-associated diseases. Albeit the mechanisms of polyphenols promoting action on symbiotic bacterial strains are not restricted to the capacity of such bacteria to breakdown phenolics. Given the important functions of the symbiotic bacteria prompted by polyphenols, it is significant to study the transcriptional response of the intestinal microbiota to those compounds.

8.2 Influence of polyphenols on the expression of adaptation mechanism by the gut microbiota

Xenobiotic compounds influence multiple genetic responses of bacterial phyla, ranging from antibiotic resistance, metabolic responses, cell surface architecture and stress response pathways (Maurice et al., 2013). The effect of polyphenols in microbial members of the gut microbiota is dependent on both the microbial species and the antimicrobial properties of the polyphenol class. As aforementioned, one of the main mechanisms of phenolics against pathogens is to attack the cell membrane (Lacombe et al., 2013). The lipopolysaccharide of Gram-negative bacterial outer membrane is considered to be the major component conferring the ability to resist antimicrobial stress (Lacombe et al., 2013b). However, some Gram-positive strains may also exhibit tolerance to phenolics. For instance, *Streptococcus gallolyticus* form a protective layer around the cells in response to tannins. Krause et al. (2005) demonstrated by *in vitro* growth assays that *Streptococcus bovis* JB1 was sensitive to condensed tannins, while *Streptococcus gallolyticus* was tolerant. In that study, a significant increase in CPS and EPS gene expression in response to tannic acid was explaining the tolerance of *Streptococcus* strains. Firrman et al. (2016) evaluated the growth patterns, cell morphology, and the genetic expression profiles of gut commensal bacteria exposed to different concentrations of quercetin for 24h. Results of this study revealed that quercetin did not affect the growth of *Ruminococcus gauvreauii*, slightly repressed *Bifidobacterium*

catenulatum, and moderately inhibited the growth of *Enterococcus caccae;* all without noticeable changes in size and cell shape. However, the molecular analysis of the bacteria response to quercetin revealed a putative mechanism tolerance/resistance. Interestingly, an ABC transporter permease belonging to cellular transporters ubiquitous in bacteria and contributing to antibiotic resistance (Blanco et al., 2016; Piddock, 2006), was significantly up-regulated in *R. gauvreauii*. The capacity of this bacterium to maintain growth under quercetin resulted from its capacity to downregulate several metabolism genes. In the case of *B. catenulatum*, ABC transporters and multidrug transporter protein were equally up-regulated, likely attempting to get rid of the toxic substrate, and genes related to catabolism and energy production were significantly reduced. Finally, *E. caccae,* which was inhibited by quercetin, induced stress response genes, while downregulating two transporters-related genes, responsible for the uptake of sugar and carbohydrates into the cell, as well as, genes involved in cell wall synthesis. In another study, Firrman et al. (2018) also evaluated the effect of the flavanone naringenin on the same gut bacteria. In this case, *R gauvreauii* overexpressed genes responsible for ferrous iron transport, but under-expressed genes coding for DNA synthesis and repair. *B. catenulatum* upregulated multiple genes associated with cell transport, including a dipeptide ABC transporter permease component, a galactoside transport protein, and DNA repair and molecular transport. However, a significant drop in gene expression related to catabolism and/or energy production in *E. caccae*, affected energy production and normal growth. Altogether, apart from the possible morphological changes in bacteria induced by polyphenols, strain-specific molecular adaptability involving either membrane transporters or energy metabolism explain the remarkable resilience of gut bacteria.

Tolerance mechanisms of bacteria to polyphenols might stem from the activation of enzymes like tannase, quercetinase (family of cupin-type dioxygenases: flavonol 2,4-dioxygenase, quercetin 2,3-dioxygenases), gallate decarboxylase, esterase, phenolic acid decarboxylase, benzyl alcohol enzymes (de Las Rivas et al., 2019; Fetzner, 2012; Filannino et al., 2018; Fritsch et al., 2016; Jiménez et al., 2013; Kawabata et al., 2019; Tabasco et al., 2011). The growth promoting activity of blueberry functional ingredients on *Bifidobacterium* and *Lactobacillus* strains has been assessed (Vendrame et al., 2011). The growth rate improvement of these two probiotic strains in presence of blueberry extracts was explained by their ability to metabolize polyphenols (Filannino

et al., 2018; Fritsch et al., 2016; Jiménez et al., 2013; Tabasco et al., 2011). A proteomic analysis of *L. plantarum* challenged with tannic acid, in addition to demonstrate the metabolic capacity by this bacterium, revealed the expression of oxidative stress and cell wall biogenesis (Curiel et al., 2011). Consistent with the propensity of polyphenols to affect the bacteria cell wall (Lacombe et al., 2013), this study demonstrated that *L. plantarum* regulates proteins playing a key role in the peptidoglycan biosynthesis in response to tannic acid. These findings unveiled that tannic acid can affect bacteria through both oxidative damage and disruption of the cell wall. In light with this, Reverón et al. (2013) reported that *L. plantarum* WCFS was morphologically affected by tannic acid. Importantly, visualization by TEM of lag-phase cells growing with tannic acid, occasionally revealed the presence of extracellular matrix through ruthenium red staining. Genes involved in cell-wall proteins and antibiotic-related genes, such as penicillin binding proteins (PBPs) involved in peptidoglycan biosynthesis, were also significantly induced. In this study, cell-envelope related genes were further assessed under gastrointestinal condition showing comparable outcomes, indicating that they are crucial for persistence and survival of bacteria in the human gut. Additionally, a study from the same research group revealed that genes involved in polyphenols degradation, in transport functions and in stress response were upregulated upon the exposure of *L. plantarum* WCFS1 to gallic acid (Reveron et al., 2015). Moreover, resveratrol was shown to affect the regulation of efflux systems and ABC transporters in the same strains (Reveron et al., 2018). The molecular structure of polyphenols account for the severity of their antimicrobial actions (Xie et al., 2014). Accordingly, PAC trimers from peanut skin extract showed stronger inhibitory activity than PACs dimers on the Gram-positive food-pathogen *Bacillus cereus*. Consistent with the aforementioned studies, analysis of the up-regulated genes suggested that PACs trimers disrupted cell membranes and walls of *B. cereus,* and altered its usual nutritional metabolism (Tamura et al., 2016).

Tannins have also been reported to reduce the hydrophobicity of bacterial cell surfaces (Wojnicz et al., 2016). For instance, Zoetendal et al. (2008) studied the gene expression profiles of *E. coli* strains grown anaerobically with or without *Acacia mearnsii* tannin extract to unravel resistance strategies. The authors demonstrated that the *mdtABCD* operon, encoding a multidrug transport system (cellular processes; toxin production and resistance), was significantly

upregulated. This *mdtABCD* operon confers tolerance of *E. coli* to tannins and gallic acid. Furthermore, cranberry pomace and two of its sub-fractions, named anthocyanins and non-anthocyanin polyphenols (flavonols), had bactericidal effects against *Salmonella* strains, the latter being the most active (Das et al., 2019). The authors observed that cranberry polyphenols reduced the expression of virulence genes, cell wall/membrane biogenesis, and a transcription regulator after 20h of incubation. Likewise, genes encoding for inner and outer membrane proteins, multidrug resistance genes and ABC transporters and permeases were modulated. Finally, polyphenols also act through another antimicrobial mechanism; they affect bacterial quorum sensing (QS). For instance, cranberry PACs were shown to reduce the production of QS-regulated virulence genes in *Pseudomonas aeruginosa* in a *Drosophila melanogaster* model (Maisuria et al., 2016).

All in all, bacteria adopt many strategies to avoid the detrimental action of antimicrobials and unfavourable growth conditions; these appear to be strain specific. As reviewed above, the genome of *Akkermansia*, in addition to possessing numerous candidate mucinase-encoding genes, also has sequences of potential antibiotic resistance genes. In particular, it presents genes coding for beta-lactamase (Amuc_0106 and Amuc_0183), 5-nitroimidazole antibiotic resistance protein (Amuc_1953) (van Passel et al., 2011), and other antibiotic resistance genes for glycopeptides (vancomycin-X, D-ala D-ala dipeptidase), phenicol, sulphonamide, tetracycline, and trimethoprim (Caputo et al., 2015). *A. muciniphila* might also have the ability to regulate self-protection by expressing genes coding for capsular polysaccharide (Amuc_1413 and Amuc_2098). Within the *Akkermansia* genome, gene encoding exosortase *EpsH* (encoded by Amuc_1470), forming a protein sorting system associated to exopolysaccharide expression has been reported (van Passel et al., 2011). Both the cell surface architecture and the genetic machinery may influence the physicochemical properties of bacteria to overcome the inhibitory effect of polyphenols.

9. Problem statement

In this review we provided insights on the role of the gut microbiota to human physiology, as well as the role of phenolics to restore gut dysbiosis and obesity disturbances. In most of the studies, polyphenols caused a bloom of *A. muciniphila* concomitantly with an improvement of

obesity markers. However, while the positive health effect of polyphenols mediated by the gut microbiota is clearly demonstrated, the phenolic fractions responsible for the effect on the mucosa-associated niche and the genetic response of *Akkermansia* need to be uncovered.

We hypothesize that the antimicrobial action of polyphenols on opportunistic pathogens associated to gut dysbiosis and host metabolic alterations might favour the increase of symbiotics, especially *A. muciniphila,* and attenuate obesity. Regarding to this statement, we surmise that polyphenols might also induce changes in the colonic histomorphology and mucin profile, generally affected in obesity, as mechanisms by which, might recover the ecological niche of *A. muciniphila.* Given the heterogeneity of data obtained on *A. muciniphila* abundance from animal and human models by dietary supplementation with polyphenol-rich foods, performing *in vitro* assays is a worthy approach to provide evidence to better understand the direct reaction of *A. muciniphila* to phenolics. To our knowledge, except for the significant colonization of *A. muciniphila* in the intestine, there is a paucity of knowledge on the transcriptional mechanisms of this bacterium to adapt to polyphenols, and a lack of information on the type of polyphenol affecting the growth of *Akkermansia.* An increasing number of molecular mechanisms have been identified to influence the bacterial resistance, sensibility and growth, upon exposure to antimicrobial polyphenols. Importantly, *A. muciniphila* appears to predominate after antibiotic administration, oxygen, and even to challenges by other microbes (Caputo et al., 2015; Chia et al., 2018; Ouwerkerk et al., 2016b). Thus, we propose that the bloom of *A. muciniphila* stems from its resilience to polyphenols and its capacity to induce resistance mechanisms, providing a selective advantage to be a prominent symbiont in the gut over phenolics susceptible pathobionts.

10. Objectives

The present PhD thesis aimed to study, using *in vivo* and *in vitro* models, the modulating effects of polyphenols on the gut microbiota, and especially one of its key members, *A. muciniphila,* and investigate the molecular response of this bacterium to phenolics. A murine model is proposed to evaluate the prebiotic potential of polyphenols and their effects on colonic epithelium histomorphology, the mucus thickness and mucin profile, as instrumentally affecting *A. muciniphila* ecological niche. An *in vitro* approach was developed to determine whether this

bacterium expresses molecular adaptations or resistance mechanisms to the presence of polyphenolic compounds. These objectives were achieved by analyzing the gut microbial community structure and predicted metagenome in a mouse model of HFHS-diet induced obesity, submitted to daily dietary supplementation with cranberry and blueberry whole fruit powders, their fibrous fractions, and polyphenol-rich extracts. Changes in the gut dysbiosis and metabolic disturbances as markers of obesity were evaluated. We also explored the molecular basis of the response of *A. muciniphila* to dietary polyphenols by carrying out *in vitro* growth static monocultures, in a mucin-rich medium.

In the **Chapter I** the prebiotic potential of cranberry and blueberry constituents, notably, fibres (cell-wall polysaccharides) and polyphenols was assessed by analyzing the modulation of the gut microbiota in a model of HFHS-diet induced obese mice. The focus was first, to validate whether the polyphenolic compounds from berries, displayed selective prebiotic-like effect on *A. muciniphila* and contributed to counteracting gut dysbiosis and obesity. The taxonomic and predicted metagenomic profile of mice gut microbiota were then characterized. Specific taxonomic markers and functions were demonstrated to be linked either to the intake of polyphenol-rich whole fruit powder or to its fibre-rich fraction. Additionally, bacterial biomarkers were also correlated to changes in mouse phenotypes associated to obesity.

The **Chapter II** aims to identify which polyphenolic category from a whole phenolic extract is causing the bloom of *A. muciniphila* in HFHS-diet induced obese mice, and their effect on the host health. To this effect, a whole wild blueberry extract and three polyphenolic sub-fractions containing anthocyanins, oligomeric PACs and polymeric PACs, in the same proportion as found in the whole extract were evaluated. Considering the complex structure of PACs and the evidence of their stronger antimicrobial impact on bacteria, we show that the PACs are responsible for the prebiotic-like effect on *A. muciniphila.* Notably, the fraction rich in oligomeric PACs significantly prompted *A. muciniphila* abundance in obese mice, and polymeric PACs remarkably improved its ecological niche by increasing the mucin-secreting GC number in the colonic epithelium. Likewise, the polymeric PACs was the fraction contributing to ameliorating the glucose homoeostasis in obese mice.

In the **chapter III,** the molecular and physiological capacity of *A. muciniphila* accounting for its adaptation or resistance to polyphenols as antimicrobials, were further investigated**.** The same approach used in the animal model described in the chapter II was followed; that is, a whole cranberry extract and three derived polyphenolic fractions, composed mainly by anthocyanins, oligomeric PACs and polymeric PACs were assessed. The sub-fractions were added to a culture medium at physiological concentrations supplied in the whole cranberry extract. The goal was to evaluate the effect of cranberry polyphenolic fractions on the growth of *A. muciniphila* and determine whether these phenolic categories distinctly enact mechanisms of resistance on this bacterium. This experimental design demonstrates that *A. muciniphila* is versatile and can cope with antimicrobial effects of polyphenolic fractions by using membrane-protection strategies, such as CPS/EPS production, by managing cell metabolism and expressing antibiotic cross-resistance mechanisms to adapt to polyphenols presence.

CHAPTER I

This chapter studies the prebiotic effects of polyphenol-rich cranberry and blueberry whole fruit powders and those of their fibrous fractions in mice fed an obesogenic diet. Cranberry and blueberry in addition to contain polyphenols, have plant cell wall polysaccharides (fibres); cellulose, pectin and hemicellulose, are found to be the predominant constituents of berries cell wall material. The objective of the present work was to discriminate the contribution of berry polyphenolic compounds from that of the fibrous material on modulating the gut microbiota, stimulating *A. muciniphila,* and attenuating metabolic and intestinal alterations associated to obesity. To this effect, the prebiotic potential of the fibrous fractions was evaluated separately. The fibre-rich fraction, either from cranberry or blueberry, were incorporated to a HFHS-diet at the same amount as found in the respective whole fruit powder. Bioinformatic tools were applied to identify taxonomic biomarkers that might be selectively favoured either by the presence of polyphenols or fibres in the diet. This research article, which was prepared for publication in the journal of *Frontiers in Microbiology,* highlights the role of polyphenol-rich whole fruit to modulate the gut microbiota structure and functions, by inhibiting pathobionts and favouring health-promoting species in a context of diet-induced obesity. The results demonstrate that beyond the taxonomic composition, the functional structure of the gut microbiota of obese mice is shifted by a dietary supplementation with polyphenol-rich whole cranberry powder to a profile comparable with that of lean mice. In particular, we could identify the selective prebiotic effect of both polyphenol-rich cranberry and blueberry powders on *A. muciniphila.* Moreover, other taxonomic biomarkers such as *Dubosiela newyorkensis, Eggerthellaceae* and *Coriobacteriales_incertae_sedis* were identified to selectively respond to the intake of a polyphenol-enriched diet; while *Muribaculaceae* and *Lachnospiraceae_NK4A136_group* were induced by the fibre-enriched diets.

Prebiotic potential of berry polyphenols and fibres on the gut microbiota composition and microbial metabolic functions of obese mice

Maria-Carolina Rodríguez-Daza,[1 2 *] Marcela Roquim,[1] Stéphanie Dudonné,[1 3] Geneviève Pilon,[1 4] Emile Levy, [1] André Marette,[1 4] Denis Roy,[1 2] Yves Desjardins[1 3 *]

1. *Institute of Nutrition and Functional Foods (INAF), Laval University, Québec, QC, Canada.*
2. *Food Science Department, Faculty of Agriculture and Food, Laval University, Québec, QC, Canada.*
3. *Plant Science Department, Faculty of Agriculture and Food, Laval University, Québec, QC, Canada.*
4. *Department of Medicine, Faculty of Medicine, Cardiology Axis of the Quebec Heart and Lung Institute, Québec, QC, Canada*

Article prepared for submission to the journal *Frontiers in Microbiology*

Résumé

Cette étude a évalué le potentiel prébiotique de poudres de canneberges et de bleuets entiers (CP et BP) riches en polyphénols, et de leurs fractions fibreuses (CF et BF) sur la composition du microbiote intestinal et leur influence sur les troubles métaboliques induits par un régime riche en gras et en sucre (HFHS) de 8 semaines. Les taxons associés aux souris maigres, y compris *Akkermansia muciniphila, Dubosiella newyorkensis* et *Angelakisella,* ont été sélectivement favorisés par les régimes CP et BP. CF a également augmenté les familles des *Coriobacteriaceae* et *Eggerthellaceae* ayant la capacité de dégrader polyphénols. La diète HFHS supplémentée avec CP, mais pas avec CF, a réduit les dépôts de masse grasse, le poids et l'efficacité énergétique des souris obèses. Cependant, CF a réduit les triglycérides hépatiques. Chez les souris obèses, le régime CP a normalisé les fonctions microbiennes à un niveau comparable à celui des témoins alimentés par Chow. À l'aide d'une modélisation d'association multivariée, les taxons bactériens et les fonctions distinguant le phénotype obèse des souris saines et des souris traitées aux baies ont été déterminés. Cette étude met en évidence le rôle prébiotique des polyphénols et leur contribution à la modulation de la composition et de la fonction du microbiote intestinal, améliorant l'obésité.

Mots clés : *Akkermansia muciniphila, Coriobacteriaceae, Eggerthellaceae, Dubosiella,* fibres, polyphénols, flavonoïdes, prébiotiques.

Abstract

This study assessed the prebiotic potential of polyphenol-rich whole cranberry and blueberry fruit powders (CP and BP), and of their fibrous fractions (CF and BF) on gut microbiota composition and their influence on metabolic disorders induced by high-fat high-sucrose (HFHS) diet for 8 weeks. Lean mice-associated taxa, including *Akkermansia muciniphila, Dubosiella newyorkensis,* and *Angelakisella*, were selectively induced by CP and BP-diets. CF also triggered polyphenols-degrading families *Coriobacteriaceae* and *Eggerthellaceae*. CP, but not CF, reduced fat mass depots, body weight and energy efficiency of HFHS-fed mice. However, CF reduced hepatic triglycerides level in HFHS-fed mice. Importantly, CP diet normalized the microbial functions to a level comparable to that of Chow-fed controls. Using multivariate association modelling, bacterial taxa and predicted functions distinguishing an obese phenotype from healthy controls and berry-treated mice were identified. This study highlights the prebiotic role of polyphenols, and their contribution to the compositional and functional modulation of gut microbiota, counteracting obesity.

Keywords: *Akkermansia muciniphila*, *Coriobacteriaceae, Eggerthellaceae*, *Dubosiella,* fibres, polyphenols, flavonoids, prebiotics.

Prebiotic potential of berry polyphenols and fibres on the gut microbiota composition and microbial metabolic functions of obese mice

Authors : Maria-Carolina Rodríguez-Daza*, Marcela Roquim, Stéphanie Dudonné, Emile Levy, Geneviève Pilon, André Marette, Denis Roy, Yves Desjardins*

Graphical abstract

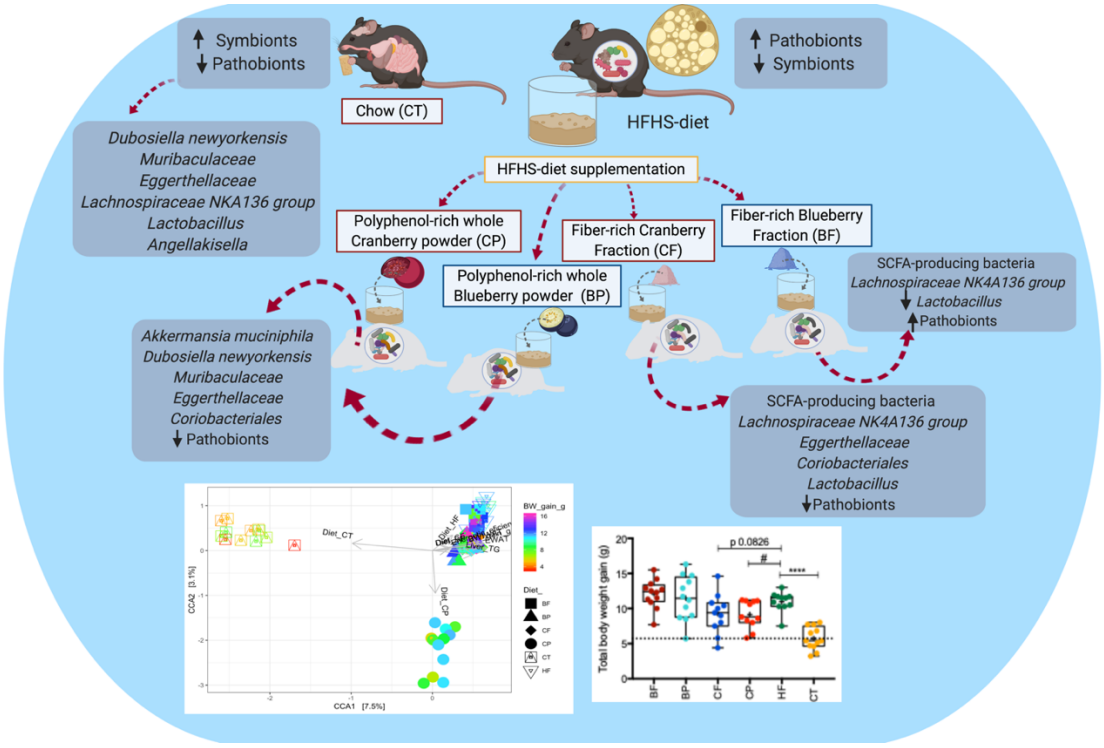

Highlights

- Polyphenol-rich CP and BP selectively prompted the growth of *A. muciniphila*, and *D. newyorkensis*
- Polyphenol-rich CP reduced body weight and energy efficiency in HFHS-diet induced obese mice
- Polyphenol-rich CP remarkably changed the gut microbiota composition and functional profile
- Fibre-rich CF, but not BF, inhibited pathobionts and prompted *Lactobacillus* and *Eggerthellaceae*

*Correspondence: Yves.Desjardins@fsaa.ulaval. ca; maria-carolina.rodriguez-daza.1@ulaval.ca

In Brief

Rodriguez-Daza et al. demonstrate that berry polyphenols are significantly modifying the gut microbiota of mice fed an obesogenic diet. HFHS-diet supplementation with polyphenol-rich whole cranberry fruit powder exerts prebiotic effects and are associated with the attenuation of obesity. Polyphenol-rich powders inhibit pathobionts overgrowth and restore intestinal eubiosis. Although fibre-rich fractions promoted SCFA-producing bacteria, only cranberry fibres inhibited pathobionts and reduced hepatic triglycerides level. Beyond the gut microbiota composition, microbiome functional analysis reveals that CP attenuate weight gain in HFHS-fed mice.

Prebiotic potential of berry polyphenols and fibres on the gut microbiota composition and microbial metabolic functions of obese mice

Maria-Carolina Rodríguez-Daza,[1 2 *] Marcela Roquim,[1] Stéphanie Dudonné,[1 3] Geneviève Pilon,[1 4] Emile Levy, [1] André Marette,[1 4] Denis Roy,[1 2] Yves Desjardins[1 3 *]

1. *Institute of Nutrition and Functional Foods (INAF), Laval University, Québec, QC, Canada.*
2. *Food Science Department, Faculty of Agriculture and Food, Laval University, Québec, QC, Canada.*
3. *Plant Science Department, Faculty of Agriculture and Food, Laval University, Québec, QC, Canada.*
4. *Department of Medicine, Faculty of Medicine, Cardiology Axis of the Quebec Heart and Lung Institute, Québec, QC, Canada*

Introduction

The gut microbiota emerges as a complex interconnected organism intimately interacting with multiple host organs and systems. A disturbed gut microbiota, characterized by reduced microbial abundance and diversity, and altered metabolic functions (i.e. dysbiosis), is conducive to many health problems and is particularly linked to the development of obesity (Turnbaugh et al., 2008; Turnbaugh et al., 2006). Indeed, the dysbiotic faecal microbiota transfer from obese donors into lean germ-free mice reproduces the obese phenotype and metabolic disturbances in the latter (Turnbaugh et al., 2008). Improving functional capabilities of the microbiota could play a crucial role in nutrient extraction, in resistance to opportunist bacteria (i.e. pathobionts), and, consequently, in the maintenance of the host fitness. Therefore, not only is it important to identify the gut microbial members conferring metabolic benefits, but it is also essential to develop strategies favoring establishment of beneficial bacteria in order to maintain or restore health.

In recent years, the use of prebiotics has gained interest to alleviate gut dysbiosis and decrease the risk of metabolic disorders (Sanders et al., 2019). Prebiotics are non-digestible food ingredients that selectively stimulate the growth and activity of one or a limited number of colonic bacteria, beneficially impacting the host health (Gibson et al., 2017). Dietary cell wall polysaccharides, such as pectin, arabinoxylans, cellulose and hemicellulose, usually considered as prebiotics, have been shown to support the growth of *Bifidobacterium* spp., *Lactobacillus* spp., *Faecalibacterium*

prausnitzii, *Eubacterium rectale*, *Bacteroides* spp. and *Prevotella* spp. (Chen et al., 2018; Larsen et al., 2019; Mao et al., 2019; Truchado et al., 2017), which have been reported to be important phylotypes with protective effects against metabolic diseases (Sanders et al., 2019). Both cellulose and hemicellulose, besides arabinans and arabino-xyloglucans rich pectin, are components of cranberry cell walls, constituting 65.5% insoluble fibre of the whole fruit (Hotchkiss et al., 2015; White et al., 2010). Likewise, blueberry cell wall hemicellulose is composed of pectin and xyloglucan (30–35%) (Blaker and Olmstead, 2015; Vicente et al., 2007). Those prebiotic fibres are fermented to short chain fatty acids (SCFAs) by the gut microbiota, and are involved in intestinal cell turnover, lipid metabolism modulation, glycaemic response regulation and gastrointestinal satiety hormones release (De Vadder et al., 2014; Makki et al., 2018; Müller et al., 2018). Furthermore, interactions between plant cell wall components and polyphenols, such as proanthocyanins (PACs), have been demonstrated in apple, cranberry and grapes (Bindon et al., 2010; Bourvellec et al., 2005; Hotchkiss et al., 2015; Sun et al., 2015). Tightly linked to fibres, polyphenols are catabolized by gut microbes to smaller phenolic acids, which exert anti-inflammatory, immuno-modulatory and antioxidant effects in the host (González-Sarrías et al., 2017).

Growing evidences indicate that polyphenols also exert prebiotic effects and reduce the risk of obesity, insulin resistance, and cardiovascular diseases (den Abbeele et al., 2018; Paturi et al., 2018; Skrovankova et al., 2015). Between 90 and 95% of the ingested polyphenols reach the colon, where they suppress gut pathobionts and stimulate health promoting bacteria (Clifford, 2004; Masumoto et al., 2016). For instance, supplementing the diet with whole wild blueberries was shown to increase the relative abundance of beneficial microbes belonging to the *Bifidobacteriaceae* and to the polyphenol-degrading family *Coriobacteriaceae* in rodent and human guts (Guglielmetti et al., 2013; Lacombe et al., 2013b; Rodríguez-Daza et al., 2020). Likewise, cranberry polyphenols and seed fibres inhibited pathogens and stimulated the probiotic species *Bacillus coagulans* and *Lactobacillus rhamnosus* (Lacombe et al., 2013c; Majeed et al., 2018). Importantly, several polyphenol-rich extracts have been shown to concomitantly inhibit opportunistic pathogens and cause a bloom of *Akkermansia muciniphila* in mice fed an obesogenic diet (Anhê et al., 2014; Collins et al., 2016a; Garcia-Mazcorro et al., 2018; Heyman-Lindén et al.,

2016a; Pan et al., 2017; Rodríguez-Daza et al., 2020; Tu et al., 2018). This bacterium is of a particular interest due to its immuno-modulatory properties in the host and its capacity to prevent obesity, type 2 diabetes and inflammation (Depommier et al., 2019; Everard et al., 2013; Schneeberger et al., 2015a). Even if many evidences point to the prebiotic effects of both berry fibres and polyphenols, more work is needed to differentiate the effects of cell wall polysaccharides from that of polyphenols on gut microbiota composition and function.

The present study aims to evaluate the effects of cranberry and blueberry whole fruit powders and their fibre-rich fractions (non-extractible polyphenols and polysaccharides) on the gut microbiota composition and functional profile, in a murine model of HFHS-diet induced obesity. Polyphenol-rich whole cranberry and blueberry fruit powders selectively favored key bacterial species linked to lean phenotypes and attenuation of obesity-related disorders. Changes in the predicted functional profile and metabolic redundancy of the gut microbiota reveal a distinct role of polyphenols-rich cranberry powder in the prevention of obesity-associated phenotypes. While the whole blueberry powder strongly modulated the taxonomic composition of the gut microbiota, it did not significantly improve microbial functions.

Results

Phytochemical composition of the whole cranberry and blueberry powders

The complete phenolic characterization and chemical composition of the berry powders and their fibre-rich fractions are presented in the Supporting Information **Table S1 - S2.** In order to compare the prebiotic effects of fibres with polyphenol-rich berry powders, the quantity (g/100 g) of each berry's fibrous fraction added to a HFHS-diet were balanced to provide an equal amount of fibres as encountered in their respective berry powder. All the diets were adjusted to be isocaloric with a total energetic density of 5.4 kcal/g. The diet compositions are presented in the **Table S3.**

Polyphenols-rich CP diet reduced body weight gain, fat mass accumulation and energy efficiency in HFHS fed mice

The HFHS-diet consumption induced a significant increase of mice body weight (BW) from the week 5 until the end of the study as compared with those of the Chow diet-fed counterparts (**Figure 1 A-B**). The diet supplementation with polyphenols-rich CP reduced the total BW gain after 8 weeks of intervention ($p<0.05$ as compared to HFHS) and the fibre-rich faction CF tended to reduce it ($p=0.0826$ as compared to HFHS). A significant decrease in body fat mass accumulation (percentage of BW) was consistent with the reduced BW gain in mice fed the CP-diet ($p<0.01$ as compared to HFHS) (**Figure 1 C-D**). There was a lower proportion of inguinal white adipose tissue (IWAT) weights in relation to the final body weight after 8 weeks of feeding ($p<0.01$ compared to HFHS-fed mice) and a trend to reduce the epididymal white adipose tissues mass (EWAT, $p=0.0847$) in CP-fed mice (**Figure 1 E-F)**. The CP reduced energy efficiency (the ratio of BW to energy intake), body fat mass percentage and BW gain in HFHS-fed obese mice (**Figure 1 G-H**). Moreover, no significant changes in BW gain of mice supplemented with BP and BF diets were observed as compared to HFHS. As a matter of fact, an increase of the EWAT in mice fed the BF-diet and of liver triglycerides level was observed compared to HFHS ($p<0.05$) (**Figure 1 F**).

The CF-enriched diet decreased the hepatic triglycerides storage in HFHS-fed mice

Triglycerides (TG) levels in the HFHS-fed control mice were significantly higher than in Chow-fed mice ($p<0.001$). Interestingly, the fibre-rich CF-fed group had reduced hepatic TG levels compared to HFHS-fed mice ($p<0.05$). However, an unexpected increase of hepatic TG was observed in mice fed the fibre-rich BF-diet as compared to HFHS-fed mice ($P<0.05$) (**Figure 1 I**).

Polyphenol-rich CP and BP and their fibrous fractions did not affect the HFHS-induced glucose metabolism disorder in mice

After a glucose load, glycemia level reached 25 mmol/L after 15 mins and remained significantly higher during the entire OGTT in the mice fed HFHS-diet as compared to Chow-fed mice ($p<0.001$) (**Figure 2 A-B)**. However, the diet enrichment with CP, BP, CF, and BF did not affect blood glucose levels in obese mice, showing similar area under the curve (AUC) as compared to HFHS-fed control mice (**Figure 2 B**). The plasma insulin levels during the OGTT were significantly increased in HFHS compared to Chow-fed mice ($p<0.05$) (**Figure 2 C-D**). Blood glucose levels and the serum insulin in the fasting state were significantly higher in the HFHS-fed mice than in the Chow control mice ($p<0.05$, **Figure 2 E-F**). The mice fed the BF diet presented an increase in fasting insulin as compared to HFHS-fed mice.

Insulin tolerance test (ITT) was also performed in the same groups of mice to assess the effects of the whole berry powders and the fibre fractions on HFHS diet-induced insulin resistance. HFHS-diet fed mice showed decreased insulin sensitivity at 5 and 10 mins timepoints of the ITT compared to Chow-fed mice ($p<0.05$) (**Figure 2 G**), but the AUC values indicated that both HFHS and Chow groups responded in a similar manner with decreases in blood glucose during the 60 min after insulin challenge (**Figure 2 H**). Likewise, the mice fed the polyphenols-enriched CP and BP diets, as well as their fibre rich fractions CF and BF, displayed similar response to exogenous insulin, with no significant changes compared to HFHS-fed control mice (**Figure 2 H**). Insulin resistance, as reflected by the homeostasis model assessment of insulin resistance (HOMA-IR) index, was higher in the HFHS-fed mice compared to Chow-fed mice, ($p<0.05$). The supplementation with the polyphenol-rich CP, BP and the fibre-rich fractions CF and BF did not significantly affect this index compared to the HFHS controls (**Figure 2 I**).

Polyphenols-rich BP-diet significantly improved colonic mucus thickness while the CP-diet increased the caecum mass in obese mice

Representative histological sections of the colon tissues of treated mice are presented in Supporting Information **Figure S1 A-F.** The HFHS-diet had a detrimental effect on the

histomorphology of the colonic mucosal epithelium compared to Chow-fed mice ($p<0.0001$) (**Figure S1 G**). Among the diets supplemented with berry powders and their fibre fractions, only the BP significantly improved the mucus thickness compared to the HFHS-fed mice ($p<0.01$). However, there was no differences in the colonic crypt depth and the number of mucus-producing goblet cells (GC) per crypt depth (μm^2) among the mice fed the CP, BP, CF, and BF as compared to the mice fed the HFHS and Chow diets (**Figure S1 H-I**). Since both the residing commensal bacteria and the diet composition influence the type of host-derived mucin (Schroeder, 2019; Sharma and Schumacher, 1995), we evaluated the proportion of acid, neutral and mixed mucins from the histopathological preparations of colon tissues. The numbers of GC stained either by Alcian blue (AB) or periodic-acid Schiff (PAS), specific for sulfated and sialiated type of acidic mucins (blue), and α-glycol neutral mucins (magenta), respectively (Deplancke and Gaskins, 2001), were evaluated; GC stained with purple color indicated the presence of both neutral and acid mucins. A significant difference was observed in the proportion of mixed mucin (neutral and acid mucins) in HFHS-fed mice compared to Chow-fed mice ($p<0.05$) (**Figure S1 J**). The HFHS-diet tended to decrease the amount of neutral mucin-filled GC ($p=0.0916$) as compared to the Chow-group. However, there was no significant difference in the types of mucin-filled GC between mice fed the CP, BP, CF and BF compared to HFHS-fed mice.

The increase in the size and mass of caecum tissues is an indication of increased dietary fibres fermentation by the gut microbiota (Adam et al., 2014). Here, the positive effect of berry constituents on the weight of the caecum content was measured to reflect gut microbial changes. HFHS-diet had a lower weight of the caecum of mice compared to Chow-fed group ($p<0.0001$, 140.0 ± 14.4 mg vs 421.2 ± 24.5 mg in HFHS and Chow respectively) (**Figure S1 K**). The diet supplementation with both berry fibre-rich fractions did not alter the weight of caecum content compared to HFHS-diet (158.6 ± 9.6 mg, and 149.0 ± 10.6 mg in CF and BF respectively compared to 140.0 ± 14.4 mg in HFHS-fed mice). The polyphenols-rich CP diet significantly increased the caecum mass in obese mice ($p<0.01$, 229.0 ± 18.0 mg) as compared to untreated HFHS control group ($p<0.001$). Even though the polyphenols-rich BP-diet tended to increase the caecum mass (162.2 ± 5.7 mg, $n=12$), it was not statistically significant as compared to HFHS (**Figure S1 K**).

The polyphenols-rich CP and BP diets and their fibrous fractions CF and BF increased gut microbial richness and diversity in HFHS fed mice

The changes in α-diversity were contrasted against both the baseline at week 0 and with the HFHS-fed control mice at week 8. HFHS-diet did not significantly affect the microbial richness (*Chao1*) and *Shannon* diversity as compared to the baseline (**Figure 3**). Importantly, the CP and BP, as well as their fibre-rich fractions CF and BF, significantly increased the microbial richness compared to both the baseline and to untreated HFHS-fed mice ($p<0.05$) (**Figure 3 A**). The mice fed the fibre-rich BF-diet presented a significantly higher microbial diversity compared to baseline (*Shannon* index, $p<0.05$); yet, it only tended to increase this parameter when compared to HFHS-fed mice at week 8 (corrected p value $q=0.0723$). Particularly, the supplementation with a polyphenols-rich BP increased the gut microbiota diversity after 8 weeks ($p<0.05$, vs HFHS) (**Figure 3 A**); At the same time, polyphenols-rich CP-diet tended to increase it (corrected p value $q=0.0944$). All treatments slightly improved the *Simpson* evenness index compared to the HFHS-fed mice, yet not significantly.

Polyphenols-rich CP and BP diets significantly influenced the gut microbiota in HFHS fed mice

The Bray-Curtis distances matrix among mice gut microbiota including both data from the baseline and week 8, revealed perfect hierarchical clustering over time (**Figure 3 B**). Thus, the dietary groups, showing similar gut microbiota composition at baseline, were all clustered in the left quadrant of the PCoA. However, the mice fed CP and BP-enriched diets clustered separately from the HFHS-fed control mice after 8 weeks of dietary intervention, as observed in the right side of the PCoA. The PERMANOVA, analysis of similarities (ANOSIM) was used to give an insight into the degree of separation between the tested dietary groups. The R statistic score obtained was R^2 0.4293 ($p<0.001$), indicating that the significant changes were diet-induced in the mice gut microbiota structure from the beginning of the intervention.

Since the groups had different distribution in the PCoA at week 8, β-diversity was measured only considering the taxonomic changes at the end of the intervention. Particularly, the berry powders containing polyphenols distinctly drove the bacterial composition away from HFHS-diet induced obese mice and their fibre-rich fractions. β-diversity measurements displayed a clear separation of mice fed the polyphenols-rich CP-diet from the HFHS-fed control group, demonstrating a dissimilar gut microbiota structure, including when the taxon-based UniFrac measure was integrated into the analyses (**Figure 3 C-D**). In a similar manner, gut microbiota of polyphenols-rich BP-fed mice diverged from that of HFHS-fed mice (**Figure 3 C**). Mice fed the fibre-rich CF clustered away from the control group HFHS; however, fibre-rich fraction BF only slightly affected the gut microbiota structure as compared to HFHS-diet (**Figure 3 C-D**). The PERMANOVA analysis revealed a significant R^2 value of 0.4030 ($p< 0.001$) for Bray-Curtis dissimilarity and R^2 0.3354 ($p<0.001$) for UniFrac phylogenetic-based distances, representing a variation in the Axis 1 of 26.3% and 22.1% respectively.

Polyphenols-rich CP and BP diets and not their fibrous fractions decreased *Firmicutes* and selectively prompted the *Verrucomicrobia* and *Actinobacteria* phyla in HFHS fed mice

Using the DADA2 pipeline for taxonomic classification analysis of ASVs, we identified 21 bacterial families, 59 genera and 5 species from bacterial sequences of mouse fecal samples. At the phylum level, the HFHS-diet induced a higher proportion of *Firmicutes* ($q<0.0001$, 76.2 ± 3.5% vs 60.9 ± 4.1% in Chow) and reduced the relative proportion of *Bacteroidetes* ($q<0.0001$, 6.7 ± 2.0% vs 29.3 ± 3.2% in Chow) (**Figure S2-A**). Remarkably, both polyphenols-rich CP and BP supplemented diets decreased the relative proportion of the phylum *Firmicutes* ($q<0.0001$, 55.6 ± 4.9% and 59.6 ± 4.4% respectively) and significantly prompted the phylum *Verrucomicrobia*, nearly doubling the relative proportion to 28.1 ± 3.9% in CP-fed mice and 25.4 ± 3.6% in BP-fed mice as compared to 14.9 ± 2.7% in HFHS-fed mice ($q<0.01$ and $q<0.05$ for CP and BP respectively). A significant increase of the phylum *Actinobacteria* was also observed in mice fed the polyphenols-rich CP-diet ($q<0.05$, 11.6 ± 2.0%), likewise, the BP-diet tended to favor this

phylum (9.3 ± 1.9%, corrected p value, q=0.0533) compared to HFHS control mice (4.5 ± 0.8%) (**Figure S2-A**).

Polyphenols-rich CP and BP diets triggered health-promoting bacterial taxa in HFHS fed mice

All treatments presented similar β-diversity distances of gut microbiota structure at baseline. Therefore, pairwise comparisons (Kruskal-Wallis test with *pos-hoc* multiple comparisons corrections) at the family and genus level were performed between groups at week 8. Taxonomic summary bar plots (**Figure S2-B**) present ASVs assigned gut bacteria families and genera, indicating the proportion in each dietary group at the end of the intervention. In the Chow-fed mice, the family *Muribaculaceae* (29.3 ± 3.2%) and *Lactobacillaceae* (17.0 ± 4.7%) covered the majority of the mouse gut microbes. However, the consumption of HFHS-diet significantly dropped the mouse faecal abundance of those families (q<0.0001, 6.7 ± 2.0% of *Muribaculaceae* and q<0.05, 7.7 ± 4.7% of *Lactobacillaceae*). On the contrary, the HFHS-fed mice had higher abundances of *Lachnospiraceae* (q<0.0001, 26.0 ± 2.5% vs 7.0 ± 1.0% in Chow), *Ruminococcaceae* (q<0.01, 21.0 ± 3.8% vs 9.0 ± 1.3% in Chow), followed by *Peptostreptococcaceae* (q<0.05, 5.8 ± 2.4% vs 0.1 ± 0.1% in Chow). Surprisingly, when compared to HFHS, the diet-supplementation with CP inhibited the growth of *Lachnospiraceae* (q<0.0001, 8.7 ± 1.3%), *Ruminococcaceae* (q<0.05, 11.3 ± 1.7%) and *Peptostreptococcaceae* (q<0.05, 0%), keeping their relative abundances close to those observed in the Chow-fed control mice (**Figure S2-B**); this was not the case for CF-supplemented mice. Although BP also contained polyphenols, the mice fed this diet did not have an altered abundance of the above-mentioned HFHS-induced opportunistic taxa. Alike, there was no differential abundance of other taxa at the family level in mice fed the fibre-rich BF-diet as compared to the HFHS-fed group.

Particularly, the polyphenols-rich CP and BP diets selectively promoted bacterial families known to confer beneficial effects to host health. Selective prebiotic-like effects on the abundance of *Akkermansiaceae* and *Coriobacteriales_Incertae_Sedis* were favored by CP and BP, but this outcome was not triggered by the diets supplemented with their corresponding fibres fractions. At

week 8, the proportions of *Akkermansiaceae* in Chow and HFHS groups were 10.0 ± 4.3% and 12.6 ± 1.6% respectively. *Akkermansiaceae* was increased in CP and BP-fed mice in 28.1 ± 3.9%, and 25.4 ± 3.6% respectively as compared to HFHS-fed mice ($q<0.05$). On the opposite, the mice fed the fibre-rich fractions presented 16.2 ± 3.9% and 15.1 ± 2.8% for CF and BF respectively. While the polyphenols-degrading family *Coriobacteriales_Incertae_Sedis* were undetected in both the mice fed the Chow and HFHS-diet after 8 weeks of the intervention, this family was distinctly promoted by the CP and BP-enriched diets, increasing up to 9.1 ± 1.9% and 5.2 ± 1.5% in HFHS-diet induced obese mice ($q<0.0001$ vs HFHS). Importantly, within the fibres-containing diets, only the CF stimulated *Coriobacteriales* as compared to HFHS-fed mice ($q<0.05$), indicating that residual non-extractible polyphenols were present in the cranberry fibres, likely, high molecular weight compounds forming non-covalent interactions with the cell wall polysaccharides. This finding was further confirmed by analyzing the PACs content in the blueberry and fibrous cranberry fractions, showing the presence of non-extractible PACs in CF (**Table S4**).

Polyphenols-rich CP and BP diets exert selective prebiotic effects on *Akkermansia muciniphila*, *Dubosiella newyorkensis* and *Angelakisella* in HFHS fed mice

By analysing ASVs at a finer-taxonomic level, 59 genera were identified in the mouse fecal microbiota composition (**Figure S2-C**). Within the taxa distinctly modulated by the diets, *Akkermansia muciniphila* was the only gut bacterial species representing the family *Akkermansiaceae,* selectively prompted in the polyphenols-rich CP and BP-diet fed mice ($q<0.05$ as compared to HFHS). These results were further confirmed by amplifying the *A. muciniphila* 16S rRNA gene copy by qPCR, which relative proportions were significantly correlated with the data obtained from the 16S rRNA sequencing (spearman $R^2>0.902$ in all the groups, $p<0.0001$, see supporting information **Figure S3**). The genera *Lactobacillus* (12.4 ± 5.2%), an unassigned genus of the family *Coriobacteriales* (9.1 ± 1.9%), the *Lachnospiraceae_NK4A136_group* (9.0 ± 1.4%) and *Dubosiella* (3.5 ± 1.1%) were particularly stimulated in CP fed mice. In the BP-fed

mice, the *Lachnospiraceae_NK4A136_group* (4.8 ± 0.9%) and unassigned genus of *Coriobacteriales* (5.2 ± 1.5%) were predominant.

Considering that a large number of genera were modulated in the mouse faecal microbiota, *DESeq2* differential analysis were performed to find out significant changes in the relative abundance of bacterial taxonomies after 8 weeks of intervention. This complementary statistical approach was used to estimate the taxa fold changes, while accounting for library size and biological variability (Love et al., 2014) between treatments as compared to the HFHS fed mice. Only the ASVs-assigned genera with the associated bacterial families that were significantly increased and decreased by more than 2-fold after p-values adjustment (FDR Bonferroni correction, $q<0.05$) are presented in the **Figure 4.**

The *DESeq2* analysis revealed that the HFHS-diet differentially influenced the abundance of 51 genera as compared to the standard Chow-diet (**Figure 4**). On the one hand, it drastically decreased bacterial taxa such as *Clostridium_senso_stricto_1* (9-fold), *Muribaculaceae*, *Eggerthellaceae* (8-fold), *Lachnospiraceae_NK4A136_group* (8-fold), *Rumicococcaceae_UCG_014* (7-fold), *Lachnospiraceae_UCG_001* (4-fold), *Angelakisella* (4-fold), and *Dubosiella* (2-fold), which bacterial species was identified as *D. newyorkensis*. On the other hand, genus such as *Romboutsia* (Family *Peptostreptococcaceae*), genera of the family *Ruminococcaceae*, (including *Ruminiclostridium*, *Oscillibacter*, *Butyricicoccus*, and *Anaerotruncus)*, genera belonging to the family *Lachnospiraceae* (including *Roseburia* and *Acetatifactor)*, and the genus *Lactococcus* were significantly over-represented in HFHS-fed mice as compared to Chow-group (**Figure 4 A**). Surprisingly, the CP-diet enrichment significantly repressed the abundance of *Romboutsia, Ruminiclostridium, Roseburia, Oscillibacter, Lactococcus,* and *Butyricicoccus*.

Within the taxa stimulated by CP-diet, there was a 5-fold and 10-fold increase in an unassigned genus belonging to the polyphenols-degrading families *Eggerthellaceae* and *Coriobacteriales_Incertae_Sedis* respectively, as compared to the HFHS-fed mice (**Figure 4 B**). Moreover, there were 2-fold up to 8-fold higher abundance of the genus *Angelakisella,*

Muribaculaceae, *Dubosiella* and *Lachnospiraceae_NK4A136_group* in mice supplemented with CP.

As found in the CP-fed mice, BP inhibited the genera *Romboutsia,*

m and *Oscillibacter* compared to HFHS-fed group. Interestingly, this treatment prompted both a 5-fold increase of *Eggerthellaceae* and a 10-fold increase of *Coriobacteriales_Incertae_Sedis* (**Figure 3 B-D**). Likewise, and in lesser proportion, it stimulated an unassigned genus of the *Muribaculaceae,* the genera *Angilakisella,* and *Dubosiella*.

The fibre-rich CF-diet decreased *Ruminiclostridium*, *Oscillibacter,* and *Anaerotruncus.* The ASVs the most promoted by both the CF and BF-diet were *Lachnospiraceae_NK4A136_group* and *Acetatifactor,* being 7- and 8-fold higher than in HFHS-fed treatment, respectively. Considering their high content in fibres, those diets promoted polysaccharides-degrading taxa, such as *Clostridium_senso_stricto_1, Muribaculaceae* and *Roseburia* (**Figure 3 C**). The BF-diet significantly reduced 5 ASVs, including the genus *Lactobacillus,* and 15 were significantly stimulated as compared to HFHS (**Figure 3 F**). However, in contrast to the CF-diet, the BF did not modulate the polyphenols-degrading families *Eggerthellaceae* and *Coriobacteriales,* as found on the diets supplemented with both cranberry constituents CP and CF.

Akkermansia muciniphila and *Coriobacteriales Incertae Sedis* are key biomarkers of polyphenols-rich diets fed mice gut microbiota

Using LEfSe analysis (**Figure 5**), we identified taxonomic biomarkers that were distinctly driven by the polyphenols-rich CP and BP diets and by their fibre-rich fractions CF and BF in HFHS-diet induced obese mice. This analysis complemented both the pairwise comparisons and the *DESeq2* analysis. Remarkably, *A. muciniphila* was revealed as the main bacterial biomarker discriminating the gut microbiota composition of mice fed the polyphenols-rich CP and BP-diets, showing a high LDA score of 4.8 for both groups. In addition, *Coriobacteriales_Incertae_Sedis, Lachnospiraceae_NK4A136_group, Eggerthellaceae,* and *Ruminococcaceae_UCG_014* were characteristics in mice fed both the CP and BP-enriched diets. Noteworthy, the CP-diet specifically

prompted the genera *Angelakisella,* and *Dubosiella* showing 3.6 LDA scores. The *Lachnospiraceae_NK4A136_group* was the most representative bacterial taxon in both CF and BF when comparing to HFHS, presenting 4.7 and 4.0 LDA scores, respectively. It is worth mentioning that within the fibre-containing diets, only that from cranberry (CF) revealed the polyphenols-degrading families *Coriobacteriales_Incertae_Sedis* and *Eggerthellaceae* as bacterial biomarkers.

Gut microbiota composition discriminates the type of diet supplementation and body weight changes in mice

To identify specific bacterial taxa significantly associated with mice phenotypes, spearman rank correlations and Canonical Correspondence Analysis (CCA) were performed. The features of BW gain, adipose tissues accretion (IWAT and EWAT), energy efficiency, caecum size, mucus thickness and the liver triglycerides were included in the correlative analyses. The correlation coefficients observed between bacterial abundances at the genus level and mouse phenotypes are illustrated in a heatmap (**Figure 6 A**). Analysis of the mice gut microbiota indicates that the abundance of predominant families *Muribaculaceae, Lactobacillus, Lachnospinaceae_NK4A136_*group and *Clostridium_sensu_stricto_1*, negatively correlated with BW gain, adipose tissues accretion, energy efficiency and liver triglycerides ($p<0.05$). Interestingly, among the polyphenols-degrading families, the family *Eggerthellaceae* was inversely correlated with the BW gain ($p<0.05$) and was positively correlated with an improved caecum size and mucus thickness (R^2 0.435 and 0.563 respectively, $p<0.0001$). On the opposite, an unassigned genus belonging to the family *Lachnospinaceae,* the family *Ruminococcaceae* and the genus *Ruminiclostridium* were positively correlated with the BW gain, energy efficiency and the reduced caecum size, which is consistent with the HFHS-diet induced obesity characterized by an increased relative abundance of those taxa.

Confirming the causal effect of diet on the gut microbiota composition and its link with the changes in the mice phenotypes, the CCA diagram reveals divergent microbial key players in mice fed the Chow-diet and CP-diet from those observed in HFHS-fed obese mice. Surprisingly, the taxa of *Muribaculaceae, Lachnospiraceae_NK4A136_group*, *Eggerthellaceae* and *Lactobacillus* assembled with Chow-diet and were correlated with the mucus thickness. Likewise, *Dubosiella,*

Coriobacteriales and *Akkermansia* characterized the CP-diet, and differed from the HFHS-fed group within the CCA. In this sense, the mice fed the HFHS-diet, as well as the groups of BP, BF and CF fed mice clustered in the same direction of the BW gain, the accretion of adipose tissues (IWAT and EWAT) and the increase of energy efficiency. In this case, the family *Lachnospiraceae* characterized this last cluster (**Figure 6 B)**. The PERMANOVA analysis for the CCA showed a R^2 score of 0.36472 ($p<0.0001$).

To assess which gut microbial communities were affected by the diet composition, we performed a multivariate association with linear models (MaAsLin) analysis. To do so, abundant ASVs were tested for their dependence on the polyphenols-rich and fibre-rich diets, demonstrating the main effects of the type of berry constituents on promoting specific bacterial taxa (**Figure 6 C)**. Interestingly, the families *Coriobacteriales_Incertae_Sedis* and *Eggerthellaceae* stood out as representative of the BP and CP diets, underlining a significant species/polyphenol interaction ($q<0.0001$). Moreover, the family *Eggerthellaceae* was strongly correlated with the Chow-diet with a positive coefficient of 0.764 ($q<0.0001$). Most of the abundant bacterial taxa in HFHS-fed mice, were significantly negatively correlated with the Chow and CP-diets. These changes in microbial composition coincided with changes in mice phenotypes such as body weight and liver triglycerides, as well as, with the functional structure of the gut microbiota inferred indirectly from 16S sequences using Tax4Fun2 software.

The polyphenols-rich CP-diet are associated with specific predicted functions of gut microbial communities in HFHS fed mice

The variation in the gut microbiota functions of animals fed the polyphenols-rich CP and BP diets and their fibre-rich CF and BF fractions were evaluated based on Bray-Curtis dissimilarities and LEfSe analyses of functional profiles obtained by Tax4Fun2. At week 8, the gut microbiota KEGG-assigned functions (level 1 and 2) of HFHS-fed mice differed consistently from those fed the Chow-diet, irrespective of the choice of analytical statistical method (LEfSe and PERMANOVA) (supporting information **Figure S4-S6** and **Figure 7**). The gut microbial communities of HFHS-fed mice displayed very divergent functions compared to the Chow-fed mice, as indicated by the separated centroid of these groups in the PCoA space (**Figure 7 A**).

Surprisingly, the gut microbial community members of the polyphenols-rich CP-diet had distinct functional profile from HFHS-diet fed obese mice. The CP-fed mice clearly shifted away from the HFHS-fed group, and remained positioned at the level of the Chow-fed mice within the PCoA axis 2 (43.4% of variation), indicating that the CP-induced microbial changes had a functional structure comparable to that of the Chow-control group (see **Figure 7 A)**. Moreover, the polyphenols-rich BP-diet and the fibre-rich CF fraction had similar microbial function patterns, as indicated by the proximity of their group centroids; however, both BP and CF centroids slightly moved away from the HFHS-fed group. Conversely, the fibre-rich BF-diet did not impact the gut microbial functions of HFHS-diet induced obese mice, remaining closely linked to the HFHS cluster centroid in the PCoA space. The PERMANOVA for the β-diversity analysis based on the diet-induced modulation of the functional pathways showed a R^2 score of 0.3007 ($p<0.001$), from variations of 42.4% and 51.1% in PCoA axes 2 and 1 respectively. In addition, the *betadisper* results showed no significant differences in the dispersions of mice within each group (*permutest* F value 0.8317, p=0.514), demonstrating that the PERMANOVA-obtained p-value was strongly influenced by the changes in the taxonomic functional structures, and was not an artifact of the heterogeneous dispersions of group's variances.

CP-enriched diet favours distinct metabolic functions by coexisting bacterial taxonomies in HFHS fed mice

We further analyzed the functional redundancy (FRI) found in bacterial community members in order to evaluate the coexistence of taxonomic assigned-sequences capable of fulfill analogous metabolic functions. The FRI was obtained by Tax4fun2 analysis and the results were plotted in a PCoA based on the Bray-Curtis distance measurement (**Figure 7 B**). In particular, as compared to the HFHS-fed group, the CP cluster centroid in the PCoA markedly diverged away from the HFHS-centroid (see **Figure 7 B**), suggesting that certain metabolic functions were distinctively represented by bacterial taxonomies prompted by the CP-enriched diet. Also, the distance-based redundancy analysis showed a clear, but less pronounced separation amongst mice belonging to the BP, BF and CF groups and those from the HFHS-control diet. The PERMANOVA analysis of functional redundancy supported the dissimilarities among the clustered diets, showing a R^2 of

0.2740 ($p<0.001$) with 17.7% and 16.2% of variations on the PCoA axis 1 and 2 respectively. Likewise, the homogeneity of dispersions within groups was confirmed (*permutest* $p>0.05$).

The PCoA of functions redundancy unveiled the overlapping of centroids of BP, BF, and CF-fed mice close to those fed the HFHS (**Figure 7 B**). This demonstrates that predicted metabolic functions are strongly conserved in the bacterial communities identified in all aforementioned groups, although the relative abundance and taxonomic composition of the gut microbiota differed across the polyphenols-rich BP and the fibre-rich BF and CF diets (as shown by the β-diversity and *DESeq2* analyses, **Figure 3** and **Figure 4**).

The LEfSe results correlated with those obtained by distances-based dissimilarities in functional redundancy between the gut microbiota of groups (supporting information **Figure S3-S5**). The LEfSe analysis based on the KEGG level 2, showed 10 functional pathways significantly overrepresented in the gut microbiota composition of HFHS-diet induced obese mice. Genes encoding for energy metabolism (mainly sulfur metabolism, nitrogen metabolism and methane metabolism at the KEGG level 1), the pathway of global and overview maps (mainly microbial metabolism in diverse environments, carbon metabolism and fatty acid metabolism), and amino acid metabolism (encompassing cysteine and methionine metabolism, histidine metabolism and arginine biosynthesis) were featured in the HFHS-fed mice as compared to the Chow control group (supporting information **Figure S4-A** and **Figure S5**). In contrast, the CP-diet favored functional pathways involved in antimicrobial drug resistance, and membrane transport, among others as compared to HFHS-fed mice (**Figure S4-B** and **Figure S6-A**). In the case of BP-fed mice, pathways related to metabolism of cofactors and vitamins, lipid metabolism and DNA replication and repair were significantly enriched when compared to HFHS-fed mice (**Figure S4-C**). The fibre-rich CF diet promoted the nucleotide metabolism, the amino acids metabolism and the carbohydrate metabolism among others functional pathways. However, the BF diet only revealed two pathways being significantly modulated (valine, leucine and isoleucine degradation, and tyrosine metabolism) as compared to HFHS-fed mice (**Figure S4 D-E**).

The predicted microbial functions profile correlates with improved liver TG, energetic efficiency and body weight changes

After assessing the relationship between diet and mice phenotypes with the gut microbiota composition in a multivariate model, we evaluated the link between mice phenotypes and energy metabolism (liver TG, energetic efficiency and BW gain) and the microbial functional pathways via MaAsLin software. The correlation between mice phenotypes performed with upregulated and downregulated functional pathways of all treatments, uncovered a number of enriched pathways, among which the glutathione metabolism was found negatively correlated with both BW gain and energy efficiency in mice after 8 weeks of dietary intervention (Supporting information **Table S5** and **Table S6**). Relative abundances of 37 functional pathway genes (level 1) were significantly correlated with body weight changes (FDR $q<0.001$). Within the top-3 microbial functions, genes coding for amino sugar and nucleotide sugar metabolism, fructose and mannose metabolism, and glutathione metabolism were negatively correlated with the BW gain in mice. In contrast, functional pathways such as biosynthesis of secondary metabolites, biosynthesis of antibiotics, and biosynthesis of phenylalanine, tyrosine and tryptophan were positively correlated to the BW gain. These findings are further supported by the LEfSe analysis (supporting information **Figure S5**), demonstrating the significant over-representation of 48 functional pathways in HFHS-fed obese mice as compared to Chow group. These observations provide an explanation of how gut microbiota functions can attenuate the obesity-associated phenotypes in HFHS-fed mice.

The reduction in liver TG level was inversely correlated with the predicted microbial pathways of degradation of aromatic compounds, ethylbenzene degradation, and alpha-linolenic acid metabolism (supporting information **Table S7**). Regarding to the changes in energy efficiency, in addition of the pathway of glutathione metabolism, the genes coding for the pathways of ABC transporters, starch and sucrose metabolism, and glycolysis/gluconeogenesis were negatively correlated.

Discussion

The approach used in the present study was helpful to appraise the prebiotic potential and influence of polyphenols-rich cranberry and blueberry powders from their fibre-rich fractions on obesity-associated disorders. We demonstrated that the polyphenols-rich CP reduced the adipose tissue accumulation, reduced BW gain, and improved the energy balance, without affecting food intake in HFHS-fed obese mice. However, these results were not reproduced by the fibrous fraction from the same fruit, even if they tended to lower the mice BW ($p=0.0826$), indicating that the polyphenols of cranberry are the functional compounds largely contributing to counteract the obesity-related phenotypes. In contrast, the BP-enriched diet did not induce significant changes on fat mass accumulation and BW gain of obese mice, even if the polyphenols-rich CP and BP were incorporated to the HFHS-diet providing an equal caloric charge. In our study, the CP was a mix of anthocyanins, phenolic acids, oligomers and polymers of PACs (degree of polymerisation DP between 1-5 and DP>10, respectively). Particularly, the PACs, which were the most abundant flavonoids in the composition of the cranberry powder used herein, have been shown to exert strong effects on the energy expenditure by different mechanisms, that is, acting on the adipose tissue, skeletal muscle and liver (Caimari et al., 2013; Zhou et al., 2019). Here, the polyphenols-rich CP-diet suppressed the HFHS-induced fat deposition in IWAT, and to a less extent, in EWAT tissues. In support of our results, previous studies showed that the gavage-based supplementation of cranberry polyphenolic extract decreased BW gain, improved glucose homeostasis, and lowered hepatic TG in obese mice, and that such effects, were strongly linked to the gut microbiota composition (Anhê et al., 2017).

The consumption of HFHS-diet reduced the colonic mucus thickness and affected the gut microbial richness and diversity. Importantly, an improved mucus thickness was induced by BP, and all the berry-based diets increased the gut microbial richness in HFHS-diet induced obese mice. The increased microbial richness and diversity stimulated by cranberry and blueberry constituents, corroborates other reports, linking the gut microbiota modulation to obesity, diabetes and IBD (Anhê et al., 2017; Henning et al., 2018; Lacombe et al., 2013b; Zhao et al., 2017). Additionally, our findings agree with several studies using polyphenols-rich diets, showing the

influence of the gut microbiota in improving energy balance, metabolic function, intestinal barrier and changes in body weight (Henning et al., 2018; Masumoto et al., 2016; Zhao et al., 2017).

When analysing at a deeper taxonomic level, individual ASVs were modulated selectively in mice fed the polyphenols-rich diets, but they were not significantly modulated in mice fed the fibre-enriched diets. Particularly, the families *Peptostreptococcaceae* (*Romboutsia* genus), *Lachnospiraceae* and *Ruminococcaceae*, (including *Ruminiclostridium*, *Oscillibacter*, and *Butyricicoccus*), shown to dominate the gut microbiota after the consumption of a high fat diet, were associated to increasing body weight in mice (Kameyama and Itoh, 2014; Qin et al., 2018; Zhao et al., 2017). Those commensal bacteria, which are able to induce intestinal inflammation or pathology under diet-induced obesity, diabetes (Gurung et al., 2020) or any gut environmental alteration, are actually pathobionts. Interestingly, these were impeded by CP and BP-diets. The suppressive effect of polyphenols-rich diets against opportunistic gut bacteria appears as one of the mechanisms involved in the prevention of obesity-associated gut dysbiosis in mice. Noteworthy, we also highlighted the prebiotic effect of polyphenols on bacterial families related to a lean phenotype and intestinal homeostasis. Indeed, polyphenols-rich CP and BP diets caused a strong bloom of *A. muciniphila*. In this respect, substantial evidence supports the role of this bacterium in improving metabolic phenotypes in obesity and diabetes, regulating the gut inflammation and host immune system (Ansaldo et al., 2019; Everard et al., 2013; Schneeberger et al., 2015a). Furthermore, an unassigned genus of *Muribaculaceae,* the taxa characteristic of Chow-fed lean mice, was stimulated by CP and BP in HFHS-fed obese mice and was negatively correlated with BW gain. Surprisingly, consistent to our findings, *Muribaculaceae* appears to be involved in the prevention of obesity (Cao et al., 2019). This family, were known as *S24-7* in GreenGenes sequences database (Lagkouvardos et al., 2019), and referred in Ribosomal Database Project (RDP) as *Porphyromonadaceae* (*Barnesiella,* is now suggested a different phylogenetic species) (DeSantis et al., 2006; Wang et al., 2007a). *Muribaculaceae* species, belonging to the phylum *Bacteroidetes,* are specialized in degrading dietary carbohydrates and are considered microbial biomarkers of a healthy mouse microbiome (Yang et al., 2019); the abundance of this species is drastically reduced by HFHS-diets as showed in other reports (Cao et al., 2019; Hou et al., 2019) and as observed in the present study.

The findings presented here underline the distinct mechanisms by which polyphenols and fibres exert their probiotic effects. The MaAslin model was useful to demonstrate how changes in the relative abundance of specific bacterial taxa are driven by the presence of cranberry and blueberry fibres and polyphenols in HFHS-fed mice; such results were based on the statistical FDR corrected significance of multivariate associations. Essentially, the family *Coriobacteriaceae* and *Eggerthellaceae* were triggered by the presence of polyphenols in the diet, yet the *Eggerthellaceae* was also associated to the Chow-diet intake, likely due to the high content of cereal derived fibres in the latter (cellulose, hemicellulose, and lignin, Harlan Teklad global diets 2018). Interestingly, *Dubosiella* and *Angelakisella* were selectively prompted by both CP and BP. *Dubosiella newyorkensis* was identified using DADA2 pipeline and SILVA sequences library. Surprisingly, this species belonging to the family *Erysipelotrichaceae*, is used as a patented probiotic for modulating weight loss and preventing metabolism and immunity associated diseases, such as obesity, diabetes, metabolic syndrome, and abnormal lipid metabolism (Cox and Blaser, 2018). Additionally, *Angelakisella* may be a biomarker of Chow-fed lean mice microbiota; it is strongly decreased by 4.0-fold in mice fed HFHS-diet. *Angelakisella* is a newly described bacterial species isolated from human ileum (Mailhe et al., 2017), for which functional benefits remain to be explored. These genera may be involved in the microbes-mediated anti-obesity effects by polyphenols.

The polyphenols-degrading bacterial families have been shown to potentiate bioactive phenolic metabolites (González-Sarrías et al., 2017). Of particular interest is the *Eggerthellaceae* family, including gut associated genera such as *Eggerthella, Paraeggerthella, Gordonibacter* and *Slackia* (Cho et al., 2016; Gupta et al., 2013), whose xenobiotic metabolism is linked to positive effects in host lipid metabolism and hepatic detoxification activity in mice (Cho et al., 2016; Claus et al., 2011; Clavel et al., 2014). Interestingly, the family *Eggerthellaceae* was 5-fold more abundant in mice fed the Chow, BP, CP and the cranberry fibres CF as compared to HFHS, and correlated to reduced BW gain, as well as to restored intestinal histomorphology (caecum weight and mucus thickness) in obese mice.

The fibre-enriched diets can promote the growth of SCFA-producing genera shown to contribute to lipid metabolism and prevent metabolic abnormalities in mice (den Besten et al.,

2015; Weitkunat et al., 2016). Noteworthy, the fibre-rich CF-diet decreased the hepatic TG in obese mice, but this was not the case with the fibre-rich BF. Non-extractible PACs were found associated with cranberry fibres, which could provide added effect on both the gut microbiota composition and related functions. Supporting this interpretation, a previous study showed that the supplementation with both fibres and polyphenols from peach by-products ameliorated insulin resistance and hepatic steatosis and decreased TG content in high-fat high-fructose fed (HFF) obese rats (Rodríguez-González et al., 2018).

In the present study, synergistic effects between cranberry fibres and polyphenols are inhibiting obesity-associated pathobionts. The CF-diet inhibited *Ruminiclostridium*, *Oscillibacter,* and *Anaerotruncus* genera that were increased in untreated HFHS-fed mice; in contrast, the BF-diet supplementation did not affect their abundance, and thus, did not improve the obesity phenotypes. In this context, a recent review summarized how unabsorbed polyphenols can be associated to fibres by non-covalent binding (Jakobek and Matić, 2018). In particular, because of their structure and spatial configuration, A-type PACs found in cranberry (Prior et al., 2001) were shown to have a higher affinity to pectin (Mamet et al., 2018), a naturally occurring polysaccharide found in berries. In addition, cranberry purified oligosaccharides exert antimicrobial and anti-adhesive properties against pathogens (Sun et al., 2015), as do polyphenols (Lacombe et al., 2013c; Lacombe and Wu, 2017). Here, we demonstrated the antimicrobial effects of cranberry fibres fraction as reported elsewhere (Hotchkiss et al., 2015; Sun et al., 2015), and the influence of repressed pathobionts on the mice metabolic status and BW gain, as sustained by the multivariate correlation analysis in the present study.

Consistent to other studies (Mykkanen et al., 2014; Prior et al., 2008), the whole berry powders and fibrous fractions supplementation failed to improve the glucose intolerance induced by HFHS diet. Several factors, including the shorter duration of dietary intervention (8 weeks), and the feeding of cranberry and blueberry fruit powders rather than concentrated polyphenols and purified fibres, likely led to these results. Nevertheless, the duration of dietary exposure was sufficient to significantly modulate the gut microbiota of mice. The improvements of metabolic, intestinal and BW phenotypes induced by the berry enriched diets were highly related to a distinct gut microbiota structure between the treated groups compared to HFHS. Within this framework, the functional

structure analysis based in Bray-Curtis distance matrix demonstrated that the CP-diet resulted in a distinct metabolic profile in the gut microbiota as compared to HFHS. Changes in the functional redundancy of the gut microbiota of CP-fed mice indicated that metabolic pathways were singularly represented by taxonomically different gut bacteria, suggesting an improved microbial functions diversity and resiliency. Surprisingly, the CP-supplementation was able to correct the microbial metabolic alterations in HFHS-fed mice and bring them closer to that of Chow control group. Noteworthy, the predicted KEGG functional categories such as energy metabolism, amino-acid and fatty acid metabolism that were dominant in untreated HFHS-fed obese mice, as observed in previous study (Daniel et al., 2014), were also significantly repressed by polyphenols-rich diets. In terms of metabolic functions, the FRI analysis explains why the BF-fed mice kept the obesity-associated phenotypes as observed in HFHS-fed obese mice. The Bray-Curtis dissimilarities, while accounting for KEGG orthologues markers, indicate that the BF-group overlapped the HFHS, emphasising that despite the fact that some taxonomic abundances were significantly modulated by this fibre-rich diet, the obesity-related metabolic functions were not influenced.

Conclusions

The present study demonstrates that polyphenols from cranberry and not their constitutive fibres are involved in the amelioration of obesity-associated disturbances. Specifically, polyphenols-rich diets improved the HFHS-diet induced gut microbiota dysbiosis in obese mice. We highlight the selective prebiotic effects of polyphenols on *A. muciniphila*, *Muribaculaceae*, *Dubosiella newyorkensis*, *Angelakisella*, *Coriobacteriaceae*, and *Eggerthellaceae*. Among those taxa, *Eggerthellaceae* and *Muribaculaceae* were revealed as key microbial players highly related to BW loss and to a restored intestinal histomorphology. To the best of our knowledge, this is the first study reporting the prebiotic effects of cranberry and blueberry polyphenols on *Dubosiella newyorkensis*, a novel bacterial marker identified to counter metabolic diseases (Cox and Blaser, 2018).

Apart from the gut microbiota composition, the assessment of its metabolic functional structure constitutes a relevant approach to understand the mechanism by which polyphenols can prevent metabolic disorders associated with obesity. The functional redundancy analysis of the gut

microbiota also emerges as useful tool to study the metabolic contribution of bacteria, and how specific taxa fulfill diversified functional roles in the host. Remarkably, cranberry powder strongly influenced energy efficiency, white adipose tissues reduction and BW loss in obese mice; these effects were associated with a shift in the predicted metabolic profile of the gut microbiota. The significant bloom of polyphenols-degrading families of *Coriobacteriaceae* and *Eggerthellaceae* by CF, point to the presence of non-extractible polyphenols interacting with the cranberry fibres; we infer that a synergy between cell wall polysaccharides and polyphenols in cranberry fibre-rich fraction ameliorates the hepatic TG and microbiota composition. Our findings support not only the use of polyphenols, but the whole berries containing polyphenols/cell wall polysaccharides, as preventative strategy against metabolic diseases by modulating the functional and compositional profile of the gut microbiota.

Star methods

Key resource table

Contact for reagent and resource sharing

Experimental model and subject details

Diet preparation

Experimental design of animal bioassay

Method details

Characterization of the whole berry powders and derived fib

Glucose homeostasis and hepatic triglycerides assessment

Colon histology

Fecal DNA extraction and 16S rRNA gene amplicon library preparation and sequencing

16S rRNA sequences processing

Microbial functional profiling

Analysis of 16S rRNA gene copies of *Akkermansia muciniphila* by quantitative real-time PCR

Quantification and statistical analysis

Microbial community composition and differential abundance statistical analysis

Mouse phenotypes Statistical analysis

Supplementary information

Supplemental Information includes six figures and seven tables.

Author contributions

Y.D., D.R, G.P., E.L. and A.M. conceived the study. M.R.D. and M.R. were involved in the animal experiments. M.R performed the metabolic assays. M.R.D. performed the histological analysis of colon tissues. M.R.D. performed the 16S rRNA sequences processing, analysis of the gut microbiota structure and functional profiling. M.R.D. performed the statistical analysis of the microbiome composition and mouse phenotypes. M.R.D. and YD discussed and wrote this manuscript. All authors contributed to reviewing and editing the manuscript.

Acknowledgments

This study was funded by Fruit D'Or, CRIBIQ, MITACS, Atrium Innovation, Diana Food Canada. M.R.D was supported by the COLCIENCIAS PhD. scholarship. We thank the internship Blanca Elizabeth Ruiz Alvarez for participating in the image analyses of histological preparations.

References

Adam, C.L., Williams, P.A., Dalby, M.J., Garden, K., Thomson, L.M., Richardson, A.J., Gratz, S.W., and Ross, A.W. (2014). Different types of soluble fermentable dietary fibre decrease food intake, body weight gain and adiposity in young adult male rats. Nutrition & Metabolism. 11(1), 36. DOI: 10.1186/1743-7075-11-36.

Anhê, F.F., Nachbar, R.T., Varin, T.V., Vilela, V., Dudonné, S., Pilon, G., Fournier, M., Lecours, M.-A., Desjardins, Y., Roy, D., et al. (2017). A polyphenol-rich cranberry extract reverses insulin resistance and hepatic steatosis independently of body weight loss. Molecular Metabolism. 6(12), 1563-1573. DOI: 10.1016/j.molmet.2017.10.003.

Anhê, F.F., Roy, D., Pilon, G., Dudonné, S., Matamoros, S., Varin, T.V., Garofalo, C., Moine, Q., Desjardins, Y., Levy, E., et al. (2014). A polyphenol-rich cranberry extract protects from diet-induced obesity, insulin resistance and intestinal inflammation in association with increased *Akkermansia* spp. population in the gut microbiota of mice. Gut. 64(6). DOI: 10.1136/gutjnl-2014-307142.

Ansaldo, E., Slayden, L.C., Ching, K.L., Koch, M.A., Wolf, N.K., Plichta, D.R., Brown, E.M., Graham, D.B., Xavier, R.J., Moon, J.J., et al. (2019). *Akkermansia muciniphila* induces intestinal adaptive immune responses during homeostasis. Science. 364(6446), 1179-1184. Published online 2019/06/22 DOI: 10.1126/science.aaw7479.

Auguie, B. (2016). gridExtra: miscellaneous functions for "grid" graphics. R package version 2.3

Barcelo, A., Claustre, J., Moro, F., Chayvialle, J.A., Cuber, J.C., and Plaisancié, P. (2000). Mucin secretion is modulated by luminal factors in the isolated vascularly perfused rat colon. Gut. 46(2), 218-224. DOI: 10.1136/gut.46.2.218.

Bindon, K.A., Smith, P.A., and Kennedy, J.A. (2010). Interaction between grape-derived proanthocyanidins and cell wall material. 1. Effect on proanthocyanidin composition and molecular mass. J Agr Food Chem. 58(4), 2520-2528. DOI: 10.1021/jf9037453.

Blaker, K., M., and Olmstead, J., W. (2015). Cell wall composition of the skin and flesh tissue of crisp and standard texture southern highbush blueberry genotypes. J Berry Res. 5(1), 9-15. DOI: 10.3233/jbr-140085.

Bourvellec, L.C., Bouchet, B., and Renard, C.M.G.C. (2005). Non-covalent interaction between procyanidins and apple cell wall material. Part III: Study on model polysaccharides. Biochimica et Biophysica Acta (BBA) - General Subjects. 1725(1), 10-18. DOI: 10.1016/j.bbagen.2005.06.004.

Caimari, A., del Bas, J.M., Crescenti, A., and Arola, L. (2013). Low doses of grape seed procyanidins reduce adiposity and improve the plasma lipid profile in hamsters. International Journal of Obesity. 37(4), 576. DOI: 10.1038/ijo.2012.75.

Callahan, B.J., McMurdie, P.J., Rosen, M.J., Han, A.W., Johnson, A.A., and Holmes, S.P. (2016). DADA2: High-resolution sample inference from Illumina amplicon data. Nature Methods. 13(7). DOI: 10.1038/nmeth.3869.

Camacho, C., Coulouris, G., Avagyan, V., Ma, N., Papadopoulos, J., Bealer, K., and Madden, T.L. (2009). BLAST+: architecture and applications. BMC Bioinformatics. 10, 421. Published online 2009/12/17 DOI: 10.1186/1471-2105-10-421.

Cao, W., Chin, Y., Chen, X., Mi, Y., Xue, C., Wang, Y., and Tang, Q. (2019). The role of gut microbiota in the resistance to obesity in mice fed a high fat diet. Int J Food Sci Nutr. 1-11. Published online 2019/11/28 DOI: 10.1080/09637486.2019.1686608.

Chen, C., You, L.J., Huang, Q., Fu, X., Zhang, B., Liu, R.H., and Li, C. (2018). Modulation of gut microbiota by mulberry fruit polysaccharide treatment of obese diabetic db/db mice. Food Funct. 9(7), 3732-3742. Published online 2018/07/12 DOI: 10.1039/c7fo01346a.

Cho, G.-S., Ritzmann, F., Eckstein, M., Huch, M., Briviba, K., Behsnilian, D., Neve, H., and Franz, C.M.A.P. (2016). Quantification of *Slackia* and *Eggerthella* spp. in human feces and adhesion of representatives strains to caco-2 cells. Frontiers in Microbiology. 7, 658. DOI: 10.3389/fmicb.2016.00658.

Claus, S.P., Ellero, S.L., Berger, B., Krause, L., Bruttin, A., Molina, J., Paris, A., Want, E.J., de Waziers, I., Cloarec, O., et al. (2011). Colonization-induced host-gut microbial metabolic interaction. mBio. 2(2), 10. DOI: 10.1128/mBio.00271-10.

Clavel, T., Desmarchelier, C., Haller, D., Gérard, P., Rohn, S., Lepage, P., and Daniel, H. (2014). Intestinal microbiota in metabolic diseases. Gut Microbes. 5(4), 544-551. DOI: 10.4161/gmic.29331.

Clifford, M.N. (2004). Diet-derived phenols in plasma and tissues and their implications for health. Planta Medica. 70(12), 1103-1114. DOI: 10.1055/s-2004-835835.

Collins, B., Hoffman, J., Martinez, K., Grace, M., Lila, M., Cockrell, C., Nadimpalli, A., Chang, E., Chuang, C.-C., Zhong, W., et al. (2016). A polyphenol-rich fraction obtained from table grapes decreases adiposity, insulin resistance and markers of inflammation and impacts gut microbiota in high-fat-fed mice. J Nutritional Biochem. 31, 150-165. DOI: 10.1016/j.jnutbio.2015.12.021.

Cox, L.M., and Blaser, M., 2018. Probiotic compositions for improving metabolism and immunity, in: N.Y. University (Ed.) Justia Patents, A61K 35/741 (20060101); A61K 45/06 (20060101) ed. New York University, New York , NY (US).

Daniel, H., Gholami, A., Berry, D., Desmarchelier, C., Hahne, H., Loh, G., Mondot, S., Lepage, P., Rothballer, M., Walker, A., et al. (2014). High-fat diet alters gut microbiota physiology in mice. The ISME Journal. 8(2), 295. DOI: 10.1038/ismej.2013.155.

De Vadder, F., Kovatcheva-Datchary, P., Goncalves, D., Vinera, J., Zitoun, C., Duchampt, A., Backhed, F., and Mithieux, G. (2014). Microbiota-generated metabolites promote metabolic benefits via gut-brain neural circuits. Cell. 156(1-2), 84-96. Published online 2014/01/15 DOI: 10.1016/j.cell.2013.12.016.

den Abbeele, P., Duysburgh, C., Jiang, A.T., Rebaza, M., Pinheiro, I., and Marzorati, M. (2018). A combination of xylooligosaccharides and a polyphenol blend affect microbial composition and activity in the distal colon exerting immunomodulating properties on human cells. 47. DOI: 10.1016/j.jff.2018.05.053.

den Besten, G., Bleeker, A., Gerding, A., van Eunen, K., Havinga, R., van Dijk, T.H., Oosterveer, M.H., Jonker, J.W., Groen, A.K., Reijngoud, D.-J., et al. (2015). Short-chain fatty acids protect against high-fat diet–induced obesity via a PPARγ-dependent switch from lipogenesis to fat oxidation. Diabetes. 64(7), 2398-2408. DOI: 10.2337/db14-1213.

Denis, M.C., Desjardins, Y., Furtos, A., Marcil, V., Dudonne, S., Montoudis, A., Garofalo, C., Delvin, E., Marette, A., and Levy, E. (2015). Prevention of oxidative stress, inflammation and mitochondrial dysfunction in the intestine by different cranberry phenolic fractions. Clin Sci (Lond). 128(3), 197-212. Published online 2014/07/30 DOI: 10.1042/CS20140210.

Deplancke, B., and Gaskins, R.H. (2001). Microbial modulation of innate defense: goblet cells and the intestinal mucus layer. Am J Clin Nutrition. 73(6). DOI: 10.1093/ajcn/73.6.1131S.

Depommier, C., Everard, A., Druart, C., Plovier, H., Van Hul, M., Vieira-Silva, S., Falony, G., Raes, J., Maiter, D., Delzenne, N.M., et al. (2019). Supplementation with *Akkermansia muciniphila* in overweight and obese human volunteers: a proof-of-concept exploratory study. Nat Med. 25(7), 1096-1103. Published online 2019/07/03 DOI: 10.1038/s41591-019-0495-2.

Derrien, M., Vaughan, E.E., Plugge, C.M., and de Vos, W.M. (2004). *Akkermansia muciniphila* gen. nov., sp. nov., a human intestinal mucin-degrading bacterium. International Journal of Systematic and Evolutionary Microbiology. 54(5), 1469-1476. DOI: 10.1099/ijs.0.02873-0.

DeSantis, T.Z., Hugenholtz, P., Larsen, N., Rojas, M., Brodie, E.L., Keller, K., Huber, T., Dalevi, D., Hu, P., and Andersen, G.L. (2006). Greengenes, a chimera-checked 16S rRNA gene database and workbench compatible with ARB. Applied and Environmental Microbiology. 72(7), 5069-5072. DOI: 10.1128/aem.03006-05.

Dowle, M. (2019). Extension of `data.frame`. R package version 1.12.6.

Dudonné, S., Dubé, P., Anhê, F., Pilon, G., Marette, A., Lemire, M., Harris, C., Dewailly, E., and Desjardins, Y. (2015). Comprehensive analysis of phenolic compounds and abscisic acid profiles of twelve native Canadian berries. Journal of Food Composition and Analysis. 44, 214-224. DOI: 10.1016/j.jfca.2015.09.003.

Everard, A., Belzer, C., Geurts, L., Ouwerkerk, J.P., Druart, C., Bindels, L.B., Guiot, Y., Derrien, M., Muccioli, G.G., Delzenne, N.M., et al. (2013). Cross-talk between *Akkermansia muciniphila* and intestinal epithelium controls diet-induced obesity. Proc National Acad Sci. 110(22), 9066-9071. DOI: 10.1073/pnas.1219451110.

Garcia-Mazcorro, J.F., Lage, N.N., Mertens-Talcott, S., Talcott, S., Chew, B., Dowd, S.E., Kawas, J.R., and Noratto, G.D. (2018). Effect of dark sweet cherry powder consumption on the gut microbiota, short-chain fatty acids, and biomarkers of gut health in obese db/db mice. PeerJ. 6, e4195. Published online 2018/01/10 DOI: 10.7717/peerj.4195.

Garnier, S. (2017). viridis: Default Color Maps from 'matplotlib'. R package version 0.5.1. [p426].

Gentleman, R., Carey, V., Huber, W., and Hahne, F. (2019). genefilter: methods for filtering genes from high-throughput experiments. R package version 1.68.0.

Gibson, G.R., Hutkins, R., Sanders, M., Prescott, S.L., Reimer, R.A., Salminen, S.J., Scott, K., Stanton, C., Swanson, K.S., Cani, P.D., et al. (2017). Expert consensus document: The International Scientific Association for Probiotics and Prebiotics (ISAPP) consensus statement on the definition and scope of prebiotics. Nature Reviews Gastroenterology & Hepatology. 14(8), 491-502. DOI: 10.1038/nrgastro.2017.75.

González-Sarrías, A., Espín, J., and Tomás-Barberán, F.A. (2017). Non-extractable polyphenols produce gut microbiota metabolites that persist in circulation and show anti-inflammatory and free radical-scavenging effects. Trends in Food Science & Technology. 69, 281-288. DOI: 10.1016/j.tifs.2017.07.010.

Guglielmetti, S., Fracassetti, D., Taverniti, V., Bo, C., Vendrame, S., Klimis-Zacas, D., Arioli, S., Riso, P., and Porrini, M. (2013). Differential modulation of human intestinal *Bifidobacterium* populations after consumption of a wild blueberry (Vaccinium angustifolium) drink. J Agr Food Chem. 61(34), 8134-8140. DOI: 10.1021/jf402495k.

Gupta, R.S., Chen, W., Adeolu, M., and Chai, Y. (2013). Molecular signatures for the class Coriobacteriia and its different clades; proposal for division of the class Coriobacteriia into the emended order Coriobacteriales, containing the emended family *Coriobacteriaceae* and *Atopobiaceae* fam. nov., and *Eggerthellales* ord. nov., containing the family *Eggerthellaceae* fam. nov. International Journal of Systematic and Evolutionary Microbiology. 63(Pt 9), 3379-3397. DOI: 10.1099/ijs.0.048371-0.

Gurung, M., Li, Z., You, H., Rodrigues, R., Jump, D.B., Morgun, A., and Shulzhenko, N. (2020). Role of gut microbiota in type 2 diabetes pathophysiology. EBioMedicine. 51, 102590. Published online 2020/01/07 DOI: 10.1016/j.ebiom.2019.11.051.

Hartman, A.L., Lough, D.M., Barupal, D.K., Fiehn, O., Fishbein, T., Zasloff, M., and Eisen, J.A. (2009). Human gut microbiome adopts an alternative state following small bowel transplantation. Proc National Acad Sci. 106(40), 17187-17192. DOI: 10.1073/pnas.0904847106.

Hastie, T., Tibshirani, R., Narasimhan, B., and Chu, G. (2019). impute: Imputation for microarray data. R package version 1.60.0.

Henning, S.M., Yang, J., Hsu, M., Lee, R.-P., Grojean, E.M., Ly, A., Tseng, C.-H., Heber, D., and Li, Z. (2018). Decaffeinated green and black tea polyphenols decrease weight gain and alter microbiome populations and function in diet-induced obese mice. European Journal of Nutrition. 57(8), 2759-2769. DOI: 10.1007/s00394-017-1542-8.

Heyman-Lindén, L., Kotowska, D., Sand, E., Bjursell, M., Plaza, M., Turner, C., Holm, C., Fåk, F., and Berger, K. (2016). Lingonberries alter the gut microbiota and prevent low-grade inflammation in high-fat diet fed mice. Food & nutrition research. DOI: 10.3402/fnr.v60.29993.

Hotchkiss, A.T., Nuñez, A., Strahan, G.D., Chau, H.K., White, A.K., Marais, J.P.J., Hom, K., Vakkalanka, M.S., Di, R., Yam, K.L., et al. (2015). Cranberry xyloglucan structure and inhibition of *Escherichia coli* adhesion to epithelial cells. J Agr Food Chem. 63(23), 5622-5633. DOI: 10.1021/acs.jafc.5b00730.

Hou, D., Zhao, Q., Yousaf, L., Khan, J., Xue, Y., and Shen, Q. (2019). Consumption of mung bean (*Vigna radiata* L.) attenuates obesity, ameliorates lipid metabolic disorders and modifies the gut microbiota composition in mice fed a high-fat diet. J Funct Food. 103687. DOI: 10.1016/j.jff.2019.103687.

Jakobek, L., and Matić, P. (2018). Non-covalent dietary fiber - polyphenol interactions and their influence on polyphenol bioaccessibility. Trends in Food Science & Technology. 83(The Journal of Nutrition 132 2002), 235-247. DOI: 10.1016/j.tifs.2018.11.024.

Johansson, M.E.V., Gustafsson, J.K., Holmén-Larsson, J., Jabbar, K.S., Xia, L., Xu, H., Ghishan, F.K., Carvalho, F.A., Gewirtz, A.T., Sjövall, H., et al. (2014). Bacteria penetrate the normally impenetrable inner colon mucus layer in both murine colitis models and patients with ulcerative colitis. Gut. 63(2), 281-291. DOI: 10.1136/gutjnl-2012-303207.

Johnson, O., Marais, S., Walters, J., van der Merwe, E.L., Alagaili, A.N., Mohammed, O.B., Bennett, N.C., and Kotzé, S.H. (2016). The distribution of mucous secreting cells in the gastrointestinal tracts of three small rodents from Saudi Arabia: Acomys dimidiatus, Meriones rex and Meriones libycus. Acta Histochemica. 118(2), 118-128. DOI: 10.1016/j.acthis.2015.12.003.

Kameyama, K., and Itoh, K. (2014). Intestinal colonization by a *Lachnospiraceae* bacterium contributes to the development of diabetes in obese mice. Microbes and Environments. 29(4), 427-430. DOI: 10.1264/jsme2.me14054.

Lacombe, A., Li, R.W., Klimis-Zacas, D., Kristo, A.S., Tadepalli, S., Krauss, E., Young, R., and Wu, V.C.H. (2013a). Lowbush wild blueberries have the potential to modify gut microbiota and xenobiotic metabolism in the rat colon. PLoS ONE. 8(6). DOI: 10.1371/journal.pone.0067497.

Lacombe, A., McGivney, C., Tadepalli, S., Sun, X., and Wu, V.C.H. (2013b). The effect of American cranberry (*Vaccinium macrocarpon*) constituents on the growth inhibition, membrane integrity, and injury of *Escherichia coli*

O157: H7 and *Listeria monocytogenes* in comparison to *Lactobacillus rhamnosus*. Food microbiology. 34(2), 352-359.

Lacombe, A., and Wu, V.C.H. (2017). The potential of berries to serve as selective inhibitors of pathogens and promoters of beneficial microorganisms. Food Quality and Safety. 1(1), 3-12. DOI: 10.1093/fqs/fyx001.

Lagkouvardos, I., Lesker, T.R., Hitch, T.C.A., Gálvez, E.J.C., Smit, N., Neuhaus, K., Wang, J., Baines, J.F., Abt, B., Stecher, B., et al. (2019). Sequence and cultivation study of *Muribaculaceae* reveals novel species, host preference, and functional potential of this yet undescribed family. Microbiome. 7(1), 28. DOI: 10.1186/s40168-019-0637-2.

Larsen, N., Bussolo de Souza, C., Krych, L., Barbosa Cahu, T., Wiese, M., Kot, W., Hansen, K.M., Blennow, A., Venema, K., and Jespersen, L. (2019). Potential of pectins to beneficially modulate the gut microbiota depends on their structural properties. Front Microbiol. 10, 223. Published online 2019/03/05 DOI: 10.3389/fmicb.2019.00223.

Lawrence, M., Huber, W., Pages, H., Aboyoun, P., Carlson, M., Gentleman, R., Morgan, M.T., and Carey, V.J. (2013). Software for computing and annotating genomic ranges. PLoS Comput Biol. 9(8), e1003118. Published online 2013/08/21 DOI: 10.1371/journal.pcbi.1003118.

Love, M.I., Huber, W., and Anders, S. (2014). Moderated estimation of fold change and dispersion for RNA-seq data with DESeq2. Genome Biology. 15(12), 550. DOI: 10.1186/s13059-014-0550-8.

Mailhe, M., Ricaboni, D., Vitton, V., Cadoret, F., Fournier, P.E., and Raoult, D. (2017). '*Angelakisella massiliensis*' gen. nov., sp. nov., a new bacterial species isolated from human ileum. New Microbes and New Infections. 16, 51-53. DOI: 10.1016/j.nmni.2017.01.003.

Majeed, M., Nagabhushanam, K., Arumugam, S., Natarajan, S., Majeed, S., Pande, A., Beede, K., and Ali, F. (2018). Cranberry seed fibre: a promising prebiotic fibre and its fermentation by the probiotic *Bacillus coagulans* MTCC 5856. International Journal of Food Science & Technology. 53(7), 1640-1647. DOI: 10.1111/ijfs.13747.

Makki, K., Deehan, E.C., Walter, J., and Bäckhed, F. (2018). The impact of dietary fiber on gut microbiota in host health and disease. Cell Host & Microbe. 23(6), 705-715. DOI: 10.1016/j.chom.2018.05.012.

Mallick, H., Rahnavard, A., and McIver, L. (2019). MaAsLin: Multivariate Analysis by Linear Models. R package, MaAsLin2 (version 1.0.0). https://git.bioconductor.org/packages/Maaslin2.

Mamet, T., Ge, Z.-z., Zhang, Y., and Li, C.-m. (2018). Interactions between highly galloylated persimmon tannins and pectins. International Journal of Biological Macromolecules. 106, 410-417. DOI: 10.1016/j.ijbiomac.2017.08.039.

Mao, G., Li, S., Shen, X., Zhou, S., Orfila, C., J. Linhardt, R., Ye, X., and Chen, S. (2019). Depolymerized RG-I enriched pectin from citrus segment membrane modulates gut microbiota, increases SCFAs production, promotes the growth of *Bifidobacterium* spp., *Lactobacillus* spp. and *Faecalibaculum* spp. Food & Function. DOI: 10.1039/c9fo01534e.

Martin, M. (2011). Cutabapt removes adapter sequences from high-throughput sequences reads. EMBnet journal 17(1), 10-12. DOI: https://doi.org/10.14806/ej.17.1.200.

Masumoto, S., Terao, A., Yamamoto, Y., Mukai, T., Miura, T., and Shoji, T. (2016). Non-absorbable apple procyanidins prevent obesity associated with gut microbial and metabolomic changes. Sci Rep-uk. 6(1), 31208. DOI: 10.1038/srep31208.

McMurdie, P.J., and Holmes, S. (2013). phyloseq: an R package for reproducible interactive analysis and graphics of microbiome census data. PloS one. 8(4). DOI: 10.1371/journal.pone.0061217.

McMurdie, P.J., and Holmes, S. (2014). Waste not, want not: Why rarefying microbiome data is inadmissible. PLoS Computational Biology. 10(4). DOI: 10.1371/journal.pcbi.1003531.

Morgan, M., Anders, S., Lawrence, M., Aboyoun, P., Pages, H., and Gentleman, R. (2009). ShortRead: a bioconductor package for input, quality assessment and exploration of high-throughput sequence data. Bioinformatics. 25(19), 2607-2608. Published online 2009/08/06 DOI: 10.1093/bioinformatics/btp450.

Müller, M., Canfora, E.E., and Blaak, E.E. (2018). Gastrointestinal transit time, glucose homeostasis and metabolic health: Modulation by Dietary Fibers. Nutrients. 10(3), 275. DOI: 10.3390/nu10030275.

Murrell, P. (2019). The Grid Graphics Package. R package version 3.6.1.

Mykkanen, O.T., Huotari, A., Herzig, K.H., Dunlop, T.W., Mykkanen, H., and Kirjavainen, P.V. (2014). Wild blueberries (*Vaccinium myrtillus*) alleviate inflammation and hypertension associated with developing obesity in mice fed with a high-fat diet. PLoS One. 9(12), e114790. Published online 2014/12/17 DOI: 10.1371/journal.pone.0114790.

Neuwirth, E. (2014). ColorBrewer Palettes. R package version 1.1-2.

Oksanen J, F.G.B., Michael Friendly, Roeland Kindt,, Pierre Legendre, D.M., Peter R. Minchin, R. B. O'Hara,, Gavin L. Simpson, P.S., M. Henry H. Stevens, Eduard Szoecs,, and Wagner, H. (2019). Vegan: Community ecology package. CRAN https://cran.r-project.org, https://github.com/vegandevs/vegan

Oleś, A., Morgan, M., and Huber, W. (2018). BiocStyle: Standard styles for vignettes and other Bioconductor documents. R package version 2.14.2.

Pagès, H., Aboyoun, P., Gentleman, R., and DebRoy, S. (2015). Biostrings: string objects representing biological sequences, and matching algorithms. R package version 2.54.0.

Pagès, H., Carlson, M., Falcon, S., and Li, N. (2019). Manipulation of SQLite-based annotations in Bioconductor. R package version 1.48.0.

Pan, P., Lam, V., Salzman, N., Huang, Y.-W., Yu, J., Zhang, J., and Wang, L.-S. (2017). Black raspberries and their anthocyanin and fiber fractions alter the composition and diversity of gut microbiota in F-344 Rats. Nutrition and Cancer. 1-9. DOI: 10.1080/01635581.2017.1340491.

Paturi, G., Butts, C.A., Monro, J.A., and Hedderley, D. (2018). Effects of blackcurrant and dietary fibers on large intestinal health biomarkers in rats. Plant Foods for Human Nutrition. 73(1), 54-60. DOI: 10.1007/s11130-018-0652-7.

Prior, R.L., Lazarus, S.A., Cao, G., Muccitelli, H., and Hammerstone, J.F. (2001). Identification of procyanidins and anthocyanins in blueberries and cranberries (*Vaccinium* spp.) using high-performance liquid chromatography/mass spectrometry. J Agr Food Chem. 49(3), 1270-1276. DOI: 10.1021/jf001211q.

Prior, R.L., Wu, X., Gu, L., Hager, T.J., Hager, A., and Howard, L.R. (2008). Whole berries versus berry anthocyanins: interactions with dietary fat levels in the C57BL/6J mouse model of obesity. J Agr Food Chem. 56(3), 647-653. DOI: 10.1021/jf071993o.

Qin, Y., Roberts, J.D., Grimm, S.A., Lih, F.B., Deterding, L.J., Li, R., Chrysovergis, K., and Wade, P.A. (2018). An obesity-associated gut microbiome reprograms the intestinal epigenome and leads to altered colonic gene expression. Genome Biology. 19(1), 7. DOI: 10.1186/s13059-018-1389-1.

Quast, C., Pruesse, E., Yilmaz, P., Gerken, J., Schweer, T., Yarza, P., Peplies, J., and Glöckner, F. (2013). The SILVA ribosomal RNA gene database project: improved data processing and web-based tools. Nucleic Acids Research. 41(D1). DOI: 10.1093/nar/gks1219.

Ram, K., and Wickham, H. (2018). wesanderson: A Wes Anderson palette generator. R package version. R package version 0.3.6.

Rodríguez-Daza, M.-C., Daoust, L., Boutkrabt, L., Pilon, G., Varin, T., Dudonné, S., Levy, É., Marette, A., Roy, D., and Desjardins, Y. (2020). Wild blueberry proanthocyanidins shape distinct gut microbiota profile and influence glucose homeostasis and intestinal phenotypes in high-fat high-sucrose fed mice. Sci Rep-uk. 10(1), 2217. DOI: 10.1038/s41598-020-58863-1.

Rodríguez-González, S., Pérez-Ramírez, I.F., Amaya-Cruz, D.M., Gallegos-Corona, M.A., Ramos-Gomez, M., Mora, O., and Reynoso-Camacho, R. (2018). Polyphenol-rich peach (Prunus persica L.) by-product exerts a greater beneficial effect than dietary fiber-rich by-product on insulin resistance and hepatic steatosis in obese rats. J Funct Food. 45(Nutrition, Metabolism and Cardiovascular Diseases 21 2011), 58-66. DOI: 10.1016/j.jff.2018.03.010.

Sanders, M.E., Merenstein, D.J., Reid, G., Gibson, G.R., and Rastall, R.A. (2019). Probiotics and prebiotics in intestinal health and disease: from biology to the clinic. Nat Rev Gastroenterol Hepatol. 16(10), 605-616. Published online 2019/07/13 DOI: 10.1038/s41575-019-0173-3.

Schliep, K.P. (2011). phangorn: phylogenetic analysis in R. Bioinformatics. 27(4), 592-593. Published online 2010/12/21 DOI: 10.1093/bioinformatics/btq706.

Schneeberger, M., Everard, A., Gomez-Valades, A.G., Matamoros, S., Ramirez, S., Delzenne, N.M., Gomis, R., Claret, M., and Cani, P.D. (2015). *Akkermansia muciniphila* inversely correlates with the onset of inflammation, altered adipose tissue metabolism and metabolic disorders during obesity in mice. Sci Rep. 5, 16643. Published online 2015/11/14 DOI: 10.1038/srep16643.

Schneider, C.A., Rasband, W.S., and Eliceiri, K.W. (2012). NIH Image to ImageJ: 25 years of image analysis. Nat Methods. 9(7), 671-675. Published online 2012/08/30 DOI: 10.1038/nmeth.2089.

Schroeder, B.O. (2019). Fight them or feed them: how the intestinal mucus layer manages the gut microbiota. Gastroenterology Report. 7(1), 3-12. DOI: 10.1093/gastro/goy052.

Segata, N., Izard, J., Waldron, L., Gevers, D., Miropolsky, L., Garrett, W.S., and Huttenhower, C. (2011). Metagenomic biomarker discovery and explanation. Genome Biology. 12(6), 1-18. DOI: 10.1186/gb-2011-12-6-r60.

Sharma, R., and Schumacher, U. (1995). Morphometric analysis of intestinal mucins under different dietary conditions and gut flora in rats. Dig Dis Sci. 40(12), 2532-2539. Published online 1995/12/01 DOI: 10.1007/bf02220438.

Skrovankova, S., Sumczynski, D., Mlcek, J., Jurikova, T., and Sochor, J. (2015). Bioactive compounds and antioxidant activity in different types of berries. International Journal of Molecular Sciences. 16(10), 24673-24706. DOI: 10.3390/ijms161024673.

Slowikowski, K., Hughes, S., Lukauskas, S., Irisson, J.-O., Kamvar, Z.N., Thompson, R., Dervieux, C., Hiroaki, Y., and Gramme, P. (2019). Automatically Position Non-Overlapping Text Labels with 'ggplot2'. R package version 0.8.1.

Sun, J., Marais, J., Khoo, C., LaPlante, K., Vejborg, R.M., Givskov, M., Tolker-Nielsen, T., Seeram, N.P., and Rowley, D.C. (2015). Cranberry (*Vaccinium macrocarpon*) oligosaccharides decrease biofilm formation by uropathogenic *Escherichia coli*. J Funct Food. 17(Planta 216 3 2003), 235-242. DOI: 10.1016/j.jff.2015.05.016.

Truchado, P., Hernandez-Sanabria, E., Salden, B.N., Abbeele, P.V.d., Vilchez-Vargas, R., Jauregui, R., Pieper, D.H., Possemiers, S., and Wiele, T.V.d. (2017). Long chain arabinoxylans shift the mucosa-associated microbiota in the proximal colon of the simulator of the human intestinal microbial ecosystem (M-SHIME). J Funct Food. 32(British Journal of Nutrition 76 1996), 226-237. DOI: 10.1016/j.jff.2017.02.004.

Tu, P., Bian, X., Chi, L., Gao, B., Ru, H., Knobloch, T.J., Weghorst, C.M., and Lu, K. (2018). Characterization of the functional changes in mouse gut microbiome associated with increased *Akkermansia muciniphila* population modulated by dietary black raspberries. ACS Omega. 3(9), 10927-10937. Published online 2018/10/06 DOI: 10.1021/acsomega.8b00064.

Turnbaugh, P.J., Bäckhed, F., Fulton, L., and Gordon, J.I. (2008). Diet-induced obesity is linked to marked but reversible alterations in the mouse distal gut microbiome. Cell Host & Microbe. 3(4), 213-223. DOI: 10.1016/j.chom.2008.02.015.

Turnbaugh, P.J., Ley, R.E., Mahowald, M.A., Magrini, V., Mardis, E.R., and Gordon, J.I. (2006). An obesity-associated gut microbiome with increased capacity for energy harvest. Nature. 444(7122), 1027. DOI: 10.1038/nature05414.

Vicente, A.R., Ortugno, C., Rosli, H., Powell, A.L., Greve, L.C., and Labavitch, J.M. (2007). Temporal sequence of cell wall disassembly events in developing fruits. 2. Analysis of blueberry (*Vaccinium* species). J Agric Food Chem. 55(10), 4125-4130. Published online 2007/04/13 DOI: 10.1021/jf063548j.

Wang, Q., Garrity, G.M., and Microbiol, T.-J.M. (2007). Naive Bayesian classifier for rapid assignment of rRNA sequences into the new bacterial taxonomy. Appl. Environ. Microbiol. DOI: 10.1128/AEM.00062-07.

Weitkunat, K., Schumann, S., Nickel, D., Kappo, K., Petzke, K., Kipp, A., Blaut, M., and Klaus, S. (2016). Importance of propionate for the repression of hepatic lipogenesis and improvement of insulin sensitivity in high-fat diet-induced obesity. Molecular Nutrition & Food Research. 60(12), 2611-2621. DOI: 10.1002/mnfr.201600305.

Wemheuer, F., Taylor, J.A., Daniel, R., Johnston, E., Meinicke, P., Thomas, T., and Wemheuer, B. (2018). Tax4Fun2: a R-based tool for the rapid prediction of habitat-specific functional profiles and functional redundancy based on 16S rRNA gene marker gene sequences. Biorxiv. 490037. DOI: 10.1101/490037.

White, B.L., Howard, L.R., and Prior, R.L. (2010). Proximate and polyphenolic characterization of cranberry pomace. J Agric Food Chem. 58(7), 4030-4036. Published online 2009/12/22 DOI: 10.1021/jf902829g.

Wickham, H. (2009). ggplot2, Elegant Graphics for Data Analysis. springer. DOI: 10.1007/978-0-387-98141-3.

Wickham, H. (2016). Tools for splitting, applying and combining data. R package version 1.8.4.

Wickham, H. (2019). Simple, consistent wrappers for common string operations. R package version 1.4.0.

Wickham, H., Hester, J., and Chang, W. (2019). Tools to make developing R packages easier. R package version 2.2.1.

Williams, J.M., Duckworth, C.A., Vowell, K., Burkitt, M.D., and Pritchard, M.D. (2016). Current protocols in mouse biology. Current protocols in mouse biology. 6(2), 148-168. DOI: 10.1002/cpmo.2.

Wright, E.S. (2016). Using DECIPHER v2.0 to analyze big biological sequence data in R. The R Journal. 8(1).

Xie, Y. (2013). knitr: A General-purpose tool for dynamic report generation in R. R package version 1.26.

Yang, J., Park, J., Park, S., Baek, I., and Chun, J. (2019). Introducing Murine Microbiome Database (MMDB): A curated database with taxonomic profiling of the healthy mouse gastrointestinal microbiome. Microorganisms. 7(11). Published online 2019/10/28 DOI: 10.3390/microorganisms7110480.

Yang, Y.-W., Chen, M.-K., Yang, B.-Y., Huang, X.-J., Zhang, X.-R., He, L.-Q., Zhang, J., and Hua, Z.-C. (2015). Use of 16S rRNA gene-targeted group-specific primers for real-time PCR analysis of predominant bacteria in mouse feces. Applied and Environmental Microbiology. 81(19), 6749-6756. DOI: 10.1128/aem.01906-15.

Zhao, L., Zhang, Q., Ma, W., Tian, F., Shen, H., and Zhou, M. (2017). A combination of quercetin and resveratrol reduces obesity in high-fat diet-fed rats by modulation of gut microbiota. Food & Function. 8(12), 4644-4656. DOI: 10.1039/C7FO01383C.

Zhou, F., Yin, M., Liu, Y., Han, X., Guo, J., Ren, C., Wang, W., Huang, W., Zhan, J., and You, Y. (2019). Grape seed flour intake decreases adiposity gain in high-fat-diet induced obese mice by activating thermogenesis. J Funct Food. 62, 103509. DOI: 10.1016/j.jff.2019.103509.

Star methods

Key resource table

REAGENT or RESOURCE	SOURCE	IDENTIFIER
Bacterial and Virus Strains		
Akkermansia muciniphila strain	Derrien et al. (2004)	ATCC BAA-835
Chemicals, Peptides, and Recombinant Proteins		
Cyanidin 3-glucoside standard	Sigma-Aldrich	Cat #PHL89616
Gallic acid standard	Sigma-Aldrich	Cat #91215
Epicatechin standard	Sigma-Aldrich	Cat #03940590
Malvidin 3-glycoside standard	Extrasynthèses, Genay, France	
PowerUp SYBR Green Master Mix	Applied Biosystems	Cat #A25742
2018 Teklad global 18% protein rodent diet	Harlan laboratories	N/A
Critical Commercial Assays		
ZR fecal DNA kit	Zymo Research Corp., Orange, CA	Cat #D6010
Experimental Models: Organisms/Strains		
C57BL/6J male mice	Jackson laboratories, Sacramento, CA USA	000664-C57BL/6J; https://www.jax.org/strain/000664
Oligonucleotides		
Primers Sequences for *A. muciniphila* forward 5′-CACACCGCCCGTCACAT-3′ and reverse 5′-TGCGGTTGGCTTCAGATACTT-3′	This work	N/A
Primers Sequences for total bacteria Uni334F 5′-ACTCCTACGGGAGGCAGCAGT-3′ Uni514R 5′-ATTACCGCGGCTGCTGGC-3′	Hartman et al. (2009)	N/A
Software and Algorithms		
R studio	R Core Team, Vienna, Austria	Version 3.6.1
Cutadapt	Martin (2011)	Version 2.4
Divisive Amplicon Denoising Algorithm (DADA2 R package)	Callahan et al. (2016)	Version 1.14.0
SILVA taxonomic database	Quast et al. (2013)	SILVA SSU Ref 132 NR, Dec 2017
DECIPHER R package	Wright (2016)	Version 2.14.0
Phyloseq R package	McMurdie and Holmes (2013).	Version 1.30.0
ggplot2 R package	Wickham (2009)	Version 3.2.1
Tax4Fun2 R package	Wemheuer et al. (2018)	Version 1.1.3
BLAST R package	Camacho et al. (2009)	Version 2.9.0
DESeq2 R package	Love et al. (2014)	Version 1.26.0
Vegan R package	Oksanen J et al. (2019)	Version 2.5-6
RColorBrewer R package	Neuwirth (2014)	Version 1.1.2
Viridis R package	Garnier (2017)	Version 0.5.1
Biostrings R package	Pagès et al. (2015)	Version 2.54.0
Knitr R package	Xie (2013)	Version 1.26
BiocStyle R package	Oleś et al. (2018)	Version 2.14.2

GridExtra R package	Auguie (2016)	Version 2.3
Phangorn R package	Schliep (2011)	Version 2.5.5
Wesanderson R package	Ram and Wickham (2018)	Version 0.3.6
ShortRead R package	Morgan et al. (2009)	Version 1.44.0
Data.table R package	Dowle (2019)	Version 1.12.6
Plyr R package	Wickham (2016)	Version 1.8.4
Grid R package	Murrell (2019)	Version 3.6.1
GenomicFeatures R package	Lawrence et al. (2013)	Version 1.38.0
AnnotationDbi R package	Pagès et al. (2019)	Version 1.48.0
Genefilter R package	Gentleman et al. (2019)	Version 1.68.0
Impute R package	Hastie et al. (2019)	Version 1.60.0
devtools R package	Wickham et al. (2019)	Version 2.2.1
ggrepel R package	Slowikowski et al. (2019)	Version 0.8.1
Stringr R package	Wickham (2019)	Version 1.4.0
GraphPad Prism 8.0	GraphPad software	https://www.graphpad.com/scientificsoftware/prism/
Software Gatan digital micrograph	Gatan	https://www.gatan.com/products/
Image-Pro software	Media Cybernetics, Silver Spring, USA	N/A
National Institute of Health image J software	Schneider et al. (2012)	N/A
Other		
Omni Bead Ruptor Homogenizer	Omni International	Bead ruptor 12
ABI 7500 Fast real-time cycling platform	Applied Biosystems	N/A
HPLC with DAD detection	Agilent technologies	Agilent 1100 series system
Reverse-phase UHPLC coupled to tandem mass spectrometry	Agilent technologies	N/A
Normal-phase HPLC	Agilent technologies	Agilent 1260/1290 infinity system
Agilent 2100 Bioanalyzer system	Agilent technologies	N/A
Gatan XP1000 camera	Gatan	https://www.gatan.com/products/
Glucometer	Bayer	Accu-Check
Vacuum Infiltration Processor	Sakura brand	Tissue-Tek VIP
BX51 microscope, equipped with a CCD Digital Camera System	Olympus America, Inc, USA	N/A
Nanodrop	Nanodrop Technologies, Wilmington, DE, USA	ND-1000

Contact for reagent and resource sharing

Further information and requests for resources and reagents should be directed to and will be fulfilled by the Lead Contact, Maria-Carolina Rodriguez (maria-carolina.rodriguez-daza.1@ulaval.ca).

Experimental model and subject details

Diet preparation

Cranberry and blueberry powders and their fibrous residue have been uniformly incorporated into a high fat high sucrose diet (HFHS). The amount of polyphenols-rich cranberry (CP) and blueberry powders (BP) was defined on the basis of the polyphenol dose of 200 mg/kg of body weight (BW) in mice, as previously determined (Anhê et al., 2014). Subsequently, the amount of cranberry and blueberry fibre-rich fractions (CF and BF respectively) was calculated considering the equivalent total fibre content as found in the corresponding berry powders (see supplementary information **Table S3**). To maintain an isocaloric level, the diets composition was adjusted to provide equivalent nutritional value of 5.4 kcal/g.

Experimental design of animal bioassay

Six-weeks old C57BL/6J male mice ($n = 72$; Jackson laboratories, Sacramento, CA USA) were randomized into six groups of 12 animals each and were single-housed in a controlled environment (1 mouse per cage; 12/12-h light-dark) with free access to food and drinking water. After two weeks of acclimation with standard-chow diet (2018 Teklad global 18% protein rodent diet, Harlan laboratories), the mice were fed either a Chow-diet (CT), a HFHS control diet or a HFHS diet containing either polyphenols-rich CP and BP, or the fibrous fractions CF and BF for 8 weeks (see table 1). Body weight (BW) gain was recorded under non-fasting condition, twice a week. Food intake was evaluated by monitoring the food consumption (g) three times per week. After 5 weeks and 7 weeks of treatment, insulin tolerance test (ITT) and oral glucose tolerance test (OGTT) were performed, respectively. Fecal material was collected from each mouse for bacterial DNA extraction before the start of the treatments (week 0) and at the end (week 8), immediately immersed in dry-ice and stored at -80°C. After 8 weeks of feeding, mice were anesthetized with isoflurane (2-3%; 0.5 – 1.5 L/min) and euthanized by cardiac puncture. Adipose tissues, organs, and intestines were carefully dissected; their weight was recorded and immediately immersed in liquid nitrogen, RNA later (Invitrogen) or into fixation solutions (Carnoy's solution, buffered formalin 10%) according to the subsequent analysis. Frozen tissues were then stored at −80 °C.

All experimental procedures were performed according to the guidelines of the animal care committee of Laval University (CPAUL). The protocols were summited and approved by Canadian Council on Animal Care.

Method details

Characterization of the whole berry powders and derived fibrous fractions

American cranberry (*Vaccinium macrocarpon* Aiton) and wild blueberry (*Vaccinium angustifolium* Aiton) fruit powders were provided by Fruits d'Or (Quebec, Canada) and fibrous residues were provided by Diana Food Canada. The fruit fibres were obtained after extraction of polyphenols with a 70 % hydroethanolic extract as described previously (Denis et al., 2015). The extraction solid residues were pressed and air dried at 50°C and powdered before inclusion in the mice feed. The phenolic characterization of the fruit powders and fibrous residues was carried out according to the methodology described by Dudonné et al. (2015). Briefly, the total phenolic content was measured by the Folin-Ciocalteu technique by quantifying on the basis of gallic acid equivalent (Sigma-Aldrich, St. Louis, MO, USA). The anthocyanins were analyzed by reverse phase HPLC with a diode array detector and quantified using a cyanidin 3-glycoside standard (Extrasynthèses, Genay, France). Proanthocyanidins were separated according to their degree of polymerization (DP) by normal phase HPLC chromatography and quantized by fluorescence using (-) -epicatechin as standard (Sigma-Aldrich, St. Louis, MO, USA). Chromatography grade solvents were purchased from EMD Millipore Chemicals (Billerica, MA, USA) and Anachemia (Montreal, Canada).

A comprehensive analysis of the fibres, proteins, lipids, carbohydrates and total energy content of the samples was conducted by Environex (Quebec, Canada) using standard AOAC methods for total lipids (AOAC 989.05), for proteins (AOAC). 992.15), for dietary fibres (AOAC 985.29) and moisture content (AOAC 44-15A). Caloric and carbohydrate contents were calculated. The carbohydrate content was obtained by subtracting the dietary fibres content from the total carbohydrate content.

Glucose homeostasis and hepatic triglycerides assessment

After 5 weeks of treatments, mice were fasted for 6 hours. Blood was drawn at baseline and immediately centrifuged (3.500 rpm, 10 min at 4°C). Insulin solution was administrated 10 µl/g of 0.65U/kg by intraperitoneal injection, followed by glycemia measurements using an Accu-Check glucometer (Bayer) before and at 5, 10, 15, 20, 30, and 60 minutes after the injection. An oral glucose tolerance test (OGTT) was performed after 7 weeks of treatment. Mice were fasted for 12 hours overnight, blood baseline sample was drawn and immediately centrifuged (3.500 rpm, 10 min at 4°C). Dextrose solution (2 µl/g of 50% dextrose) was administrated by gavage and blood samples (60 µl) were obtained from the mouse lateral saphenous vein. Glycemia was determined using an Accu-Check glucometer (Bayer) at time 15, 30, 60, 90, and 120 minutes relative to the glucose load. The area under the curve (AUC-OGTT) was determined considering the glucose levels measured between baseline and 120 minutes after glucose overload (GraphPad Prism 7.0, USA). Insulin resistance index (HOMA-IR) was calculated using the formula: HOMA-IR = [fasting glycemia (nmol/L)*fasting insulinemia (µU/mL)/22.5]. The 12h fasting blood samples were collected for determinations of plasma insulin. Samples were stored at -80°C until the assay. Mouse insulin was determined using an ultrasensitive ELISA kit (Alpco, Salem, USA).

Liver triglyceride (TG) content was assessed after chloroform–methanol extraction and enzymatic reactions using commercial kits (Randox Laboratories, Crumlin, UK).

Colon histology

Colon tissues were prepared as previously described (Williams et al., 2016). The PBS-flushed colon tissues were cut into two equal sized sections (transverse incision), and then were transferred into the tube containing a large excess of cold Methanol-Carnoy's solution (60% methanol, 30% chloroform and 10% glacial acetic acid). The samples were stored for 3hr at 4°C to allow the fixation. After fixation, the tissues were washed with cold 70% ethanol once, and stored in the same solution at 4°C until they were processed. Tissue processing was performed at IBIS laboratory of Molecular Imaging and Microscopy, Laval University (Québec, QC, Canada). The samples were placed into a tissue cassette indelibly labeled with a unique animal identifier. The

cassettes were subjected to a tissue processor for standard processing to allow embedding in paraffin wax (Tissue-Tek VIP, vacuum Infiltration Processor Sakura brand). The protocol applied was: Alcohol 95% 45 min, Alcohol 100% 3 x 45 min, Toluene 2 x 45 min, Paraffin 1h30, 2h00 and 4h00. Paraffin-embedded sections of colon tissues were cut and stained with both periodic acid Schiff and Alcian blue (AB-PAS). AB-PAS staining enables the differentiation between acid mucins and neutral mucins, with blue color showing acid mucins, purple color indicating a mixture of neutral and acid mucins, and red/magenta color indicating neutral mucins alone (Barcelo et al., 2000).

Goblet cell quantification, mucus thickness and crypts depth measurements

The relative proportions and distribution of mucous secreting goblet cells was quantified following Johnson et al. (2016) protocols with some modifications (Johansson et al., 2014). All images were captured using a BX51 microscope (Olympus America, Inc, USA) equipped with a CCD Digital Camera System and Image-Pro software. Number of goblet cells (GC) was counted for a defined distance (using 20X objective lens, 50 μm scale). Initially, images were taken with the 4X objective lens (200 μm scale bars) in order to examine the whole tissue section. This was used to ensure that the total area of the images taken at a higher magnification would cover at least 50% of the tissue section. Afterwards, under 20X objective lens, each section was divided into four equal quadrants and taking representative images. A total of 12 crypts (3 crypts per section) were analyzed for each mouse. In each quadrant, within a delineated area (from epithelium towards the colonic crypts), mucin secreting GC types (acid, neutral and mixed) were counted and the data were expressed as the relative cell numbers per crypt (12 crypts of 12 mice per group). To determine the specific mucin GC types for the colon for each animal, the cell counts were totaled separately in acid, neutral and mixed mucin-filled GC, and the data normalized to reflect the total numbers of each mucin cell type per crypt. Crypt lengths (μm) were calculated from an average of 12 crypts per tissue section, for 12 mice. Average of mucus thickness was calculated in a similar manner, measuring the lengths of the inner mucus layer closely adhered to the epithelium, for 12 mice. The National Institute of Health image J software was used for supporting the cell quantifications and crypts length measurements.

Fecal DNA extraction and 16S rRNA gene amplicon library preparation and sequencing

The microbial genomic DNA was extracted from approximately 100 mg of feces using a ZR fecal DNA kit (D6010; Zymo Research Corp., Orange, CA) following the manufacturer protocols. The concentration and quality of DNA was determined spectrophotometrically using a ND-1000 Nanodrop (Nanodrop Technologies, Wilmington, DE, USA).

Degenerate primers 341F (5'-CCTACGGGNGGCWGCAG-3') and 805R (5'-GACTACHVGGGTATCTAATCC-3') targeting the 16S rRNA V3-V4 region were used for the amplicon library preparation of 16S rRNA fragments. The primers were adapted to incorporate the transposon-based Illumina Nextera adapters (Illumina, USA) and a sample barcode sequence allowing multiplexed paired-end sequencing. Constructed 16S metagenomic libraries were purified using 35 μL of magnetic beads (AxyPrep Mag PCR Clean up kit; Axygen Biosciences, USA) per 50 μL PCR reaction. Library quality control was performed with a Bioanalyzer 2100 using DNA 7500 chips (Agilent Technologies, USA). An equimolar pool was obtained and checked for quality prior to further processing. The pool was quantified using picogreen (Life Technologies, USA) and loaded on a MiSeq platform using 2 x 300 bp paired-end sequencing (Illumina, USA). High-throughput sequencing was performed at the IBIS (Institut de Biologie Intégrative et des Systèmes - Université Laval).

16S rRNA sequences processing

Demultiplexed RAW data files covering all of the samples were imported into the R studio environment, (version 3.6.1, R Core Team, Vienna, Austria). Paired forward and reverse reads from raw data files were trimmed (primer removal) using Cutadapt (version 2.4) (Martin, 2011). Reads were quality-filtered and bases with low-quality scores (<20) were discarded. These filtered files were then processed using Divisive Amplicon Denoising Algorithm (DADA2) pipeline which included the steps of dereplication, core denoising algorithm (that models and corrects Illumina-sequenced amplicon errors) and the merging of the base pairs. The advantage of using DADA2 over traditional clustering methods is that it determines exact sequences based on an error model

for the sequencing run, resolving differences of as little as one nucleotide (Callahan et al., 2016), merging function provided global ends-free alignment between paired forward and reverse reads. The reads were merged together if they overlapped exactly, and a table for amplicon sequence variants (ASVs, a higher analog of operational taxonomic units—OTUs) was constructed, recording the number of times each amplicon sequence variant was observed in each sample. Chimeras were removed using the *removeBimeraDenovo* function of the same DADA2 package. ASVs sequences were assigned a taxonomy using the most recent SILVA taxonomic database (SILVA SSU Ref 132 NR, Dec 2017) as reference dataset (Quast et al., 2013). A phylogenetic tree of the ASVs was obtained using the function *AlignSeq* implemented in DECIPHER R package (Wright, 2016) to create the multiple sequence alignment used to inform downstream analyses in *phyloseq* package, especially the calculation of phylogeny-aware distances between microbial communities. Afterward, a phyloseq data object was created using *phyloseq* function of the *phyloseq* package in R (McMurdie and Holmes, 2013). Unassigned taxa and singletons were removed. Estimates of observed α-diversity, richness (Chao1) and diversity (Shannon and Simpson Indices) were measured within sample categories using *estimate_richness* function of the *phyloseq* package. Relative abundances of microbial genera and phylum were plotted using the *ggplot2* package (Wickham, 2009) after transforming abundance data into relative abundances. For β-diversity analysis, multidimensional scaling (MDS, also known as principal coordinate analysis; PCoA) was performed while using different distance measures: the Bray-Curtis dissimilarity that considers the species abundance count and the unweighted UniFrac that account for phylogenetic closeness of ASVs (OTUs) observed in different samples without taking into account the abundances. The plots of community data were visualized by using their base functions in the *phyloseq* package.

Microbial functional profiling

To evaluate whether the cranberry and blueberry powders or their fibre fractions drive microbes with distinct functional repertoires, we investigated the functional profile of each ASV inferred against SILVA database. Predicted functions of each sample were extracted based on the Kyoto Encyclopaedia of Genes and Genomes (KEGG) Ontology (KO) functional and pathway profiles

using Tax4Fun2 (Wemheuer et al., 2018). A current default reference dataset of 16S rRNA gene data from 12,002 bacterial genomes (NCBI RefSeq database assessed on 19 August 2018) is available through the KEGG database to generate reference data (Wemheuer et al., 2018). The ASV count table and the taxonomic classification were merged and then, used to predict functional profiles. ASV fasta file were initially aligned against the supplied 16S rRNA reference sequences ("Ref100NR") with copy number correction enabled by BLAST (version 2.9.0), using the *runRefBlast* function. Functional predictions were subsequently calculated using the *makeFunctionalPrediction* function incorporating the abundance of each ASV. Only ASVs that were matched with a 97% similarity to sequences present in the SILVA database were included. ASVs assigned to a taxonomic key (i.e. a particular genus) having no functional reference profiles were not included in the prediction (called Fraction of Unexplained; FTU). The obtained profile is subsequently normalised: the sum of all functions in a sample is 1. The functional redundancy index (FRI) with respect to single functions was also calculated. The FRI denote the proportion of species capable of performing a particular function and their phylogenetic relationship to each other. A specific function is almost ubiquitous in all community members when there is a high FRI , whereas functions that are present in a few closely related species or that have been detected in only one community member is indicated by a low FRI (Wemheuer et al., 2018). We subsequently compared these FRI values based on the actual genomic information of the observe bacterial abundance changes by calculating the Bray-Curtis distances and analysis of similarities (PERMANOVA); principal coordinate analyses were performed to visualize the closeness of functions displayed by bacterial communities making up the gut microbiota of each group.

Multivariate association analysis

Multivariate microbial Association with Linear Models (MaAsLin) was performed for overlapping the diet composition (polyphenols-containing diets, the fibre-rich diets and the control diets) as covariates, while accounting for bacterial taxonomies (at the genus level), potentially determining the significance to a specific variable. The MaAsLin system uses an arcsine square root transformed analysis of the microbial community abundance or function in a standard multivariable linear model, pertinent to determine the significance of putative relationships from

clinical or environmental metadata set (Mallick et al., 2019). Using the MaAsLin model, the analysis was focused on the diet composition as a single variable of interest, "subtracting out" the effect of the other confounding metadata variables evaluated in the present study. The minimum percentage relative abundance of 0.01% was applied within the MaAsLin parameters, p values across all associations were then adjusted using the Benjamini–Hochberg FDR method, with a threshold of $p < 0.05$ and $q < 0.05$. Only the microbial features with $q<0.05$ were reported.

To evaluate the association of the gut microbiota functional profiling with changes in the liver TG, the energetic efficiency and BW, MaAsLin was run with same settings across all. Then, functional pathways at the KEGG level 1 from Tax4Fun2 data were included. The functional features presented were representatives pathways that were significantly modulated by the diets as determined by LEfSe analysis ($q<0.05$) (Segata et al., 2011).

Likewise, all the covariates such as BW gain, liver TG, IWAT, EWAT, energetic efficiency, caecum weight and mucus thickness were also analyzed to look for significant changes that could be driven by specific bacterial taxa during the 8-weeks dietary intervention. The co-occurrence relationships between the relative abundances of taxa (at the genus level) found to be significantly associated with the above variables were evaluated by calculating Spearman ranked correlations. The resulting association were visualized using a heatmap representing the R correlation coefficients. In the heatmap, the p values across all associations are presented as *$p<0.05$, **$p<0.01$, ***$p<0.001$ and ****$P<0.0001$. Relations between bacterial communities and mouse phenotypes of the different groups of mice were further represented using Ordination of Canonical Correspondence Analysis (CCA). CCA allows exploration of relations between sets of variables—in this case, microbiota composition according to the diet and the mouse phenotypes found with significant changes during the intervention. CCA strives to maximizes the correlations of the gut microbiota structure with one set of variables while accounting for the microbiota composition and the type of diet. CCAs were computed using R studio and *Vegan* package.

Analysis of 16S rRNA gene copies of *Akkermansia muciniphila* by quantitative real-time PCR

The determination of 16S rRNA gene copies of total bacteria was carried out per sample through quantitative PCR amplification using the bacterial universal primers Uni334F (5′-ACTCCTACGGGAGGCAGCAGT-3′) and Uni514R (5′-ATTACCGCGGCTGCTGGC-3) (Hartman et al., 2009). The proportion of *Akkermansia muciniphila* 16S rRNA gene copy relative to the total bacteria were analyzed in fecal samples from all groups. Home designed 16S rRNA primer sequences (Geneious software, version 9.0) were used for *A. muciniphila* (forward 5′-CACACCGCCCGTCACAT-3′ and reverse 5′-TGCGGTTGGCTTCAGATACTT-3′). Primer amplification efficiencies and standard curves were determined by making dilution series of pure total DNA for this bacterium (ATCC BAA-835 strain), calculating a linear regression based on the CT data points, and inferring the efficiency from the slope of the line. The reaction mixture (20 µl) contained 10 µL of 2X PowerUP SYBR Green Master mix (Applied Biosystem), 6.4 µL of water, 0.8 µL of a 5 µM Forward and Reverse primers, and 2 µL of extracted DNA in DNase/RNase-free water. The qPCR amplifications were performed on an Applied Biosystems ABI 7500 Fast real-time cycling platform. The thermocycling protocol consisted in 50°C for 2 min, 95°C for 10 min for hot-start polymerase activation, followed by 40 cycles of denaturation at 95°C for 15 s, annealing at 60°C for 1 min, and a melting curve stage as default setting from 60°C to 95°C. Twelve samples were analyzed for each group, duplicate qPCR reactions were performed. The average CT value obtained from each primer pair was used to calculate the proportion of bacterial taxa over total bacteria in mouse feces. The data were transformed into a percentage using the ΔΔCT-based following formula as described elsewhere (Yang et al., 2015):

$$\boldsymbol{X = \frac{(Eff.Univ.)^{CT\ univ}}{(Eff.Spec.)^{CT\ spec}}\ \mathbf{x\ 100}}$$

Where *Eff.Univ* is the calculated efficiency of the universal primers and *Eff.Spec* refers to the efficiency of the taxon-specifc primers. *CT univ* and *CT spec* are the CT mean values registered by the Fast real-time thermocycling platform. “X” represents the percentage of 16S taxon-specific copy number existing in each fecal sample. Finally, spearman correlations analyses were

performed for comparing the data from 16S rRNA sequencing versus the 16S rRNA relative proportion obtained by qPCR; p values <0.05 were considered statistically significant.

Quantification and statistical analysis

Microbial community composition and differential abundance statistical analysis

To detect differences in richness and α-diversity between groups, either Mann-Whitney U tests or Kruskal-Wallis test were performed among sample categories while measuring the observed estimates of α-diversity (richness of unique ASVs). Stratified permutational multivariate analysis of variance (PERMANOVA) with 999 permutations was conducted on all principal coordinates that were obtained during PCoA with the *adonis* function of the *vegan* package in R, to observe the statistical significance ($p<0.05$) of clusters according to the sample categories. To understand multivariate homogeneity of groups dispersions (variances) between multiple conditions, *Vegan's betadisper* function was performed with pairwise comparisons of group mean dispersions.

Differential abundance analyses of taxa between cranberry and blueberry-fed mice and HFHS-fed control group was determined at finer taxonomic level (the ASVs level) using the *DESeq2* package in R (Love et al., 2014). Only taxa found to be significant ($P <0.05$ after multiple-hypothesis testing) were reported. *DESeq2* is a statistical method for differential analysis of count data, using shrinkage estimation for dispersions and fold changes while accounting for library size differences and biological variability (Love et al., 2014). It has recently been demonstrated that adopting these methods to microbiome taxonomy count data, as a direct analogy to differential expression from RNA-Seq, leads to improvements in detecting differential abundance compared to simple proportions or rarefying (McMurdie and Holmes, 2014). Results were expressed as $\log_2$-fold change in HFHS relative to Chow-fed mice and in CP, CF, BP and BF groups relative to HFHS-fed control mice. To detect differentially abundant features, relative abundance comparisons at the genus, family, and phylum levels were performed on normalized data, employing non-parametric Mann-Whitney U-tests, as well as,

Kruskal-Wallis test with multiple comparison correction according to false discovery rate (FDR) method of Benjamini and Hochberg (Prism 8.0, GraphPad software, California). Similarly, those tests were used as appropriate to analyze the changes in the relative proportion of *A. muciniphila* examined by qPCR analysis in all the groups.

Comparisons at finer taxonomic levels (family through genus) were performed with linear discriminant analysis (LDAs) by LEfSe to identify microbial taxa biomarkers (Segata et al., 2011), that characterize the differences between groups of mice. The alpha value for Kruskal-Wallis and Wilcoxon tests was set at 0.05, the logarithmic LDA score threshold was 2.0, and per-sample normalization of sum values was applied (LEfSe default parameters). These biomarkers are microbial taxa that differ in abundance between groups, as identified by a Wilcoxon rank-sum test. The effect size of each biomarker was then estimated by determining an LDA score (Segata et al., 2011). Alike, LEfSe analysis and q-value were employed to identify microbial functions and KEGG pathways statistically over-represented in cranberry and blueberry-fed mice compared to HFHS-fed mice.

Mouse phenotypes Statistical analysis

To compute individual pairwise comparisons of means of histological analysis, Student's *t*-tests and one-way ANOVA with a Dunnett post hoc test (Graph Pad Prism 8.0) were performed between the berries-enriched diets CP, BP and the fibre-enriched diets CF and BF compared to HFHS control group. Significance changes on the metabolic phenotypes (OGTT, ITT) between groups at different time points were calculated using a two-way repeated measures ANOVA with Dunnett's post hoc test correction (Graph Pad Prism 8.0). p-values less than 0.05 were considered statistically significant whereas p-values between 0.05 and 0.1 were considered as showing a trend. Results were expressed as means ± standard error of the mean (SEM).

Additional used R-Packages

DECIPHER v2.14.0 (Wright, 2016), *ggplot2* v3.2.1 (Wickham, 2009), BLAST v1.26.0 (Camacho et al., 2009), *RColorBrewer v*1.1.2 (Neuwirth, 2014), *Viridis* v0.5.1 (Garnier, 2017),

Biostrings v2.54.0 (Pagès et al., 2015), *Knitr* v1.26 (Xie, 2013), *BiocStyle* v2.14.2 (Oleś et al., 2018), *GridExtra* v2.3 (Auguie, 2016), *Phangorn* v2.5.5 (Schliep, 2011), *Wesanderson* v0.3.6 (Ram and Wickham, 2018), *Data.table* v1.12.6 (Dowle, 2019), *Plyr* v1.8.4 (Wickham, 2016), *Grid* v3.6.1 (Murrell, 2019), *GenomicFeatures* v1.38.0 (Lawrence et al., 2013), *AnnotationDbi* v1.48.0 (Pagès et al., 2019), *Genefilter* v1.68.0 (Gentleman et al., 2019), *Impute* v1.60.0 (Hastie et al., 2019), *devtools* v2.2.1 (Wickham et al., 2019), *ggrepel* v0.8.1 (Slowikowski et al., 2019), *Stringr* v1.4.0 (Wickham, 2019), *ShortRead* v1.44.0 (Morgan et al., 2009).

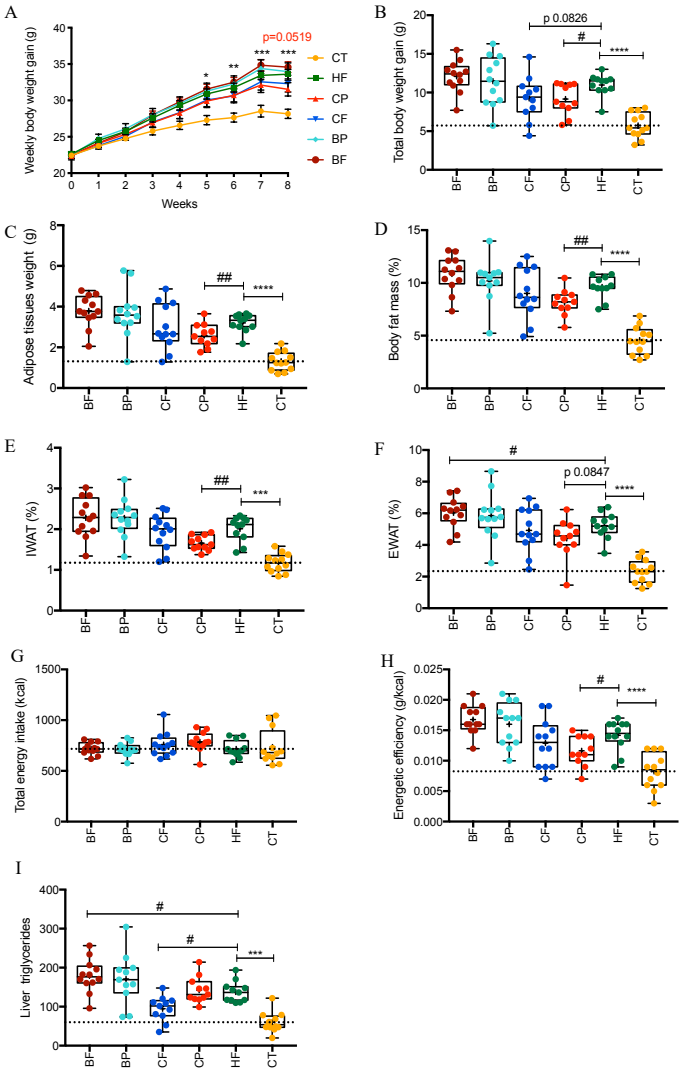

Figure 1. The whole cranberry powder decreases body weight gain, percentage of body fat mass and energy efficiency in HFHS-diet induced obese mice.

Six weeks-old C57BL/6J mice were fed with standard chow-diet (CT), HFHS-diet (HF) or HFHS-diet supplemented with either the whole cranberry powder (CP), cranberry fibres (CF), the whole blueberry powder (BP) and blueberry fibres (BF) for 8 weeks. A) Weekly body weight , B) total body weight gain, C) Adipose tissues weights of mice at the end of the dietary intervention, D) The percentage of fat mass expressed relative to body weight at the time of sacrifice, E) Inguinal white adipose tissue (IWAT) weight, F) Epididymal white adipose tissues (EWAT) weight expressed relative to body weight at the end of the study G) Total energy intake and H) Energetic efficiency corresponding to the ratio of body weight to energy intake, I) Hepatic triglycerides accumulation. Values are expressed as the mean ± SEM (n = 12). Dotted lines correspond to the mean values of CT-fed mice. *p < 0.05 ** p<0.01 *** p<0.001 and ****p<0.0001 as compared to CT-fed control group. ##p<0.01 #p<0.05 compared to HFHS. p-values indicated in the graph “A” are compared to the control HF and color-coded as the legend.

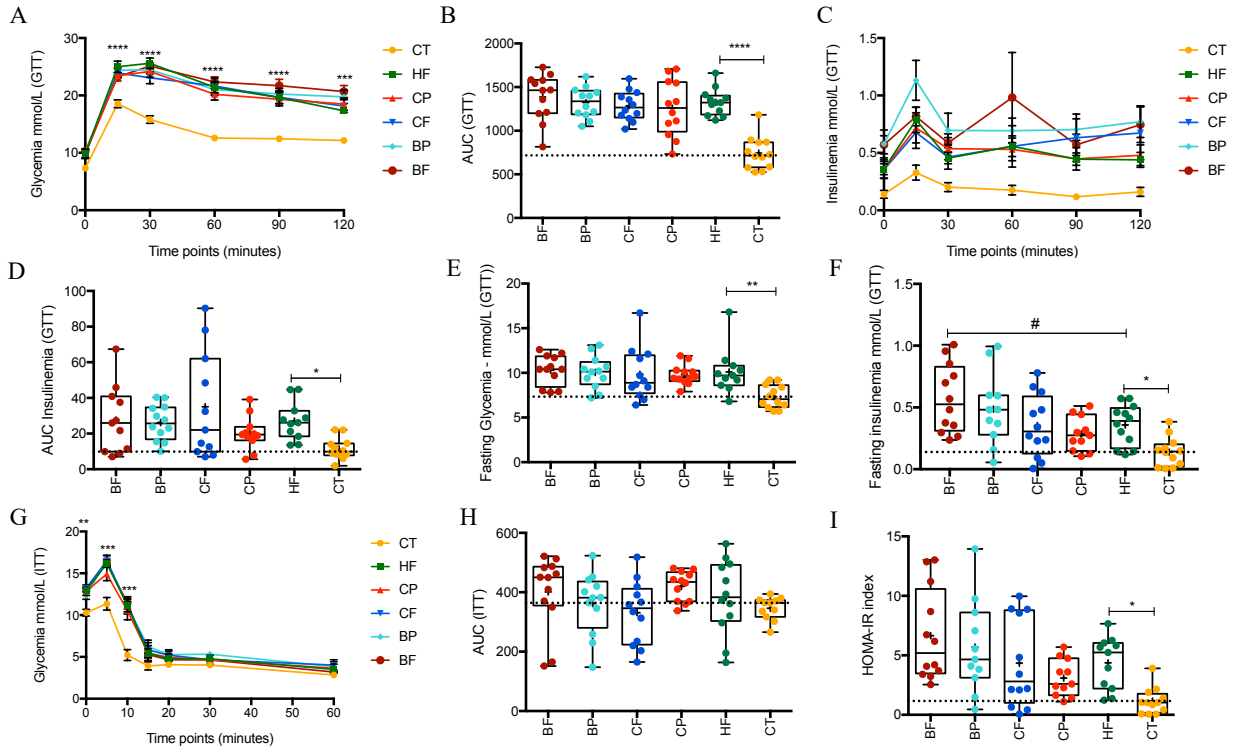

Figure 2. Diet-enrichment with berry powders and their fibre-rich fractions did not affect glucose homeostasis in HFHS-diet induced obese mice.

Six weeks-old C57BL/6J male mice were fed with standard chow-diet (CT), HFHS-diet (HF) or HFHS-diet enriched either with the whole cranberry powder (CP), cranberry fibre fraction (CF), the whole blueberry powder (BP) and blueberry fibre fraction (BF) for 8 weeks. A) Oral glucose tolerance test (OGTT) was performed at 7 weeks of treatment after a 12 h fast. Blood glucose levels were measured at baseline and at the indicated times after glucose injection. B) Area under the curve (AUC) during OGTT. C) Plasma insulin was measured at the same timepoint of the OGTT test. D) AUC of plasma insulin measurements during OGTT, E) Changes in glycemia levels after 12 h fast, F) Changes in fasting plasma insulin levels during OGTT, G) Insulin tolerance test (ITT) performed at 6 weeks of treatment after a 6 h fast. Time-course of blood glucose levels measured after intraperitoneal injection of insulin. H) AUC during ITT, I) Homeostatic model assessment of insulin resistance (HOMA-IR). Dotted lines correspond to the mean values of CT-fed mice. *p < 0.05 ** p<0.01 *** p<0.001 and ****p<0.0001 as compared to CT-fed control group. #p<0.05 compared to HFHS.

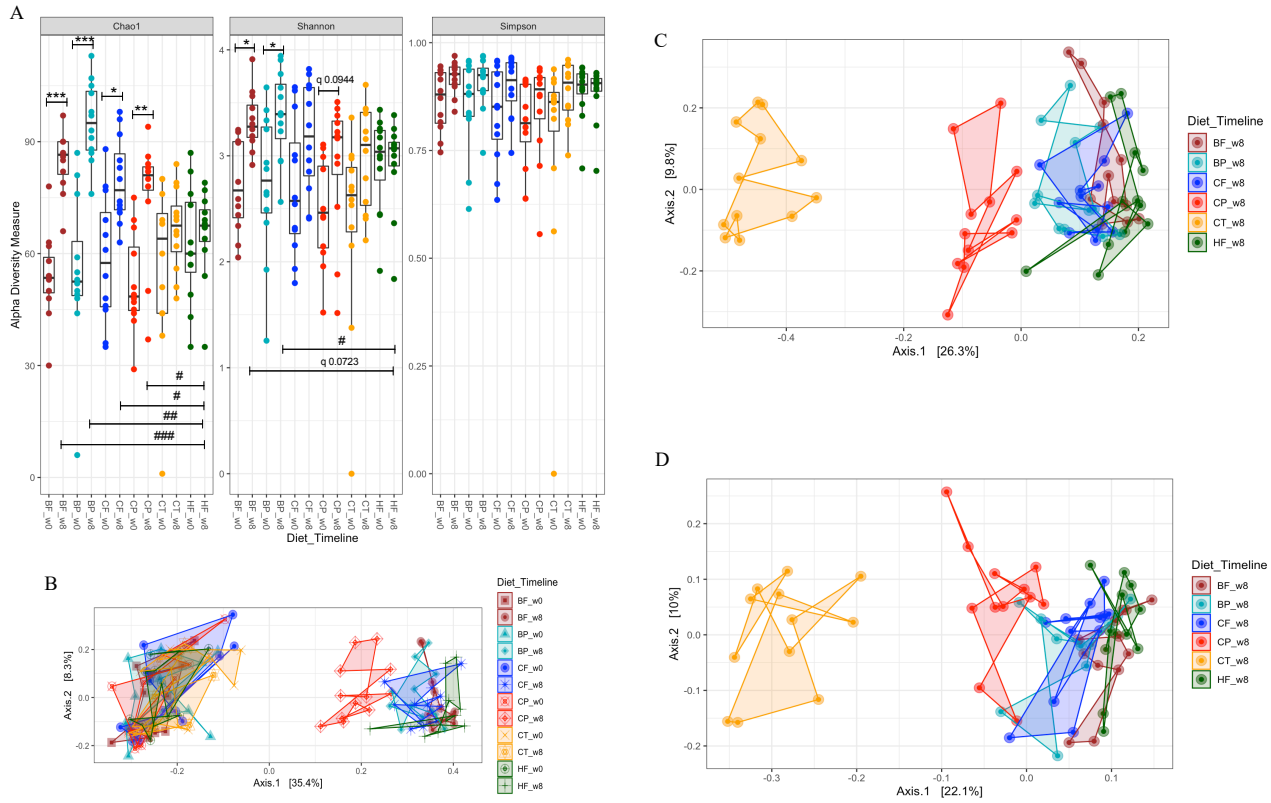

Figure 3. Polyphenols-rich CP and BP and their fibre-rich fractions CF and BF distinctly influenced the gut microbiota structure of HFHS-diet induced obese mice.

The mice were fed a HFHS-diet (HF), Chow diet (CT), HFHS-diet supplemented either with polyphenols-rich whole cranberry powder (CP), cranberry fibre-rich fraction (CF), polyphenols-rich whole blueberry powder (BP) and blueberry fibre-rich fraction (BF) for 8 weeks. A) Alpha-diversity, considering gut species richness determined by Chao1 index; gut bacterial diversity measured by Shannon-diversity and Simpson-evenness indices are plotted for each dietary group at the baseline (week 0) and at the end of the intervention (week 8). Values are individual data points representing each mouse at baseline and week 8. The line inside the box represents the median, while the whiskers represent the lowest and highest values within 1.5 interquartile range (IQR). B) Principal Coordinates Analysis (PCoA) plots of Bray Curtis dissimilarities between samples from the baseline (denoted as w0) to the end of the intervention (denoted as w8), with the % explained variance by the principle coordinates (PERMANOVA R2 0.4293, p<0.001); C) PCoA plot of Bray Curtis dissimilarities between samples at week 8 shows clustering of mice on chow and the polyphenol-rich and fibre-rich diets (PERMANOVA R2 0.40295, p< 0.001), and D) PCoA plot of taxon phylogenetic tree-based distances determined by unweighted UniFrac of samples at week 8 (PERMANOVA R2 0.3354, p<0.001) are presented. The microbiome of mice on CP and CT-diets are clearly distinct versus the HF-diet. Within the HFHS-supplemented mice, mice on CP-diet showed the strongest separation versus the HF. Statistical testing showed a difference in alpha diversity for dietary groups in Chao1 index, Shannon-diversity and Simpson evenness are represented as *p<0.05, **p<0.01, ***p<0.001, ****p<0.0001 as compared to baseline within the same group, and #p<0.05, ##p<0.01, ###P<0.001 and #### p<0.0001 as compared to HFHS group at week 8. Corrected p values having a tendency are indicated as “q” values in the graph. Each sample point (n=12 per group) is color-coded based on the administrated diet for 8 weeks (W8), as shown in each figure legend.

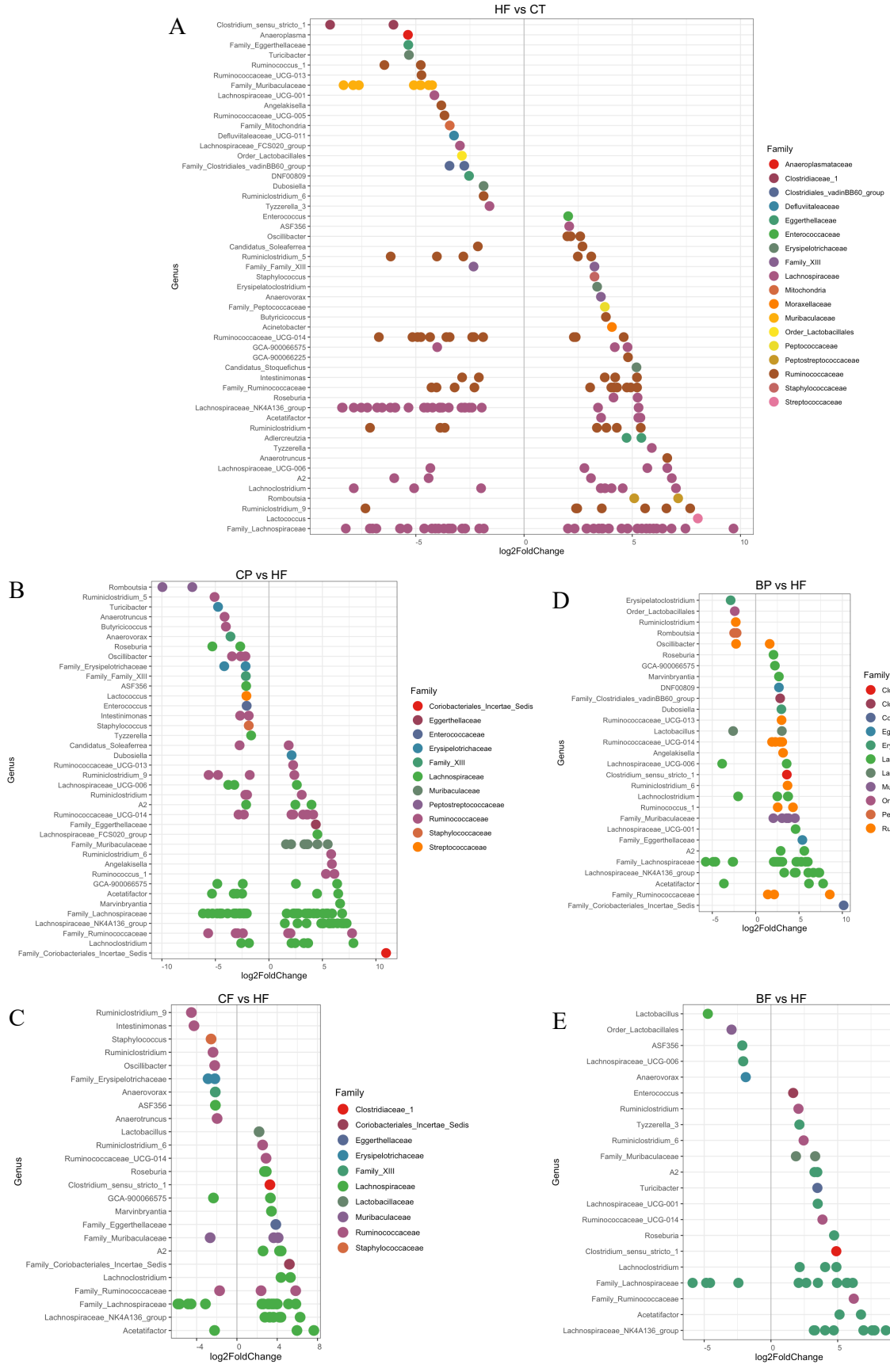
A
HF vs CT
Genus
log2FoldChange
Family
Anaeroplasmataceae
Clostridiaceae_1
Clostridiales_vadinBB60_group
Defluviitaleaceae
Eggerthellaceae
Enterococcaceae
Erysipelotrichaceae
Family_XIII
Lachnospiraceae
Mitochondria
Moraxellaceae
Muribaculaceae
Order_Lactobacillales
Peptococcaceae
Peptostreptococcaceae
Ruminococcaceae
Staphylococcaceae
Streptococcaceae
B
CP vs HF
C
CF vs HF
D
BP vs HF
E
BF vs HF

Figure 4. Bacterial taxa significantly up-regulated and down-regulated by polyphenols-rich CP and BP and their fibre-rich fractions CF and BF as compared to HFHS-fed mice.

Differential abundance analysis (DESeq2) assessing ASVs significantly changed in the microbiota of mice fed the HFHS-diet (HF) and the mice fed the HFHS-diet supplemented either with the polyphenol-rich whole cranberry powder (CP), the cranberry fibre-rich fraction (CF), the polyphenols-rich whole blueberry powder (BP), and the blueberry fibre-rich fraction (BF) after 8 weeks of intervention. A) DESeq2 analysis identified 51 ASVs that were significantly modulated in HFHS-fed obese mice (HF) relative to lean Chow-fed mice (CT); B) 38 ASVs were modulated in CP-fed mice relative to HFHS-fed obese mice; C) 25 ASVs were modulated in CF-fed mice relative to HFHS-fed obese mice; D) 29 ASVs were modulated in BP-fed mice relative to HFHS-fed obese mice; E) 21 ASVs were modulated in BF-fed mice relative to HFHS-fed obese mice. Significant ASVs ($p < 0.05$, FDR-corrected) are represented by single data points (with some data points overlapping) within each genus grouped on the x-axis, and by colour fitting to which taxonomic family the ASVs belong. Data are plotted as log2 fold change; ASVs are ordered by decreasing log2 of fold change. ASVs to the right of the zero line are more abundant and ASVs to the left of the zero line are less abundant in the groups as showed in the legends.

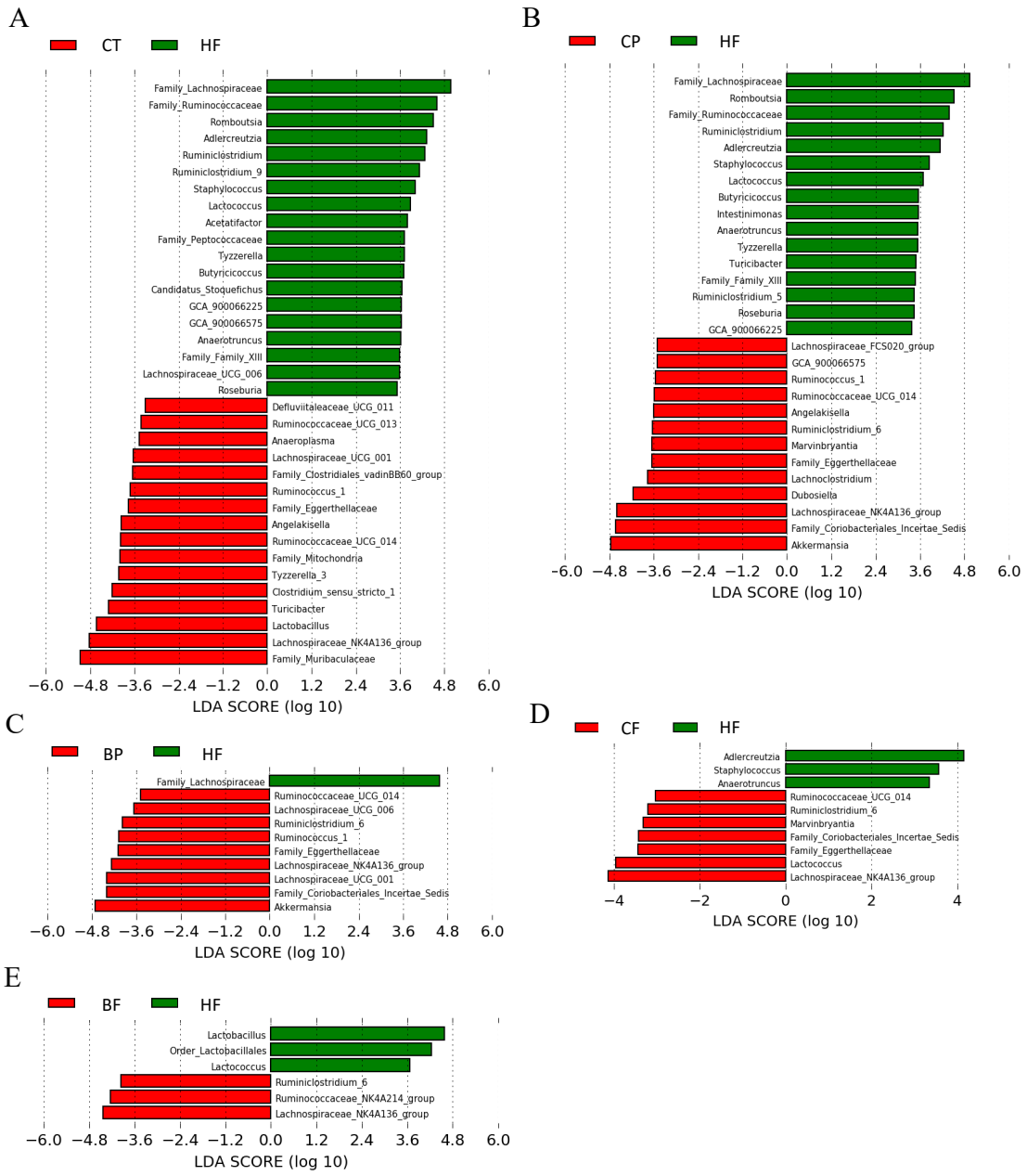

Figure 5. Bacterial taxa featured as biomarkers in mice fed the polyphenols-rich CP and BP and their fibre-rich fractions CF and BF determined by LEfSe analysis as compared to HFHS-fed mice.

Key phylotypes of differently abundant taxa were identified using linear discriminant analysis (LDA) combined with effect size (LEfSe) algorithm. A) LEfSe analysis showing taxa distinguishing mice fed the Chow-diet (CT) as compared to HFHS-fed mice (HF); B) Taxa distinguishing mice fed the polyphenol-rich whole cranberry powder

(CP); C) Taxa distinguishing mice fed the polyphenol-rich whole blueberry powder (BP); D)Taxa distinguishing mice fed the fibre-rich cranberry fraction (CF); and E) Taxa distinguishing mice fed the fibre-rich blueberry fractions (BF). The threshold for the logarithmic LDA score was 2.0. Positive LDA scores (green bars) are enriched in HF, while negative LDA scores (red bars) are enriched in CT, CP, BP, CF and BF as shown on the figure legends. Statistically significant taxa enrichment among groups was obtained with Kruskal-Wallis test among classes (Alpha value = 0.05).

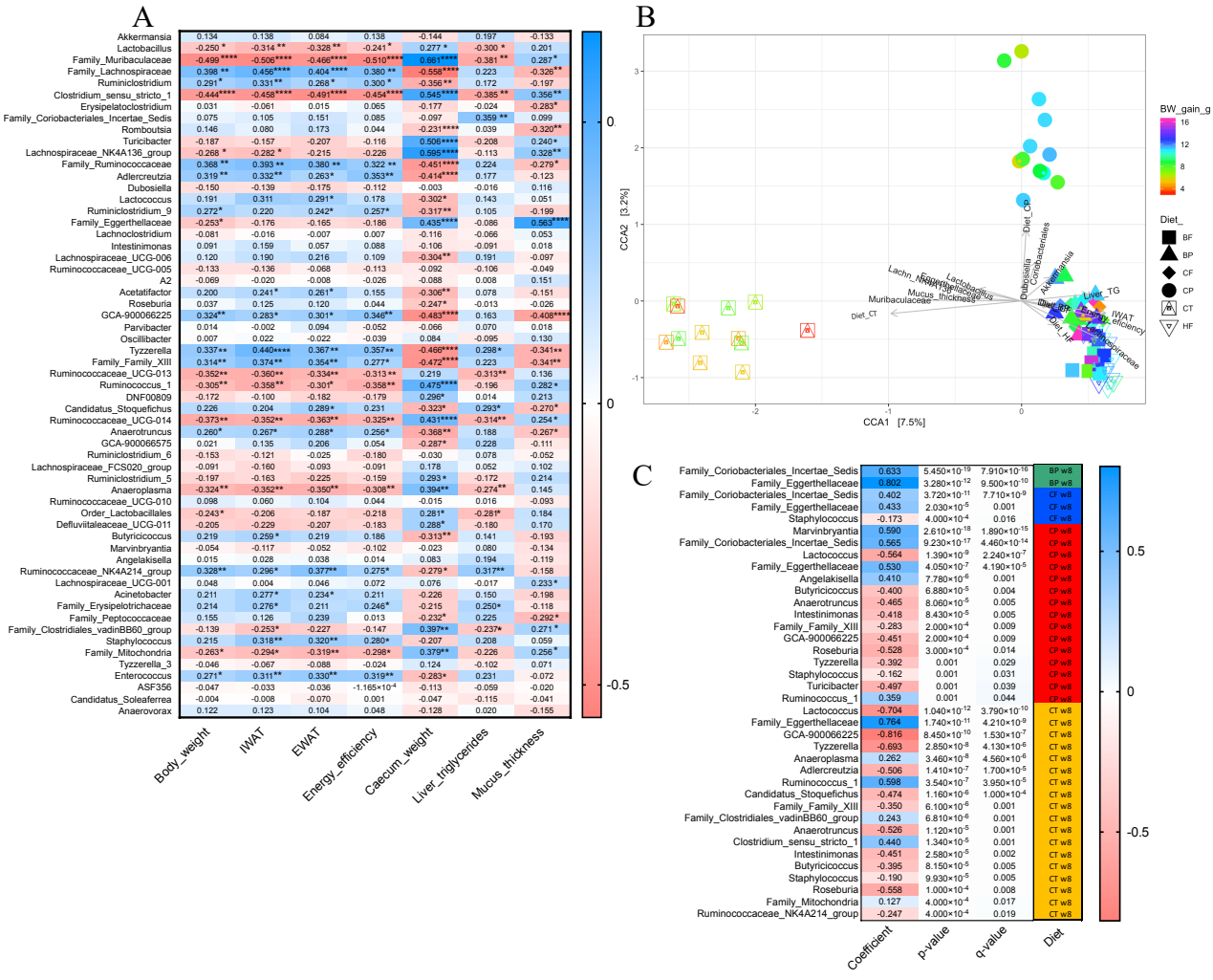

Figure 6. Widespread prebiotic role of the type of diet supplementation on relative abundances of bacterial ASVs and their correlations with mice phenotypes.

The mice were fed a HFHS-diet (HF), Chow diet (CT), HFHS-diet supplemented either with polyphenols-rich whole cranberry powder (CP), cranberry fibre-rich fraction (CF), polyphenols-rich whole blueberry powder (BP) and blueberry fibre-rich fraction (BF) for 8 weeks. A) Heatmap showing microbial associations with obesity phenotypes in mice. Each row in the heatmap represents the effects of one of the 59 ASVs (averaging >0.05% relative abundance) in each of the mouse phenotypes in columns. Blue color indicates ASVs whose relative abundance increases concomitant with the mouse phenotypes measures, and red color indicates the ASVs whose relative abundance decreases when the mouse phenotypes measure increases. On the right side of the figure, we indicate the color scale for the spearman correlation R2 scores. Asterisks indicate bacterial taxa for which the association was significant, *p<0.05, **p<0.01, ***p<0.001, ****p<0.0001. B) Ordination of Canonical Correspondence Analysis (CCA) showing the connection between samples and environmental variables along with representative taxonomies significantly modulated by the diets in mice gut microbiota. The mice of each group of diet while accounting for gut microbiota composition are coded by different symbols as shown in the legend on the right side of the figure. The arrows indicate environmental variables and bacterial taxa discriminating the different treatments: Diet_CT, Diet_HF,

Diet_CP, Diet_BP, Diet_CF, Diet_BF, Mucus_tickness, IWAT, Liver_TG, Energy_efficiency, *Lactobacillus, Muribaculaceae, Lachnospiraceae, Lachnospiraceae_NK4A136, Eggerthellaceae, Coriobacteriales,* and *Akkermansia*. The color of the symbols from each group represents the changes in mouse body weight gain in grams (denoted as BW_gain_g in the figure legend) after 8-week of intervention. C) Bacterial taxa showing opposing or compatible connection with the type of diet supplementation based on the MaAslin model applied for uncovering the prebiotic effects of berry constituents. Rows represent different bacterial taxa that exhibit significant main interaction with each of the type of diet supplementation. Columns represent the coefficient scores, the p-value ($p<0.05$), the FDR corrected p-value ($q<0.05$) and the diet interaction. Taxa showing compatible correlation are indicated with the blue color and those negatively correlated are indicated with the red color as denoted by the scale legend.

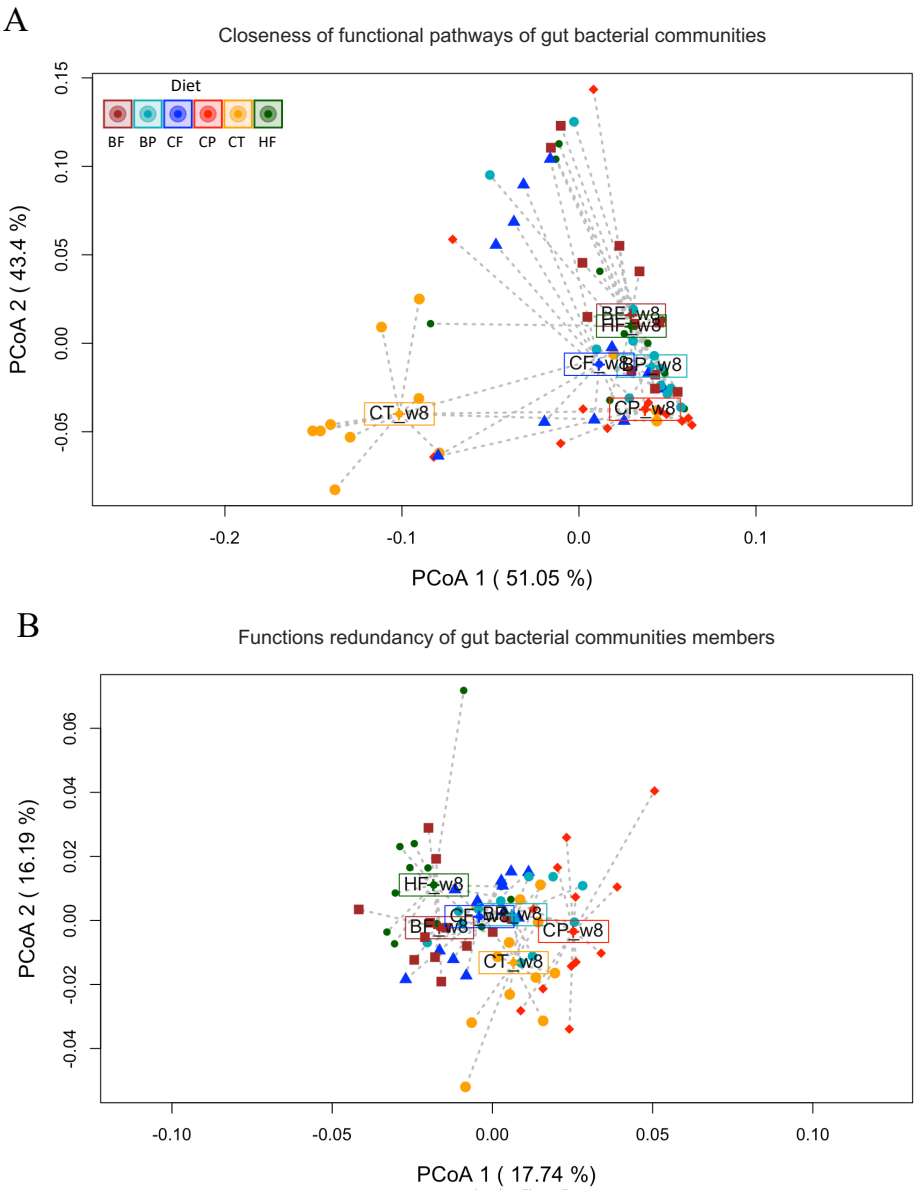

Figure 7. Gut microbiota structure of mice fed the polyphenol-rich CP-diet is showed functionally distinct to HFHS-diet induced obese mice.

Principal coordinate analyses (PCoA) of metabolic profiles across mice fed the HFHS-diet (HF), Chow diet (CT), HFHS-diet supplemented either with polyphenols-rich whole cranberry powder (CP), cranberry fibre-rich fraction (CF), polyphenols-rich whole blueberry powder (BP) and blueberry fibre-rich fraction (BF) for 8 weeks. A) Closeness of predicted functional pathways of gut bacterial communities. PCoA ordination under Bray-Curtis distance metric were performed for predicted functional composition. The functional profile of mouse microbiota on CF and BP diets are clearly distinct to HF as indicated by the centroid locations, with the strongest separation between mice on CP versus the HF diet. Contrary, the mice on the BF-diet were similar to HF. PERMANOVA comparison in terms of predicted metabolic functions resulted in a significant R^2 0.30065 ***$p<0.001$. The axis 2 and 1 explain 43.4% and

51.5% of the total variation. No significant differences in the dispersion of samples were observed, as confirmed by permutest F=0.6323 p=0.679 indicating significant dissimilarities founded in the functional structure. B) Functional redundancy of gut bacterial community members. PCoA ordination under Bray-Curtis distance metric was performed to evaluate the changes in the functional redundancy of gut bacterial communities according to the type of diet supplementation. Constrained distance-based redundancy analysis shows a clear separation of the functional profiles of mice fed the CP-diet and CT-diet from HF-group. The BP, BF and CF were confined together slightly separated from HF. The axis 2 and 1 explain 16.19% and 17.74 of the total variation. PERMANOVA accounting for predicted functional redundancy of gut microbial communities was R^2 0.27394 ***p<0.001. No significant differences in the dispersion of samples were observed, as confirmed by permutest F=0.8317 p=0.514, indicating significant dissimilarities founded in the functional redundancy of the gut microbiota. Each small-scale dot represents one faecal microbiome sample, coloured by the type of diet. Each large-scale centroid (shown as enclosed diet name) is representing the mean functional/redundancy composition of each group. The dotted lines are connecting the faecal microbiome sample to the centroids of each groups.

Supplementary information

Prebiotic potential of berry polyphenols and fibres on the gut microbiota composition and microbial metabolic functions of obese mice

Maria-Carolina Rodríguez-Daza,[1 2 *] Marcela Roquim,[1] Stéphanie Dudonné,[1 3] Geneviève Pilon,[1 4] Emile Levy, [1] André Marette,[1 4] Denis Roy,[1 2] Yves Desjardins[1 3 *]

1. *Institute of Nutrition and Functional Foods (INAF), Laval University, Québec, QC, Canada.*
2. *Food Science Department, Faculty of Agriculture and Food, Laval University, Québec, QC, Canada.*
3. *Plant Science Department, Faculty of Agriculture and Food, Laval University, Québec, QC, Canada.*
4. *Department of Medicine, Faculty of Medicine, Cardiology Axis of the Quebec Heart and Lung Institute, Québec, QC, Canada*

*Correspondence: Yves.Desjardins@fsaa.ulaval.ca; maria-carolina.rodriguez-daza.1@ulaval.ca

Table S1. Phenolic characterisation of cranberry a blueberry dry powder

Polyphenol content	Cranberry powder	Blueberry powder
Total Anthocyanins (mg C3GE/100 g DW)	**138.7 ± 19.0**	**974.4 ± 103.8**
Delphinidin 3-galactoside	-	92.8± 9.7
Delphinidin 3-glucoside	-	101.4± 10.5
Cyanidin 3-galactoside	39.1 ± 5.0	41.4 ± 3.9
Delphinidin 3-arabinoside	-	57.5 ± 6.0
Cyanidin 3-glucoside	1.6 ± 0.3	44.0 ± 4.5
Petunidin 3-galactoside	-	50.9 ± 5.3
Cyanidin 3-arabinoside	24.5 ± 3.5	25.9± 5.3
Petunidin 3-glucoside	-	75.8 ± 8.1
Peonidin 3-galactoside	51.0 ± 7.7	14.4 ± 1.4
Petunidin 3-arabinoside	-	278 ± 2.6
Peonidin 3-glucoside	4.9 ± 0.1	32.7 ± 33.6
Malvidin 3-galactoside	-	84.0 ± 12.2
Malvidin 3-glucoside	-	130.8 ± 13.7
Peonidin 3-arabinoside	17.7 ± 2.6	-
Malvidin 3-arabinoside	-	49.8 ± 4.5
Delphinidin 3-(6"-acetoyl) glucoside	-	30.0 ± 3.0
Cyanidin 3-(6"-acetoyl) glucoside	-	16.4 ± 2.9
Malvidin 3-(6"-acetoyl) glucoside	-	18.4 ± 3.1
Petunidin 3-(6"-acetoyl) glucoside	-	22.3 ± 3.4
Peonidin 3-(6"-acetoyl) glucoside	-	10.2 ± 0.9
Malvidin 3-(6"-acetoyl) glucoside	-	47.9 ± 5.9
Total Proanthocyanins (mg EE/100 g DW)	**182.2 ± 10.9**	**574 ± 11.0**
Monomers	16.3 ± 3.7	35.4 ± 4.6
Dimers	47.0 ± 3.3	55.2 ± 1.1
Trimers	15.2 ± 1.2	34.1 ± 0.3
Tetramers	9.6 ± 0.7	33.5 ± 0.8
Pentamers	5.1 ± 0.3	22.7 ± 0.3
Hexamers	ND	19.9 ± 0.3
Heptamers	ND	9.4 ± 0.4
Octamers	ND	6.9 ± 0.6
Nonamers	ND	6.6 ± 0.2
Decamers	ND	2.4 ± 0.7
Polymers >10	88.9 ± 10.9	348.4 ± 7.1

Table S2. Chemical composition of cranberry and blueberry dry powders and fibrous fractions

Composition (g/100)	Cranberry powder	Cranberry fibrous fraction	Blueberry powder	Blueberry fibrous fraction
Protein	1.4	9.0	2.5	10.4
Carbohydrates	58.6	-	76.8	5.3
Total fibres	25.1	65.4	15.4	68.3
Lipids	10.8	22.1	3.4	5.5
Residual moisture	2.1	2.0	<0.5	6.0
Ash	2.0	4.6	1.9	4.5
Energy (Kcal / 100g)	437.01	484.11	409.14	385.84

Table S3. Diets adjustment with berry powders and fibrous fractions

Ingredients (g/100 g)	HFHS	HFHS + CP		HFHS + CF		HFHS + BP		HFHS + BF	
Protein (Casein/ L-cystine)	20.18	20.04	0.14	19.84	0.35	20.06	0.12	20.06	0.12
Carbohydrate (sucrose)	26.89	21.03	5.84	26.89	-	23.05	3.84	26.83	0.06
Fibres (Cellulose/berry's fibres)	5	2.5	2.5	2.6	2.4	4.2	0.8	4.2	0.8
Fat (lard/corn oil)	39.6	38.53	1.1	38.7	0.85	39.43	0.17	39.54	0.06
Mineral mix	6.7	6.7	-	6.7	-	6.7	-	6.7	-
Vitamin mix	1.4	1.4	-	1.4	-	1.4		1.4	-
Choline bitartrate	0.2	0.2	-	0.2	-	0.2	-	0.2	-
Tert-butylhydrytoluene (BHT)	0.03	0.03	-	0.03	-	0.03	-	0.03	-
Residual humidity + ashes	-	-	0.4	-	0.25	-	0.1	-	0.12
TOTAL (g)	**100**	**100.41**		**100.21**		**100.13**		**100.12**	
Energetic density (kcal/g)	**5.45**	**5.42**		**5.43**		**5.44**		**5.44**	

Table S4. Proanthocyanidins (PACs) content in berry fibrous fractions

PACs degree of polymerization (DP)	Cranberry fibrous fraction		Blueberry fibrous fraction	
	Extractible PACs	Non-extractible PACs	Extractible PACs	Non-extractible PACs
Monomers	0,24 ± 0,023	0,06 ± 0,002	0,10 ± 0,001	0
Dimers	0,38 ± 0,003	0	0,06 ± 0,003	0
Trimers	0,17 ± 0,007	0	0,06 ± 0,003	0
Tetramers	0,11 ± 0,004	0	0	0
Pentamers	0,07 ± 0,001	0	0	0
Hexamers	0,06 ± 0,002	0	0	0
Heptamers	0,04 ± 0,003	0	0	0
Octamers	0,02 ± 0,019	0	0	0
Nonamers	0	0	0	0
Decamers	0	0	0	0
Polymers>10	0,13 ± 0,034	0	0,71 ± 0,113	0
Total	**1,21 ± 0,095**	**0,06 ± 0,002**	**0,93 ± 0,12**	**0**

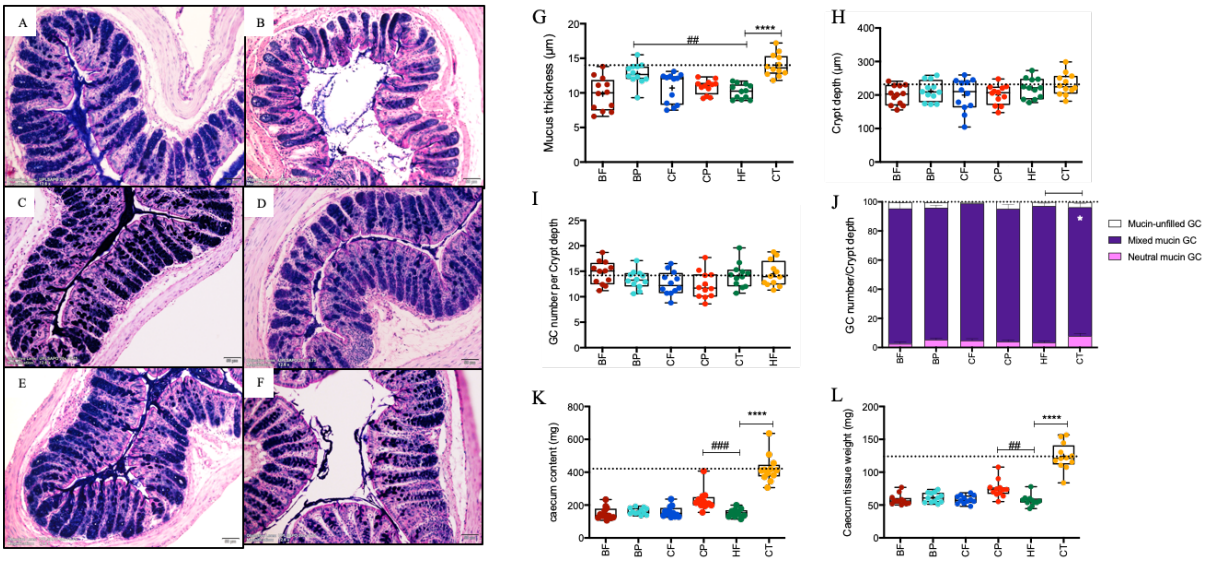

Figure S1. BP-diet improved the colonic mucus thickness and the CP-diet increased the caecum size and mass in HFHS diet induced obese mice.

Representative histological images of the colon tissues of examined mice (n=12) fed the A) CT, B) HFHS, C) CP, D) CF, E) BP, and F) BF diets. A combination of Alcian Blue and periodic acid–Schiff staining (AB/PAS) was used to distinguish acidic (dark blue) and neutral (red) mucins. A purple color indicates the presence of both acidic and neutral mucins. Images were taken using objective lens UPLSAPO 20X/0.75, magnification 12.6X, Scale 50 µm. Histological parameters were evaluated in cross-sections of colon tissues stained with AB/PAS staining: G) Mucus thickness, H) Crypt depth I) Total goblet cells number per µm of crypt, and J) Total mucin-filled goblet cells number. The weight of K) caeca content and L) tissues were also registered as indicative of the impact of diets on the microbial community changes. Data are shown as Mean ± SEM (n = 12/group). Significant differences were determined by ordinary one-way ANOVA. Values are expressed as mean +/- SEM. ****p<0.0001, **p<0.01 and *p<0.05 compared to HFHS. Chow group is represented by the dotted line.

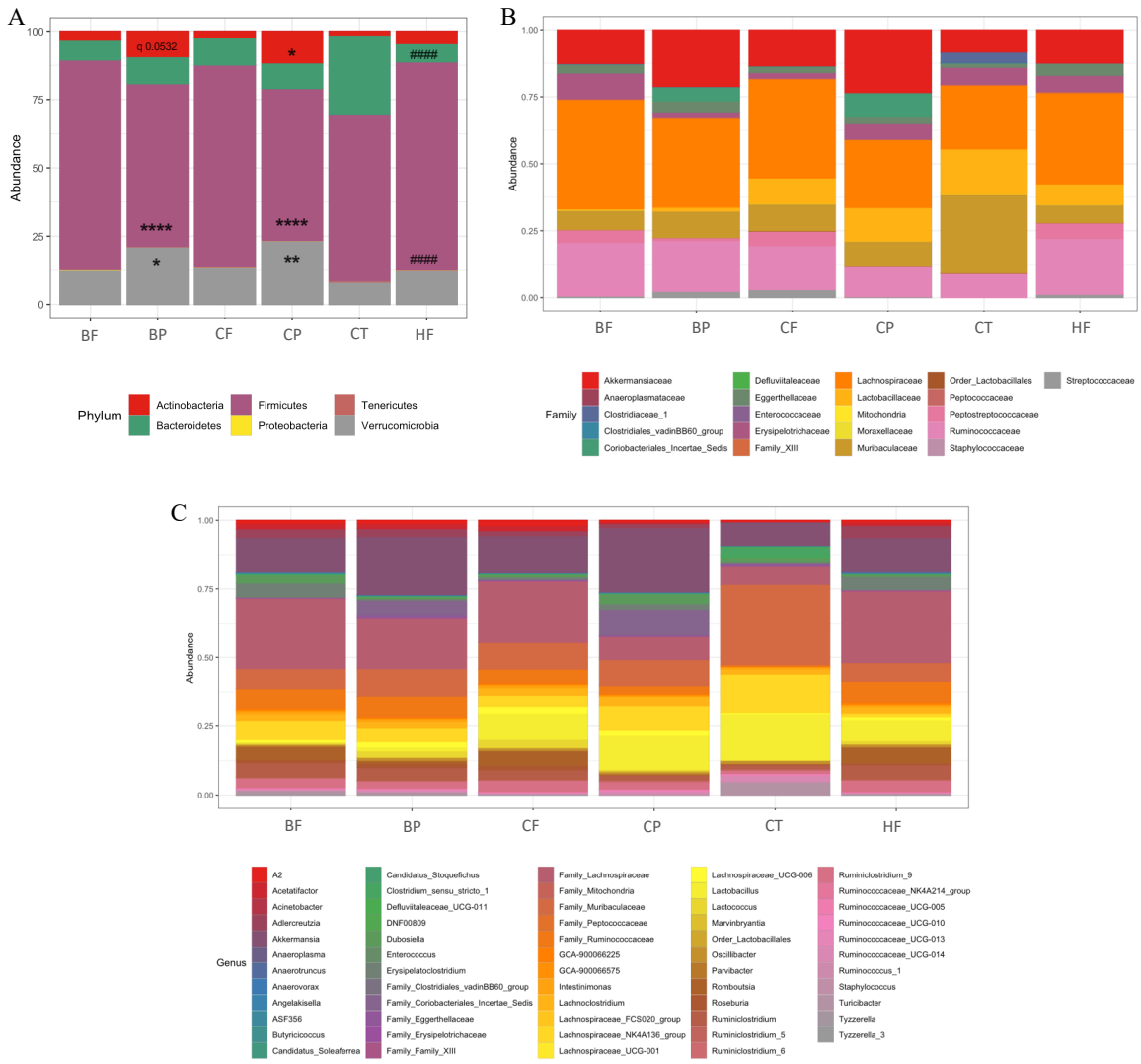

Figure S2. Polyphenols-rich CP and BP diets reduced the relative proportions of gut opportunistic bacteria and triggered health-promoting taxonomies in HFHS-diet induced obese mice.

Polyphenols-rich CP and BP diets significantly decreased the relative abundance of phylum Firmicutes and selectively increased the phyla Verrucomicrobia and Actinobacteria in HFHS-diet induced obese mice. A) Bar graph shows the changes in the relative abundance of gut microbiota phyla at 8 weeks in mice fed the HFHS diet (HF), Chow diet (CT), HFHS-diet supplemented with either cranberry powder (CP), cranberry fibre-rich fraction (CF), blueberry powder (BP) and blueberry fibre-rich fraction (BF) are presented. B) Bar graph of the relative abundances of the bacterial families across the gut microbiota composition of each group. C) Bar graph of the relative abundances of the genera composing the gut microbiota of each group. Kruskal-Wallis test with FDR Benjamini and Hochberg post-hoc multiple comparison correction was performed to compare taxonomic abundance among groups and Mann-Whitney U test was performed to compare the F/B ratio. #### $p<0.0001$, ### $p<0.001$ as compared to CT-group and *$p<0.05$, **$p<0.01$, ***$p<0.001$, ****$p<0.0001$ as compared to HFHS.

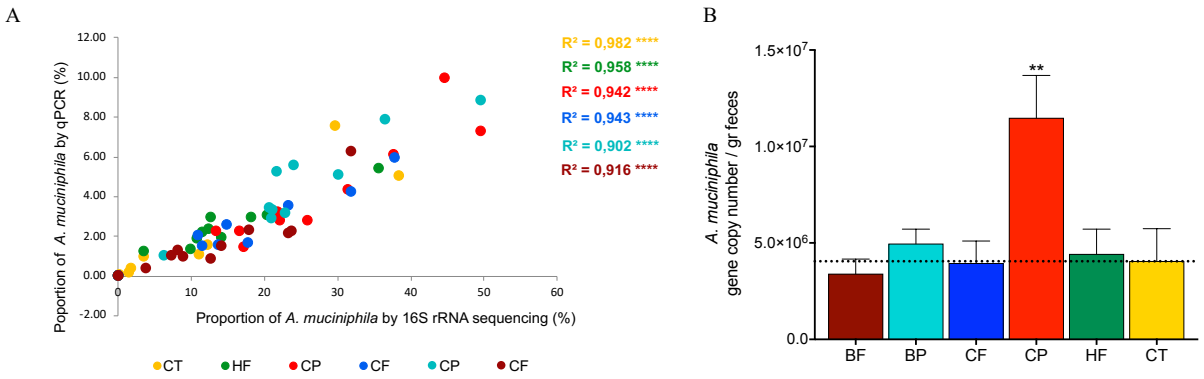

Figure S3. Absolute quantification of 16S rRNA gene copy of Akkermansia muciniphila in mice fecal samples.

A) Correlation between the relative abundance of Akkermansia muciniphila analyzed by 16S rRNA gene sequencing and by qPCR. Each point in a plot represents the values of the linear combinations for a sample pair in the correlation. Spearman correlation R^2 scores are indicated in the graphs. Asterisks indicate bacterial taxa for which the association was significant, *p<0.05, **p<0.01, ***p<0.001, ****p<0.0001. Points representing the faecal relative abundance are color-coded by groups being HFHS-diet (HF), Chow diet (CT), HFHS-diet supplemented either with polyphenols-rich cranberry powder (CP), cranberry fibre-rich fraction (CF), polyphenols-rich blueberry powder (BP) and blueberry fibre-rich fraction (BF). B) Absolute quantification of 16S rRNA gene copy of *A. muciniphila* per gr of fecal samples. Kruskal-Wallis test with FDR Benjamini and Hochberg post-hoc multiple comparison correction was performed to compare taxonomic abundance among groups. *p<0.05, **p<0.01, ***p<0.001, ****p<0.0001 as compared to HFHS.

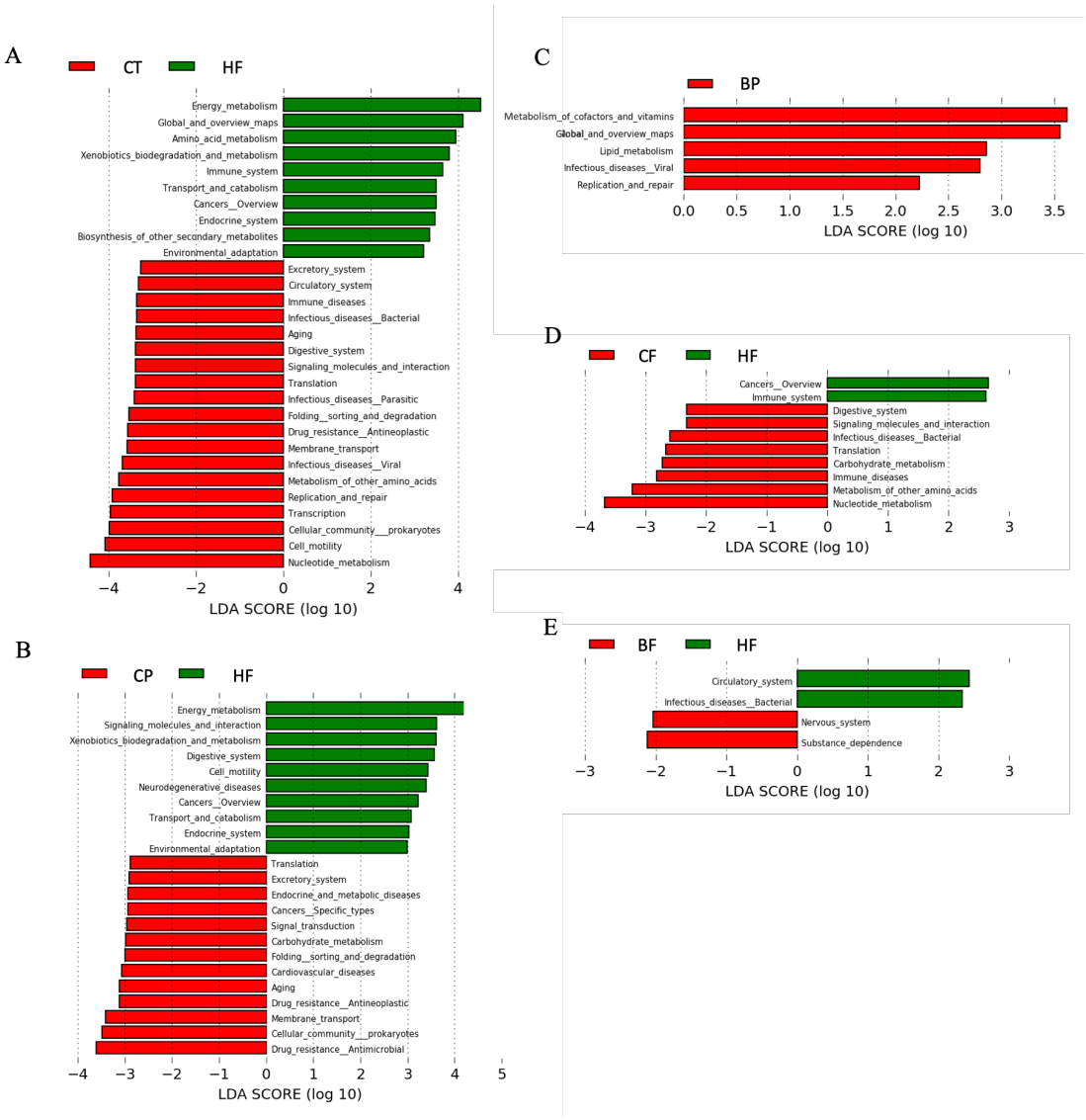

Figure S4. Key Predicted level 2 KEGG functional pathways differently enriched in the gut microbiota of mice.

Level 2 KEGG pathways characterizing the microbial functional composition were identified using linear discriminant analysis (LDA) combined with effect size (LEfSe) algorithm. A) Predicted microbial function capacities enriched in the mice fed HFHS-diet (HF) as compared to Chow diet (CT); B) Microbial functional pathways enriched in mice fed the polyphenols-rich cranberry powder (CP) as compared to HF; C) Microbial functional pathways enriched in mice fed the polyphenols-rich blueberry powder (BP) as compared to HF; D) Microbial functional pathways enriched in mice fed the cranberry fibre-rich fraction as compared to HF (CF); and E) Microbial functional pathways enriched in mice fed the blueberry fibre-rich fraction (BF) as compared to HF. The threshold for the logarithmic LDA score was 2.0. Positive LDA scores (green bars) are enriched in HF, while negative LDA scores (red bars) are enriched in CT, CP, BP, CF and BF as shown on the figure legends. Statistically significant taxa enrichment among groups was obtained with Kruskal-Wallis test among classes (Alpha value = 0.05).

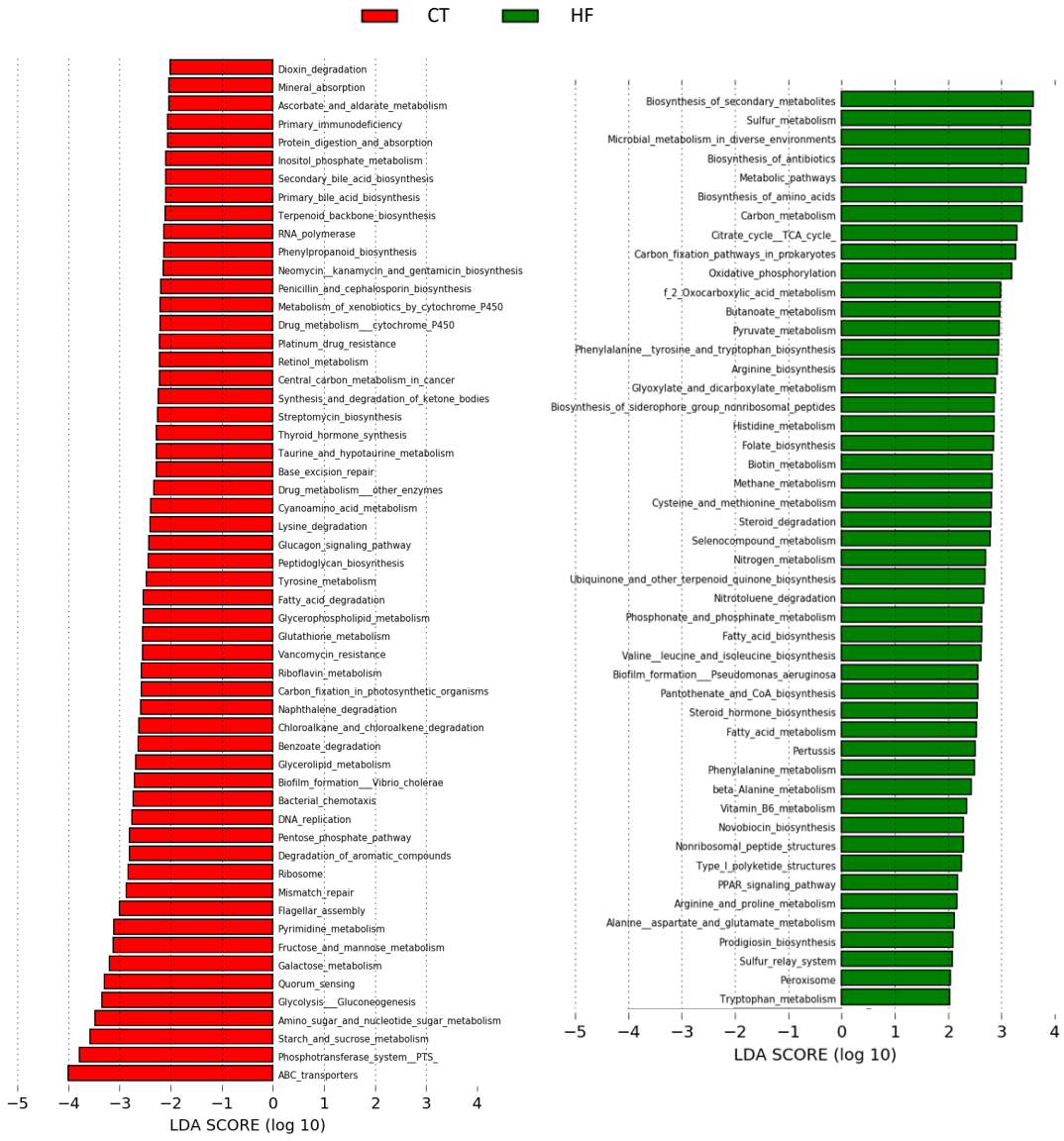

Figure S5. Level 1 KEGG pathways distinguishing the functional composition of the gut microbiota of mice fed the HFHS-diet and the Chow-diet.

Level 1 KEGG pathways characterizing the microbial functional composition were identified using linear discriminant analysis (LDA) combined with effect size (LEfSe) algorithm. The threshold for the logarithmic LDA score was 2.0. Positive LDA scores (green bars) are enriched in HFHS-fed mice (HF), while negative LDA scores (red bars) are enriched in Chow-fed mice (CT) as shown on the figure legends. Statistically significant taxa enrichment among groups was obtained with Kruskal-Wallis test among classes (Alpha value = 0.05).

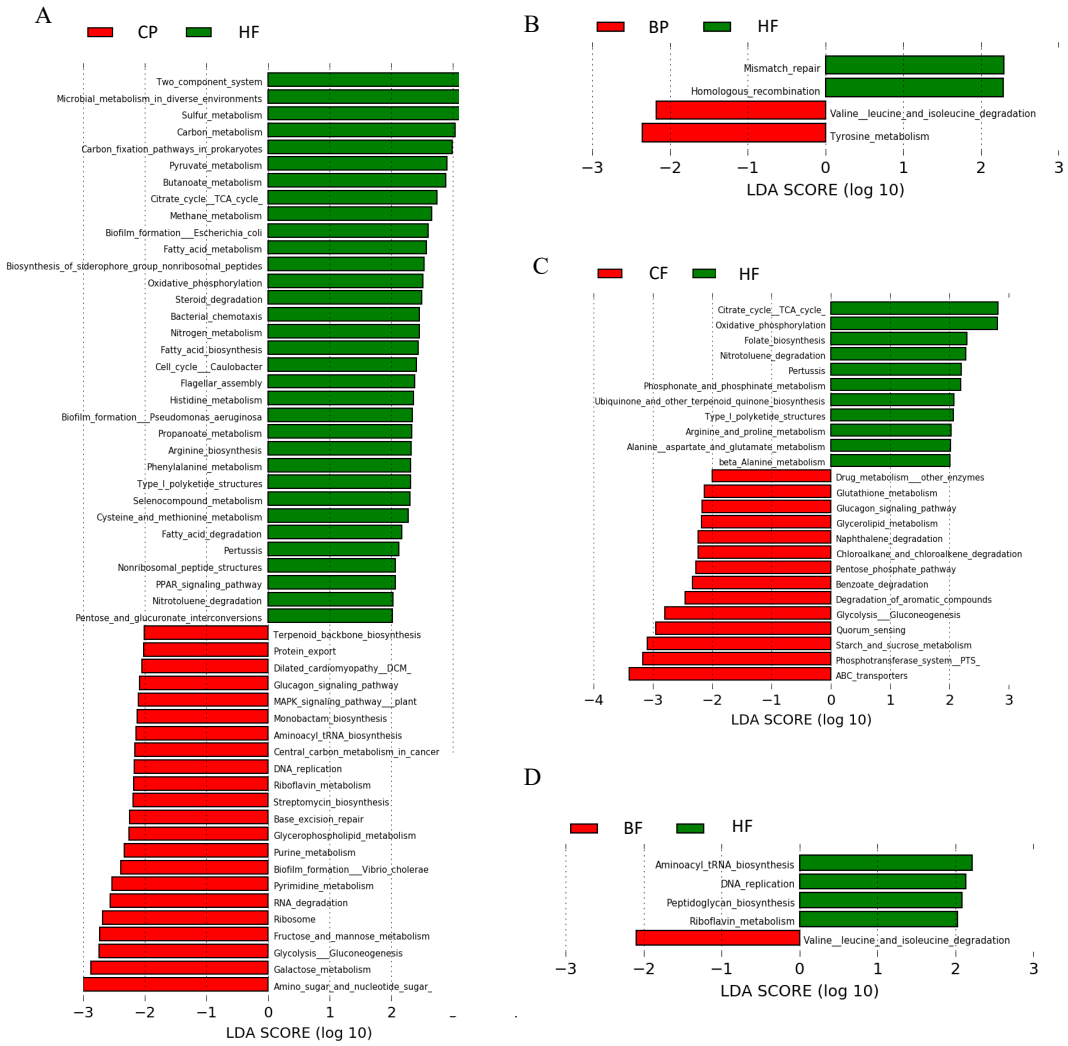

Figure S6. Level 1 KEGG pathways significantly differentiating the functional composition of the gut microbiota of mice fed the polyphenols-rich CP and BP and their fibre-rich fractions CF and BF as compared to HFHS-fed mice.

Level 1 KEGG pathways distinguishing the functional profile of the gut microbiota were identified using linear discriminant analysis (LDA) combined with effect size (LEfSe) algorithm. A) Microbial functional pathways enriched in mice fed the polyphenols-rich cranberry powder (CP) as compared to HFHS (HF); B) Microbial functional pathways enriched in mice fed the polyphenols-rich blueberry powder (BP) as compared to HF; C) Microbial functional pathways enriched in mice fed the cranberry fibre-rich fraction as compared to HF (CF); and D) Microbial functional pathways enriched in mice fed the blueberry fibre-rich fraction (BF) as compared to HF. The threshold for the logarithmic LDA score was 2.0. Positive LDA scores (green bars) are enriched in HF, while negative LDA scores (red bars) are enriched in CP, BP, CF and BF as shown on the figure legends. Statistically significant taxa enrichment among groups was obtained with Kruskal-Wallis test among classes (Alpha value = 0.05).

Table S5. Level 1 KEGG microbial functions significantly correlated with changes in mouse body weight as determined by MaAsLin multivariate model

Variable	Microbial Functional Feature	Coefficient	N	N.not.0	p-value	q-value
Body_weight	Phosphotransferase system (PTS)	-0.0059225	72	72	7.49E-05	0.00292188
Body_weight	Amino sugar and nucleotide sugar metabolism	-0.0020872	72	72	0.00042764	0.00902506
Body_weight	Fructose and mannose metabolism	-0.0013018	72	72	0.00076182	0.01313482
Body_weight	Glutathione metabolism	-0.0011398	72	72	0.00019422	0.00571234
Body_weight	Primary bile acid biosynthesis	-0.0008386	72	72	0.00085033	0.01400381
Body_weight	DNA replication	-0.0008198	72	72	5.24E-05	0.00290966
Body_weight	Pentose phosphate pathway	-0.0007384	72	72	5.48E-06	0.00161805
Body_weight	Riboflavin metabolism	-0.0006695	72	72	0.00129273	0.0191842
Body_weight	Prolactin signaling pathway	-0.0006553	72	72	0.0015496	0.02213708
Body_weight	Penicillin and cephalosporin biosynthesis	-0.0006482	72	72	0.00130453	0.0191842
Body_weight	Cyanoamino acid metabolism	-0.0006368	72	72	1.91E-05	0.00161805
Body_weight	Homologous recombination	-0.0005034	72	72	0.00061627	0.01100476
Body_weight	Phenylpropanoid biosynthesis	-0.0004368	72	72	0.00048596	0.00913766
Body_weight	Peptidoglycan biosynthesis	-0.0003806	72	72	0.00046376	0.00913766
Body_weight	RNA polymerase	-0.0003797	72	72	0.00031094	0.00706675
Body_weight	Proteasome	-0.0002985	72	60	0.00259651	0.03606261
Body_weight	Type II diabetes mellitus	-0.0001315	72	72	2.27E-05	0.00161805
Body_weight	Choline metabolism in cancer	0.00042113	72	72	0.00010017	0.00357748
Body_weight	Vitamin B6 metabolism	0.00060283	72	72	0.0004332	0.00902506
Body_weight	Novobiocin biosynthesis	0.00062698	72	72	0.00015897	0.00496791
Body_weight	Valine, leucine and isoleucine biosynthesis	0.00091862	72	72	0.00086824	0.01400381
Body_weight	Phosphonate and phosphinate metabolism	0.00092898	72	72	1.62E-05	0.00161805
Body_weight	2-Oxocarboxylic acid metabolism	0.00111864	72	72	0.00028409	0.00676395
Body_weight	Oxidative phosphorylation	0.00115897	72	72	7.60E-05	0.00292188
Body_weight	Glyoxylate and dicarboxylate metabolism	0.00118521	72	72	0.00024553	0.00641461
Body_weight	Biosynthesis of antibiotics	0.00146004	72	72	2.14E-05	0.00161805
Body_weight	Biosynthesis of amino acids	0.00150048	72	72	0.00013508	0.00450258
Body_weight	Phenylalanine, tyrosine and tryptophan biosynthesis	0.00152835	72	72	0.00049343	0.00913766
Body_weight	Biosynthesis of secondary metabolites	0.00170713	72	72	0.00023538	0.00641461
Body_weight	Citrate cycle (TCA cycle)	0.00174812	72	72	7.50E-05	0.00292188

Table S6. Level 1 KEGG microbial functions significantly correlated with the energy efficiency measures in mice determined by MaAsLin multivariate model.

Variable	Microbial Functional Feature	Coefficient	N	N.not.0	p-value	q-value
Energy_efficiency	Phosphotransferase system (PTS)	-4.3164784	72	72	0.00013883	0.00079608
Energy_efficiency	ABC transporters	-2.8608865	72	72	3.82E-05	0.0005455
Energy_efficiency	Starch and sucrose metabolism	-2.5602155	72	72	8.51E-05	0.00079003
Energy_efficiency	Glycolysis / Gluconeogenesis	-1.2523014	72	72	3.38E-05	0.0005455
Energy_efficiency	Glutathione metabolism	-0.8400877	72	72	0.00028179	0.00136617
Energy_efficiency	Pyrimidine metabolism	-0.7761125	72	72	3.87E-05	0.0005455
Energy_efficiency	Mismatch repair	-0.7462071	72	72	3.93E-05	0.0005455
Energy_efficiency	Degradation of aromatic compounds	-0.716631	72	72	3.68E-05	0.0005455
Energy_efficiency	cGMP-PKG signaling pathway	-0.7095958	72	72	0.00013102	0.00079003
Energy_efficiency	cAMP signaling pathway	-0.7095958	72	72	0.00013102	0.00079003
Energy_efficiency	Cardiac muscle contraction	-0.7095958	72	72	0.00013102	0.00079003
Energy_efficiency	Adrenergic signaling in cardiomyocytes	-0.7095958	72	72	0.00013102	0.00079003
Energy_efficiency	Insulin secretion	-0.7095958	72	72	0.00013102	0.00079003
Energy_efficiency	Aldosterone synthesis and secretion	-0.7095958	72	72	0.00013102	0.00079003
Energy_efficiency	Aldosterone-regulated sodium reabsorption	-0.7095958	72	72	0.00013102	0.00079003
Energy_efficiency	Endocrine and other factor-regulated calcium reabsorption	-0.7095958	72	72	0.00013102	0.00079003
Energy_efficiency	Gastric acid secretion	-0.7095958	72	72	0.00013102	0.00079003
Energy_efficiency	Pancreatic secretion	-0.7095958	72	72	0.00013102	0.00079003
Energy_efficiency	Protein digestion and absorption	-0.7030792	72	72	5.87E-05	0.0006376
Energy_efficiency	Bile secretion	-0.6918516	72	72	0.00016622	0.00090336
Energy_efficiency	Mineral absorption	-0.6725455	72	72	9.75E-05	0.00079003
Energy_efficiency	Chloroalkane and chloroalkene degradation	-0.6582353	72	72	9.29E-06	0.0005455
Energy_efficiency	Primary immunodeficiency	-0.6458242	72	72	0.00012589	0.00079003
Energy_efficiency	Glycerolipid metabolism	-0.6306738	72	72	0.00012953	0.00079003
Energy_efficiency	Naphthalene degradation	-0.6204404	72	72	3.73E-05	0.0005455
Energy_efficiency	DNA replication	-0.6050003	72	72	7.96E-05	0.00079003
Energy_efficiency	Pentose phosphate pathway	-0.5481787	72	72	8.15E-06	0.0005455
Energy_efficiency	Cyanoamino acid metabolism	-0.4711767	72	72	2.89E-05	0.0005455
Energy_efficiency	Carbon fixation in photosynthetic organisms	-0.4094607	72	72	4.37E-05	0.00055539
Energy_efficiency	Drug metabolism - other enzymes	-0.3110524	72	72	9.40E-05	0.00079003
Energy_efficiency	Ribosome biogenesis in eukaryotes	-0.2547038	72	72	0.00014011	0.00079608
Energy_efficiency	Vancomycin resistance	-0.2472966	72	72	0.00013273	0.00079003
Energy_efficiency	Type II diabetes mellitus	-0.0987267	72	72	2.52E-05	0.0005455

Energy_efficiency	Peroxisome	0.23960372	72	72	0.0001501	0.00083389
Energy_efficiency	Choline metabolism in cancer	0.31476786	72	72	0.00011818	0.00079003
Energy_efficiency	Ubiquinone and other terpenoid-quinone biosynthesis	0.47828201	72	72	0.00021295	0.00111461
Energy_efficiency	Selenocompound metabolism	0.55908577	72	72	0.00021401	0.00111461
Energy_efficiency	Phosphonate and phosphinate metabolism	0.69850007	72	72	1.74E-05	0.0005455
Energy_efficiency	Folate biosynthesis	0.71703049	72	72	3.92E-05	0.0005455
Energy_efficiency	Arginine biosynthesis	0.81467295	72	72	1.98E-05	0.0005455
Energy_efficiency	Biotin metabolism	0.84148802	72	72	1.90E-05	0.0005455
Energy_efficiency	Nitrotoluene degradation	0.86780223	72	72	2.07E-05	0.0005455
Energy_efficiency	Oxidative phosphorylation	0.89092059	72	72	5.32E-05	0.00061504
Energy_efficiency	Biosynthesis of antibiotics	1.06334308	72	72	4.44E-05	0.00055539
Energy_efficiency	Biosynthesis of amino acids	1.08551728	72	72	0.00026873	0.00136617
Energy_efficiency	Citrate cycle (TCA cycle)	1.34168133	72	72	5.41E-05	0.00061504

Table S7. MaAsLin significant correlations between the KEGG microbial functions and the levels of liver triglycerides in mice

Variable	**Microbial Functional Feature**	**Coefficient**	**N**	**N.not.0**	**p-value**	**q-value**
Liver_TG	Degradation of aromatic compounds	-4.75E-05	72	72	3.89E-05	0.00353277
Liver_TG	Ethylbenzene degradation	-4.56E-05	72	72	3.30E-06	0.00058828
Liver_TG	alpha-Linolenic acid metabolism	-4.53E-05	72	72	3.53E-06	0.00058828
Liver_TG	Quorum sensing	-4.40E-05	72	72	0.00010669	0.0088905
Liver_TG	Naphthalene degradation	-4.35E-05	72	72	1.18E-05	0.00131009
Liver_TG	Pentose phosphate pathway	-3.79E-05	72	72	3.06E-06	0.00058828
Liver_TG	Vancomycin resistance	-1.83E-05	72	72	1.56E-05	0.00155561
Liver_TG	Folate biosynthesis	5.07E-05	72	72	1.04E-05	0.00129991
Liver_TG	Biosynthesis of antibiotics	7.83E-05	72	72	4.51E-06	0.00064361

CHAPTER II

We have previously studied the effects of polyphenols-rich cranberry and blueberry powders and of their fibrous fractions on the attenuation of metabolic disorders, uncovering the instrumental role that polyphenols exert in promoting *A. muciniphila* and other key bacterial species driving beneficial effects to host health. However, it is well known that the berries contain a wide array of polyphenols that may act in a different manner on the host depending of their structure. The present chapter evaluates the effect of wild blueberry polyphenolic extract and three derived polyphenolic fractions on the gut microbiota composition, the colonic histomorphology, and on the progress of diet-induced obesity and insulin resistance. The phenolic sub-fractions constituted by F1) anthocyanidins and phenolic acids, F2) oligomeric PACs and flavovols, and F3) polymeric PACs, were administrated to mice at the same concentration as encountered in the total blueberry extract. This approach led to identify which polyphenols contributed the most to stimulate *A muciniphila*, restore its ecological niche, and improve metabolic alterations in mice fed an obesogenic diet. Here, the colonic histomorphology and mucin profile was targeted as instrumental mechanisms by which, blueberry unabsorbed phenolics, mainly those of high molecular weight, can act to promote *A. muciniphila* growth. PACs polymer-enriched fractions were demonstrated to significantly improve the glucose tolerance and restore the colonic epithelium, by inducing a thicker mucus layer and a higher number of mucin-secreting goblet cells than the untreated controls counterpart. The scientific manuscript was published in the *Nature's Scientific Reports* journal, February 2020 (https://doi.org/10.1038/s41598-020-58863-1).

Wild blueberry proanthocyanidins shape distinct gut microbiota profile and influence glucose homeostasis and intestinal phenotypes in high-fat high-sucrose fed mice

Maria-Carolina Rodríguez-Daza[1 2 a], Laurence Daoust[1 2 a], Lemia Boutkrabt[1], Geneviève Pilon[1 3], Thibault Varin[1], Stéphanie Dudonné[1], Émile Levy[1], André Marette[1 3], Denis Roy[1 2] and Yves Desjardins[1 2]

[1] Institute of Nutrition and Functional Foods (INAF), Laval University, Québec, QC, Canada.

[2] Food Science Department, Faculty of Agriculture and Food, Laval University, Québec, QC, Canada.

[3] Department of Medicine, Faculty of Medicine, Cardiology Axis of the Quebec Heart and Lung Institute, Québec, QC, Canada.

[a] These authors contributed equally to this work

Corresponding Author:

Yves Desjardins

Institute of Nutrition and Functional Foods (INAF)

Laval University, Québec

Pavillon des Services, # 2736

2440, Boulevard Hochelaga, Québec, QC, Canada G1V 0A6

Telephone: 418-262-0897; email: yves.desjardins@fsaa.ulaval.ca

Article published in the Journal of Scientific Reports

10, Article number: 2217 (2020), https://doi.org/10.1038/s41598-020-58863-1

Résumé

Les bleuets sont une source importante de polyphénols et sont largement étudiés pour la prévention ou l'atténuation des maladies métaboliques. Cependant, la contribution santé et les mécanismes d'action des polyphénols dépendent de leur type et de leur structure. Cette étude a évalué les effets d'un extrait polyphénolique de bleuet (WBE) (*Vaccinium angustifolium* Aiton) sur les paramètres cardiométaboliques, la composition du microbiote et l'histologie de l'épithélium intestinal des souris nourries d'une diète obesogène (HFHS), et elle visait à déterminer quelles fractions polyphénoliques (BPF) dérivées de l'extrait, étaient responsables des effets observés. Pour ce faire, l'extrait entier a été séparé en trois fractions, F1) anthocyanes et acides phénoliques, F2) proanthocyanidines oligomeriques (PACs), acides phénoliques et flavonols (PACs degré de polymérisation DP<4), et F3) polymères de PACs (PACs DP>4) et ajouté à la diète HFHS aux concentrations équivalant respectivement à celles retrouvées dans l'extrait entier. Après 8 semaines, le WBE a réduit de 18,3 % l'AUC de l'OGTT par rapport aux souris traitées par le HFHS, et F3 a contribué le plus à cet effet. La fraction F1 riche en anthocyanes n'a pas reproduit cette réponse. WBE et le BPF ont restauré la couche de mucus colique. En particulier, la fraction F3 riche en PAC polymères a augmenté le nombre de cellules caliciformes sécrétant du mucus. WBE a augmenté de 2 fois la proportion d'*Adlercreutzia equolifaciens,* tandis que la fraction F2 riche en PACs oligomères a augmenté de 2,5 fois la proportion d'*Akkermansia muciniphila*. Cette étude révèle le rôle des PACs de WBE sur la modulation du microbiote intestinal et la restauration de la couche du mucus épithélial du côlon qui constitue une importante niche écologique pour les bactéries symbiotiques associées à la muqueuse, dont la présence peut être fondamentale dans l'apparition des effets santé induits par des polyphénols du bleuet.

Mots clés : polyphénols, proanthocyanidines, microbiote intestinale, *Akkermansia muciniphila, Adlercreutzia equolifaciens*, homéostasie du glucose.

Abstract

Blueberries are a rich source of polyphenols, widely studied for the prevention or attenuation of metabolic diseases. However, the health contribution and mechanisms of action of polyphenols depend on their type and structure. Here, we evaluated the effects of a wild blueberry polyphenolic extract (WBE) (*Vaccinium angustifolium* Aiton) on cardiometabolic parameters, gut microbiota composition and gut epithelium histology of high-fat high-sucrose (HFHS) diet-induced obese mice and determined which constitutive polyphenolic fractions (BPF) was responsible for the observed effects. To do so, the whole extract was separated in three fractions, F1) Anthocyanins and phenolic acids, F2) oligomeric proanthocyanidins (PACs), phenolic acids and flavonols (PACs degree of polymerization DP<4), and F3) PACs polymers (PACs DP>4) and supplied at their respective concentration in the whole extract. After 8 weeks, WBE reduced OGTT AUC by 18.3% compared to the HFHS treated rodents and the F3 contributed the most to this effect. The anthocyanin rich F1 fraction did not reproduce this response. WBE and the BPF restored the colonic mucus layer. Particularly, the polymeric PACs-rich F3 fraction increased the mucin-secreting goblet cells number. WBE caused a significant 2-fold higher proportion of *Adlercreutzia equolifaciens* whereas oligomeric PACs-rich F2 fraction increased by 2.5-fold the proportion of *Akkermansia muciniphila.* This study reveals the key role of WBE PACs in modulating the gut microbiota and restore colonic epithelial mucus layer, providing a suitable ecological niche for mucosa-associated symbiotic bacteria, which may be crucial in triggering health effects of blueberry polyphenols.

Keywords**:** polyphenols, proanthocyanins, gut microbiota, *Akkermansia muciniphila, Adlercreutzia equolifaciens,* glucose homeostasis.

Introduction

Wild blueberries *(Vaccinium angustifolium* Aiton*)* are recognized as a rich source of bioactive phenolic compounds, the consumption of which has been associated with the attenuation of metabolic disorders through its beneficial action on glucose homoeostasis and the reduction the oxidative stress and intestinal inflammation[1,2]. Until now, these positive effects have predominantly been attributed to flavonoids and in particular to anthocyanins[3,4]. However, wild blueberry has a complex profile of bioactive polyphenols; in addition to anthocyanins, it contains chlorogenic acid, and oligomers and polymers of flavan-3-ols, such as proanthocyanidins (PACs) [5]. Interestingly, there is increased evidence showing that PACs can attenuate the progression of metabolic syndrome, including type 2 diabetes and obesity[6]. Preclinical studies have suggested different mechanisms by which PACs regulate metabolic health, ranging from immunomodulatory signaling, stimulation of glucose and lipid metabolism, dampening of metabolic endotoxemia, as well as through inhibition of digestive enzymes[7-9]. However, since high molecular weight PACs are poorly absorbed in the small intestine[10], they reach the large intestine where they interact with the gut microbiota and exert prebiotic-like effects[11].

A disrupted intestinal homoeostasis and alterations in the gut microbiota diversity and taxonomic composition (i.e., dysbiosis) have been found to affect intestinal immune response[12] and contribute to the pathogenesis of obesity and type 2 diabetes; it may therefore represent novel risk factors for these metabolic disorders. Likewise, gut epithelial inflammation and altered mucus layer lead to increased epithelial permeability and are specifically associated with an altered gut microbiota [13-15]. Among the lifestyle factors affecting gut microbial diversity, diet quality is of paramount importance and contributes significantly to the determination of gut microbiota composition [16]. In this context, berry polyphenols, including wild blueberry, have recently been shown to significantly promote the abundance of beneficial bacteria involved in the attenuation of obesity-associated disorders and dysbiosis [17,18]. Indeed, in rats fed a high-fat diet, the supplementation of blueberry powder for 8-weeks improved insulin sensitivity and systemic inflammation in association with major changes in gut microbiota composition[19]. In human, a cross-over dietary intervention study revealed prebiotic-like effects of wild blueberry on the

Bifidobacterium spp. relative abundance[20]. Furthermore, a highbush blueberry polyphenolic fraction and an anthocyanin-enriched fraction were found to attenuate gut barrier dysfunction induced by *E. coli* in a model of Caco-2 epithelial cell culture[21]. Whilst those findings have been obtained using different methodologies and model systems, together they provide strong evidence to suggest that wild blueberry polyphenols can selectively modulate the gut microbiota composition and prevent intestinal and metabolic obesity-associated disorders. However, we still do not know which type of polyphenol are providing those beneficial effects and the underlying mechanisms.

A better understanding of the influence of specific blueberry polyphenols on the gut microbiota and intestinal epithelium is crucial to understand their role in metabolic disorders associated with obesity. We hypothesize that the gut microbiota, the host colonic epithelium and the mucus profile are key features by which non-absorbable oligomeric and polymeric PACs may improve the perturbed intestinal and metabolic homoeostasis associated with an obesogenic diet. Furthermore, the identification of bacterial communities displaying unique phenolic degrading capability may reveal specific bacterial consortia triggering beneficial bioactivities in the host.

In the current study, we evaluated the contribution of specific polyphenolic fractions found in whole wild blueberries to their beneficial impact on intestinal and metabolic endpoints in a mouse model of diet-induced obesity. We investigated the impact of the oral administration of wild blueberry extract (hydro-ethanolic extract, WBE) or three polyphenolic fractions (anthocyanins and phenolic acids, oligomeric PACs with flavonols and phenolic acids, and PACs polymers in the respective amounts found in the whole blueberry extract) on the diet-induced glucose intolerance, insulin sensitivity and on the gut microbiota composition, as well as on intestinal epithelium histology.

Results

Phenolic characterization of WBE and polyphenolic fractions

The polyphenolic characterization of the extracts and fractions is shown in the Supplementary information **Table S1.** The rationale for the fractionation of the wild blueberry polyphenolic extract (WBE) was to determine which polyphenol class and type, that is, anthocyanins, PACs oligomers or PACs polymers, was responsible for the effects observed in the whole WBE. To do so, the whole WBE was fractionated in three parts, F1) anthocyanins and phenolic acids, F2) oligomeric proanthocyanidins (PACs), phenolic acids and flavonols (PACs degree of polymerization DP<4), and F3) PACs polymers (PACs DP>4) (**Fig 1)** and supplied at their respective concentration in the whole extract. That is, two hundred mg of WBE per kg mouse body weight (BW) provided a daily dose of 17.03 mg of total polyphenols, including phenolic acids, flavonols, anthocyanins, PACs oligomers and polymers. 32.01 mg/kg BW of fraction F1 administrated to mice represented the proportion of anthocyanins contained in the whole 200 mg/kg BW WBE (i.e. 1.68 mg), while 53 mg/kg BW of fraction F2 supplied the equivalent daily dose of oligomeric PACs (i.e. 4.43 mg) and 37.21 mg/kg BW of fractions F3, provided an equivalent dose of polymeric PACs supplied by the WBE (i.e. 1.95 mg). The detailed characterization of extracts dosage per mouse is presented in **Fig 1.** Noteworthy, the dose used in this study in mice represents a feasible dose in humans. By applying the US Food and Drug Administration's guidelines to establish the human equivalent dose based on body surface area[22], we found that a 17 mg/kg dose would be the human equivalent of a 200 mg/kg dose in mice.

Weight gain and adiposity were not affected by the WBE and BPF

As expected, the consumption of a HFHS diet for 8 weeks significantly increased mouse body weight and body weight gain as compare to the chow-fed mice (Supplementary information **Fig. S1A-B**). This was explained by increased energy intake (Supplementary information **Fig. S1 C**). The energy intake was slightly, but significantly decreased at week 2 in the animals treated with the WBE and with fraction F2 as compared to the HFHS control group ($p<0.05$) (Supplementary information **Fig. S1 C**). This effect was transient and no difference in total energy intake was

observed for the whole duration of the experiment (HFHS, 600.7±15.88 kcal; WBE, 583.2±9.69 kcal; F1, 589.0±12,17 kcal; F2, 577.6±11.49 kcal; F3, 574.7±9.06 kcal). Visceral adipose tissues were significantly increased in the HFHS control group compared to chow-fed mice ($p<0.05$). However, mice gavaged with WBE and BPF showed similar visceral mass with no significant differences compared to HFHS-vehicle treated mice (Supplementary information **Fig. S1D**).

Total WBE and F3 rich in polymeric PACs improved glucose tolerance in HFHS-fed mice

Further assessment of glucose homeostasis was determined by the oral glucose tolerance test (OGTT) (**Fig. 2 A**). Glucose tolerance was markedly deteriorated in the vehicle-treated HFHS mice as revealed by the significant increase of the area under the curve (AUC) of the OGTT as compared to the chow-fed mice ($p<0.05$). While fasting glycemia was not different between WBE and BPF-treated mice and the vehicle-treated HFHS group, we observed a significant improvement in glucose tolerance in mice treated with the WBE and F3 polymeric PACs as indicated by a significant AUC reduction of 18.25 and 18.52%, respectively ($p<0.05$), whereas a trend in decreased AUC (17.68%, $p=0.0566$) was also observed in mice fed the F2 fraction as compared to HFHS.(**Fig. 2 B**).. HFHS-fed mice were insulin-resistant compared to chow-fed mice as indicated by the elevated glucose-stimulated insulin secretion (GSIS) (**Fig. 2 C-D),** the impaired insulin tolerance (**Fig. 2 E**) and the HOMA-IR index (**Fig. 2 F**). However, no significant effect on the above parameters was observed in mice fed the WBE and BPF compared to HFHS-fed group.

The polymeric PACs fraction (F3) increased the total GC number in HFHS-fed mice

The intestinal mucus layer has important protective and lubricative properties in the colon and may be affected by a HFHS-diet induced dysbiosis, thereby augmenting the risk of colonic mucosa exposition to the commensal microbiota. This prompted us to investigate the effects of wild blueberry polyphenols on mouse colon mucosal histomorphology, including the crypts length, the mucin secreting goblet cells (GC) number and the mucus layer thickness. Representative images

of AB-PAS stained colonic tissues are presented in the **Fig. 3 A 1-6**. In chow-fed mice, a thick purple stained layer of mucus was consistently observed, with inner mucus layer closely associated to the colonic epithelium and a secreted mucus scattered in the luminal space. Mucus layer was thinner and sparse in the vehicle-treated HFHS group (**Fig. 3 A-2**) as compared to the chow-fed animals. However, the WBE and BPF-treated mice displayed a restored mucus thickness as compared to the HFHS control group (**Fig. 3 A 3-6**). HFHS-fed mice presented a thinner mucus layer compared to the Chow-fed mice ($p<0.01$, **Fig. 3 B**). However, all mice orally supplemented with either WBE- ($p<0.01$), F1- ($p<0.01$), F2- ($p<0.05$) or F3 had a significantly thicker mucus layer as compared to the vehicle-treated HFHS-fed mice ($p<0.05$). No difference in the crypt's depth was observed among the WBE and all the BPF-treated mice and vehicle-treated HFHS control mice (**Fig. 3 C**). Although we observed that the mucus layer in the vehicle-treated HFHS-fed mice was thinner as compared to the chow group, there was no significant differences in the number of total mucin-secreting GC. Once normalized over the length of the crypt (GC number per μm of colonic crypts), only mice fed the F3 fraction rich in polymeric PACs presented an increased number of total GC compared to vehicle treated HFHS fed mice ($p<0.05$) (**Fig. 3 D**).

Consistent with the multiple functions of mucus, it is well established that GC produce a heterogeneous range of secretory mucins subtypes [23] and can be identified as acid, neutral and as a mix of both mucins. The acid mucin are further differentiated into sialomucins or sulfomucins groups, based on the presence of terminal sialic acid or sulfate group on the O-linked oligosaccharide chains [14]. Therefore, we classified the total number of GC considering the polychromatic AB/PAS mucin type separately, resulting in the specific determination of acid mucin-filled GC, mixed mucin-filled GC, and neutral mucin-filled GC, as well as, those GC without mucin that were considered as mucin empty GC. A mix of neutral and acidic mucins (purple stained mucin, mixed mucin GC) was predominantly found in colonic GC in BPF-treated groups (F1, 84.2%; F2, 85.3%; and F3, 83.4%; compared to vehicle-treated HFHS-fed mice, 80.2%) (**Fig. 3 E**). However, in mice fed WBE, the neutral mucin-filled GC showed an increased proportion (20.2%) compared to HFHS-fed mice (8.6%, $p<0.05$) (**Fig. 3 E**). In contrast, the remaining GC in HFHS-fed mice had a higher proportion of mucin-unfilled GC (11%) compared

to the WBE (2.2%) (p=0.0358, q=0.093 after multiple comparison corrections), and BPF treated mice (F1, 3.3%; F2. 2.7%; and F3, 6.4%) (F1, p=0.0536 q=0.0938; F2, p=0.0338 q=0.093).

To investigate the influence of wild blueberry polyphenols on intestinal permeability *Tjp1* (Tight junction protein, also known as Zonula occludin, ZO-1) and *Ocln* (Occludin) gene expression were measured using RT-qPCR and found no significant changes between vehicle treated HFHS and chow-fed mice or as compared to mice treated with WBE and BPF (**Fig. S2 A-B**).

WBE and BPF did not affect the microbial richness of the gut microbiota of HFHS-diet induced obese mice

To determine whether HFHS-diet affected fecal microbial diversity and whether the blueberry polyphenol treatments could modify this parameter, we next analyzed alpha and beta diversity indices. Rarefaction curves of the normalized sequences showed that our sequencing was deep enough to include all of the OTUs in the diet groups (**Fig. S3**). All treatments, including vehicle-treated chow and HFHS fed mice exhibited nearly the same α-diversity index using the *Chao1* index, an estimate of OTU richness for microbial communities (**Fig. S3 A**). There were no significant differences in the number of observed species in the polyphenols-treated mice compared to the HFHS-fed mice, as determined by Kruskal-Wallis test with Benjamini multiple comparison correction. A similar response was observed between the BPF-treated mice and the HFHS-fed mice on species abundance and Shannon's diversity index (P>0.05) (**Fig. S3 B**).

As expected, the HFHS-diet drastically changed the gut microbiota composition compared to the chow-diet. PERMANOVA for the Bray Curtis matrix revealed significant differences between vehicle-treated chow and HFHS and BPF-treated groups (PERMANOVA, R-squared: 0.37968; p-value<0.001). The Bray Curtis β-diversity index further showed that the communities associated with the chow-group and the vehicle-treated HFHS-fed mice diverged upon a confined region within the PCoA **(Fig. 4 A**). Specifically, the distribution of mice across the PC1 axis reflected the difference of microbial profile between mice fed chow vs HFHS diets, explaining 39% of the variance. Although there were differences in the relative proportion of some identified bacterial

OTUs, the β-diversity of the gut microbiota remained similar between the mice fed the polyphenols-containing diets. The mice fed the WBE, the BPF and the control HFHS-diet clustered similarly, this was not the case for mice fed the WBE who tended to spread out of the vehicle-treated HFHS-group.

Bacterial taxa within the families *Coriobacteriaceae* and *Verrucomicrobiacea* were influenced by the WBE and the F2 fraction rich in oligomeric PACs in HFHS-diet induced obese mice

Analysis of bacterial relative abundance confirmed prior reports[24] that the consumption of a HFHS diet consistently affects the proportion of *Bacteroidetes* (19%) and *Firmicutes* (59%), compared to a chow diet (53% and 35%, respectively) ($p<0.001$), leading to a higher *Firmicutes/Bacteroidetes* ratio (*F/B*) in the HFHS treated groups (**Fig. 4 B-C**). Phylum level analysis showed that most of the compositional differences between vehicle-treated HFHS-fed mice, WBE and BPF treated mice were reflected in the relative abundance of *Firmicutes, Bacteroidetes* and, to a lesser extent, *Verrucomicrobia* and *Actinobacteria* **(Fig. 4 C**). In the WBE and BPF treated mice, the family *Coriobacteriaceae*, *S24-7, Verrucomicrobia* and the order *Clostridiales* were favored as compared to HFHS (**Fig. 4 D**). Within the families, 20 different genera were identified (**Fig. 4 E**). Important changes in the relative proportion of the genera *Adlercreutzia, Akkermansia,* an unknown genus of order *Clostridiales*, family *S24-7,* as well as a genus of *Ruminococcaceae* and *Peptostreptococcaceae* were observed (**Fig. 5 A-E)**. Kruskal-Wallis tests with Benjamini's multiple corrections showed a significant reduction of an unassigned genus of the family *S24-7* by WBE compared to vehicle-treated HFHS-group ($p<0.05$). Although it was not supported statistically, we noted that BPF tended to increase *Akkermansia* (family *Verrucomicrobiaceae*) abundance, presenting the higher proportion in the mice treated by the F2 fraction rich in oligomeric PACs (24.8%) and the F3 rich in polymeric PACs (21.2%) compared to HFHS (17.9%). The WBE did not stimulate *A. muciniphila*. Moreover, unassigned genera belonging to the families *Ruminococcaceae* and *Peptostreptocaccaceae* were increased in WBE and reduced in F2 treated mice (**Fig. 5 D-E**). Similarly, an increased proportion of *Adlercreutzia*

(family *Coriobacteriaceae*) was observed in the WBE (7.8%) and F2-fed mice (6.8%) compared to HFHS-fed mice (4.5%).

qPCR analyses of mouse fecal samples confirmed the stimulatory effects of WBE and the F2 fraction rich in oligomeric PACs on the relative proportion of *A. muciniphila* and *A. equolifaciens*

The relative abundance of distinctive bacterial genus found in the 16S rRNA data sequencing by the BPF were further analyzed by qPCR. We focused our attention on two bacterial species considered important for the degradation of polyphenols and the attenuation of metabolic issues; *Adlercreutzia equolifaciens,* and *Akkemansia muciniphila*. Interestingly, *A. muciniphila* proportion was significantly stimulated by the F2 fraction rich in oligomeric PACs, showing a 2.5-fold higher relative proportion of the bacterium in the feces of those mice as compared to that of the HFHS group ($p<0.05$). At the same time, the WBE, which contained similar amount of oligomeric PAC, did not stimulate *A. muciniphila* (**Fig. 5 F-G**). In a similar way, the *A. equolifaciens* relative proportion was 2.0-fold higher in both mouse groups treated with the WBE and the F2 fraction ($p<0.01$ and $p<0.05$ respectively) (**Fig. 5 H**). Both qPCR and 16S rRNA gene sequencing sets of data were correlated in order to validate the observed abundance. Significant spearman coefficients were obtained for the groups ($p<0.01$) and showed comparable profile of those bacterial taxa by the two quantification methods (**Fig. 5 I).**

Functional analysis of microbial communities within wild blueberry polyphenols fed mice revealed pathways related to xenobiotic metabolism

LEfSe analysis of PICRUSt predictions in vehicle-treated HFHS-fed mice demonstrated fluctuations in the functional pathways attributed to carbohydrate, lipid, and energy metabolism and membrane transport as compared to chow-fed mice. In total, 21 pathways were significantly affected by the HFHS-diet, compared to WBE supplementation, which were shown to affect only 6 pathways (Supplementary information **Fig. S5**). The WBE repressed microbial pathways were linked to LPS biosynthesis and glycosaminoglycan degradation in HFHS-fed mice, while WBE-

fed mice revealed changes in xenobiotics metabolic pathways like benzoate degradation. Noteworthy is the fact that some functions linked to xenobiotics metabolism and cell motility stood out in mice treated with the BPF. Among them, seleno-compound metabolism, butanoate metabolism and benzoate degradation are pathways highly associated to phytochemical metabolism, such as polyphenols [25]. Those results are consistent to the increased abundance of the polyphenols-degrading family *Coriobacteriaceae.* However, the F1-treated group was the only one that revealed starch and sucrose metabolism as important feature included within the category of carbohydrate metabolism. In the case of F2 fraction rich in oligomeric PACs, the butanoate metabolism pathway was significantly overrepresented and for the F3 polymeric PACs group, the ketone body's metabolism and plant-pathogens interaction pathways were induced. Those predicted functional changes induced by PACs suggest adaptation of the gut microbial environmental that are likely related to microbial energy metabolism.

Discussion

The purpose of this study was to identify blueberry polyphenolic fractions that can contribute to the reported beneficial effects of the WBE on metabolic health, the gut microbiota composition and on the intestinal histology of HFHS-diet induced obese mice. We observed that WBE improvements of glucose tolerance coincided with a modulation of the abundance of bacterial families such as *Coriobacteriaceae* and *Verrucomicrobiacea* and the maintenance of the colonic mucus layer in a murine model of diet-induced obesity and insulin resistance. We also provide new evidence that this effect is largely attributable to the blueberry proanthocyanidin polymers enriched fraction.

Indeed, within the BPF, the F3 fraction rich in polymeric PACs appears to contribute the most to the overall beneficial effect of the wild blueberry extract on intestinal histology and glucose tolerance of HFHS-fed mice, while the F2 fraction, rich in PACs oligomers, also tended to ameliorate this last parameter ($p=0.0566$). Notwithstanding the fact that PACs polymers represented only a small fraction of the total polyphenols found in the whole WBE, they exerted significant effects on glucose tolerance. During the OGTT, despite no significant changes in insulin secretion in PAC treated animals as compared to the control group, an improved glucose

tolerance was observed. These results may suggest an amelioration of the insulin action, an insulin independent effect or a reduced intestinal glucose absorption in the PAC treated group. Indeed, previous studies reported that polyphenols may interfere with SGLT1 and GLUT2 in the small intestine. In this regard, proanthocyanidins have been shown to mimic insulin effects by affecting intestinal glucose transporters[26] and stimulating intestinal hormones which are involved in the modulation of digestion and metabolism[27]. For instance, Casanova-Martí et al. (2017)[27] demonstrated, both *in vivo* and *ex vivo,* the role of grape seed proanthocyanidins (GSPE) on the induction of enterohormones secretion in different parts of the intestine, leading to glucose homeostasis regulation. The authors showed that GSPE treatment increased GLP-1 levels in the ileum, while the unabsorbed GSPE's and phenolic microbial metabolites did so in the colon. These findings suggest that unabsorbed polyphenols with high degree of polymerization and microbiota-metabolized phenolic compounds act on enteroendocrine L-cells to promote GLP-1 secretion[27]. Further studies will be needed to determine whether the protection from glucose intolerance that are linked to unabsorbed polymeric PACs from blueberry can be linked to other intestinal targets that are linked to pancreatic beta-cell insulin secretion or hepatic insulin clearance.

In this study, the improved glucose tolerance was found to be independent of changes in body weight, consistent with previous studies[28-30]. For instance, Seymour et al. (2011)[30] did not observe any change in body weight gain, lean and fat mass despite improved glucose tolerance in obese Zucker rats fed a high-fat diet (HFD) supplemented with 2% of blueberry powder. Also, Elks et al. (2015)[29] found that blueberry powder supplementation (4%) did not affect body weight gain, but significantly attenuated the glucose intolerance and hepatic steatosis in HFD fed obese postmenopausal female mice.

A recent meta-analysis of human gut microbes associated with obesity shows weak or non-significant associations of particular taxa or overall diversity with the body mass index[31], but it is becoming apparent that polyphenolic compounds can distinctly reshape gut bacteria and exert local and systemic protective effects against HFD-induced metabolic dysfunctions. We observed that blueberry polyphenols had no effect on the *F/B* ratio, as a marker of diet-induced gut dysbiosis[24]; however, we observed a stimulation of key bacterial species such as *A. muciniphila* and *A. equolifaciens* belonging to *Verrucomicrobia* and *Actinobacteria* phyla, respectively, in mice fed

the WBE and the F2 fraction. In mice fed the WBE, a decrease in the relative abundance of *S24-7* (taxonomically classified as *Muribaculaceae*) was coherent with the reduced *Bacteroidetes* phylum abundance. The *S24-7*, is a bacterial family believed to be involved in the degradation of plant glycan, host glycan, and α-glucan carbohydrates[32], but within the gut microbiota composition of C57-BL6 mice, it was shown to be sensitive to the administration of antibiotics [33]. Thus, we surmise that the decreased abundances of *S24-7* taxon, is the result of the antibacterial action of the total WBE[34].

Changes in the gut microbiota have been proposed as an important mechanism of action of poorly absorbed high molecular weight polyphenols against obesity-associated metabolic disorders. The blooming of *A. muciniphila* by the oligomeric PACs-rich F2 fraction is particularly interesting since it was shown to drive colonic epithelial immunomodulatory response and to protect against metabolic disorders[17,35-37]. Similar effects on *A. muciniphila* abundance were also triggered by an ellagitannin-rich extract from pomegranate [38] and camu-camu[39], by a B-type proanthocyanins-rich grape extract[40], by an A-type proanthocyanins-rich cranberry extract[17], as well as by lingonberries[41]. In the present experiment, there was no association of this bacterium with body weight gain. Likewise, Shin et al.[37] demonstrated that blooming of *A. muciniphila* upon metformin treatment did not affect body weight gain or fat mass accumulation, but did improve glucose tolerance in HFD-fed mice. A recent study demonstrated that the administration of *A. muciniphila* counteracted diet-induced metabolic endotoxemia, restored colon mucosal barrier dysfunction and glucose homeostasis in obese type 2 diabetic mice[36]. In our study, the changes induced by the F2 fraction on the gut microbiota, and particularly on *A. muciniphila,* while compelling, are somewhat surprising, since they were not reproduced in the WBE treatment containing the same polyphenols as F2 (PAC oligomers, phenolic acids such as protocatechuic acid and 5- caffeoylquinic acid, as well as flavonols such as quercetin). We surmise that the polyphenols not present in F2, namely anthocyanin and PAC polymers have blunted the *Akkermansia* bloom in the WBE treated mice, probably by stimulating the growth of bacteria competing with *A. muciniphila.* We indeed observed that the mucus associated bacterial families, *Ruminococcaceae* and *Peptostreptococcaceae* were stimulated in the WBE and reduced in F2

treated mice (**Fig. 5 D-E**). These species may be mutually co-exclusive to *Akkermansia* as shown by Lavelle et al. (2015) in a human ulcerative colitis human model[42].

Noteworthy, the F2 fraction also favored *A. equolifaciens* belonging to the family *Coriobacteriaceae,* involved in the degradation of phenolic compounds including flavan-3-ols[43,44], a feature that explains its increased relative proportion in WBE and PACs treatments compared to HFHS-vehicle treated mice. Recently, Jiao et al. (2019)[18] found that *Adlercreutzia* was prevalent in low fat diet-fed mice compared to high-fat diet-induced obesity in C57BL/6J mice, and that the supplementation with blueberry polyphenolic extract increased its relative abundance. Interestingly, recent studies have not only demonstrated *Adlercreutzia*'s capacity to convert – epigallocatechin (–EGC), -epicatechin (−EC), -catechin (−C), and +catechin (+C) into their corresponding metabolites, but also that it can catalyze the above metabolites by hydroxylation reactions[44] and produce a range of phenyl-valerolactones metabolites presumed to have metabolic bioactivities[45]. Moreover, *A. equolifaciens* has also been observed to be decreased in subjects suffering of inflammatory bowel disease (IBD)[46]. In that study, *A. equolifaciens* was considered a microbial biomarker of the reestablishment of mucosal function in those patients who positively responded to an immunomodulators monotherapy [46].

Directly involved in intestinal homeostasis, the mucus layer covering the colonic epithelium acts as a protective barrier against the luminal commensal microbes. We observed that the supplementation with the total WBE and all the BPF prevented the loss of mucus thickness that was induced by the HFHS-rich diet. Interestingly, only the mice fed the F3 fraction rich in PACs polymers presented a higher number of colonic mucin-secreting GC on the epithelium as compared to HFHS-fed mice. Our results are comparable to those of another study which examined how cranberry PACs administration counteracted the altered intestinal morphology and function, induced by elemental enteral nutrition in mice[47]. Although in the present study the *Muc2* gene expression was not analyzed, it is well known that the mucin exocytosis and mucus function is largely regulated at the post-translational level and therefore, the analysis of *Muc2* protein content by using an *ex vivo* technique, histological or by immunostaining preparations in future studies will be useful to provide complementary evidence of improved mucus function and the potential mechanisms involved at the molecular level[48]. The histological assessment of mouse colonic

tissues showed a clear improvement of the mucus barrier by the BPF, however, the innate immune pathways involved in the regulation and exocytosis of mucin remain to be explored to further understand the mechanisms underlying the enhanced colonic mucus thickness. For instance, the NLRP6-inflammasome pathway has been shown as an essential factor for mucosal self-renewal, cell proliferation, and regulation of intestinal flora through mucus secretion from GC and the epithelium[49]. Interestingly, a recent study demonstrated that a freeze-dried powder of a polyphenol-rich mulberry juice promotes the formation of NLRP6 inflammasomes and provides mucosal protection by modifying the bacterial content and preserving the GC number in mice with DSS-induced acute colitis[50].

The type of secreted mucins is an important parameter that can be affected in intestinal metabolic disorders[51]. The proportions between neutral and acid mucins are normally constant and are modified in obesity and IBD[14]. In our experiment, significant differences were observed in the proportion of neutral mucin-filled GC between the WBE-treated (20.2%) and HFHS-fed mice (8.6%). Neutral mucins have usually been associated with mono-sulfated mucin in GC residing on the colonic crypt bottom[14], a location where cell divisions and mucin maturation appear to be active[52]. The GC located in the top of colonic crypt primarily harbor acid-sialomucins[14]. In the case of the BPF-treated mice, a trend toward increased acidic-mixed mucin was observed, suggesting that BPF may induce the secretion of sialomucins which are more resistant against microbiological degradation than neutral mucins and are impervious to bacterial glycosidases and host proteases[53]. Similar mucin profile has been reported in normal human colonic tissues, with a predominance of acidic-mixed mucin (~80%) and sparse neutral mucin (20%)[54]. These results highlight the modulation of maturation and mucin-type profile as an emerging mechanism through which wild blueberry polyphenol may maintain intestinal homeostasis.

One limitation of the present study is that our methodological approach for the preparation of polyphenolic fractions did not permit the obtention of pure phenolic classes, as it was the case for the anthocyanins rich fraction (F1) and the oligomeric PACs rich fraction (F2). To confirm the effects of WBE and the BPF, in particular, an improved fractionation of wild blueberry polyphenols will be required in order to test the selective effects of PAC oligomers and polymers

on the gut microbiota composition (*Akkermansia* and *Adlercreutzia*) and histology, as well as on the related metabolic phenotypes in further studies.

In summary, we demonstrated that the oral administration of all BPF reestablished the colonic mucus thickness in obese mice and thus created an ecological niche for the symbiotic mucosa-associated bacteria. Specifically, the F2 fraction exerted a selective prebiotic action on the mucin-degrading bacterium *A. muciniphila,* but this was not the case with the WBE. Interestingly, we also observed a bloom of the polyphenols-degrading family *Coriobacteriaceae*, in particular of *A. equolifaciens*, which suggest their involvement in the metabolism of polyphenols, which is particularly relevant as it can generate bioactive molecules involved into the amelioration of metabolic disturbances in obesity and diabetes[55]. Our study also unraveled the important role that polymeric PACs play on the gut epithelial barrier function, especially promoting a thicker mucus layer, possibly through increasing mucin-secreting GC number, as well as mediating non-insulin dependent intestinal glucose response in obese mice. While the administration of WBE attenuated HFHS-induced glucose tolerance, only the F3 fraction replicated this effect, even though this fraction was in lower proportion in the whole WBE.

Methods

Polyphenols fractionation

A polyphenol-rich wild blueberry hydro-ethanolic extract (70%) *(Vaccinium angustifolium* Aiton*)* (WBE) provided by Diana Food Canada was fractionated by gel-filtration chromatography as described by Gu et al. (2002)[56] to produce three different fractions, the first, rich in anthocyanins and phenolic acids (F1), the second, rich in PACs oligomers, phenolic acids and flavonols (F2) and the last one, rich in PACs polymers (F3). The purification of anthocyanin compounds was carried out using 30 g of cation exchange resin (siliaPrepX SCX, silicycle, Canada). Briefly, 75g/l of crude WBE solubilized in acidified water (1% acetic acid) was deposited on the resin, and the WBE was eluted with 50 % ethanol (Fraction containing flavonoids and PACs), and further with acidified methanol with 5% of HCl (F1 containing anthocyanins). Anthocyanins-containing fraction was then passed through XAD 7 resin in order to eliminate the HCl that may be toxic for

mice and further evaporated and lyophilized. The fraction containing flavonoids and PACs was also evaporated and recovered in Ethanol/water solution (50/50: v/v). The purification of the PACs-rich fraction was further performed on a Sephadex LH-20 column using an adaptation of the protocol of Feliciano et al (2012)[57]. Redisep column (Teledyne, Isco) containing 65 g of Sephadex LH-20 (bed volume = 100 ml) was placed on a Spot Prep system (Armen Instrument, France). The system is coupled to a UV detector set at 254 nm, and a fluorescence detector (emission wavelength: 230 nm - reception wavelength: 321 nm). The flow rate used was 5 ml/min. PACs oligomers and flavonoids were isolated by elution with methanol/ethanol 50/50 (F2); and the PACs polymers were eluted with 70% acetone (F3). In order to produce the needed amount for the preclinical study, several consecutive separations were carried out. The fractions were then homogenized and characterized.

Phenolic characterization of blueberry extract and polyphenolic fractions

The polyphenol composition analysis was carried out as described previously[58]. Flavonols, flavan-3-ols and phenolic acids were analyzed as published before[58] using reverse-phase UHPLC–MS/MS, where data were acquired in scan mode (m/z 100–1000). Anthocyanins were analyzed by reverse-phase HPLC with DAD detection using an Agilent 1100 series system (Santa Clara, CA). The separation was performed with a flow rate of 1 mL/min using a Develosil C18 reverse phase column (250 mm × 4 mm, 5 μm particle size), protected with an Ultrasep C18 guard column (Phenomenex, CA). Binary gradient of 5% formic acid in ultrapure water (solvent A) and methanol (solvent B) was as follows for the anthocyanins separation: 0−2 min, 5% B; 2−10 min, 5−20% B; 10−15 min, 20% B; 15−30 min, 20−25% B; 30− 35 min, 25% B; 35−50 min, 25−33% B; 50−55 min, 33% B; 55− 65 min, 33−36% B; 65−70 min, 36−45% B; 70−75 min, 45− 53% B; 75−80 min, 53−55% B; 80−84 min, 55−70% B; 84−88 min, 70−5% B; 88−90 min, 5% B [59]. Chromatographic data were acquired at 520 nm and the quantification was performed using a cyanidin 3-glucoside standard. The identification of anthocyanins was achieved by comparison of chromatographic retention times and mass spectral information obtained with previously published data. PACs were analyzed by normal-phase HPLC with fluorescence detection using an Agilent 1260/1290 infinity system (Santa Clara, CA). The fluorescence was monitored at excitation and emission wavelengths

of 230 nm and 321 nm respectively, and the quantification of polymerization degree (DP) from 1 to >10, was performed using an external calibration curve of epicatechin, applying a correction factor according to their respective responses in fluorescence[59].

Experimental design of animal study

All experimental procedures were performed according to the guidelines of the animal care committee of Laval University (CPAUL). The protocols were summited and approved by Canadian Council on Animal Care (CCA). Six-weeks old C57BL/6J male mice ($n = 72$; Jackson laboratories, Sacramento, CA USA) were single-housed in a controlled environment (1 mouse per cage; 12/12-h light-dark) with free access to food and drinking water. After two weeks of acclimation with standard-chow diet (2018 Teklad global 18% protein rodent diet, Harlan laboratories), the mice were randomly divided into six groups (n=12/group) and fed a Chow diet or a HFHS diet (65% lipids, 15% proteins and 20% carbohydrates). The animals on the control diets (HFHS, and Chow) were treated daily by gavage with the vehicle (water). The polyphenols-treated groups were fed with HFHS-diet and supplemented daily by gavage either with the wild blueberry polyphenol extract (WBE, 200 mg/kg, providing 17 mg of polyphenols per day) or its polyphenolic fractions (BPF), that were rich in anthocyanins and phenolic acids (F1), in oligomeric PACs, phenolic acids and flavonols (F2), or in PACs polymers (F3). In order to determine the contribution of the different blueberry polyphenol classes on the modulation of the gut microbiota composition and the host intestinal and metabolic profile, the amount of BPF administrated to the mice represented the respective proportion of polyphenol of anthocyanins (F1), PACs oligomers (F2), and PACs polymers (F3) contained in the whole WBE. According to the group, the animals received 32 mg/kg of F1 fraction, 53 mg/kg of the F2 fraction, and 37 mg/kg of the F3 fraction (**Fig.1**). Body weight gain was taken under non-fasting condition, twice a week. Food intake was evaluated by monitoring the food consumption (g) three times per week. After 5 weeks and 7 weeks of treatment, insulin tolerance test (ITT) and oral glucose tolerance test (OGTT) were performed, respectively. Feces were collected before the start of the treatments (week 0) and at the end (week 8), immediately immersed in dry-ice and stored at -80°C for subsequent metagenomics analysis. After 8 weeks of feeding, mice were anesthetized with isoflurane (2-3%; 0.5 – 1.5 L/min)

and euthanized by cardiac puncture. Adipose tissues, organs, and intestines were carefully dissected; their weight was recorded and immediately immersed in liquid nitrogen, RNA later (Invitrogen) or into fixation solutions (Carnoy's solution, buffered formalin 10%) according to the subsequent analysis. Frozen tissues were then stored at −80 °C.

Glucose homeostasis

After 5 weeks of treatments, mice were fasted for 6 hours. Blood was drawn at baseline and immediately centrifuged (3,500 rpm, 10 min at 4°C). Insulin solution was administrated (10 µl/g of 0.65U/kg) by intraperitoneal injection, followed by glycemia measurements using an Accu-Check glucometer (Bayer) before and at 5, 10, 15, 20, 30, and 60 minutes after the injection. An oral glucose tolerance test (OGTT) was performed after 7 weeks of dietary treatment. Mice were fasted for 12 hours overnight, blood baseline sample was drawn and immediately centrifuged (3,500 rpm, 10 min at 4°C). Dextrose solution (2 µl/g of 50% dextrose) was administrated by gavage and blood samples (60 µl) were obtained from the mouse lateral saphenous vein. Glycemia was determined using an Accu-Check glucometer (Bayer) at time 15, 30, 60, 90 and 120 minutes relative to the glucose load. The area under the curve (AUC-OGTT) was determined considering the glucose levels measured between baseline and 120 minutes after glucose overload (GraphPad Prism 7.0, USA). Insulin resistance index (HOMA-IR) was calculated using the formula: HOMA-IR = [fasting glycemia (nmol/L) * fasting insulinemia (µU/mL)/22.5]. The 12-h fasting blood samples were collected for determinations of plasma insulin. Samples were stored at -80°C until the assay. Mouse insulin was determined using an ultrasensitive ELISA kit (Alpco, Salem, USA).

Colon histology

Colon tissues were prepared as previously described [60]. The PBS-flushed colon tissues were cut into two equal sized sections (transverse incision). Each section (approximately 0.5 cm) of colon was placed side by side on a piece of tape (3M Micropore surgical tape, 2.5 cm width), and then tightened with forceps. The bundles enclosing the colon pieces were transferred into a tube containing a large excess of cold Methanol-Carnoy's solution (60% methanol, 30% chloroform and 10% glacial acetic acid), at least 10X the volume of fixative to the volume of tissue. The

samples were stored for 3hr at 4°C to allow the fixation. After fixation, the tissues were washed with cold 70% ethanol once, and stored in the same solution at 4°C until they were processed. Tissue processing was performed at IBIS laboratory of Molecular Imaging and Microscopy, Laval University (Québec, QC, Canada). The samples were placed into a tissue cassette indelibly labeled with a unique animal identifier and the name of the intestinal segment. The cassettes were subjected to a tissue processor for standard processing to allow embedding in paraffin wax (Tissue-Tek VIP, vacuum Infiltration Processor Sakura brand). The protocol applied was: Alcohol 95% 45 min, Alcohol 100% 3 x 45 min, Toluene 2 x 45 min, Paraffin 1h30, 2h00 and 4h00. Paraffin-embedded sections of colon tissues were cut and stained with both periodic acid Schiff and Alcian blue (AB-PAS). AB-PAS staining enables the differentiation between acid mucins and neutral mucins, with blue color showing acid mucins, purple color indicating a mixture of neutral and acid mucins, and red/magenta color indicating neutral mucins alone[61].

Goblet cell quantification, mucus thickness and crypts depth measurements

The relative proportions and distribution of mucous secreting GC was quantified following Johnson *et al.* (2016)[62] protocols with some modifications[63]. All images were captured using a BX51 microscope (Olympus America, Inc, USA) equipped with a CCD Digital Camera System and Image-Pro software. Number of GC was counted for a defined distance (using 20X objective lens, 50 µm scale). A total of 12 crypts (3 crypts per section) were analyzed for each mouse. Initially, images were taken with the 4X objective lens (200 µm scale bars) in order to examine the whole tissue section. This was used to ensure that the total area of the images taken at a higher magnification would cover at least 50% of the tissue section. Afterwards, under 20X objective lens, each section was divided into four equal quadrants and taking representative images. In each quadrant, within a delineated area (from epithelium towards the colonic crypts), the total GC number was counted, and the data were expressed as the relative cell numbers per crypt (12 crypts of 12 mice per group). To determine the specific mucin cell types for the colon for each animal, the total CG counts were totaled separately (neutral and mixed mucin-filled GC, including mucin unfilled GC) and the data were normalized to reflect the proportion of each mucin cell type per crypt. Crypt lengths (µm) were calculated from an average of 12 crypts per tissue section, for 12

mice. Average of mucus thickness was calculated in a similar manner, measuring the lengths of the inner mucus layer closely adhered to the epithelium, for 12 mice. The National Institute of Health image J software was used for supporting the cell quantifications and crypts length measurements.

Colon mRNA expression by quantitative RT-PCR

Colon tissues stored in RNAlater (Invitrogen) at -80°C were thawed on ice, and total RNA was extracted using a RNeasy mini kit (Qiagen, #74104), according to the manufacturer's instructions. Samples were DNase treated using the RNase-Free DNase kit (Qiagen; #79254) and RNA concentration and quality was assessed using RNA NanoChips in Agilent 2100 Bioanalyzer (Agilent Technologies, Germany). First-strand cDNA syntheses were prepared from 700 ng of RNA using the RT2 First Strand Kit (Qiagen/SABiosciences). The reaction included one additional step to eliminate traces of genomic DNA. The resultant cDNA product was immediately amplified by qPCR using RT2 SYBR Green qPCR Master Mix (Qiagen/SABiosciences) on an Applied Biosystems ABI 7500 Fast real-time cycling platform. Quantitative RT-PCR was performed in a 25 µl reaction containing 1 µl cDNA, 1 µl of 10 µM reverse and forward primers and 12.5 µl RT2-SYBR Green Master Mix. The thermocycling protocol was as follows: 95°C for 10 min for hot-start polymerase activation, followed by 40 cycles of denaturation at 95°C for 15 s, annealing at 60°C for 1 min, and a melting curve stage as default setting from 60°C to 95°C. Each sample was analyzed in duplicate and 10-12 biological replicates were utilized for each treatment. For the analysis of the intestinal permeability, ready-made individual primers encoding regulatory genes of differentiation were used (RT2 qPCR Primer Assay, Qiagen). Occludin (*Ocln*, Qiagen #PPM05314A), and Tight junction protein 1 (*Tjp1,* Qiagen #PPM25091A) mouse genes were the targets; Glyceraldehyde-3-phosphate dehydrogenase (*GAPDH*, Qiagen #PPM02946E), Hypoxanthine guanine phosphoribosyl transferase (*Hprt,* Qiagen #PPM03559F), and Peptidylprolyl isomerase B (*Ppib,* Qiagen #PPM03728A) were amplified as housekeeping controls genes (HKGs). Stability of HKGs was further evaluated by geNorm and NormFinder applications. Mouse XpressRef Universal total mRNA (Qiagen #338114) was also used as reference template in order to verify and compare the quality of gene expressions on our mouse

experimental mRNA. Data were analyzed using the ΔΔCT method to determine the expression level of each gene normalized to the expression level of the housekeeping gene *Gapdh.*

Fecal DNA extraction and 16S rRNA gene amplicon library preparation and sequencing

Total DNA was extracted from approximately 100 mg of feces using a ZR fecal DNA kit (D6010; Zymo Research Corp., Orange, CA) which included a bead-beating step for the mechanical lysis of the microbial cells and silica column purification. The DNA extraction was carried out as recommended in the respective kit manuals, with some modifications including a double step of pre-wash and washes during subsequent filtration to remove humic acids/polyphenols that could inhibit PCR. The concentration and quality of DNA was determined spectrophotometrically by measuring the A260/280 using a ND-1000 Nanodrop (Nanodrop Technologies, Wilmington, DE, USA). Fecal DNA sample's sequencing (12 samples per group diet) were processed at IBIS laboratory, Laval University, Québec, QC, Canada.

Amplicons of the 16S rRNA V3-V4 region were generated using degenerate primers 341F (5'-CCTACGGGNGGCWGCAG-3') and 805R (5'-GACTACHVGGGTATCTAATCC-3') adapted to incorporate the transposon-based Illumina Nextera adapters (Illumina, USA) and a sample barcode sequence allowing multiplexed paired-end sequencing. Constructed 16S metagenomic libraries were purified using 35 µL of magnetic beads (AxyPrep Mag PCR Clean up kit; Axygen Biosciences, USA) per 50 µL PCR reaction. Library quality control was performed with a Bioanalyzer 2100 using DNA 7500 chips (Agilent Technologies, USA). An equimolar pool was obtained and checked for quality prior to further processing. The pool was quantified using picogreen (Life Technologies, USA) and loaded on a MiSeq platform using 2 x 300 bp paired-end sequencing (Illumina, USA). High-throughput sequencing was performed at the IBIS (Institut de Biologie Intégrative et des Systèmes - Université Laval).

16S rRNA sequence processing

Demultiplexed reads were analyzed using the QIIME software package (version 1.9.1) and customs scripts. The Paired-End read mergeR (PEAR) v.0.9.5[64] was used to pair the forward and reverse reads of sequences in each sample with at least a 50-bp overlap. Sequences were discarded if they had ambiguous base (N) or a Phred score ≤ 25 or were shorter than 450 bp in length. Chimeras were filtered with a reference-based approach using UCHIME version 4.2[65] and a representative set of chimera-checked sequences[66]. The resulting sequences were clustered into OTUs (Operational Taxonomic Units) at 97% identity threshold using an open-reference methodology performed with USEARCH 61 version 6.1.544[67]. Taxonomy of OTUs was assigned to a representative set of 16S rRNA sequences in the Greengenes database using the RDP-classifier[68]. All *OTUs* that were observed fewer than 2 times (i.e., *singletons*), or with a number of sequences < 0.1% of total number of reads were discarded. The RDP classifier against the RDP database release 11[69] was used to further classified OTUs that were unassigned against Greengenes at the genus level.

Gut microbiota diversity and composition analysis

OTUs that had prevalence in at least 20% of the mice in a treatment group and had a variance value higher than 10% in a treatment group were included in the analysis. The QIIME α-rarefaction analysis into a depth of 6957 sequences per sample was performed. Individual samples were rarified based on α-diversity estimates, to ensure even sequencing depth for diversity and relative abundance measurements. The α-diversity of each sample was analyzed using the *Shannon-Weaver* diversity index for microbial community composition combining species richness and abundance per sample. The *Chao1* index was determined for richness and observed Species estimation (number of unique OTUs). Non-parametric Mann-Whitney U-tests as well as Kruskal-Wallis test with Benjamini's multiple comparison correction were conducted to compare diversity between diet types using Prism 7.0 (GraphPad software, California).

β-diversity metrics were calculated using Bray-Curtis distance measure, considering the OTU table rarefied at 6957 sequences per sample for all samples to account for variations in sequencing

depth. Principle Coordinate Analyses (PCoA) plots were performed on calculated distance matrices. The statistical significance on β-diversity across sample groups was assessed with the non-parametric Permutational Multivariate Analysis of Variance (PERMANOVA, 999 Monte Carlo permutations) test[70]. PERMANOVA analyses return a *p*-value for significance and also the R^2-value, which is indicative of the amount of variation attributed to a specific treatment within a model. The significance cutoff for *P* values (PERMANOVA) and corrected *P* values (Kruskal-Wallis) was set at 0.05. Relative frequencies of different taxonomic categories obtained were calculated using the Statistical Analysis of Metagenomic Profiles program (STAMP v.2.1.3).

Quantitative real-time PCR analysis. Quantitative real-time Polymerase chain reaction (qPCR) was used to confirm the proportion of specific bacterial taxa found distinctively stimulated on the metagenomic data. *Akkermansia muciniphila* and *Adlercreutzia equolifaciens* relative abundances were analyzed in fecal samples from all groups. Home designed 16S rRNA primer sequences (Geneious software, version 9.0) were used for both *A. muciniphila* (forward 5′-CACACCGCCCGTCACAT-3′ and reverse 5′-TGCGGTTGGCTTCAGATACTT-3′), and *A. equolifaciens* (forward 5′-TTAGGTAGACGGCGGGGTAA-3′ and reverse 5′-TAGGAGTCTGGGCCGTATCT-3′). Total bacteria were quantified by using the universal primers Uni334F (5′-ACTCCTACGGGAGGCAGCAGT-3′) and Uni514R (5′-ATTACCGCGGCTGCTGGC-3)[71]. Primer amplification efficiencies and standard curves were determined by making dilution series of pure total DNA for each bacterium (ATCC BAA-835 and DSM 19450 strains), calculating a linear regression based on the CT data points, and inferring the efficiency from the slope of the line. Each qPCR was performed in a 20 µl reaction containing 10 µL of 2X PowerUP SYBR Green Master mix (Applied Biosystem), 6.4 µL of water, 0.8 µL of a 5 µM Forward and Reverse primers, and 2 µL of extracted DNA in DNase/RNase-free water. The qPCR amplifications were performed on an Applied Biosystems ABI 7500 Fast real-time cycling platform. The thermocycling protocol consisted in 50°C for 2 min, 95°C for 10 min for hot-start polymerase activation, followed by 40 cycles of denaturation at 95°C for 15 s, annealing at 60°C for 1 min, and a melting curve stage as default setting from 60°C to 95°C. Twelve samples were analyzed for each group, duplicate qPCR reactions were performed. The average CT value obtained from each primer pair was used to calculate the proportion of bacterial taxa over total

bacteria in mouse feces. The data were transformed into a percentage using the ΔΔCT-based following formula as described elsewhere[72]:

$$\boldsymbol{X = \frac{(Eff.Univ.)^{CT\ univ}}{(Eff.Spec.)^{CT\ spec}}\ \mathbf{x\ 100}}$$

Where *Eff.Univ* is the calculated efficiency of the universal primers and *Eff.Spec* refers to the efficiency of the taxon-specific primers. *CT univ* and *CT spec* are the CT mean values registered by the Fast real-time thermocycling platform. "X" represents the percentage of 16S taxon-specific copy number existing in each fecal sample. Finally, spearman correlations analyses were performed for comparing the data from 16S rRNA sequencing versus the 16S rRNA relative proportion obtained by qPCR; p values <0.05 were considered statistically significant.

Inferred metagenomic functions by PICRUSt. The predictions of metagenome's functionality, grouped by diet, was predicted using the PICRUSt 1.0.0 software (http://picrust.github.io)[73]. The resulting BIOM table (a collection of closed-reference OTUs) obtained from the QIIME filtered reads and the matched data against a reference collection (GreenGenes database, May 2013 version; http://greengenes.lbl.gov) with 97% identity, was then categorized by KEGG pathways (i.e., KEGG Orthology groups [KOs] were placed into functional categories). The data were analyzed statistically by using STAMP v 2.1.3. LEfSe analysis was performed to identify the microbial functional pathways that were differentially expressed in the different group of diets.

Statistical analysis

To compute individual pairwise comparisons of means from parametric data, Student's t-tests and one-way ANOVA with a Dunnett post hoc test (Graph Pad Prism 8) were performed between WBE and BPF groups compared to HFHS group. The significance between groups at different time points was calculated using a two-way repeated measures ANOVA with Dunnett's post hoc test (Sigma-plot, USA). Kruskal-Wallis or Mann-Whitney U-tests of median were used to analyze nonparametric data as appropriate, considering the samples size and data distribution. The effects

of dietary treatments on the abundance of bacterial taxa were analyzed by White's non-parametric t-test with Benjamini's correction for multiple comparisons (STAMP; version 2.1.3). To examine differences on the abundance of individual taxa between two groups, a non-parametric Mann-Whitney U-test was applied. p values less than 0.05 were considered statistically significant whereas p values between 0.05 and 0.1 were considered as showing a trend. Results were expressed as means ± standard error of the mean (SEM).

Data availability

The datasets generated during and/or analysed during the current study are available from the corresponding author on reasonable request.

References

1 García-Lafuente, A., Guillamón, E., Villares, A., Rostagno, M. A. & Martínez, J. Flavonoids as anti-inflammatory agents: implications in cancer and cardiovascular disease. *Inflammation Research* **58**, 537-552, doi:10.1007/s00011-009-0037-3 (2009).

2 Wu, V. C. H., Qiu, X., Bushway, A. & Harper, L. Antibacterial effects of American cranberry (*Vaccinium macrocarpo*n) concentrate on foodborne pathogens. *LWT-Food Science and Technology* (2008).

3 Nair, A. R., Mariappan, N., Stull, A. J. & Francis, J. Blueberry supplementation attenuates oxidative stress within monocytes and modulates immune cell levels in adults with metabolic syndrome: a randomized, double-blind, placebo-controlled trial. *Food & Function* **8**, 4118-4128, doi:10.1039/c7fo00815e (2017).

4 Overall, J. *et al.* Metabolic effects of berries with structurally diverse anthocyanins. *International Journal of Molecular Sciences* **18**, 422, doi:10.3390/ijms18020422 (2017).

5 Shi, M., Loftus, H., McAinch, A. J. & Su, X. Q. Blueberry as a source of bioactive compounds for the treatment of obesity, type 2 diabetes and chronic inflammation. *J Funct Food* **30**, 16-29, doi:10.1016/j.jff.2016.12.036 (2017).

6 Nie, Y. & Stürzenbaum, S. R. Proanthocyanidins of natural origin: molecular mechanisms and implications for lipid disorder and aging-associated diseases. *Advances in Nutrition* **10**, 464-478, doi:10.1093/advances/nmy118 (2019).

7 Salvadó, J. M., Casanova, E., Fernández-Iglesias, A., Arola, L. & Bladé, C. Roles of proanthocyanidin rich extracts in obesity. *Food & Function* **6**, 1053-1071, doi:10.1039/c4fo01035c (2015).

8 Ogura, K. *et al.* Oral administration of apple procyanidins ameliorates insulin resistance via suppression of pro-inflammatory cytokines expression in liver of diabetic ob/ob mice. *J Agr Food Chem* **64**, 8857-8865, doi:10.1021/acs.jafc.6b03424 (2016).

9 Zhang, Y., Chen, S., Wei, C., Chen, J. & Ye, X. Proanthocyanidins from chinese bayberry (*Myrica rubra* Sieb. et Zucc.) leaves regulate lipid metabolism and glucose consumption by activating AMPK pathway in HepG2 cells. *J Funct Food* **29**, 217-225, doi:10.1016/j.jff.2016.12.030 (2017).

10 Deprez, S., Mila, I., Huneau, J.-F., Tome, D. & Scalbert, A. Transport of proanthocyanidin dimer, trimer, and polymer across monolayers of human intestinal epithelial caco-2 cells. *Antioxidants & redox signaling* **3**, 957-967, doi:10.1089/152308601317203503 (2001).

11 Masumoto, S. *et al.* Non-absorbable apple procyanidins prevent obesity associated with gut microbial and metabolomic changes. *Sci Rep-uk* **6**, 31208, doi:10.1038/srep31208 (2016).

12 Sommer, F. & Bäckhed, F. The gut microbiota — masters of host development and physiology. *Nature Reviews Microbiology* **11**, 227, doi:10.1038/nrmicro2974 (2013).

13 Bischoff, S. C. *et al.* Intestinal permeability–a new target for disease prevention and therapy. *BMC Gastroenterology* (2014).

14 Deplancke, B. & Gaskins, R. H. Microbial modulation of innate defense: goblet cells and the intestinal mucus layer. *Am J Clin Nutrition* **73**, doi:10.1093/ajcn/73.6.1131S (2001).

15 Ding, S. & opinion in clinical nutrition and, L.-P. K. Role of intestinal inflammation as an early event in obesity and insulin resistance. *Current opinion in clinical nutrition and metabolic care* (2011).

16 Zhernakova, A. *et al.* Population-based metagenomics analysis reveals markers for gut microbiome composition and diversity. *Science* **352**, 565-569, doi:10.1126/science.aad3369 (2016).

17 Anhê, F. F., Roy, D., Pilon, G., Dudonné, S. & Matamoros, S. A polyphenol-rich cranberry extract protects from diet-induced obesity, insulin resistance and intestinal inflammation in association with increased *Akkermansia* spp population of the gut microbiota of mice. *Gut* (2015).

18 Jiao, X. *et al.* Blueberry polyphenols extract as a potential prebiotic with anti-obesity effects on C57BL/6 J mice by modulating the gut microbiota. *J Nutritional Biochem* **64**, 88-100, doi:10.1016/j.jnutbio.2018.07.008 (2019).

19 Lee, S. *et al.* Blueberry supplementation influences the gut microbiota, inflammation, and insulin resistance in high-fat-diet-fed rats. *J Nutrition* **148**, 209-219, doi:10.1093/jn/nxx027 (2018).

20 Vendrame, S. *et al.* Six-week consumption of a wild blueberry powder drink increases bifidobacteria in the human gut. *J Agr Food Chem* **59**, 12815-12820, doi:10.1021/jf2028686 (2011).

21 Polewski, M. A., Esquivel-Alvarado, D., Wedde, N. S., Kruger, C. G. & Reed, J. D. Isolation and characterization of blueberry polyphenolic components and their effects on gut barrier dysfunction. *J Agr Food Chem*, doi:10.1021/acs.jafc.9b01689 (2019).

22 Reagan-Shaw, S., Nihal, M. & Ahmad, N. Dose translation from animal to human studies revisited. *FASEB J* **22**, 659-661, doi:10.1096/fj.07-9574LSF (2008).

23 Stanley, C. M. & Phillips, T. E. Selective secretion and replenishment of discrete mucin glycoforms from intestinal goblet cells. *The American journal of physiology* **277**, 200, doi:10.1152/ajpgi.1999.277.1.g191 (1999).

24 Turnbaugh, P. J. *et al.* An obesity-associated gut microbiome with increased capacity for energy harvest. *Nature* **444**, 1027, doi:10.1038/nature05414 (2006).

25 Lacombe, A. *et al.* Lowbush wild blueberries have the potential to modify gut microbiota and xenobiotic metabolism in the rat colon. *PLoS ONE* **8**, doi:10.1371/journal.pone.0067497 (2013).

26 Farrell, T. L., Ellam, S. L., Forrelli, T. & Williamson, G. Attenuation of glucose transport across Caco-2 cell monolayers by a polyphenol-rich herbal extract: Interactions with SGLT1 and GLUT2 transporters. *BioFactors* **39**, 448-456, doi:10.1002/biof.1090 (2013).

27 Casanova-Martí, À. *et al.* Acute selective bioactivity of grape seed proanthocyanidins on enteroendocrine secretions in the gastrointestinal tract. *Food & Nutrition Research* **61**, 1321347, doi:10.1080/16546628.2017.1321347 (2017).

28 DeFuria, J. *et al.* Dietary blueberry attenuates whole-body insulin resistance in high fat-fed mice by reducing adipocyte death and its inflammatory sequelae. *J Nutrition* **139**, 1510-1516, doi:10.3945/jn.109.105155 (2009).

29 Elks, C. M., Terrebonne, J. D., Ingram, D. K. & Stephens, J. M. Blueberries improve glucose tolerance without altering body composition in obese postmenopausal mice. *Obesity* **23**, 573-580, doi:10.1002/oby.20926 (2015).

30 Seymour, M. E. *et al.* Blueberry intake alters skeletal muscle and adipose tissue peroxisome proliferator-activated receptor activity and reduces insulin resistance in obese rats. *Journal of Medicinal Food* **14**, 1511-1518, doi:10.1089/jmf.2010.0292 (2011).

31 Walters, W. A., Xu, Z. & Knight, R. Meta-analyses of human gut microbes associated with obesity and IBD. *FEBS Letters* **588**, 4223-4233, doi:10.1016/j.febslet.2014.09.039 (2014).

32 Ormerod, K. L. *et al.* Genomic characterization of the uncultured Bacteroidales family *S24-7* inhabiting the guts of homeothermic animals. *Microbiome* **4**, 36, doi:10.1186/s40168-016-0181-2 (2016).

33 Yao, J. *et al.* A Pathogen-Selective Antibiotic Minimizes Disturbance to the Microbiome. *Antimicrobial Agents and Chemotherapy* **60**, 4264-4273, doi:10.1128/AAC.00535-16 (2016).

34 Lacombe, A., Wu, V. C. H., White, J., Tadepalli, S. & Andre, E. E. The antimicrobial properties of the lowbush blueberry *(Vaccinium angustifolium)* fractional components against foodborne pathogens and the conservation of probiotic *Lactobacillus rhamnosus*. *Food microbiology* **30**, 124-131, doi:doi:10.1016/j.fm.2011.10.006 (2012).

35 Gómez-Gallego, C., Pohl, S., Salminen, S., Vos, D. W. M. & Kneifel, W. *Akkermansia muciniphila*: a novel functional microbe with probiotic properties. *Beneficial microbes* **7**, 571-584, doi:10.3920/bm2016.0009 (2016).

36 Everard, A. *et al.* Cross-talk between *Akkermansia muciniphila* and intestinal epithelium controls diet-induced obesity. *Proc National Acad Sci* **110**, 9066-9071, doi:10.1073/pnas.1219451110 (2013).

37 Shin, N.-R. *et al.* An increase in the *Akkermansia* spp. population induced by metformin treatment improves glucose homeostasis in diet-induced obese mice. *Gut* **63**, 727, doi:10.1136/gutjnl-2012-303839 (2014).

38 Li, Z., Henning, S. M., Lee, R. P., Lu, Q. Y. & function, S.-P. H. Pomegranate extract induces ellagitannin metabolite formation and changes stool microbiota in healthy volunteers. *Food & function*, doi:10.1039/C5FO00669D (2015).

39 Anhe, F. F. *et al.* Treatment with camu camu (*Myrciaria dubia*) prevents obesity by altering the gut microbiota and increasing energy expenditure in diet-induced obese mice. *Gut*, doi:10.1136/gutjnl-2017-315565 (2018).

40 Roopchand, D. E., Carmody, R. N., Kuhn, P. & Diabetes, M.-K. Dietary polyphenols promote growth of the gut bacterium *Akkermansia muciniphila* and attenuate high fat diet-induced metabolic syndrome. *Diabetes*, doi:10.2337/db14-1916 (2015).

41 Heyman-Lindén, L. *et al.* Lingonberries alter the gut microbiota and prevent low-grade inflammation in high-fat diet fed mice. *Food & Nutrition Research* **60**, 29993, doi:10.3402/fnr.v60.29993 (2016).

42 Lavelle, A. *et al.* Spatial variation of the colonic microbiota in patients with ulcerative colitis and control volunteers. *Gut* **64**, 1553-1561, doi:10.1136/gutjnl-2014-307873 (2015).

43 Braune, A. & Blaut, M. Bacterial species involved in the conversion of dietary flavonoids in the human gut. *Gut Microbes* **7**, 216-234, doi:10.1080/19490976.2016.1158395 (2016).

44 Takagaki, A. & and Bulletin, N.-F. Bioconversion of (−)-epicatechin,(+)-epicatechin,(−)-catechin, and (+)-catechin by (−)-epigallocatechin-metabolizing bacteria. *Biological and Pharmaceutical Bulletin*, doi:10.1248/bpb.b14-00813 (2015).

45 Mena, P. *et al.* Phenyl-γ-valerolactones and phenylvaleric acids, the main colonic metabolites of flavan-3-ols: synthesis, analysis, bioavailability, and bioactivity. *Natural Product Reports* **36**, 714-752, doi:10.1039/c8np00062j (2018).

46 Kelly A. Shaw *et al.* Dysbiosis, inflammation, and response to treatment: a longitudinal study of pediatric subjects with newly diagnosed inflammatory bowel disease. *Genome Medicine* **8:75** doi:DOI 10.1186/s13073-016-0331-y (2016).

47 Pierre, J. F. *et al.* Cranberry proanthocyanidins improve the gut mucous layer morphology and function in mice receiving elemental enteral nutrition. *Journal of Parenteral and Enteral Nutrition* **37**, 401-409, doi:10.1177/0148607112463076 (2013).

48 Schroeder, B. O. Fight them or feed them: how the intestinal mucus layer manages the gut microbiota. *Gastroenterology Report* **7**, 3-12, doi:10.1093/gastro/goy052 (2019).

49 Wlodarska, M. *et al.* NLRP6 inflammasome orchestrates the colonic host-microbial interface by regulating goblet cell mucus secretion. *Cell* **156**, 1045-1059, doi:10.1016/j.cell.2014.01.026 (2014).

50 Wang, Y. & Hatabu, T. Mulberry juice freeze-dried powder attenuates the disease severity by the maintaining of colon mucosa in mice with DSS-induced acute colitis. *Bioscience, Biotechnology, and Biochemistry* **83**, 1-9, doi:10.1080/09168451.2019.1580135 (2019).

51 Kober, O. I. *et al.* γδ T-cell-deficient mice show alterations in mucin expression, glycosylation, and goblet cells but maintain an intact mucus layer. *American journal of physiology. Gastrointestinal and liver physiology* **306**, 93, doi:10.1152/ajpgi.00218.2013 (2014).

52 Forder, R. E. A., Howarth, G. S., Tivey, D. R. & Hughes, R. J. Bacterial modulation of small intestinal goblet cells and mucin composition during early oosthatch development of poultry1. *Poultry Science* **86**, 2396-2403, doi:10.3382/ps.2007-00222 (2007).

53 Tarabova, L., Makova, Z., Piesova, E., Szaboova, R. & Faixova, Z. Intestinal mucus layer and mucins (a review). *Folia Veterinaria* **60**, 21-25, doi:10.1515/fv-2016-0003 (2016).

54 Danquah, K. *et al.* Mucin expression patterns in histological grades of colonic cancers in Ghanaian population. *The Pan African Medical Journal* **27**, 267, doi:10.11604/pamj.2017.27.267.9793 (2017).

55 Clavel, T. *et al.* Intestinal microbiota in metabolic diseases. *Gut Microbes* **5**, 544-551, doi:10.4161/gmic.29331 (2014).

56 Gu, L. *et al.* Fractionation of polymeric procyanidins from Lowbush blueberry and quantification of procyanidins in selected foods with an optimized normal-phase HPLC−MS fluorescent detection method. *J Agr Food Chem* **50**, 4852-4860, doi:10.1021/jf020214v (2002).

57 Feliciano, R., P. *et al.* Comparison of Isolated Cranberry (*Vaccinium macrocarpon* Ait.) Proanthocyanidins to Catechin and Procyanidins A2 and B2 for Use as Standards in the 4-(Dimethylamino)cinnamaldehyde Assay. *J Agr Food Chem* **60**, 4578-4585, doi:10.1021/jf3007213 PMID - 22533362 (2012).

58 Dudonné, S. *et al.* Comprehensive analysis of phenolic compounds and abscisic acid profiles of twelve native Canadian berries. *Journal of Food Composition and Analysis* **44**, 214-224, doi:10.1016/j.jfca.2015.09.003 (2015).

59 Dudonné, S. *et al.* Modulation of Strawberry/Cranberry Phenolic compounds glucuronidation by co-supplementation with onion: Characterization of phenolic metabolites in rat plasma using an optimized μSPE-UHPLC-MS/MS Method. *Journal of agricultural and Food Chemistry* **62**, 3244-3256, doi:10.1021/jf404965z (2014).

60 Williams, J. M., Duckworth, C. A., Vowell, K., Burkitt, M. D. & Pritchard, M. D. Current protocols in mouse biology. *Current protocols in mouse biology* **6**, 148-168, doi:10.1002/cpmo.2 (2016).

61 Barcelo, A. *et al.* Mucin secretion is modulated by luminal factors in the isolated vascularly perfused rat colon. *Gut* **46**, 218-224, doi:10.1136/gut.46.2.218 (2000).

62 Johnson, O. *et al.* The distribution of mucous secreting cells in the gastrointestinal tracts of three small rodents from Saudi Arabia: Acomys dimidiatus, Meriones rex and Meriones libycus. *Acta Histochemica* **118**, 118-128, doi:10.1016/j.acthis.2015.12.003 (2016).

63 Johansson, M. E. V. *et al.* Bacteria penetrate the normally impenetrable inner colon mucus layer in both murine colitis models and patients with ulcerative colitis. *Gut* **63**, 281-291, doi:10.1136/gutjnl-2012-303207 (2014).

64 Zhang, J., Kobert, K., Flouri, T. & Stamatakis, A. PEAR: a fast and accurate Illumina Paired-End reAd mergeR. *Bioinformatics* **30**, 614-620, doi:10.1093/bioinformatics/btt593 (2014).

65 Edgar, R. C., Haas, B. J., Clemente, J. C., Quince, C. & Knight, R. UCHIME improves sensitivity and speed of chimera detection. *Bioinformatics* **27**, 2194-2200, doi:10.1093/bioinformatics/btr381 (2011).

66 DeSantis, T. Z. *et al.* Greengenes, a chimera-checked 16S rRNA gene database and workbench compatible with ARB. *Applied and Environmental Microbiology* **72**, 5069-5072, doi:10.1128/aem.03006-05 (2006).

67 Edgar, R. C. Search and clustering orders of magnitude faster than BLAST. *Bioinformatics* **26**, 2460-2461, doi:10.1093/bioinformatics/btq461 (2010).

68 Wang, Q., Garrity, G. M., Tiedje, J. M. & Cole, J. R. Naïve bayesian classifier for rapid assignment of rRNA sequences into the new bacterial taxonomy. *Applied and Environmental Microbiology* **73**, 5261-5267, doi:10.1128/aem.00062-07 (2007).

69 Cole, J. R. *et al.* Ribosomal Database Project: data and tools for high throughput rRNA analysis. *Nucleic Acids Research* **42**, doi:10.1093/nar/gkt1244 (2014).

70 Dhariwal, A. *et al.* MicrobiomeAnalyst: a web-based tool for comprehensive statistical, visual and meta-analysis of microbiome data. *Nucleic Acids Research* **45**, doi:10.1093/nar/gkx295 (2017).

71 Hartman, A. L. *et al.* Human gut microbiome adopts an alternative state following small bowel transplantation. *Proc National Acad Sci* **106**, 17187-17192, doi:10.1073/pnas.0904847106 (2009).

72 Yang, Y.-W. *et al.* Use of 16S rRNA gene-targeted group-specific primers for real-time PCR analysis of predominant bacteria in mouse feces. *Applied and Environmental Microbiology* **81**, 6749-6756, doi:10.1128/aem.01906-15 (2015).

73 Langille, M. G. I. *et al.* Predictive functional profiling of microbial communities using 16S rRNA marker gene sequences. *Nature Biotechnology* **31**, 814-821, doi:10.1038/nbt.2676 (2013).

Acknowledgements

This study was funded by CRIBIQ, MITACS, Fruit d'Or, Atrium Innovation, Diana Food Canada, and the Wild Blueberry Association of North America (WBANA). AM group was also funded by a Canadian Institutes of Health Research (CIHR) grant, the J. A. De Sève Foundation and a CIHR/Pfizer research chair in the pathogenesis of insulin resistance and cardiovascular diseases. We also extent our acknowledgments to COLCIENCIAS for granting PhD. scholarship to MCR.

Author contributions

YD, AM, DR, EL, GP designed the study. MCR and LD performed the experiments. LB and SD were involved on the preparation and technical analysis of WBE and BPF. MCR and TV performed the 16S rRNA sequences pre-processing. MCR performed the metataxonomic analysis, PCRs assays, intestinal histology and gene expression analysis. MCR and LD worked on the analysis and discussion of the data. MCR, LD, YD and AM wrote the manuscript. All authors reviewed and approved the final manuscript.

Additional Information

Competing interests: The authors declare no competing interests.

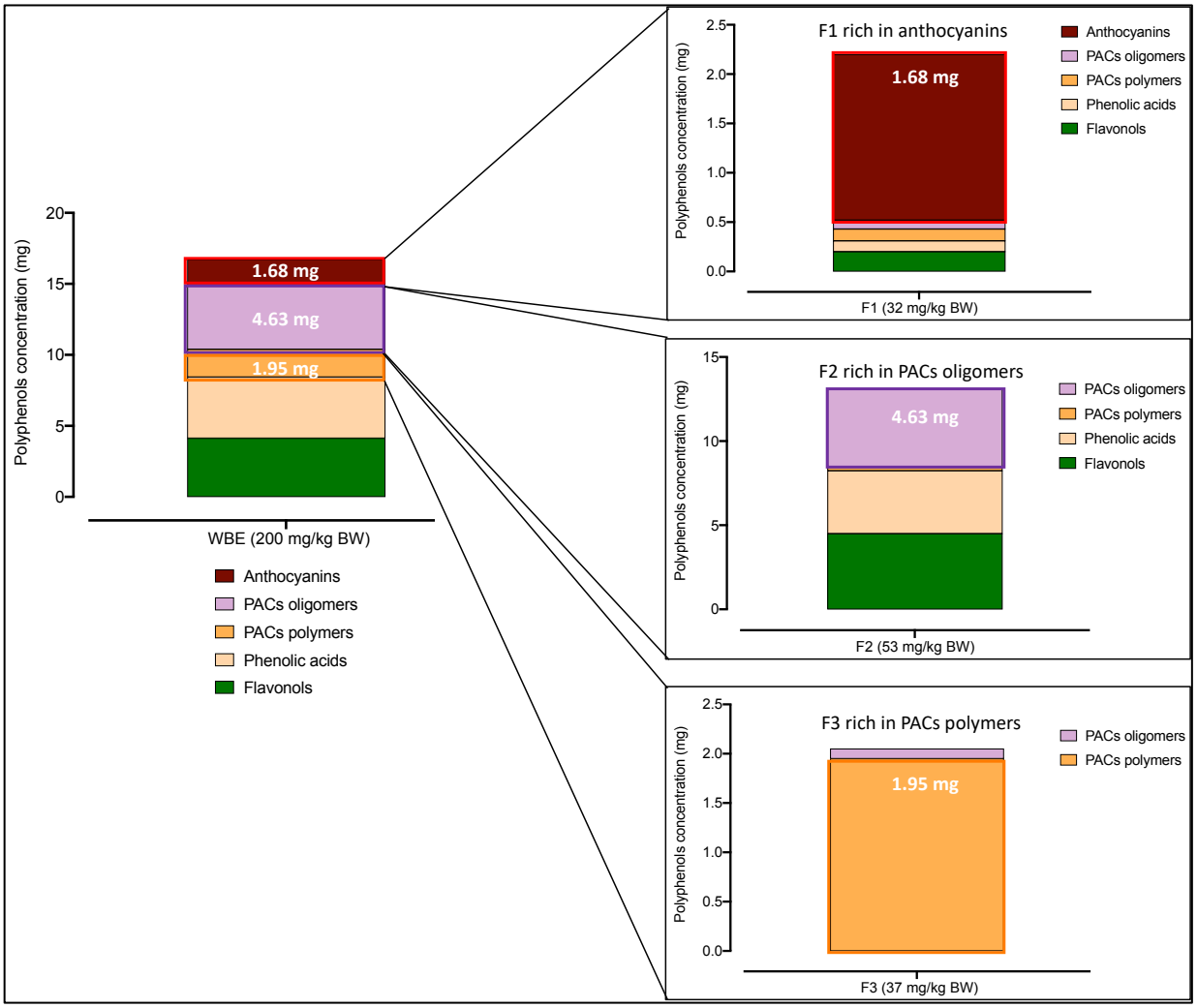

Figure 1. Phenolic content in mouse dosage of blueberry extract and polyphenolic fractions.

C57BL/6J mice were fed an HFHS diet and treated either with the vehicle (water); 200 mg/kg body weight (BW) of whole blueberry extract (WBE) containing 17 mg of polyphenols; 37 mg/kg BW of the F1 fraction rich in anthocyanin and phenolic acids; 53 mg/kg BW of the F2 fraction rich in oligomeric PACs, phenolic acids and flavonols, and 37 mg/kg BW of the F3 fraction rich in polymeric PACs for 8 weeks. The dose of each fraction administrated to mice were calculated to provide the same concentration of anthocyanins, PACs oligomers and PACs polymers as encountered in the whole blueberry extract (F1, F2, and F3 fractions respectively).

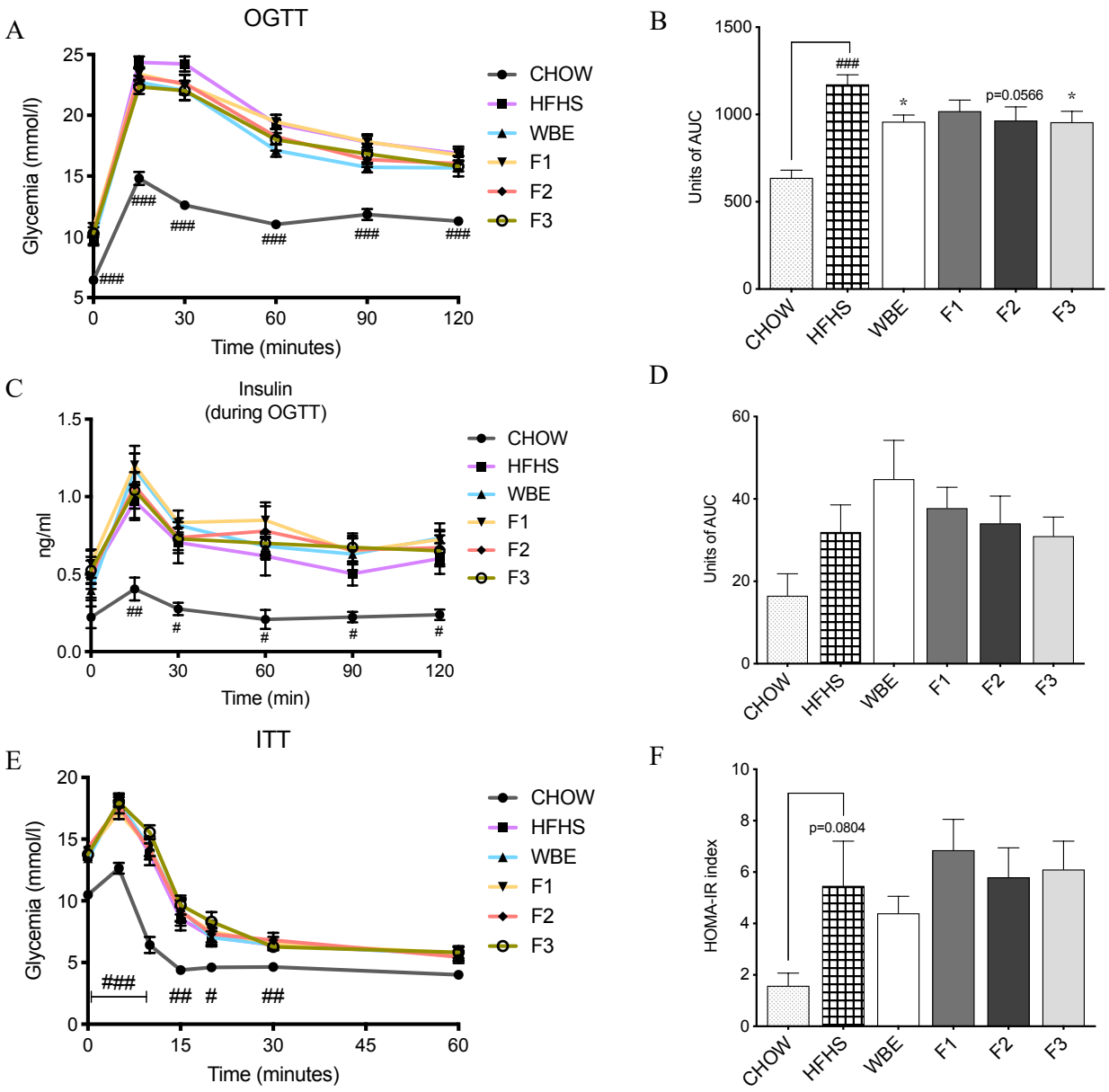

Figure 2. Total WBE and polymeric PACs-rich fraction fed mice presented an improved glucose tolerance.

C57BL/6J mice were fed a HFHS diet and treated either with the vehicle (water), the WBE or a BPF: anthocyanin and phenolic acids (F1), oligomeric PACs, phenolic acids and flavonols (F2) and polymeric PACs (F3) for 8 weeks. A) Oral glucose tolerance test (OGTT) was performed with 12h fasted at 8 weeks of treatment; B) Area under the curve (AUC) of OGTT calculated between baseline and 120 min; C) Insulin levels were measured during the OGTT; D) AUC of insulin level during OGTT was calculated; E) Blood glucose measurements over insulin tolerance test (ITT)

was performed on fasted mice for 6h at 6 weeks of treatment; F) Homeostatic model assessment of insulin resistance (HOMA-IR). A student-t test was applied to calculate the significance of the difference between the chow and the HFHS group. One-way ANOVA with a Dunnett post hoc test was applied to calculate the significant differences between groups. Two-way repeated measures ANOVA with a Dunnett post hoc test was applied to calculate the significance between groups at different time points. Values are expressed as the mean ± SEM (n=12/groups). *p<0.05 compared to HFHS; Chow vs HFHS # p<0,05 ### p<0,001.

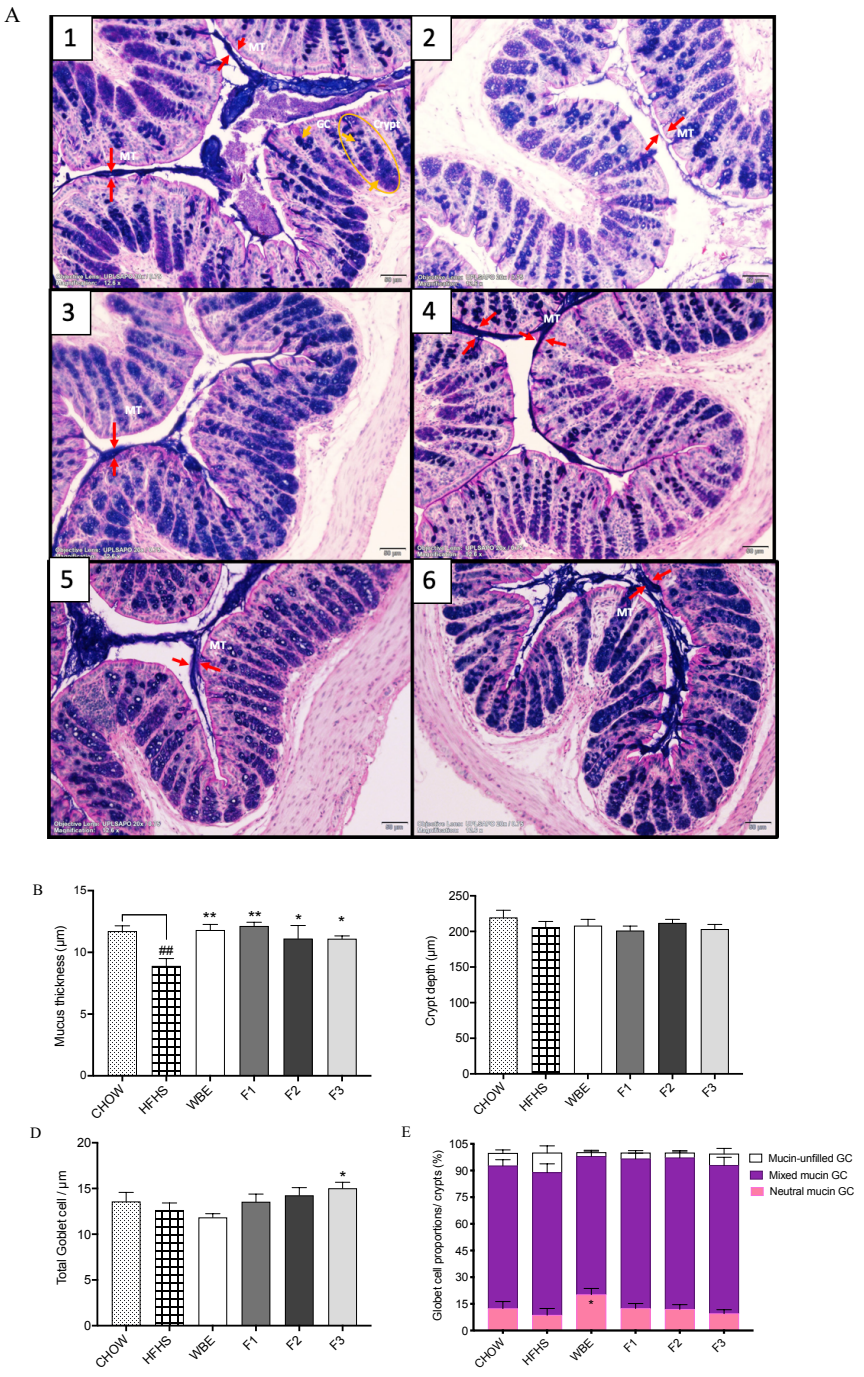

Figure 3. Wild blueberry polyphenolic fractions restore the mucus thickness and polymeric PACs-rich fraction significantly stimulated mucin-secreting goblet cells number in HFHS-fed mouse colon

The effect of HFHS-diet and the supplementation with WBE and BPF: anthocyanin and phenolic acids (F1), oligomeric PACs, phenolic acids and flavonols (F2) and polymeric PACs (F3) were studied in mouse colon morphology. A combination of Alcian Blue and periodic acid–Schiff staining (AB/PAS) was used to distinguish acidic (dark blue) and neutral (red) mucins. A purple color indicates the presence of both acidic and neutral mucins. Images shown are representatives of examined mice (n=12) in each group: A-1) Chow; A-2) HFHS; A-3) WBE; A-4) F1; A-5) F2; A-6) F3. Images were taken using objective lens UPLSAPO 20X/0.75, magnification 12.6X, Scale 50 µm. Arrows indicate mucus thickness (MT) measured using Image J software. The circle is enclosing a colonic crypt. Within each crypt mucin-filled goblet cells (GC) were counted. Histological parameters were evaluated in cross-sections of colon tissues stained with AB/PAS staining: B) Mucus thickness, C) Crypt depth D) Total GC number per µm of crypt, and E) Mucin-filled GC types. Data are shown as Mean ± SEM (n = 12/group). Significant differences were determined by ordinary one-way ANOVA. Values are expressed as mean +/- SEM. $p<0.01$## compared to Chow $p<0.01$** and $p<0.05$ * compared to HFHS, respectively.

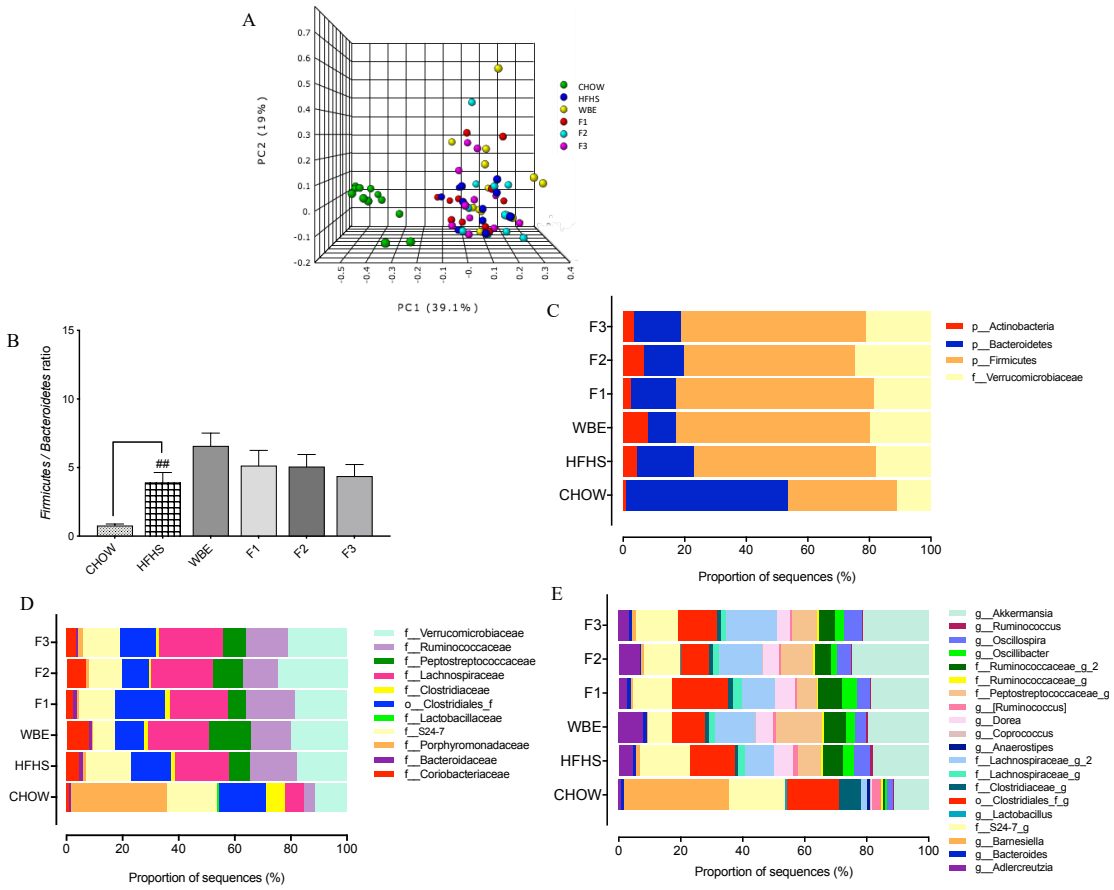

Figure 4. Dissimilarity analysis of the gut microbiota composition between groups and the mean relative abundance of bacterial taxonomies at phylum, family and genus level after 8-weeks of dietary supplementation.

Principal coordinate (PCoA) plots exhibited a different dispersion of WBE fecal microbial communities. Quantitative non-phylogenetic measures were applied as β-diversity metrics to calculate distances among all fecal mouse samples. A) Bray Curtis matrix of samples rarefied to 6,957 sequences revealed significant differences between groups (PERMANOVA, R-squared: 0.37968; p-value<0.001). Each sample point (n=12/group) is color-coded based on the administrated diet for 8 weeks (W8), as shown in each figure legend. B) Different *Firmicutes* to *Bacteroides* ratio are shown for Chow and HFHS-fed controls mice at week 8. Mice fed HFHS-diet and supplemented with WBE and BPF: anthocyanin and phenolic acids (F1), oligomeric PACs, phenolic acids and flavonols (F2) and polymeric PACs (F3) showed variations on the proportions of sequences distributed in C) Four bacterial phyla, D) Eleven families and E) twenty assigned genus. The statistical significance on β-diversity across sample groups was assessed with the non-parametric Permutational Multivariate Analysis of Variance (PERMANOVA, 999 Monte Carlo permutations) test. Kruskal-Wallis test with Benjamini post-hoc multiple comparison correction compared to HFHS were used to found out significant changes in the taxonomic proportions, p<0.01 ##. Values are expressed as mean +/- SEM

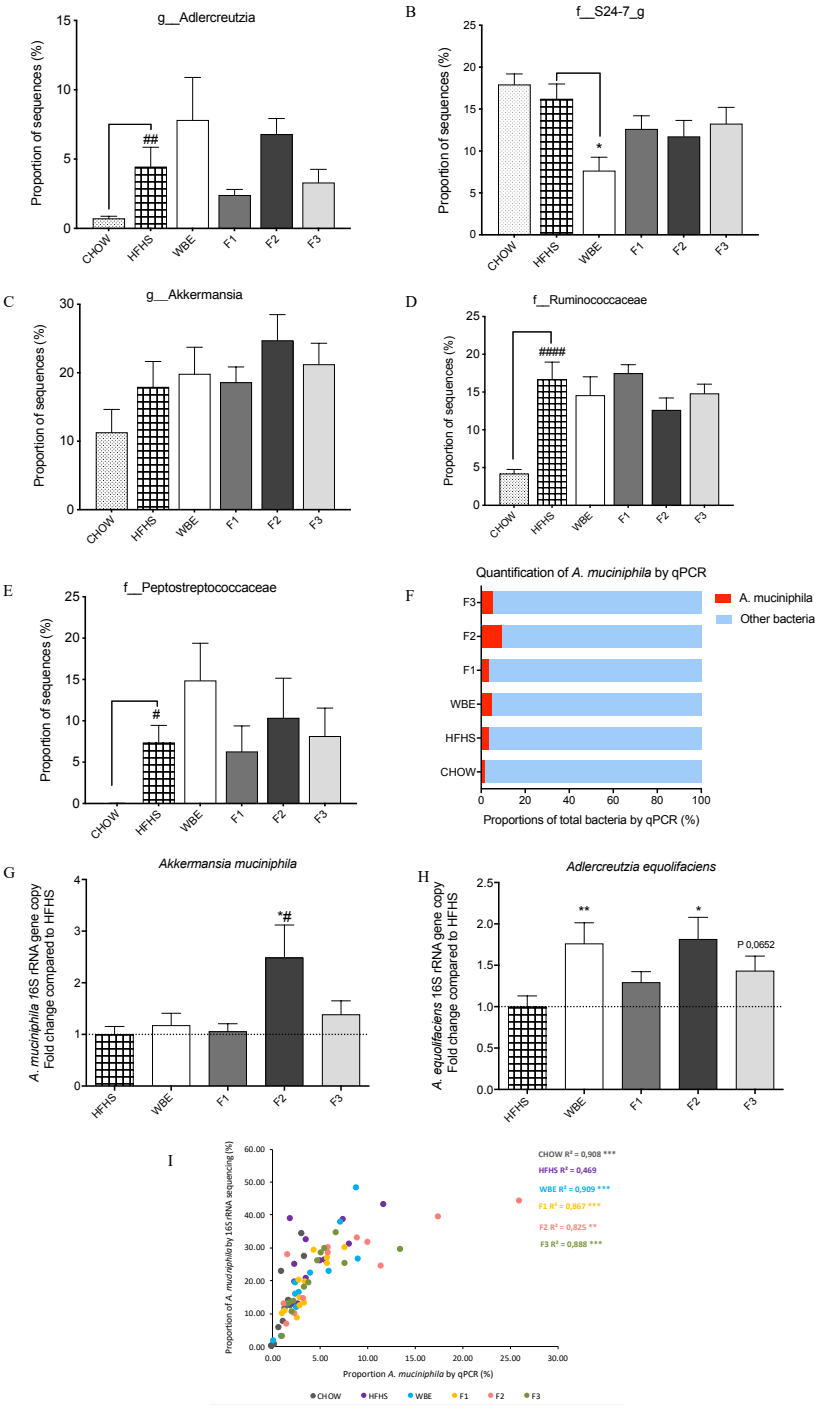

Figure 5. Mean proportions of bacterial taxa by 16S rRNA gene sequencing and significant differences in relative mean proportion of A. muciniphila and A. equolifaciens by qPCA on blueberry polyphenols treated mice and HFHS control group.

HFHS-fed mouse fecal samples were analyzed by 16S rRNA gene sequencing and qPCR analysis of 16S rRNA gene copy for *Adlercreutzia equolifaciens* and *Akkermansia muciniphila* were performed to validate the data obtained by high-throughput 16S rRNA sequencing method after 8 weeks of dietary treatment with WBE and BPF: anthocyanin and phenolic acids (F1), oligomeric PACs, phenolic acids and flavonols (F2) and polymeric PACs (F3). Relative proportion of sequences of A) *Adlercreutzia equolifaciens,* B) An unassigned genus of the family *S24-7* and C) *Akkermansia muciniphila*; the relative proportion of 16S rRNA gene copy determined by qPCR of D) An unassigned genus of the family *Ruminococcaceae;,* E) An unassigned genus of the family *Peptostreptococcaceae;* F) The relative proportion of *Akkermansia muciniphila* relative to the total bacteria; G) Fold-change of the *Akkermansia muciniphila* proportion relative to HFHS H) Fold-change of the *Adlercreutzia equolifaciens* proportion relative to HFHS; I) Spearman correlations analysis was performed for comparing the data obtained from 16S rRNA sequencing versus the 16S rRNA relative proportion obtained by qPCR, Statistic: *$p<0.05$, **$p<0.01$, ***$p<0.001$ for qPCR vs 16S rRNA gene sequencing data. Values are expressed as mean +/- SEM. Kruskal-Wallis test with Benjamini post-hoc multiple comparison correction compared to HFHS *$p<0.05$ and **$p<0.01$. Mann-Whitney U-Test PACs<4 vs HFHS #$p<0.05$.

Supplementary information

Wild blueberry proanthocyanidins shape distinct gut microbiota profile and influence glucose homeostasis and intestinal phenotypes in high-fat high-sucrose fed mice

Maria-Carolina Rodríguez-Daza[1 2 a], Laurence Daoust[1 2 a], Lemia Boutkrabt[1], Geneviève Pilon[1 3], Thibault Varin[1], Stéphanie Dudonné[1], Émile Levy[1], André Marette[1 3], Denis Roy[1 2] and Yves Desjardins[1 2]

[1] Institute of Nutrition and Functional Foods (INAF), Laval University, Québec, QC, Canada.
[2] Food Science Department, Faculty of Agriculture and Food, Laval University, Québec, QC, Canada.
[3] Department of Medicine, Faculty of Medicine, Cardiology Axis of the Quebec Heart and Lung Institute, Québec, QC, Canada.
[a] These authors contributed equally to this work

Corresponding Author:
Yves Desjardins
Institute of Nutrition and Functional Foods (INAF)
Laval University, Québec
Pavillon des Services, # 2736
2440, Boulevard Hochelaga, Québec, QC, Canada G1V 0A6
Telephone: 418-262-0897; email: yves.desjardins@fsaa.ulaval.ca

Table S1. Phenolic characterization of blueberry extract and polyphenolic fractions

	Polyphenols content (mg/100 g dry weight)			
	Crude extract	**Polyphenolic fractions**		
Polyphenol type	**WBE**	**F1**	**F2**	**F3**
Anthocyanins	**840.1 ± 24.8**	**5248.2 ± 427.0**	**29.2 ± 0.8**	**ND**
Delphinidin 3-galactoside	9.6 ± 0.6	57.7 ± 5.5	0.7 ± 0.1	ND
Delphinidin 3-glucoside	28.4 ± 4.6	262.2 ± 47.8	2.2 ± 0.1	ND
Cyanidin 3-galactoside	18.5 ± 2.4	66.5 ± 57.9	1.0 ± 0.1	ND
Delphinidin 3-arabinoside	10.3 ± 2.6	12.7 ± 0.2	0.9 ± 0.2	ND
Cyanidin 3-glucoside	68.8 ± 3.4	612.3 ± 49.3	3.2 ± 0.1	ND
Petunidin 3-galactoside	14.6 ± 1.5	83.1 ± 5.3	0.7 ± 0.3	ND
Cyanidin 3-arabinoside	25.5 ± 2.4	25.8 ± 1.3	1.6 ± 0.03	ND
Petunidin 3-glucoside	53.0 ± 3.3	512.8 ± 40.2	2.4 ± 0.2	ND
Peonidin 3-galactoside	10.3 ± 1.5	48.5 ± 3.4	0.3 ± 0.03	ND
Petunidin 3-arabinoside	14.3 ± 2.3	8.3 ± 0.2	0.7 ± 0.1	ND
Peonidin 3-glucoside	56.5 ± 2.9	554.2 ± 33.8	1.2 ± 0.1	ND
Malvidin 3-galactoside	74.0 ± 5.1	526.7 ± 52.9	1.2 ± 0.2	ND
Malvidin 3-glucoside	207.8 ±4.8	2397.5 ± 198.8	6.8 ± 0.1	ND
Malvidin 3-arabinoside	52.2 ± 4.4	32.3 ± 4.4	ND	ND
Delphinidin 3-(6"-acetoyl) glucoside	11.4 ± 0.5	13.8 ± 1.3	ND	ND
Cyanidin 3-(6"-acetoyl) glucoside	27.0 ± 2.5	7.2 ± 2.1	1.2 ± 0.1	ND
Malvidin 3-(6"-acetoyl) galactoside	26.0 ± 3.1	ND	ND	ND
Petunidin 3-(6"-acetoyl) glucoside	24.0 ± 1.6	ND	1.1 ± 0.2	ND
Peonidin 3-(6"-acetoyl) glucoside	19.2 ± 1.2	7.9 ± 3.2	1.6 ± 0.05	ND
Malvidin 3-(6"-acetoyl) glucoside	88.5 ± 4.1	18.7 ± 3.5	2.2 ± 0.1	ND
Proanthocyanins	**3290.4 ± 89.3**	**670.2 ± 83.4**	**7047.7 ± 242.2**	**5520.3 ± 294.2**
Monomers	322.0 ± 8.6	121.4 ± 5.5	1074.4 ± 41.7	27.8 ± 2.2
Dimers	1544.9 ± 24.9	141.1 ± 5.8	4676.1 ± 137.5	89.3 ± 6.5
Trimers	449.3 ± 3.7	27.0 ± 4.1	924.3 ± 35.9	162.5 ± 7.4
Tetramers	255.9 ± 0.5	11.0 ± 1.1	163.9 ± 8.8	412.5 ± 16.1
Pentamers	143.5 ± 3.0	7.3 ± 1.1	ND	296.1 ± 8.7
Hexamers	99.7 ± 4.8	10.4 ± 1.1	ND	210.0 ± 3.7
Heptamers	46.6 ± 3.2	ND	ND	68.2 ± 0.7
Octamers	34.0 ± 1.0	ND	ND	43.2 ± 6.3
Nonamers	26.1 ± 2.5	ND	ND	35.1 ± 5.7
Decamers	16.6 ± 2.5	ND	ND	ND
Polymers >10	351.6 ± 65.1	352.0 ± 64.7	209.0 ± 18.3	4175.5 ± 236.8

Polyphenols content (mg/100 g dry weight)				
	Crude extract	**Polyphenolic fractions**		
Polyphenol type	**WBE**	**F1**	**F2**	**F3**
Flavonols, flavan-3-nols and phenolic acids	**4389.5**	**986.06**	**18531.6**	**86.04**
Catechin	97.7 ± 3.6	1.7 ± 1.8	298.2 ± 1.0	5.7 ± 3.4
Epicatechin	75.5 ± 3.1	0.9 ± 0.8	214.1 ± 27.4	8.9 ± 4.3
Gallic acid	115.3 ± 2.2	34.1 ± 2.6	650.2 ± 21.1	1.1 ± 0.2
Protocatechuic acid	355.9 ± 1.6	295.8 ± 9.0	1330.0 ± 80.1	6.6 ± 0.8
P-coumaric acid	116.2 ± 13.3	ND	41.0 ± 7.0	ND
Caffeic acid	134.3 ± 5.3	4.6 ± 0.9	598.7 ± 24.4	ND
Ferulic acid	15.4 ± 2.1	ND	3.2 ± 1.1	ND
3-caffeoylquinic acid	23.8 ± 1.9	0.5 ± 0.5	81.8 ± 11.9	1.4 ± 0.3
4-caffeoylquinic acid	28.4 ± 1.4	0.4 ± 0.2	327.3 ± 8.5	5.3 ± 1.5
5-caffeoylquinic acid	1363.3 ± 42.7	13.0 ± 1.7	4015.3 ± 257.2	27.5 ± 1.5
Quercetin	739.1 ± 17.7	630.9 ± 13.4	4424.1 ± 196.8	11.4 ± 0.8
Quercetin-glucoside	414.5 ± 11.1	0.4 ± 0.4	2273.2 ± 91.0	7.5 ± 1.4
Quercetin-galactoside	135.7 ± 5.3	1.26 ± 0.45	760.7 ± 29.4	2.0 ± 0.6
Quercetin-rhamnoside	250.3 ± 13.0	ND	1422.9 ± 63.3	3.6 ± 2.3
Quercetin-xyloside	133.8 ± 10.6	ND	726.8 ± 64.0	1.1 ± 0.7
Quercetin-arabinoside	101.6 ± 4.2	ND	344.1 ± 8.0	0.4 ± 0.5
Rutin	288.7 ± 3.8	2.5 ± 0.4	1020.0 ± 27.9	3.5 ± 0.6

Results are expressed as mean of triplicate ± SD. ND, not detected. DP, Degree of polymerisation.

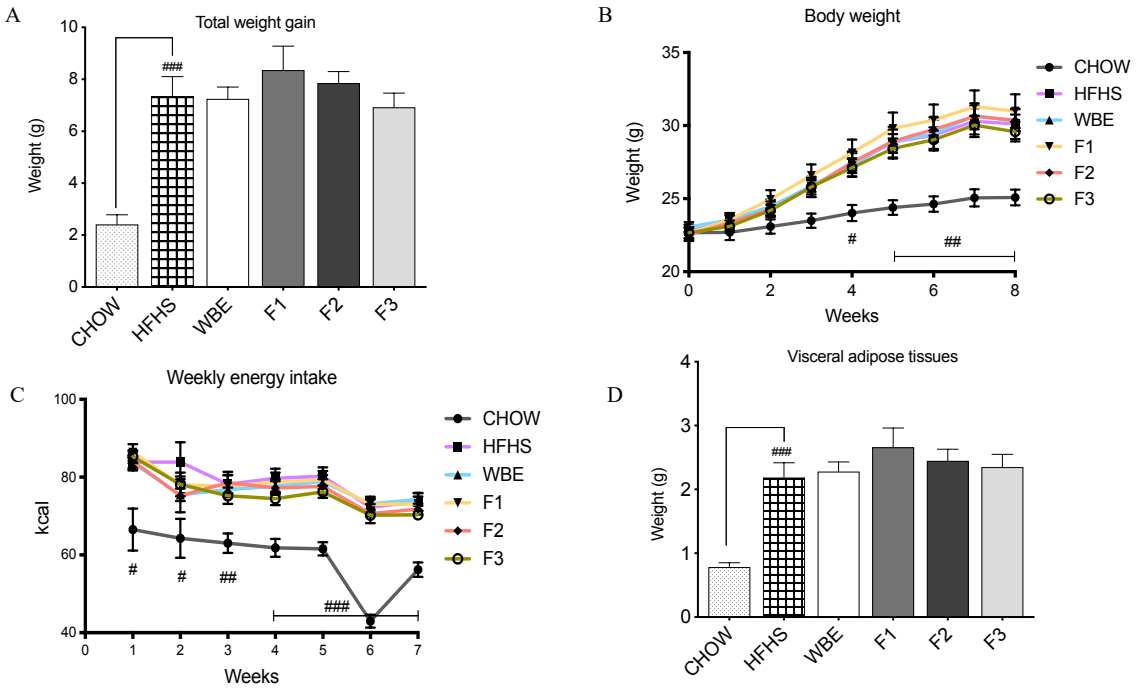

Figure S1. Body weight gain in treated mice are not affected by the administration of a WBE and BPF.

C57BL/6J mice were fed an HFHS diet and treated with the vehicle (water), the WBE or a BPF: Fraction rich in anthocyanin and phenolic acids (F1), oligomeric PACs, phenolic acids and flavonols (F2) and polymeric PACs (F3) enriched fractions for 8 weeks. A) Body weight gain; B) weight gain curves; C) energy intake; D) visceral adipose tissue weight. One-way ANOVA with a Dunnett post hoc test was applied to calculate the significance of the differences between groups. Two-way repeated measures RM-ANOVA with a Dunnett post hoc test was applied to calculate the significance between groups at different time points. Values are expressed as the mean ± SEM (n = 12). *p < 0.05 compared to HFHS; Chow vs HFHS # p<0,05 ### p<0,001, #### p<0.0001.

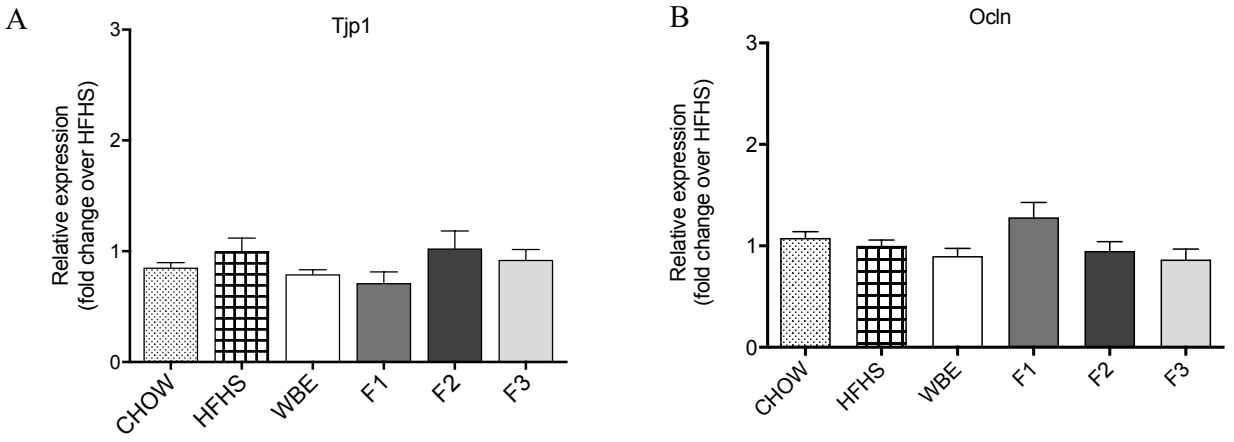

Figure S2. Effects of WBE and BPF on colonic mucin secretion and tight junction integrity of HFHS-fed mice.

Relative gene expression determined by RT-qPCR were evaluated in colon tissues of HFHS and BPF fed mice. A) mRNA levels for Tight junction protein 1 (Tjp1) and B) Occludin (Ocln) (n=10-12 per group). Ordinary one-way ANOVA a Dunnett post hoc test was performed, mean +/- SEM. $p<0.01$## compared to Chow.

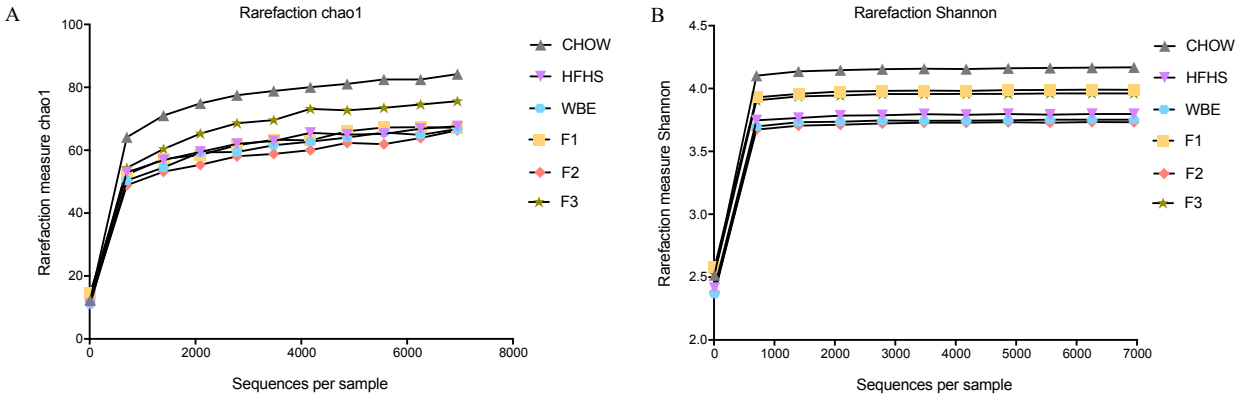

Figure S3. Rarefaction curves graphing within-sample using alpha Chao1 and Shannon diversity measures on mouse fecal bacterial communities.

A) Chao1 alpha diversity indicated HFHS-fed mice had reduced species richness than Chow controls. Curves are shown for samples treated with WBE and BPF: anthocyanin and phenolic acids (F1), oligomeric PACs, phenolic acids and flavonols (F2) and polymeric PACs (F3). Kruskal-Wallis test with Benjamini multiple comparison correction were conducted to compare diversity between groups after 8 weeks of dietary treatment. Significant differences were not found between groups ($P > 0.05$ at all sampling depth) B) Shannon diversity considering the abundance and richness showed curves similar depth of sequences among HFHS-fed mice and polyphenols treated mice.

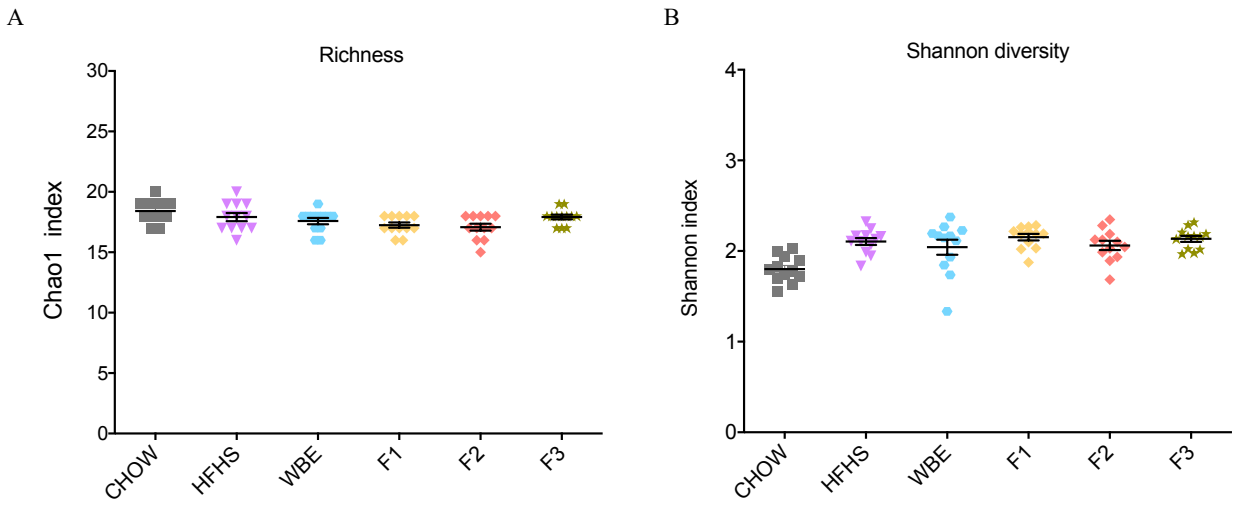

Figure S4 Alpha diversity indices.

The effect of HFHS-diet and the supplementation with WBE and BPF: anthocyanin and phenolic acids (F1), oligomeric PACs, phenolic acids and flavonols (F2) and polymeric PACs (F3) on the microbial alpha diversity were studied. A) Richness: the number of bacterial species assigned by OTUs detected in the samples was obtained using Chao1 index. B) Shannon's diversity index: Incorporates both richness and evenness. Kruskal-Wallis test with Benjamini multiple comparison correction were conducted to compare diversity between diets after 8 weeks of feeding. Mean values ±SEM are plotted, no significant differences were found.

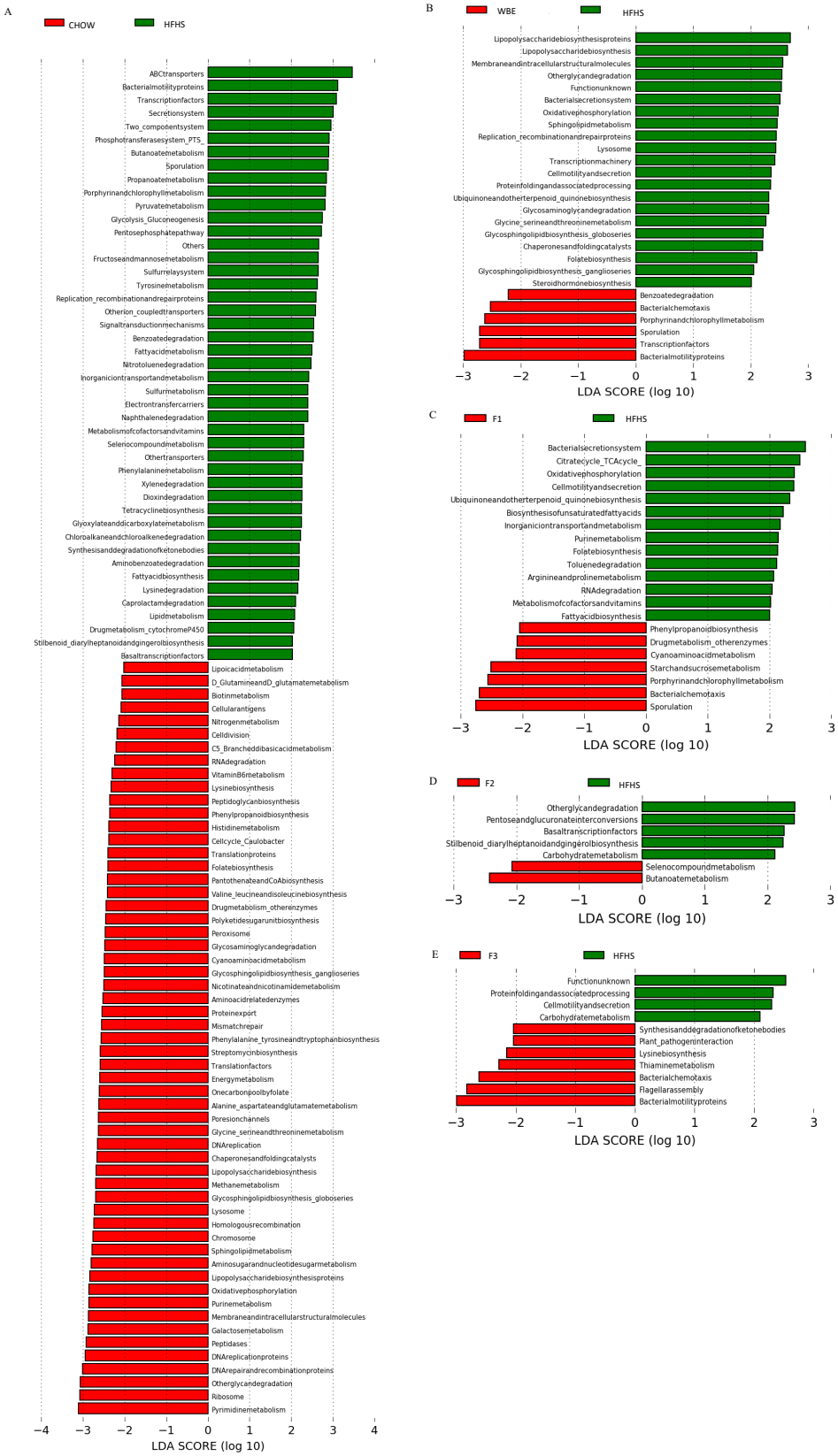
A
CHOW
HFHS
ABCtransporters
Bacterialmotilityproteins
Transcriptionfactors
Secretionsystem
Two_componentsystem
Phosphotransferasesystem_PTS
Butanoatemetabolism
Sporulation
Propanoatemetabolism
Porphyrinandchlorophyllmetabolism
Pyruvatemetabolism
Glycolysis_Gluconeogenesis
Pentosephosphatepathway
Others
Fructoseandmannosemetabolism
Sulfurrelaysystem
Tyrosinemetabolism
Replication_recombinationandrepairproteins
Otherion_coupledtransporters
Signaltransductionmechanisms
Benzoatedegradation
Fattyacidmetabolism
Nitrotoluenedegradation
Inorganiciontransportandmetabolism
Sulfurmetabolism
Electrontransfercarriers
Naphthalenedegradation
Metabolismofcofactorsandvitamins
Seleniocompoundmetabolism
Othertransporters
Phenylalaninemetabolism
Xylenedegradation
Dioxindegradation
Tetracyclinebiosynthesis
Glyoxylateanddicarboxylatemetabolism
Chloroalkaneandchloroalkenedegradation
Synthesisanddegradationofketonebodies
Aminobenzoatedegradation
Fattyacidbiosynthesis
Lysinedegradation
Caprolactamdegradation
Lipidmetabolism
Drugmetabolism_cytochromeP450
Stilbenoid_diarylheptanoidandgingerolbiosynthesis
Basaltranscriptionfactors
Lipoicacidmetabolism
D_GlutamineandD_glutamatemetabolism
Biotinmetabolism
Cellularantigens
Nitrogenmetabolism
Celldivision
C5_Branchedd ibasicacidmetabolism
RNAdegradation
VitaminB6metabolism
Lysinebiosynthesis
Peptidoglycanbiosynthesis
Phenylpropanoidbiosynthesis
Histidinemetabolism
Cellcycle_Caulobacter
Translationproteins
Folatebiosynthesis
PantothenateandCoAbiosynthesis
Valine_leucineandisoleucinebiosynthesis
Drugmetabolism_otherenzymes
Polyketidesugarunitbiosynthesis
Peroxisome
Glycosaminoglycandegradation
Cyanoaminoacidmetabolism
Glycosphingolipidbiosynthesis_ganglioseries
Nicotinateandnicotinamidemetabolism
Aminoacidrelatedenzymes
Proteinexport
Mismatchrepair
Phenylalanine_tyrosineandtryptophanbiosynthesis
Streptomycinbiosynthesis
Translationfactors
Energymetabolism
Onecarbonpoolbyfolate
Alanine_aspartateandglutamatemetabolism
Poresionchannels
Glycine_serineandthreoninemetabolism
DNAreplication
Chaperonesandfoldingcatalysts
Lipopolysaccharidebiosynthesis
Methanemetabolism
Glycosphingolipidbiosynthesis_globoseries
Lysosome
Homologousrecombination
Chromosome
Sphingolipidmetabolism
Aminosugarandnucleotidesugarmetabolism
Lipopolysaccharidebiosynthesisproteins
Oxidativephosphorylation
Purinemetabolism
Membraneandintracellularstructuralmolecules
Galactosemetabolism
Peptidases
DNAreplicationproteins
DNArepairandrecombinationproteins
Otherglycandegradation
Ribosome
Pyrimidinemetabolism
−4 −3 −2 −1 0 1 2 3 4
LDA SCORE (log 10)
B
WBE
HFHS
Lipopolysaccharidebiosynthesisproteins
Lipopolysaccharidebiosynthesis
Membraneandintracellularstructuralmolecules
Otherglycandegradation
Functionunknown
Bacterialsecretionsystem
Oxidativephosphorylation
Sphingolipidmetabolism
Replication_recombinationandrepairproteins
Lysosome
Transcriptionmachinery
Cellmotilityandsecretion
Proteinfoldingandassociatedprocessing
Ubiquinoneandotherterpenoid_quinonebiosynthesis
Glycosaminoglycandegradation
Glycine_serineandthreoninemetabolism
Glycosphingolipidbiosynthesis_globoseries
Chaperonesandfoldingcatalysts
Folatebiosynthesis
Glycosphingolipidbiosynthesis_ganglioseries
Steroidhormonebiosynthesis
Benzoatedegradation
Bacterialchemotaxis
Porphyrinandchlorophyllmetabolism
Sporulation
Transcriptionfactors
Bacterialmotilityproteins
−3 −2 −1 0 1 2 3
LDA SCORE (log 10)
C
F1
HFHS
Bacterialsecretionsystem
Citratecycle_TCAcycle_
Oxidativephosphorylation
Cellmotilityandsecretion
Ubiquinoneandotherterpenoid_quinonebiosynthesis
Biosynthesisofunsaturatedfattyacids
Inorganiciontransportandmetabolism
Purinemetabolism
Folatebiosynthesis
Toluenedegradation
Arginineandprolinemetabolism
RNAdegradation
Metabolismofcofactorsandvitamins
Fattyacidbiosynthesis
Phenylpropanoidbiosynthesis
Drugmetabolism_otherenzymes
Cyanoaminoacidmetabolism
Starchandsucrosemetabolism
Porphyrinandchlorophyllmetabolism
Bacterialchemotaxis
Sporulation
−3 −2 −1 0 1 2 3
LDA SCORE (log 10)
D
F2
HFHS
Otherglycandegradation
Pentoseandglucuronateinterconversions
Basaltranscriptionfactors
Stilbenoid_diarylheptanoidandgingerolbiosynthesis
Carbohydratemetabolism
Selenocompoundmetabolism
Butanoatemetabolism
−3 −2 −1 0 1 2 3
LDA SCORE (log 10)
E
F3
HFHS
Functionunknown
Proteinfoldingandassociatedprocessing
Cellmotilityandsecretion
Carbohydratemetabolism
Synthesisanddegradationofketonebodies
Plant_pathogeninteraction
Lysinebiosynthesis
Thiaminemetabolism
Bacterialchemotaxis
Flagellarassembly
Bacterialmotilityproteins
−3 −2 −1 0 1 2 3
LDA SCORE (log 10)

Figure S5. LEfse analysis of fecal microbial functional profiles between HFHS-fed mice and wild blueberry polyphenols treated mice.

LDA scores for the bacterial taxa differentially abundant between HFHS-fed mice, WBE and BPF: anthocyanin and phenolic acids (F1), oligomeric PACs, phenolic acids flavonols (F2) and polymeric PACs (F3). Positive and negative LDA scores indicate the bacterial taxa enriched in A) WBE-fed mice vs HFHS, B) F1-fed mice vs HFHS, C) F2 vs HFHS and D) F3 vs HFHS. Only the taxa having a $p < 0.05$ (Wilcoxon-Mann Whitney rank-sum test) and LDA >2.0 are shown in the figure legend.

CHAPTER III

We previously demonstrated, using *in vivo* models, the role of polyphenols to modulate the gut microbiota and attenuate metabolic and intestinal disorders induced by a HFHS-diet in mice. The chapter I, confirmed the selective prebiotic effect of cranberry and blueberry polyphenol-rich powders on *A. muciniphila* as compared to the fibrous fractions from the same fruit. Additionally, it was demonstrated the role of polyphenol-enriched diets to significantly inhibit opportunistic pathobionts associated to diet-induced obesity, and to promote symbiotic bacteria, bearing positive outcomes in the host. Subsequently, in the chapter II, we identified the phenolic category responsible for the stimulation of *A. muciniphila* and showed that it restored the ecological niche of this bacterium. Particularly, the polymeric PACs enriched fraction were shown to increase the number of colonic mucin-secreting goblet cells and restore the mucus layer in mice fed an obesogenic diet; but this fraction contributed as well to lower the glycemic level. All those outcomes, including the crucial role of polyphenols to inhibit pathobionts and stimulate symbionts, led us to delve into an *in vitro* experiment to study the transcriptional response of this bacterium to polyphenols. We surmise that the antimicrobial properties of polyphenols are an important factor to modulate the gut microbial communities and that such impact might be species-specific. It is also worthy to note that *A. muciniphila* has been shown to be resistant and predominate the gut microbiota upon the administration of broad-spectrum antibiotics. In the present work, we use cranberry as a rich source in phenolic acids, anthocyanidins and A-type PACs, to evaluate the effects of polyphenolic fractions on the expression of genes linked to mechanisms of bacterial resistance and adaptation to antimicrobials in *A. muciniphila*. Particularly, cranberry A-type PACs are well known for inhibiting pathogens by membrane-based perturbations, and affecting bacteria cell adhesion and metabolism, among other mechanisms. To elucidate whether cranberry phenolics might induce distinct genetic and phenotypic response on *A. muciniphila,* a comparable approach to that applied in the murine model presented in the chapter II was followed. Three polyphenolic sub-fractions: F1) phenolic acids and anthocyanidins, F2) oligomeric PACs and flavonols, and F3) polymeric PACs, were added to a mucin-rich culture medium at the same concentration as found in the total cranberry extract supplemented medium. The present manuscript, prepared for publication in the scientific journal *Cell,* uncovers the *Akkermansia's* capacity to resist cell wall

attack and induce antibiotic cross-resistance mechanisms to overcome the flavonoids inhibitory effects; we particularly highlight the significant stimulation of EPS and CPS by polymeric PACs, which might have beneficial immunomodulatory implications in the host. In addition, we reveal that the Urolithin A, a microbial phenolic metabolite shown to correlate with a higher *Akkermansia* proportion, especially stimulated the growth of this bacterium, as well as induced the formation of a thick CPS. Given the originality of those findings, the present research article, which remains confidential, was peer evaluated and considered potentially patentable. Currently, further studies on the induction and production of CPS/EPS in *A. muciniphila* by using cranberry polyphenolic fractions are being performed.

Polyphenolic fractions induce capsular exopolysaccharide biosynthesis and antibiotic-resistance molecular mechanisms in *Akkermansia muciniphila*

María Carolina Rodríguez Daza,[a b *] Denis Roy,[a b *] and Yves Desjardins[a b *]

[a] *Food Science Department, Faculty of Agriculture and Food, Laval University, Québec, QC, Canada.*
[b] *Institute of Nutrition and Functional Foods (INAF), Laval University, Québec, QC, G1V 0A, Canada*

Correspondence: maria-carolina.rodriguez-daza.1@ulaval.ca (M.C.R.), Denis.Roy@fsaa.ulaval.ca (D.R.), yves.desjardins@fsaa.ulaval.ca (Y.D.)

Article prepared to be submitted to the scientific journal *Cell*

Résumé

Les polyphénols sont associés à la prolifération d'*Akkermansia muciniphila (Akk),* une bactérie intestinale montrant des propriétés anti-obésité et ayant la capacité de maintenir la muqueuse en santé. Dans cette étude, les caractéristiques phénotypiques, génotypiques, ainsi que de la croissance de cette bactérie ont été évaluées afin de déterminer les mécanismes sous-jacents aux effets prébiotiques induits par les polyphénols. L'analyse de l'expression des gènes a révélé que le locus codant la protéine H des exopolysaccharides (*EpsH* Amuc_1470) ainsi que la protéine de biosynthèse d'exopolysaccharide capsulaire (CPS) (Amuc_1413) étaient induits chez *Akk* cultivée par l'extrait de canneberge - la fraction riche en flavan-3-ols - et par l'urolithine A, un métabolite polyphénolique. L'analyse par microscopie électronique à transmission des cellules traitées par les extraits polyphénoliques a montré une couche de CPS plus épaisse que celle des cellules témoins. Les polyphénols ont induit chez *Akk* l'expression d'un transporteur de type ABC-2 probablement impliqué dans la sécrétion des exopolysaccharides. La croissance d'*Akk* n'a pas été inhibée par des fractions polyphénoliques antimicrobiennes. Nous suggérons que la production des CPS/EPS et les stratégies moléculaires liées à la résistance aux antibiotiques confèrent à *Akk* un avantage concurrentiel pour coloniser l'écosystème colique en présence de flavonoïdes. Cette étude identifie les mécanismes bactériens impliqués dans l'augmentation induite par les polyphénols des populations d'*Akk*, une bactérie associée à l'amélioration des phénotypes cardiométaboliques.

Mots clés : *Akkermansia muciniphila*, exopolysaccharides capsulaires, antimicrobiens, polyphénols, flavonoïdes, transporteur de type ABC 2, mécanismes d'adaptation moléculaire.

Abstract

Dietary polyphenols induce bloom of *Akkermansia muciniphila (Akk),* a gut bacterium associated to anti-obesity and healthy mucosa phenotype. Here, the growth, phenotypic and genotypic features of this bacterium were evaluated to uncover mechanisms underlying polyphenols-induced prebiotic effects. RT-qPCR analysis revealed that the exopolysaccharides locus protein-H (*EpsH* Amuc_1470) and the capsular exopolysaccharide (CPS) biosynthesis protein (Amuc_1413) were significantly upregulated in *Akk* grown under cranberry extract, flavan-3-ols-rich fraction, and microbial polyphenolic metabolite urolithin A. Transmission electron microscopy analysis of ruthenium red-treated cells exhibited a thicker CPS layer than control cells. Polyphenols induced ABC 2-type transporter complex involved in exopolysaccharides secretion. *A. muciniphila's* growth was not inhibited by antimicrobial polyphenolic fractions. We suggest that CPS-EPS apparatus and antibiotic-related molecular strategies confer *Akk* a microbial competitive advantage for colonizing the colonic ecosystem in presence of flavonoids. This study provides insights on tentative mechanisms by which polyphenols trigger *Akk* bloom linked to improved cardiometabolic phenotypes.

Keywords: *Akkermansia muciniphila*, capsular exopolysaccharides, antimicrobial, polyphenols, flavonoids, ABC 2-type transporter, molecular adaptation mechanisms.

Polyphenolic fractions induce capsular exopolysaccharide biosynthesis and antibiotic-resistance molecular mechanisms in *Akkermansia muciniphila*

Graphical abstract

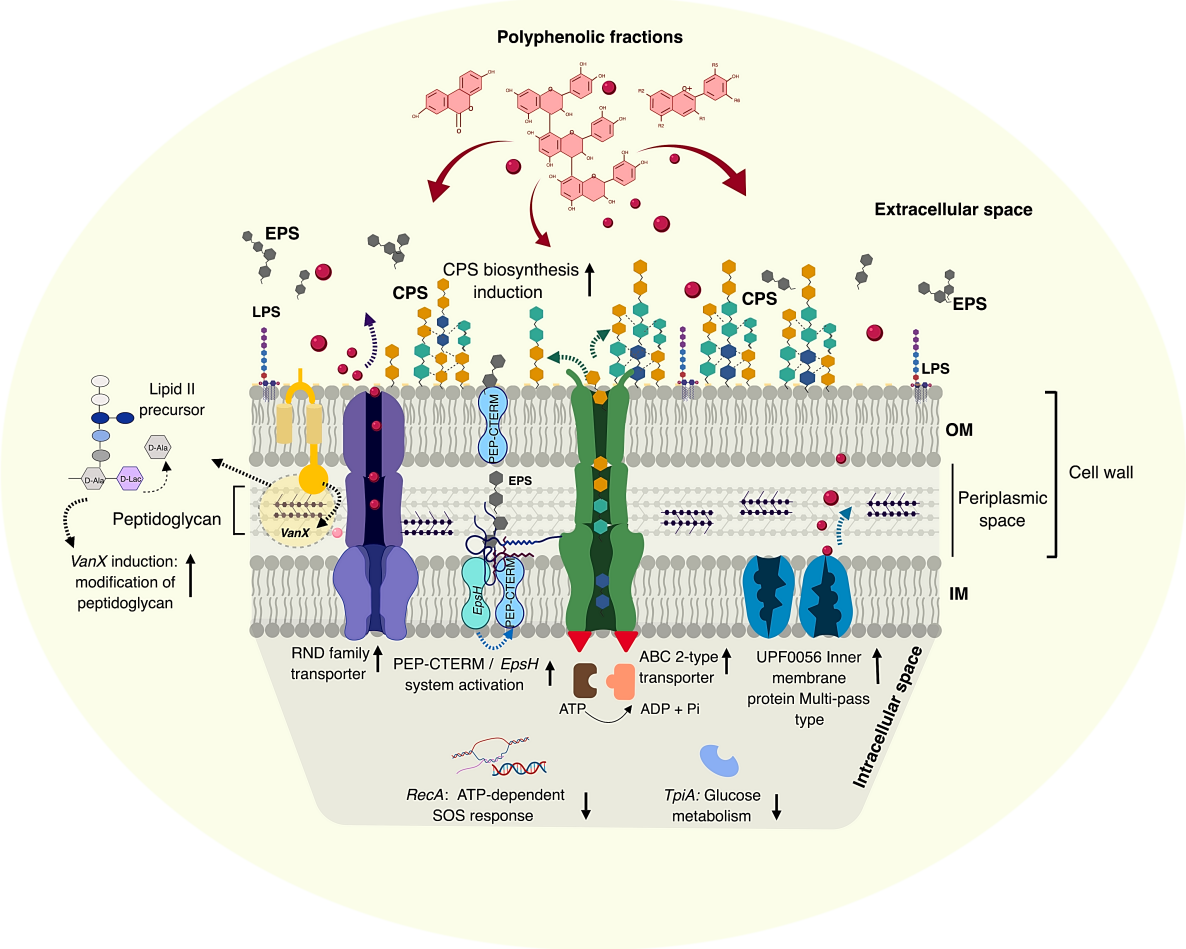

Authors

María-Carolina Rodríguez-Daza, Denis Roy, and Yves Desjardins

Correspondence

yves.desjardins@fsaa.ulaval.ca

maria-carolina.rodriguez-daza.1@ulaval.ca

In brief

The antimicrobial properties of dietary polyphenols modulate *A. muciniphila* fecal abundance. Rodríguez-Daza et al. provide evidence of *Akkermansia*'s molecular adaptation mechanisms to specific polyphenolic fractions. The induction of cell wall protection strategies and changes in metabolic and stress adaptation explain *A. muciniphila* bloom observed when adding polyphenols to culture media.

Highlights

- Polyphenolic fractions induce *A. muciniphila* to form capsular polysaccharide (CPS)
- *A. muciniphila* significantly activate the polysaccharide sorting system PEP-CTERM/EpsH
- Transmembrane RND family, and multi-pass efflux pumps are upregulated
- *A. muciniphila* increases *VanX* expression involved in peptidoglycan modification

Introduction

Dietary polyphenols are bioactive molecules displaying numerous biological properties. Among them, flavonoids have high antioxidant capacity, anti-inflammatory and antimicrobial activities (Esposito et al., 2014; Ma et al., 2018; Xie et al., 2014). In particular, owing to their antimicrobial action and their limited absorption in the small intestine (Clifford, 2004), flavonoids have been shown to potently modulate the colonic microbiota composition (Mosele et al., 2015).

Flavonoids can selectively inhibit gut pathogenic bacteria and stimulate symbiotic and probiotic bacteria, contributing to the amelioration of dysbiosis-associated disorders (Anhê et al., 2014; Jiao et al., 2019). Specifically, *Akkermansia muciniphila,* a Gram-negative mucus-living bacterium (Derrien et al., 2004), is stimulated by cranberry proanthocyanins-rich extract and other fruit polyphenols (Anhê et al., 2014; Henning et al., 2017; Masumoto et al., 2016; Morissette et al., 2020; Rodríguez-Daza et al., 2020), as well as, by the ellagitannin microbial metabolite urolithin A (Li et al., 2015a). Moreover, blooms of *A. muciniphila* have been associated with improved gut barrier function and cardiometabolic parameters (Everard et al., 2013). *A. muciniphila* thus appears to mediate the beneficial effects of polyphenols on host's metabolism and immunity. However, the mechanisms underlying such polyphenols-induced effects on *A. muciniphila* remain unclear and poorly studied.

It is well known that the antimicrobial activities of polyphenols, such as PACs and gallotannins are attributable to both the inactivation of membrane-bound proteins and to their affinity to mineral micronutrients including iron and zinc via chelation with metals (Tamura et al., 2016). Accordingly, the molecular adaptability and capacity of bacteria to attenuate the antimicrobial effect of polyphenols partly explain how these compounds modulate the microbiota composition. Indeed, bacteria exposed to polyphenols can up-regulate the expression of genes involved in cell wall protection and to nutrient limitations (Reverón et al., 2013; Tamura et al., 2016). Likewise, bacterial genes involved in nucleotide transport and metabolism, energy production and conversion, as well as, transcription–translation processes can be significantly affected by polyphenols (Curiel et al., 2011; Xue et al., 2016).

The capacity of bacteria to adapt to polyphenols may explain how they compete to occupy specific ecological niches. For instance, *Lactobacillus* spp. has the ability to metabolize polyphenols through the action of tannase, gallate decarboxylase, galloyl-esterase, and benzyl alcohol dehydrogenase enzymes (Jiménez et al., 2013; Reverón et al., 2013; Tabasco et al., 2011), conferring it the advantage to colonize the colon after polyphenols intake. Moreover, in Gram-negative bacteria, antibiotic-induced genetic responses may provide cross-resistance against polyphenols antimicrobial activity. The *mdtABCD* operon of *Escherichia coli*, which encodes a multidrug transport system, was significantly up-regulated in response to procyanidins, a phenomenon that explains the tolerance of the bacteria to condensed tannins (Zoetendal et al., 2008). Modification of the cell shape of bacteria exposed to high molecular weight polyphenols support the hypothesis that they interact with the cell surface and alter the integrity of the cell wall as antibiotics do (Lacombe et al., 2010b; Lacombe et al., 2012). The capacity of bacteria to induce cell wall protection mechanisms appears critical to their ability to resist to antimicrobials. Particularly, the production of extracellular polysaccharides (EPS) and capsule by bacteria have been shown to cope membrane damage by polyphenols. For instance, *Streptococcus gallolyticus* was resistant to condensed tannins (gallic acid derivatives) by producing EPS (Krause et al., 2005).

One of the reasons explaning the bloom of *A. muciniphila* in response to antimicrobials like polyphenols and antibiotics, is its capacity to induce defence mechanisms allowing it to withstand the imposed stress. Indeed, *A. muciniphila* was found to be the dominant species after vancomycin oral treatment in non-obese diabetic (NOD) mice (>80%) (Hansen et al., 2012) and its growth was spurred after the consumption of broad-spectrum antibiotics in humans (Dubourg et al., 2013). Unsurprisingly, the genome of *Akkermansia* harbours numerous antibiotic resistance genes (Caputo et al., 2015; Guo et al., 2017a; van Passel et al., 2011b) some of which may also confer the capacity to overcome polyphenols-induced cellular disturbances. Likewise, *Akkermansia*'s genome is positive for the PEP-CTERM proteins sorting systems, associated to exopolysaccharide production (the *EpsH* gene encoded by Amuc_1470*,* an exopolysaccharide locus protein H, and a family of the genes of EPS biosynthesis encoded by Amuc_1413 and Amuc_2077) (Ottman et al., 2016; van Passel et al., 2011b), which might be regulated as strategies to provide protection.

Research on prebiotic-like effects of polyphenols on *A. muciniphila* has mainly evaluated changes in its fecal abundance in preclinical and clinical models. This study is thus aimed to understand the molecular response of *A. muciniphila* to flavonoids in absence of confounding factors that take place in a competitive microbial community pool. This knowledge may provide innovative approaches to promote its persistence in the colon.

The objective of the present study is to elucidate the molecular adaptation of *A. muciniphila* to tannins-rich extract and a cranberry extract rich in phenolic acids, anthocyanidins, flavonols and flavan-3-ols. Quantitative reverse transcription PCR (RT-qPCR), scanning electron microscopy (SEM) and transmission electron microscopy (TEM) analyses were performed to evaluate the growth, genotypic, and phenotypic response of *A. muciniphila*. We focused on the evaluation of genes coding for products involved in capsular and exopolysaccharide (EPS) biosynthesis, polysaccharide-related transporters, vancomycin resistance gene, efflux pumps membrane transporters, and metabolism.

Results

Phenolic characterization of cranberry extract, polyphenolic fractions and tannin-rich extract TAN-active

The polyphenolic characterization of the cranberry extract is shown in the supplementary information **Table S1**. 600 mg of CE per liter of broth provided 192 mg of total polyphenols, including 74.2 mg of flavonoids. The polyphenolic fraction F1 (221 mg/L) provided 12.48 mg of flavonoids; the fraction F2 (381 mg/L) provided 47.06 mg of flavonoids; and the fraction F3 (115 mg/L) provided 34.22 mg of flavan-3-ols. The high concentration (H) of CE (CE-H) delivered 766.29 mg of total polyphenols per liter of broth from which 296.81 mg were flavonoids. A high concentration of F3 (F3-H, 460 mg/L) provided 136.47 mg of flavan-3-ols. The tannin-rich extract TAN-active (143 mg/L) extract was composed by 83.57 mg of flavan-3-ols (**Figure S1**). The proanthocyanins content of the TAN-active is presented in the supplementary information **Table S2.**

The growth of *A. muciniphila* was not inhibited by the presence of flavonoids but was enhanced by the polyphenolic microbial metabolite Urolithin A

The presence of the total CE and the polyphenolic fractions showed no inhibitory effects on the growth of *A. muciniphila* (supplementary information **Figure S2**). However, likely due to the high concentration of oligomeric proanthocyanins (78 mg/L), the TAN-active extract had some growth-reducing effects, but it was not statistically significant ($p=0.0904$).

Considering the strong correlation of the polyphenolic metabolite Urolithin A (Uro-A) with *Akkermansia's* fecal abundance in humans (Li et al., 2015a), we decided to evaluate whether this metabolite was exerting a direct stimulatory effect on *A. muciniphila* through *in vitro* culture assays. Interestingly, the presence of Uro-A in the culture broth stimulated *A. muciniphila* growth; the proportion of viable cells represented 167.31% ($p < 0.05$) compared to BHI-Muc control broth (normalized to 100%).

A. muciniphila enact a cell-defence molecular repertoire during the first 24 hours of growth as adaptation mechanisms to polyphenolic fractions

To examine the primary response of *A. muciniphila* during the exponential growth phase as an adaptation to the environmental changes induced by polyphenols, the genetic profile was compared between cells harvested from the same treatment at 24h and 30h after incubation. In addition to the analysis of *Akk*-cells submitted to cranberry polyphenolic fractions, the gene expressions of cells exposed to vancomycin were evaluated as a reference treatment of an antimicrobial agent targeting the bacterial membranes (Turner et al., 2013). Statistical analysis indicated that the fold change of gene expressions involving in antibiotic-related defence mechanisms diminished at 30h of culture compared to 24h (**Figure 1**).

Genes associated with bacterial resistance to antibiotic cell disturbances at the membrane level were significantly upregulated. In the case of vancomycin-treated cells (VAN), the expressions of the gene coding for the inner membrane protein (Amuc_1018), the efflux transporter resistance-nodulation-cell division (RND) family (Amuc_0889), and the D-alanyl-D-alanine dipeptidase

(*VanX*, Amuc_1627) were significantly lower at 30h than at 24h of incubation ($p<0.0001$). However, they were still considerably upregulated relative to the BHI-Muc control ($p<0.001$), indicating that it was necessary to keep the molecular cell-protection mechanisms to allow the cell to survive (**Figure 1-A**). Conversely, two genes related to the exopolysaccharide biosynthesis (*EpsH* Amuc_1470 and polysaccharide export protein Amuc_2077), as well as a gene related to DNA repair process (protein *RecA,* Amuc_0663) were down regulated at 30h compared to cells grown in the BHI-Muc control.

The *A. muciniphila* genetic profile at 30h of culture changed depending on the polyphenolic fraction present in the media. Notably, at 30h of growth, the F1-treated cells had a decreased expression of the inner membrane protein (Amuc_1018) and of the efflux transporter RND family (Amuc_0889) compared to the control level (**Figure 1-B**). However, like the VAN treatment, the F1 induced the downregulation of the exopolysaccharide related genes (Amuc_1470 and Amuc_2077), as well as the DNA metabolic process (*RecA* Amuc_0663) ($p<0.0001$).

Polymers of PAC appeared to elicit a stronger antimicrobial response on *Akk* cells versus smaller polyphenols such as PACs monomers and dimers. The results obtained herein show that the inner membrane protein and the multidrug efflux membrane transporter (Amuc_1018 and Amuc_0889), both involved in antibiotic resistance, diminished at 30h compared to 24h in F2 and F3 supplemented media, but they were significantly kept 2-fold higher than the *Akk*-control cells at the same growth phase ($p<0.01$) (**Figure 1 C-D**). In addition, a gene involved in energy metabolism (Glutamate dehydrogenase, Amuc_2051) was significantly down regulated at 30h of growth in presence of both F2 and F3 fractions ($p<0.05$ compared to control). Interestingly, only the F3 induced the expression of glyceraldehyde-3-phosphate dehydrogenase implicated in the glycolysis pathway (*Gapdh,* Amuc_1417*,* $p<0.01$ compared to control) and the polysaccharide transport protein (Amuc_2077*,* $p<0.0001$ compared to control) at 30h*,* suggesting that *A. muciniphila* activates additional molecular machinery for the exopolysaccharide slime secretion, a strategy allowing it to maintain growth in the presence of high molecular weight polyphenols.

A. muciniphila displays antibiotic-related molecular adaptation to the presence of polyphenolic fractions

Once established that *A. muciniphila* displayed a substantial transcriptional shift during the first 24h of contact with polyphenolic fractions, we analyzed the differential expression of those specific genes during that period of growth. Surprisingly, the *Akk*-cells grown in F1-supplemented broth exhibited 6-fold higher the expression of both the UPF0056 inner membrane protein (Amuc_1018) and the efflux transmembrane transporter RND family (Amuc_0889) compared to the untreated *Akk*-cells ($p<0.01$) (see **Figure 2 A-B**). Although the same genes were stimulated by other polyphenolic treatments, this stimulation was not statistically significant.

The Uro-A also induced the expression of efflux transmembrane transporter RND family (5.7-fold compared to control, $p<0.05$). Since, the Uro-A stimulated the number of viable *Akk*-cells (CFU/mL), the importance of this type of transmembrane transporter should be elucidated. Aside from the CE-H, the F3-H and the Uro-A, all the polyphenolic fractions, including the TAN-active extract, significantly induced the expression of the *VanX* gene (**Figure 2-C**), suggesting that polyphenols may act at the membrane level, targeting cell wall biosynthesis and reparation.

The polyphenolic fraction F3 induces, in a dose-dependent manner, the expression of capsular exopolysaccharides biosynthesis and putative exopolysaccharide locus protein-H *(Eps-H)* in *A. muciniphila*

In addition to the total CE and F3 fraction, the latter was also evaluated at a higher concentration. In this case, both treatments significantly induced the biosynthesis of capsular exopolysaccharide (Amuc_1413); it was 2-fold higher than for the BHI-Muc grown cells ($p<0.05$) (**Figure 3-A**). Surprisingly, along with the Uro-A (5.2-fold), only the CE-H and the F3-H substantially increased the *Eps-H* by 6.0 and 7.4-fold respectively relative to the *Akk*-cells cultured in the BHI-Muc ($p<0.001$ and $p<0.0001$ respectively compared to control) (**Figure 3-B)**. Moreover, the ABC-2 type transporter was up-regulated by all polyphenolic fractions ($P<0.01$) (**Figure 3 C**). This type of transporter has been involved in capsular polysaccharide export system,

but it belongs to a family of inner membrane proteins. Therefore, the increased expression of Amuc_1379 can be attributed to *A. muciniphila* response to the antimicrobial action that polyphenolic compounds and the vancomycin antibiotic exert at the bacterial membrane level.

Genes down regulated by polyphenolic fractions in *A. muciniphila* are involved in glycolytic and DNA metabolic processes

Genes involved in bacterial metabolism and DNA damage were examined to assess whether *A. muciniphila* could modulate energy requirements in presence of polyphenols. RT-qPCR analysis of the metabolic response of *A. muciniphila* to polyphenols during the exponential growth phase pointed to flavan-3-ols as down regulating the most carbohydrate metabolism. The F2 and F3-H induced a respective 0.87-fold and 0.8-fold lower expression of triosephosphate isomerase enzyme *(tpiA)* involved in both glycolysis and gluconeogenesis pathway ($p<0.05$ compared to BHI-Muc grown control cells) (**Figure S3-C**).

The *RecA* was analyzed to evaluate whether polyphenols could interfere with the DNA integrity. This gene is upregulated in response of a direct DNA damage, or indirectly from metabolic and oxidative stress, activating a SOS system to induce DNA repair and conferring resistance to stress (Alam et al., 2016a). Our result showed a down regulation of *RecA* (Amuc_0663) ranging from 0.7 to 0.98-fold less ($p<0.0001$ compared to BHI-Muc grown control cells) (**Figure S3-D**) in cell grown with the polyphenolic fractions. Altogether, the decreased expression of *RecA* and *tpiA* pathways in *Akk* cells are indicative of the shift of energy metabolism and survival response against a polyphenol-induced stress.

SEM and TEM analysis reveal different cell wall surface features and confirm the formation of capsular exopolysaccharides in *A. municiphila* submitted to polyphenolic fractions

SEM and TEM were used to evaluate the phenotypic features that *A. muciniphila* may exhibit in presence of polyphenolic fractions. SEM clearly show that *Akk*-cells grown in the BHI-Muc control broth displayed their typical morphology with smooth and rounded surfaces. Since the *Akk*-

cells were harvested in the exponential growth phase (overnight culture), dividing cells were frequently observed (**Figure 4-A**). In the case of the VAN-supplemented broth, the micrographs demonstrated that this antibiotic targeted the bacterial cell wall. The *Akk*-cells had a rough partially wrinkled surface, and a tendency to be of larger cellular size, known as cell elongation (**Figure 4-B**).

In contrast, the total CE showed no substantial effect on *A. muciniphila* phenotype, presenting a regular cellular size and morphology compared to control (**Figure 4-C**). However, after incubating with the F1 fraction of the total CE, *Akk*-cells were of irregular shape with a wrinkled surface (**Figure 4-D**). *Akkermansia's* cellular morphology was not altered when cultured with F2 fraction. Cell divisions were also observed (**Figure 4-D**). Interestingly, the *Akk*-cells submitted to F3 fraction were surrounded by a considerable layer of mucous slime (**Figure 4-E**). Though the F3 presence in the culture media did not affect the *A. muciniphila* cellular division, it induced cellular elongation.

We further carried out TEM observations to study the capsular exopolysaccharide formation (CPS) and to detect possible differences at the ultrastructural level between the *Akk*-cells grown in the BHI-Muc control broth and those *Akk*-cells grown under polyphenolic fractions. The differences in the formation and stability of the polysaccharide-rich protective layer around the cells were clearly demonstrated after they were stained with ruthenium red and osmium tetroxide. The visualization by TEM of ultrathin sections prepared from cells harvested after overnight cultures showed changes in the density and in the cohesion of the polysaccharide-rich layer at the *Akk*-cells surface (**Figure 5**). *A. muciniphila* cells grown in the BHI-Muc control broth had an intact cell wall, and the characteristic double compartmentalization, enclosed by a thick exopolysaccharide-rich layer of fibrous appearance (51.0 ± 3.2 nm) (**Figure 5-A**).

The outline of the double cell membrane and the CPS were clearly reduced in the *Akk*-cells submitted to the VAN-antibiotic (25.7 ± 4.3 nm) (**Figure 5-B**). Similarly, the supplementation with the total CE resulted in partial depletion of the CPS in most of the cells (**Figure 5-C**). The F1-enriched broth elicited a disperse but fuzzy CPS (23.7 ± 4.3 nm) compared to the BHI-Muc grown *Akk*-cells (**Figure 5-D**). In contrast, the cell treated with F2 showed an increased CPS

thickness (63.0 ± 2.6 nm); this loosely meshed polysaccharides-rich material was, however, scattered in the outside media, forming a slime polysaccharide layer (**Figure 5-E**). The F3 fraction used at low concentration showed to affect the typical cell wall phenotype of *A. muciniphila*. A partial cellular degradation and envelope disruption were evident in the cells, probably as a consequence of the observed diffused CPS around the cells. In this case, the ruthenium red stained a dispersed, but fibrous non-adherent exopolysaccharides slime to the cell wall (**Figure 5-F**). When a high concentration of the cranberry extract CE-H and F3-H were added to the culture media, *Akk*-cells secreted a thicker CPS layer, being 86.7 ± 11.2 nm and 67 ± 5.6 nm respectively (**Figure 5 G-H**). Interestingly, the *Akk*-cells grown with the microbial metabolite Uro-A presented the highest density of CPS layer with 108.7 ± 8.0 nm, compact around the cell (**Figure 5-I**).

Discussion

Cellular elongation and preserved growth are indicative of *Akkermansia'*s antimicrobial adaptation to polyphenolic fractions

Within the colonic microbial communities, *A. muciniphila* was shown to be stimulated by the administration of a range of dietary polyphenolic extracts and antibiotic therapies in both humans and animals. The antibiotics impact the colonization of commensal bacteria and perturb the microbial capacity to occupy intestinal niches and harvest nutrients (Modi et al., 2014). Additionally, the iron scavenging properties and the membrane-protein affinity of antimicrobial polyphenols can reduce nutrient availability and affect bacteria membrane interactions (Tamura et al., 2016), depleting opportunist pathogens and modifying the microbial ecology. In this sense, *A. muciniphila* has the capacity to resist antimicrobials, adapt its metabolism, and prevent the invasion of virulent microbes by both outcompeting for space and mucous nutrients, and by inducing host defences of the colonic epithelium. This study clearly reveals the phenotypic cellular changes induced by polyphenols on *A. muciniphila*, including the ability to develop a polysaccharides-rich protective layer, and molecular features linked to cell-defence mechanisms to antimicrobials.

The degree of polymerization and consequently the number of hydroxyl groups have been the major factor associated with antibacterial activities of PACs (Rempe et al., 2017). They may interact with the cellular membrane and target the cell wall biosynthesis as shown by some antibiotics (Blair et al., 2014; Lacombe et al., 2013d; Tropini et al., 2014). *A. muciniphila* was able to grow not only under the presence of VAN, but also under the CE, F1, F2 and F3 enriched culture media. VAN-treated *Akk*-cells presented distinguishable cellular deformation from the typical short rods shape to long ones. Importantly, the F3 fraction induced similar cell elongation in *Akk*-cells, but they were surrounded by a recognizable loosely meshed mucous material. The cell elongation is an indicator of interferences in bacterial peptidoglycan biosynthesis, in some case regulating penicillin-binding proteins (PBPs), which lead to an elongated rod morphology. For instance, phase contrast microscopy revealed that *Bacillus subtilis* cells treated with EGCG displayed a specific morphological phenotype characterized by cell elongation (Nakayama et al., 2015). It was demonstrated that EGCG binds with various PBPs in *B. subtilis*, resulting in growth inhibition and cell elongation. However, in the case of *A. muciniphila*, inhibitory effects on growth were not observed. The SEM micrographs of VAN, CE and F1 treatments showed a partial disturbance of the cell surface and also showed high number of regular sizes of *Akk* dividing cells as observed in the control, which depicts the maintenance of constant growth rate under the polyphenols-induced stress. Once analyzed by TEM, *A. muciniphila* grown with VAN, CE, the fractions F1 and F3 displayed altered cell wall integrity. Our results are consistent with those of Lacombe et al. (2010b) who found that *E. coli* O157:57 treated with a cranberry extract, and in particular with anthocyanins and phenolic acids fractions, displayed a localized disintegration of outer membrane resulting in irregular shape cells. In our study, the F1 affected the cell wall surface regular morphology, but it did not affect vital functions, since *A. muciniphila* maintained cellular growth as compared to control.

Surprisingly, the presence of Uro-A was found to stimulate the *A. muciniphila* survival as compared to untreated control culture. The urolithin A is a metabolite from the colonic microbial degradation of ellagitannins and is considered a biomarker of a so-called urolithin metabotype A associated with reduced cardiometabolic risk (Li et al., 2015a; Tomás-Barberán et al., 2017). To our knowledge, this is the first *in vitro* assay of *A. muciniphila* culture with urolithin A, and the

first showing a promoted growth activity by this metabolite in *Akk*-cells pure culture. These findings are complementary to a recent study demonstrating the bloom of *Akkermansia* in the fecal microbiota of Urolithin-A-producer volunteers after the administration of ellagitannins-rich pomegranate extract using a TWIN-SHIME system (Garcia-Villalba et al., 2017). In that study, a positive correlation of *A. muciniphila* and the production of Uro-A was not found, but yet, this bacterium was significantly correlated with the co-occurrence of Uro-A producer gut microbes.

Gene expression analysis unravel mechanisms linked to phenotype changes in *A. muciniphila*

The RT-qPCR-analysis provided insights on the autonomous molecular response associated with metabolic functions and defence to antimicrobials by *A. muciniphila* exposed to polyphenolic fractions. Changes in cellular sizes and shapes have been linked to cell-wall molecular organization and architecture of peptidoglycan (UniProt KW-0961) (Turner et al., 2013). Thus, we measured the gene coding for D-alanyl-D-alanine dipeptidase (*VanX,* Amuc_1627) in *A. muciniphila.* Although vancomycin is an antibiotic usually targeting the peptidoglycan-rich layer in Gram-positive bacteria, the genome of *A. muciniphila*, a gram-negative bacterium, harbour vancomycin-resistance gene cluster. Surprisingly, not only the cells grown in VAN-supplemented broth presented an increased relative expression of *VanX* gene, but this gene was also significantly increased in *Akk*-cells cultured under CE, F1, F2, F3 and TAN-active. Vancomycin inhibits the peptidoglycan crosslinking by binding to the D-Ala-D-Ala dipeptide of the lipid II precursor, blocking the transpeptidation reaction required for the cell wall synthesis (Lessard and Walsh, 1999). It is intriguing that *A. muciniphila* acquired a *VanX* enzyme, but this notion leads us to infer that the bacteria disposes of this machinery to modify its cell wall structure by replacing the terminal D-alanine, thus improving membrane rigidity under a stress condition. In Gram-negative bacteria, modifying the peptidoglycan crosslinks has been used as an important survival strategy under stress conditions (Lessard and Walsh, 1999). For instance, in *E. coli*, the homologous *VanX* is involved in D-Ala-D-Ala removal, necessary to peptidoglycan synthesis, from the periplasm back to the cytoplasm. In the cytoplasm, the D-Ala-D-Ala terminus was shown to be used by *E. coli* as a metabolic energy source to sustain the cell in nutritional starvation (Lessard and Walsh,

1999). In the case of *A. muciniphila*, the penetration of polyphenolic compounds across the outer membrane to access these peptides structures in the periplasm, could be further limited by the formation of CPS, but whether this bacterium may use the D-Ala-D-Ala terminus as an energy source under polyphenol-induced stress, remains to be explored.

In addition to the insights obtained by microscopic analysis, the RT-qPCR molecular response of *A. muciniphila* pointed to a marked induction of products involved in the capsular and slime exopolysaccharides proteins, with an important role in counteracting polyphenol inhibitory effects at the membrane level. We demonstrated that the CE-H, its derived F3-H fraction and the Uro-A induced the gene expression of *EpsH* (Amuc_1470). *EpsH* is a putative membrane protein based on its eight predicted transmembrane segments, forming the exopolysaccharide-associated protein sorting PEP-CTERM/EpsH system. *A. muciniphila* possess a PEP-CTERM positive genome, indicating that it has both an outer membrane (CPS) and exopolysaccharide (EPS) production genes. Interestingly, STRING analysis (Search tool for the retrieval of interacting genes, version 11.0 available online https//string-db.org) (Szklarczyk et al., 2015) demonstrated that the genes Amuc_1470 and Amuc_1413 have a high degree of connectivity (score 0.547), including neighborhood, cooccurrence and text-mining interactions, suggesting that both jointly contribute to polysaccharides complex secretion. The *EpsH* in *A. muciniphila* appears similar to *Methylobacillus* sp. 12S *EpsH*, a transpeptidase that belongs to the locus associated with biosynthesis of the exopolysaccharide methanolan, which is a heteropolymer composed of glucose, mannose and galactose residues (NCBI conserved protein domain family pfam09721, available online https://www.ncbi.nlm.nih.gov, Marchler-Bauer et al. (2017)). Both the CE-H and the F3-H fraction significantly stimulated the transcription of the CPS biosynthesis protein. This CPS protein (NCBI accession GenBank: ACD05236.1) presents a conserved domain that is typical of this proteins family involved in extracellular colanic acid exopolysaccharides synthesis (InterPro database IPR003856, IPR005700 and IPR005702), a polymer associated with the surfaces of a wide variety of bacteria and causes bacterial colonies to become extremely mucoid (Scott et al., 2019).

Induction of distinctive EPS-CPS phenotypes in *A. muciniphila* by polyphenolic fractions and immunomodulatory implications

The use of the F3-H fraction of the total CE-H, highlighted the role of flavonoids in selectively contributing to the expression of CPS-EPS related genes. Moreover, the *A. muciniphila* molecular response to F3 was dependent of the dose added in the culture media. Indeed, 34.22 mg of flavonoids induced 1.7 and 2.1-fold the gene expression of CPS biosynthesis protein and the *Eps-H* gene in *A. muciniphila*, but 136.47 mg (F3-H) induced their expression 2.12 and 7.4-fold higher expression relative to controls, a very statistically significant increase (see **Figure 3 A-B**). Therefore, the production of CPS clearly represents a strategy by *A. muciniphila* to insulate the cell wall from the interaction with polyphenols and to protect against stress conditions. Interestingly, a family 2 glycosyl transferase (Amuc_2081), another gene encoding function involved in CPS biosynthesis pathways was over-expressed by 1.8-fold, as a transcriptional adaptation against the presence of oxygen around *A. muciniphila* (Ouwerkerk et al., 2016a).

It is possible that the composition of the CPS-EPS glycoconjugates could be strongly related to the CPS density. The extracellular polysaccharides-rich envelop in *A. muciniphila* was more or less thick depending on the polyphenolic fractions to which it was exposed, being denser in F3 and Uro-A treated cells. In that context, it has been reported that the CPS profile may change according to the conditions of the bacterial habitat or to the xenobiotic substance they are exposed. For instance, polyphenols such as catechin and gallic acid have shown to influence the probiotic attributes of *Streptococcus thermophilus* CHCC 3534 through the CPS production. It was demonstrated that catechin adapted cells displayed higher amounts of CPS that the control cells, while gallic acid adapted cells showed a distinct CPS glycolytic profile (Khalil, 2010). We speculate that the different thickness and phenotypes of *A. muciniphila's* CPS such as the fuzzy, dispersed and the compact feature could relate to a different glycosylation pattern of this layer induced by the presence of specific polyphenolic fractions. Importantly, distinct CPSs profile has been shown to provide advantages in the gut environment, in face of various selective pressures, including antibiotic pressure, diet, and changing host immune responses in the gut symbiont *Bacteroides thetaiotaomicron* (Porter et al., 2017).

The CPS-EPS induction by polyphenolic fractions in *A. muciniphila* can have major applications in clinical studies. It is possible that the CPS-EPS secretion by *A. muciniphila* may improve the intestinal mucus layer viscosity, protecting the epithelium from opportunistic bacteria colonization. Here, the CPS-EPS induced by F3 and Uro-A in *Akk*-cells may represent a bridge connecting the immunomodulatory effects associated to *A. muciniphila* abundance after polyphenols intake reported from *in vivo* studies (Anhê et al., 2014; Derrien et al., 2011; Masumoto et al., 2016; Ottman et al., 2017b). Further analyses are needed after the isolation and characterization of *A. muciniphila* CPS-EPS found in the present study to elucidate their specific potential action on metabolic and immune host response by both *in vivo* and the culture of intestinal epithelial cells *in vitro*, since we know these glycoprotein complex have important roles in both microbial ecology and host physiology. The EPS, as well as, the CPS from other gut symbiotic Gram-negative bacteria such as *Bacteroides* species have shown the ability to directly act on multiple host immune cell types, modulating anti-inflammatory responses and influencing intestinal pathogens exclusion (Neff et al., 2016; Porter et al., 2017; Porter and Martens, 2015).

Ecological role of transmembrane transporters in resistance and cellular adaptation to polyphenols

Besides to the expression of CPS as membrane-related protection mechanisms, the efflux pumps and membrane transporters constitute the most ubiquitous strategy used by bacteria to resist to antimicrobial xenobiotics (Blanco et al., 2016). The gene Amuc_1379 an ABC 2-type transporter complex (UniProt B2UKT0_AKKM8) was up-regulated in *A. muciniphila* grown in the presence of all polyphenolic fractions, except in the *Akk*-cells grown in the Uro-A-supplemented broth. ATP-binding cassette (ABC) transporters participate in the export of molecules with remarkable structural diversity such as oligo- and polysaccharides (Cuthbertson et al., 2010). The permease protein is homologous to proteins encoded by a set of genes that comprise capsule polysaccharide export systems (UniRule UR000127467, source ID RU361157, available online https://www.uniprot.org/unirule) and they have been used by Gram-negative bacteria to translocate polysaccharides to the cell surface (Willis and Whitfield, 2013). Amuc_1379 shares similarities with *E. coli* inner membrane transport permease *YbhR* and with *B. subtilis* putative

transport permeases *YfiM* and *YfiN*, which contribute to drug transmembrane transport, cellular response damage stimulus (UniProtKB - P0AFP9), as well as, bacterial competition and biofilm formation functions (PubMed:28461449) (Stubbendieck and Straight, 2017). The blocking and down regulation of efflux pumps have been reported as an antibacterial action mechanism by plant polyphenols (Rempe et al., 2017). However, considering the inner-membrane location of this permease protein along with the CPS production in *A. muciniphila,* the polyphenols were expected to have reduced direct interactions with these types of transporters. Thus, the induced relative expression could be related to stress-responsive proteins inducing the secretion of a wide range of substances, including exopolysaccharides.

Although not all polyphenolic fractions significantly induced the expression of Amuc_1413 and Amuc_1470 CPS-EPS related genes and the exopolysaccharide exporter protein Amuc_2077, the ruthenium red stained exopolysaccharides-rich film either attached or not to *Akk*-cells. These findings lead us to hypothesize that *A. muciniphila* may employ ABC 2-type transporters as alternative modes of exopolysaccharides-translocation across the inner membrane to periplasm and cellular surface. Knockout of exopolysaccharides biosynthetic and transporter gene clusters in *A. muciniphila* could be an interesting approach to explore and uncover genes playing pivotal roles in mechanisms involved in CPS-EPS production and export machinery, which in the future, would be suitable for improving their yield. Other gut commensal microbes also take advantage of the different ABC transporters functions against antimicrobial compounds like polyphenols. For instance, Firrman et al. (2016b) found that *Ruminococcus gauvreauii* and *Bifidobacterium catenulatum* increased the expression of the ABC-transporter permease systems when grown with quercetin, but neither of these were increased in *Enterococcus caccae*. The up regulation of these particular genes by two of the gut commensal bacteria was related to their antimicrobial resistance to quercetin by rejecting this substrate out of the cells.

The RND transmembrane transporters family (Amuc_0889) and the inner membrane protein (Amuc_1018) known to confer multidrug resistance in both pathogenic and commensal bacteria (Alvarez-Ortega et al., 2013; Blanco et al., 2016), were significantly up-regulated in *A. muciniphila* cultured in F1-supplemented medium. As discussed above, the F1 fraction provoked a wrinkled cell surface and a fuzzy CPS, partially exposing the *Akk*-cells outer

membrane. *A. muciniphila* then, appears to operate these transmembrane transporters to pump the stressor-like agent phenolic compounds out from the cells. The anthocyanidins have been reported, among other polyphenols, to cause the formation of membrane pores and to increase cell permeability (Lacombe et al., 2013b). The increased expression of inner membrane protein is consistent with the irregular wall shape found in the *Akk*-cells grown in the F1-supplemented broth, suggesting that the flavonoids may be able to reach the periplasmic space.

Surprisingly, the efflux transmembrane transporter Amuc_0889 (RND family) was also up-regulated by Uro-A supplemented broth. Because the Uro-A exerted direct prebiotic effects on *A. muciniphila,* sustained by the increased cell viability and regular phenotype and the fact that it also up-regulated this multidrug efflux transporter drew our attention. Apart from these triggers, we do not know whether this microbial metabolite may promote other functional processes on *A. muciniphila.* Since the TEM images along with the increased expression of Amuc_1470 shed light on the formation of a thick CPS without apparent membrane damage, the urolithin A metabolite might act as a signalling molecule driving exopolysaccharides genetic apparatus in *A. muciniphila*. Further studies are needed to elucidate additional molecular responses of *A. muciniphila* induced by urolithin A. Whether the RND transporters may have primary functions in translocating the Uro-A into the *Akkermansia*'s intracellular space should be further investigated.

The increased transcription of RND-transporter is not only indicative of the active rejection of unwanted molecules from the cells, but it may also play a role in symbiotic bacterial-plant interactions at different levels, including host specificity and interspecies signal trafficking (Alvarez-Ortega et al., 2013; Blanco et al., 2016). This is interesting because the regulation of RND transporters in the gut ecosystem may intervene in symbiotic crosstalk between *A. muciniphila* and other gut commensal strains. Specifically, efflux transporter RND family, MFP subunit (Amuc_2041) and the outer membrane lipoprotein NodT family from RND efflux systems (Amuc_2043), predicted to primarily export small molecules rather than proteins, were down-regulated by *A. muciniphila* in co-culture with *Anaerostipes caccae* (Chia et al., 2018), perhaps needed to keep balancing competitiveness and ecological interactions for both bacteria. Here, the

transporter RND family was stimulated in the presence of Uro-A without apparent damage to the cells, indicating a balanced interaction between *A. muciniphila* and the urolithin-enriched media.

Moving beyond membrane-based mechanisms of antimicrobial resistance in *A. muciniphila*

Non-membrane adaptation mechanisms can also be a pivotal bacterial strategy to counteract the antimicrobial actions of flavonoids. The cytoplasmic proteins *tpiA* and *RecA* were down regulated by polyphenolic fractions. Metabolic response of *A. muciniphila* submitted to F3 during the exponential growth phase indicated down regulation of the carbohydrate metabolism system as directed by the *tpiA* enzyme. *TpiA* catalyzes the interconversion of dihydroxyacetone phosphate and glyceraldehyde-3-phosphate, which is required for both glycolysis and gluconeogenesis (UniRule: UR000079063, available online https://www.uniprot.org/unirule). Given that cell viability was not affected, we suggest that *A. muciniphila* manages the carbohydrate metabolic flux to mitigate the deleterious effect of flavonoids presence in the culture media. The development of distinctive energy generation mechanisms by this bacterium likely could provide clues to the factors explaining conserved growth. However, bacterial CPS biosynthesis may optimize cell energy expenditures by synthesizing CPSs similar in composition to glycans that the bacterium is used to metabolize (Porter et al., 2017).

Antimicrobial agents were reported to trigger the activation of the bacterial stress response (SOS response) by increasing the expression of *RecA,* acting in recombination and DNA repair (Cooper et al., 2018) (UniRule: UR000083075, https://www.uniprot.org/unirule). In this context, the DNA damage induces the relative transcript of *RecA* (Wang et al., 2016), thus, this gene is essential for increasing tolerance to antibiotic treatment. Respectively, the inhibition of *RecA*-associated SOS response has been reported to improve the bactericidal power of antibiotics, leading more sensitive the bacteria to cell death. Interestingly, a recent study demonstrated that bacteria mutants for the *RecA* SOS-system, were very sensitive to the inhibitory effects of tannic acid (Samoilova et al., 2019). These authors evaluated the effect of two polyphenols, notably tannic acid (TA) and gallic acid (GA), on the SOS-response and biofilm formation in a model of *E. coli* mutant for *RecA* and EPS production genes. In this study, the TA and GA increased the

EPS and biofilm formation in the wild-type *E. coli*, but it was 3-fold higher in *RecA* mutants. Particularly, the absence of *RecA* gene decreased the growth rate of *E. coli* in TA-enriched media, but in turn, this stimulated stress response pathways, especially the EPS secretion. Noteworthy, in case of *A. muciniphila*, while polyphenols down regulated *RecA* relative expression, they significantly increased the EPS biosynthesis as compared to untreated cells. The cytoplasmic *RecA* protein catalyzes the hydrolysis of ATP in the presence of single-stranded DNA (UniRule: UR000083075, gene ontology GO:0008094 https://www.uniprot.org/unirule). However, we demonstrated that this is not essential to maintain growth rates in *A. muciniphila* and that this bacterium expresses alternative adaptive pathways to cope the stress and DNA damage induced by polyphenols. Of note, the *RecA* SOS-system activation is not a primary mechanism to stimulate the EPS production in *A. muciniphila*. Likewise, the under-expression of bacterial SOS response relative to DNA damage is not a significant *modus operandi* by which polyphenols would inhibit *A. muciniphila* as has been demonstrated for its *E. coli* counterpart.

Conclusions

The present study provides a new understanding of the antimicrobial molecular adaptation of *A. muciniphila* to dietary polyphenols. The *in vitro* growth assays using specific polyphenolic fractions enabled us to unravel direct mechanisms to explain the prebiotic-like effects of flavonoids on the fecal abundance of *A. muciniphila.* This bacterium can adapt to the presence of polyphenols, not only by modulating cell wall protection and membrane stability, but also by interfering with intracellular metabolic process.

The antibiotic-related molecular responses may confer ecological benefits to *A. muciniphila* within the colonic microbiota, supporting its increased competitive colonization when dietary flavonoids are present. The induction in *A. muciniphila* of CPS, RND efflux pumps, and ABC 2-type transmembrane transporter, as defence mechanisms to antimicrobial polyphenolic fractions, provides added support for considering the use of these compounds as preventative dietary treatments. We suggest that *A. muciniphila* subjected to specific polyphenols causes the production of unique CPS and EPS, which may drive immunological response and host symbiotic interactions.

This work opens interesting research avenues for the use of dietary flavonoids to promote the EPS-CPS production in *Akk*-cells. The isolation of those glycoproteins would allow the exploration of direct biological and therapeutic benefits against gastrointestinal metabolic disorders by *in vitro* and *in vivo* systems.

Star methods

Key resource table

Contact for reagent and resource sharing

Experimental model and subject details

Polyphenolic fractions *A. muciniphila* culture conditions

Method details

Characterization of polyphenolic fractions

RNA isolation and cDNA synthesis

Target genes and quantitative reverse transcription PCR

Phenotypic analysis by scanning electron microscopy (SEM) and transmission electron microscopy (TEM)

Quantification and statistical analysis

Statistical analysis

Supplementary information

Supplemental Information includes three figures and three tables.

Author contributions

M.R.D., D.R and Y.D. conceived the study. M.R.D. designed and performed the experiments. M.R.D. analyzed the data and interpreted the results. D.R and Y.D. mentored and supervised this project. M.R.D. wrote this manuscript. All authors contributed to reviewing and editing the manuscript.

Acknowledgments

M.R.D was supported by the COLCIENCIAS PhD. scholarship. We thank Véronique Richard and Perrine Feutry from The Plant analysis laboratory at INAF-Laval University for the chemical analysis of the polyphenolic extracts.

Declaration of interest

The authors declare no competing interests.

References

Alam, M., Alhhazmi, A., DeCoteau, J.F., Luo, Y., and Geyer, R.C. (2016). *RecA* inhibitors potentiate antibiotic activity and block evolution of antibiotic Resistance. Cell Chemical Biology *23*, 381-391.

Alvarez-Ortega, C., Olivares, J., and Martínez, J.L. (2013). RND multidrug efflux pumps: what are they good for? Frontiers in Microbiology *4*, 7.

Andersen, C., Jensen, J., and Ørntoft, T. (2004). Normalization of real-time quantitative reverse transcription-PCR data: A model-based variance estimation approach to identify genes suited for normalization, applied to bladder and colon cancer data sets. Cancer Research *64*, 5245-5250.

Anhê, F.F., Roy, D., Pilon, G., Dudonné, S., Matamoros, S., Varin, T.V., Garofalo, C., Moine, Q., Desjardins, Y., Levy, E.*, et al.* (2014). A polyphenol-rich cranberry extract protects from diet-induced obesity, insulin resistance and intestinal inflammation in association with increased *Akkermansia* spp. population in the gut microbiota of mice. Gut *64*.

Appelbaum, P.C. (2006). The emergence of vancomycin-intermediate and vancomycin-resistant *Staphylococcus aureus*. Clinical Microbiology and Infection *12*, 16-23.

Blair, J.M.A., Webber, M.A., Baylay, A.J., Ogbolu, D.O., and Piddock, L.J.V. (2014). Molecular mechanisms of antibiotic resistance. Nature Reviews Microbiology *13*, 42-51.

Blanco, P., Hernando-Amado, S., Reales-Calderon, J., Corona, F., Lira, F., Alcalde-Rico, M., Bernardini, A., Sanchez, M., and Martinez, J. (2016). Bacterial multidrug efflux pumps: Much more than antibiotic resistance determinants. Microorganisms *4*, 14.

Caputo, A., Dubourg, G., Croce, O., Gupta, S., Robert, C., Papazian, L., Rolain, J.M., and Raoult, D. (2015). Whole-genome assembly of *Akkermansia muciniphila* sequenced directly from human stool. Biology Direct *10:5*.

Chia, L., Hornung, B.V.H., Aalvink, S., Schaap, P.J., de Vos, W.M., Knol, J., and Belzer, C. (2018). Deciphering the trophic interaction between *Akkermansia muciniphila* and the butyrogenic gut commensal *Anaerostipes caccae* using a metatranscriptomic approach. Antonie van Leeuwenhoek *111*, 859-873.

Clifford, M.N. (2004). Diet-Derived Phenols in Plasma and Tissues and their Implications for Health. Planta Medica *70*, 1103-1114.

Cooper, B., Islam, N., Xu, Y., Beard, H.S., Garrett, W.M., Gu, G., and Nou, X. (2018). Quantitative proteomic analysis of *Staphylococcus aureus* treated with Punicalagin, a natural antibiotic from pomegranate that disrupts iron homeostasis and induces SOS. Proteomics *18*, 1700461.

Curiel, J.A., Rodríguez, H., De la Rivas, B., Anglade, O., Baraige, F., Zagorec, M., Champomier-Vergès, M., Muñoz, R., and de Felipe, F. (2011). Response of a *Lactobacillus plantarum* human isolate to tannic acid challenge assessed by proteomic analyses. Molecular nutrition & Food research *55*, 1454-1465.

Cuthbertson, L., Kos, V., and Whitfield, C. (2010). ABC transporters involved in export of cell surface glycoconjugates. Microbiology and Molecular Biology Reviews *74*, 341-362.

Derrien, M., Baarlen, P., Hooiveld, G., Norin, E., Müller, M., and de Vos, W.M. (2011). Modulation of mucosal immune response, tolerance, and proliferation in mice colonized by the mucin-degrader *Akkermansia muciniphila*. Frontiers in Microbiology *2*, 166.

Derrien, M., Vaughan, E.E., Plugge, C.M., and de Vos, W.M. (2004). *Akkermansia muciniphila* gen. nov., sp. nov., a human intestinal mucin-degrading bacterium. International Journal of Systematic and Evolutionary Microbiology *54*, 1469-1476.

Dubourg, G., Lagier, J.-C., Armougom, F., Robert, C., Audoly, G., Papazian, L., and Raoult, D. (2013). High-level colonisation of the human gut by *Verrucomicrobia* following broad-spectrum antibiotic treatment. International Journal of Antimicrobial Agents *41*, 149-155.

Dudonné, S., Dubé, P., Anhê, F., Pilon, G., Marette, A., Lemire, M., Harris, C., Dewailly, E., and Desjardins, Y. (2015). Comprehensive analysis of phenolic compounds and abscisic acid profiles of twelve native Canadian berries. Journal of Food Composition and Analysis *44*, 214-224.

Dudonné, S., Dubé, P., Pilon, G., Marette, A., Jacques, H., Weisnagel, J., and Desjardins, Y. (2014). Modulation of strawberry/cranberry phenolic compounds glucuronidation by co-supplementation with onion: characterization of phenolic metabolites in rat plasma using an optimized μSPE-UHPLC-MS/MS method. J Agr Food Chem *62*, 3244-3256.

Espín, J., Larrosa, M., García-Conesa, M., and Tomás-Barberán, F. (2013). Biological significance of Urolithins, the gut microbial ellagic acid-derived metabolites: The evidence so far. Evidence-Based Complementary and Alternative Medicine *2013*, 1-15.

Esposito, D., Chen, A., Grace, M.H., Komarnytsky, S., and Lila, M. (2014). Inhibitory effects of wild blueberry anthocyanins and other flavonoids on biomarkers of acute and chronic inflammation *in vitro*. J Agr Food Chem *62*, 7022-7028.

Everard, A., Belzer, C., Geurts, L., Ouwerkerk, J.P., Druart, C., Bindels, L.B., Guiot, Y., Derrien, M., Muccioli, G.G., Delzenne, N.M.*, et al.* (2013). Cross-talk between *Akkermansia muciniphila* and intestinal epithelium controls diet-induced obesity. Proc National Acad Sci *110*, 9066-9071.

Firrman, J., Liu, L., Zhang, L., Argoty, G., Wang, M., Tomasula, P., Kobori, M., Pontious, S., and Xiao, W. (2016). The effect of quercetin on genetic expression of the commensal gut microbes *Bifidobacterium catenulatum, Enterococcus caccae* and *Ruminococcus gauvreauii*. Anaerobe *42*, 130-141.

Garcia-Villalba, R., Vissenaekens, H., Pitart, J., Romo-Vaquero, M., Espín, J., Grootaert, C., Selma, M.V., Raes, K., Smagghe, G., Possemiers, S.*, et al.* (2017). The gastrointestinal simulation model TWIN-SHIME® shows differences between human Urolithin-metabotypes in gut microbiota composition, pomegranate polyphenol metabolism, and transport along the intestinal tract. J Agr Food Chem *65*, 5480-5493.

Gu, L., Kelm, M., Hammerstone, J.F., Beecher, G., Cunningham, D., Vannozzi, S., and Prior, R.L. (2002). Fractionation of polymeric procyanidins from Lowbush blueberry and quantification of procyanidins in selected foods with an optimized normal-phase HPLC−MS fluorescent detection method. J Agr Food Chem *50*, 4852-4860.

Guo, X., Li, S., Zhang, J., Wu, F., Li, X., Wu, D., Zhang, M., Ou, Z., Jie, Z., Yan, Q.*, et al.* (2017). Genome sequencing of 39 *Akkermansia muciniphila* isolates reveals its population structure, genomic and functional diverisity, and global distribution in mammalian gut microbiotas. BMC Genomics *18*, 800.

Hansen, C.H.F., Krych, L., Nielsen, D.S., and Diabetologia, V.-F.K. (2012). Early life treatment with vancomycin propagates *Akkermansia muciniphila* and reduces diabetes incidence in the NOD mouse. Diabetologia *55*, 2285-2294.

Henning, S.M., Summanen, P.H., Lee, R.-P., Yang, J., Finegold, S.M., Heber, D., and Li, Z. (2017). Pomegranate ellagitannins stimulate the growth of *Akkermansia muciniphila* in vivo. Anaerobe *43*, 56-60.

Jiao, X., Wang, Y., Lin, Y., Lang, Y., Li, E., Zhang, X., Zhang, Q., Feng, Y., Meng, X., and Li, B. (2019). Blueberry polyphenols extract as a potential prebiotic with anti-obesity effects on C57BL/6 J mice by modulating the gut microbiota. J Nutritional Biochem *64*, 88-100.

Jiménez, N., Curiel, J., Reverón, I., Rivas, B., and Muñoz, R. (2013). Uncovering the *Lactobacillus plantarum* WCFS1 gallate decarboxylase involved in tannin degradation. Applied and environmental microbiology *79*, 4253-4263.

Khalil, R.K.S. (2010). Influence of gallic acid and catechin polyphenols on probiotic properties of *Streptococcus thermophilus* CHCC 3534 strain. World Journal of Microbiology and Biotechnology *26*, 2069-2079.

Krause, D.O., Smith, W.J.M., Brooker, J.D., and McSweeney, C.S. (2005). Tolerance mechanisms of streptococci to hydrolysable and condensed tannins. Animal feed science and Technology *121*, 59-75.

Lacombe, A., Li, R.W., Klimis-Zacas, D., Kristo, A.S., Tadepalli, S., Krauss, E., Young, R., and Wu, V.C.H. (2013a). Lowbush wild blueberries have the potential to modify gut microbiota and xenobiotic metabolism in the rat colon. PLoS ONE *8*.

Lacombe, A., Tadepalli, S., A., H.-C., and Wu, C.H. (2013b). Phytochemicals in lowbush wild blueberry inactivate *Escherichia coli* O157:H7 by damaging its cell membrane. Foodborne pathogens and disease *10*, 9.

Lacombe, A., Wu, V.C.H., Tyler, S., and journal of food, E.K. (2010). Antimicrobial action of the American cranberry constituents; phenolics, anthocyanins, and organic acids, against *Escherichia coli* O157: H7. International journal of Food Microbiology *139*, 102-107.

Lacombe, A., Wu, V.C.H., White, J., Tadepalli, S., and Andre, E.E. (2012). The antimicrobial properties of the lowbush blueberry *(Vaccinium angustifolium)* fractional components against foodborne pathogens and the conservation of probiotic *Lactobacillus rhamnosus*. Food microbiology *30*, 124-131.

Lessard, I.A.D., and Walsh, C.T. (1999). *VanX*, a bacterial d-alanyl-d-alanine dipeptidase: Resistance, immunity, or survival function? Proc National Acad Sci *96*, 11028-11032.

Li, Z., Henning, S.M., Lee, R.-P., Lu, Q.-Y., Summanen, P.H., Thames, G., Corbett, K., Downes, J., Tseng, C.-H., Finegold, S.M.*, et al.* (2015). Pomegranate extract induces ellagitannin metabolite formation and changes stool microbiota in healthy volunteers. Food & Function *6*, 2487-2495.

Ma, H., Johnson, S.L., Liu, W., DaSilva, N.A., Meschwitz, S., Dain, J.A., and Seeram, N.P. (2018). Evaluation of polyphenol anthocyanin-enriched extracts of blackberry, black raspberry, blueberry, cranberry, red raspberry, and strawberry for free radical scavenging, reactive Ccrbonyl species trapping, anti-glycation, anti-β-amyloid aggregation, and microglial neuroprotective effects. International Journal of Molecular Sciences *19*, 461.

Marchler-Bauer, A., Bo, Y., Han, L., He, J., Lanczycki, C.J., Lu, S., Chitsaz, F., Derbyshire, M.K., Geer, R.C., Gonzales, N.R.*, et al.* (2017). CDD/SPARCLE: functional classification of proteins via subfamily domain architectures. Nucleic Acids Research *45*.

Masumoto, S., Terao, A., Yamamoto, Y., Mukai, T., Miura, T., and Shoji, T. (2016). Non-absorbable apple procyanidins prevent obesity associated with gut microbial and metabolomic changes. Sci Rep-uk *6*, 31208.

Modi, S.R., Collins, J.J., and Relman, D.A. (2014). Antibiotics and the gut microbiota. Journal of Clinical Investigation *124*, 4212-4218.

Morissette, A., Kropp, C., Songpadith, J.P., Junges Moreira, R., Costa, J., Marine Casado, R., Pilon, G., Varin, T.V., Dudonne, S., Boutekrabt, L.*, et al.* (2020). Blueberry proanthocyanidins and anthocyanins improve metabolic health through a gut microbiota-dependent mechanism in diet-induced obese mice. Am J Physiol Endocrinol Metab.

Mosele, J.I., Macià, A., and Motilva, M.-J. (2015). Metabolic and microbial modulation of the large intestine ecosystem by non-absorbed diet phenolic compounds: A review. Molecules *20*, 17429-17468.

Nakayama, M., Shimatani, K., Ozawa, T., Shigemune, N., Tomiyama, D., Yui, K., Katsuki, M., Ikeda, K., Nonaka, A., and Miyamoto, T. (2015). Mechanism for the antibacterial action of epigallocatechin gallate (EGCg) on *Bacillus subtilis*. Bioscience, Biotechnology, and Biochemistry *79*, 845-854.

Neff, P.C., Rhodes, M.E., Arnolds, K.L., Collins, C.B., Donnelly, J., Nusbacher, N., Jedlicka, P., Schneider, J.M., McCarter, M.D., Shaffer, M.*, et al.* (2016). Diverse intestinal bacteria contain putative zwitterionic capsular polysaccharides with anti-inflammatory properties. Cell host & microbe *20*, 535-547.

Ottman, N., Huuskonen, L., Reunanen, J., Boeren, S., Klievink, J., Smidt, H., Belzer, C., and de Vos, W.M. (2016). Characterization of outer membrane proteome of *Akkermansia muciniphila* reveals sets of novel proteins exposed to the human intestine. Frontiers in Microbiology *7*, 1157.

Ottman, N., Reunanen, J., Meijerink, M., Pietilä, T.E., Kainulainen, V., Klievink, J., Huuskonen, L., Aalvink, S., Skurnik, M., Boeren, S.*, et al.* (2017). Pili-like proteins of *Akkermansia muciniphila* modulate host immune responses and gut barrier function. PLOS ONE *12*.

Ouwerkerk, J.P., van der Ark, K.C.H., Davids, M., Claassens, N.J., Finestra, T., de Vos, W.M., and Belzer, C. (2016). Adaptation of *Akkermansia muciniphila* to the oxic-inoxic Interface of the mucus layer. Applied and Environmental Microbiology *82*, 6983-6993.

Porter, N.T., Canales, P., Peterson, D.A., and Martens, E.C. (2017). A subset of polysaccharide capsules in the human symbiont *Bacteroides thetaiotaomicron* promote increased competitive fitness in the mouse gut. Cell Host & Microbe *22*, 494.

Porter, N.T., and Martens, E.C. (2015). The critical roles of polysaccharides in gut microbial ecology and physiology. Annual Review of Microbiology *71*, 1-21.

Rempe, C.S., Burris, K.P., Lenaghan, S.C., and Stewart, N.C. (2017). The Potential of systems biology to discover antibacterial mechanisms of plant phenolics. Frontiers in Microbiology *8*, 422.

Reverón, I., Rodríguez, H., Campos, G., Curiel, J., Ascaso, C., Carrascosa, A.V., Prieto, A., de las Rivas, B., Muñoz, R., and de Felipe, F. (2013). Tannic acid-dependent modulation of selected *Lactobacillus plantarum* traits linked to gastrointestinal survival. PLoS ONE *8*.

Rodríguez-Daza, M.-C., Daoust, L., Boutkrabt, L., Pilon, G., Varin, T., Dudonné, S., Levy, É., Marette, A., Roy, D., and Desjardins, Y. (2020). Wild blueberry proanthocyanidins shape distinct gut microbiota profile and influence glucose homeostasis and intestinal phenotypes in high-fat high-sucrose fed mice. Sci Rep-uk *10*, 2217.

Samoilova, Z., Tyulenev, A., Muzyka, N., Smirnova, G., and Oktyabrsky, O. (2019). Tannic and gallic acids alter redox-parameters of the medium and modulate biofilm formation. AIMS Microbiol *5*, 379-392.

Scott, P.M., Erickson, K.M., and Troutman, J.M. (2019). Identification of the functional roles of six key proteins in the biosynthesis of *Enterobacteriaceae* colanic acid. Biochemistry *58*, 1818-1830.

Stubbendieck, R.M., and Straight, P.D. (2017). Linearmycins activate a Two-component signaling system involved in Bacterial competition and biofilm morphology. Journal of Bacteriology *199*, 17.

Szklarczyk, D., Franceschini, A., Wyder, S., Forslund, K., Heller, D., Huerta-Cepas, J., Simonovic, M., Roth, A., Santos, A., Tsafou, K.P.*, et al.* (2015). STRING v10: protein–protein interaction networks, integrated over the tree of life. Nucleic Acids Research *43*.

Tabasco, R., Sánchez-Patán, F., Monagas, M., Bartolomé, B., Moreno-Arribas, V.M., Peláez, C., and Requena, T. (2011). Effect of grape polyphenols on lactic acid bacteria and bifidobacteria growth: Resistance and metabolism. Food Microbiology *28*, 1345-1352.

Tamura, T., Ozawa, M., Tanaka, N., Arai, S., and Mura, K. (2016). *Bacillus cereus* response to a proanthocyanidin trimer, a transcriptional and functional analysis. Current Microbiology *73*, 115-123.

Tomás-Barberán, F.A., González-Sarrías, A., García-Villalba, R., Núñez-Sánchez, M.A., Selma, M.V., García-Conesa, M.T., and Espín, J. (2017). Urolithins, the rescue of "old" metabolites to understand a "new" concept:

Metabotypes as a nexus among phenolic metabolism, microbiota dysbiosis, and host health status. Molecular Nutrition & Food Research *61*, 1500901.

Tropini, C., Lee, T.K., Hsin, J., Desmarais, S.M., Ursell, T., Monds, R.D., and Huang, K. (2014). Principles of bacterial cell-size determination revealed by cell-wall synthesis perturbations. Cell reports *9*, 1520-1527.

Turner, R.D., Hurd, A.F., Cadby, A., Hobbs, J.K., and Foster, S.J. (2013). Cell wall elongation mode in Gram-negative bacteria is determined by peptidoglycan architecture. Nature Communications *4*, 1496.

van Passel, M.W.J., Kant, R., Zoetendal, E.G., M., P.-C., Derrien, M., Malfatti, S.A., Chain, P.S.G., Woyke, T., Palva, A., de Vos, W.M.*, et al.* (2011). The genome of *Akkermansia muciniphila*, a dedicated intestinal mucin degrader, and its use in exploring intestinal metagenomes. PloS one *6*, e16876.

Vandesompele, J., Preter, K., Pattyn, F., Poppe, B., Roy, N., Paepe, A., and Speleman, F. (2002). Accurate normalization of real-time quantitative RT-PCR data by geometric averaging of multiple internal control genes. Genome Biology *3*, 1-12.

Wang, J., Liu, Q., Feng, J., Lv, J.-p., and Xie, S.-l. (2016). Effect of high-doses pyrogallol on oxidative damage, transcriptional responses and microcystins synthesis in *Microcystis aeruginosa* TY001 (Cyanobacteria). Ecotoxicology and Environmental Safety *134*, 273-279.

Willis, L.M., and Whitfield, C. (2013). Structure, biosynthesis, and function of bacterial capsular polysaccharides synthesized by ABC transporter-dependent pathways. Carbohydrate Research *378*, 35-44.

Xie, Y., Yang, W., Tang, F., Chen, X., and Ren, L. (2014). Antibacterial activities of flavonoids: Structure-activity relationship and mechanism. Current Medicinal Chemistry *22*, 132-149.

Xue, B., Xie, J., Huang, J., Chen, L., Gao, L., Ou, S., Wang, Y., and Peng, X. (2016). Plant polyphenols alter a pathway of energy metabolism by inhibiting fecal *Bacteroidetes* and *Firmicutes in vitro*. Food & Function *7*, 1501-1507.

Zoetendal, E.G., Smith, A.H., A., S.-M., and Mackie, R.I. (2008). The *BaeSR* two-component regulatory system mediates resistance to condensed tannins in *Escherichia coli*. Applied and Environmental Microbiology, 535-539.

Star methods

Key resource table

REAGENT or RESOURCE	SOURCE	IDENTIFIER
Bacterial and Virus Strains		
Akkermansia muciniphila strain	Derrien et al. (2004)	ATCC BAA-835
Chemicals, Peptides, and Recombinant Proteins		
Porcine gastric mucin Type II	Sigma-Aldrich	Cat #M2368
Brain heart infusion broth	BD Difco	Cat #B237500
RNA*later* stabilization solution	Ambion – Life technologies	Cat #AM7021
Cranberry polyphenolic extract	This work	N/A
Tannin-rich extract, Superior Tan'Activ	Silvateam S.p.a. Italy, https://www.silvateam.com	TAN-Active QS-SOL
Urolithin A	Dr. Tomás-Barberán, CEBAS, Murcia, Spain	N/A
Vancomycin hydrochloride	Sigma-Aldrich	Cat #1709007
Cyanidin 3-glucoside standard	Sigma-Aldrich	Cat #PHL89616
Gallic acid standard	Sigma-Aldrich	Cat #91215
Epicatechin standard	Sigma-Aldrich	Cat #03940590
Polyvinylpyrrolidone (PVP 10%)	Sigma-Aldrich	Cat # PVP40
ß-mercaptoethanol	Invitrogen	Cat #21985023
PowerUp SYBR Green Master Mix	Applied Biosystems	Cat #A25742
Critical Commercial Assays		
RNeasy Mini Kit	QIAGEN	Cat #74104
BashingBead Lysis Tubes	ZR, Zymo research	Cat #S6012-50
RNase-Free DNase kit	QIAGEN	Cat #79254
TURBO DNA-free Kit	Ambion – Life technologies	Cat #AM1907
Agilent RNA6000 Nano kit	Agilent technologies	Cat # 5067-1511
High Capacity cDNA Reverse Transcription Kit	Applied Biosystems	Cat #4368814
Experimental Models: Organisms/Strains		
Akkermansia muciniphila strain	ATCC	ATCC BAA-835
Oligonucleotides		
Primers Sequences for housekeeping and target genes	This work	See **Table S3**
Software and Algorithms		
NormFinder software	Andersen et al. (2004)	N/A
geNorm	Vandesompele et al. (2002)	N/A
GraphPad Prism 7.0	GraphPad	https://www.graphpad.com/scientificsoftware/prism/
Software Gatan digital micrograph	Gatan	https://www.gatan.com/products/
Other		
Anaerobic chamber	Plas-Labs™	818 series
Omni Bead Ruptor Homogenizer	Omni International	Bead ruptor 12

ABI 7500 Fast real-time cycling platform	Applied Biosystems	N/A
Sephadex LH-20	Sigma-Aldrich	Cat #LH20100
HPLC with DAD detection	Agilent technologies	Agilent 1100 series system
Reverse-phase UHPLC coupled to tandem mass spectrometry	Agilent technologies	N/A
Normal-phase HPLC	Agilent technologies	Agilent 1260/1290 infinity system
Agilent 2100 Bioanalyzer system	Agilent technologies	N/A
Scanning electron microscope	JEOL	JSM-6360LV
Transmission electron microscope	JEOL	JEM-1230
Gatan XP1000 camera	Gatan	https://www.gatan.com/products/

Contact for reagent and resource sharing

Further information and requests for resources and reagents should be directed to and will be fulfilled by the Lead Contact, Maria-Carolina Rodriguez (maria-carolina.rodriguez-daza.1@ulaval.ca).

Experimental model and subject details

Polyphenolic fractions

A polyphenol-rich cranberry extract *(Vaccinium macrocarpon)* (CE) was fractionated by gel-filtration chromatography as described previously (Gu et al., 2002). Then, three different cranberry polyphenolic fractions were generated, one, rich in anthocyanins, other containing a mix of flavan-3-ols and flavonols, and the last one, rich in flavan-3-ols. Additionally, to compare the response to another source of flavan-3-ols and to get insight about the polyphenolic-metabolite effects on *A. muciniphila*, two more extracts were used. An extract rich in tannins (TAN-Active QS-SOL, Silvateam S.p.a. Italy), and the polyphenolic microbial metabolite Urolithin A (kindly supplied by Dr. Tomás-Barberán, CEBAS, Murcia, Spain).

A. muciniphila culture conditions

Akkermansia muciniphila MucT (*Akk*) (ATCC BAA-835) growth experiments were performed in Brain heart infusion broth 37g/L (BHI) (BD Difco) supplemented with 5 g/L of porcine gastric

mucin (BHI-Muc) (Type II; Sigma-Aldrich, St. Louis, MO, USA), with addition of L-cysteine hydrochloride (0.5 g/L) as reducing agent, and salt solution 20 mL/L ($CaCl_2$ 0.25 g, $MgSO_4$ 0.50 g, K_2HPO_4 1 g, KH_2PO_4 1 g, $NaHCO_3$ 10 g, NaCl 0.5 g, distilled water 1000 mL). All anaerobic broths were autoclaved under pressure at 121ºC for 30 min. After autoclaving, the broths were dispensed in an anaerobic chamber (Plas-Labs™, gas phase of 182 kPa, 1.5 atm) under an atmosphere of 80% N_2 and 20% CO_2 and conserved for 24h to allow pre-reduce the media.

The filtered-sterilized total aqueous CE was added to the BHI-Muc media at a final concentration of 600 mg/L. In order to elucidate the degree of contribution of the polyphenolic compounds found in the CE, the derived polyphenolic fractions were added to the broths at the same concentration found in the total CE (see supplementary information **Figure S1**). Then, the concentration for the first fraction (F1) was 221 mg/L, for the second fraction (F2) 381 mg/L, and for the third fraction (F3) 115 mg/L. Additional assays were performed using a higher concentration (H) of CE (2400 mg/L) and F3-H fraction (460 mg/L) to evaluate a possible dose-dependent response.

Considering that the tannins have known antimicrobial effects, we additionally assessed a commercial condensed tannins-rich extract (143 mg/L) (TAN-Active QS-SOL). Likewise, since previous studies have demonstrated a significant stimulation of *A. muciniphila* by the consumption of antibiotics, growing bacteria were also submitted to 6 mg/L vancomycin as reference antimicrobial treatment (Appelbaum, 2006). In the same way, we evaluated the influence of 6.85 mg/L Urolithin A (equivalent to 30µM) (Espín et al., 2013) as a microbial metabolite in the growth and genetic response of *A. muciniphila*.

A. muciniphila cells (*Akk*-cells) were grown in the presence and absence of CE, and polyphenolic fractions. Growing cells of *A. muciniphila* (1.6×10^9 cells/mL) were inoculated to a final concentration of 1% of the total volume broth. *Akk*-inoculated polyphenolic BHI-Muc broths, broths devoid of polyphenolic extracts and their respective *Akk*-cells free controls were held at 37ºC under static incubation conditions in the anaerobic chamber for 48 hours. Bacterial growth was quantified after serial dilutions from collected samples poured onto BHI-Muc agar plates (0,8% agar, soft agar media) and viable colony counts. Two replica plates at each time point were

used to evaluate the growth rate. Samples were also streaked out and incubated as described above to verify colony morphology and purity from each assay. Colony forming units (CFU) were recorded and the percentage of viable cells was calculated as follows:

$$\% \text{ of viable cells} = [(CFU_{target})/CFU_{control}] \times 100$$

Duplicate aliquots of 2 mL were collected at 24h and 30h of growth after inoculation. Pellets were harvested by centrifugation at 6000 g for 10 min at 4°C and resuspended in 3 mL of RNA stabilization reagent *RNAlater (*Ambion – Life technologies*).* The suspensions were incubated at 4°C overnight and then, transferred at −20 °C until RNA isolation. Biological independent experiments were performed in triplicate with two technique repetitions per culture assay.

Method details

Characterization of polyphenolic fractions

The phenolic composition analysis was carried out as described previously (Dudonné et al., 2015). The Folin-Ciocalteu method and the gallic acid standard were used to determine the total phenolic content. The analysis of phenolic acids, flavonols and flavan-3-ols were analyzed using reverse-phase UHPLC coupled to tandem mass spectrometry (Dudonné et al., 2015). The analysis of anthocyanins was performed by reverse-phase HPLC with DAD detection using an Agilent 1100 series system (Santa Clara, CA); the standard of cyanidin 3-glucoside and chromatographic data acquired at 520 nm were considered for the anthocyanins quantification. Their identification was achieved by comparison of chromatographic retention times and mass spectral information obtained with previously published data. Proanthocyanins (PACs) were analyzed by normal-phase HPLC with fluorescence detection using an Agilent 1260/1290 infinity system (Santa Clara, CA). The fluorescence was monitored at excitation and emission wavelengths of 230 nm and 321 nm respectively, and the quantification of polymerization degree (DP) from 1 to >10, was performed using an external calibration curve of epicatechin, applying a correction factor according to their respective fluorescence responses(Dudonné et al., 2014).

RNA isolation and cDNA synthesis

Total RNA was extracted using a RNeasy mini kit (Qiagen, #74104) with some modifications. Briefly, culture samples stored in *RNAlater* at -20°C were thawed on ice, mixed with equal volumes of cold phosphate-buffered saline (PBS), and centrifuged at 6000 g for 10 min at 4ºC. *Akk*-cells were then washed three times to remove the stabilization reagent. Bacterial pellets were resuspended in RLT solution (lysis buffer) with the addition of 2.5% (v/v) polyvinylpyrrolidone (PVP 10%) and 1% (v/v) of ß-mercaptoethanol which helped to remove the remaining polysaccharides and polyphenols from samples. The suspension was transferred to 2 ml BashingBead Lysis Tubes (ZR, Zymo research #S6012-50) and submitted to cellular disruption using the Omni Bead Ruptor Homogenizer (Omni International, NW Kennesaw, GA, USA).

In order to guarantee DNA-free samples, samples were DNase treated on the column during the purification process using the RNase-Free DNase kit (Qiagen; #79254). Once the RNA was isolated, a second DNase I digestion was performed with Ambion's Turbo DNA-free kit (Applied Biosystems) according to the manufacturer's protocol. The RNA concentration and quality were assessed using a NanoDrop 2000 spectrophotometer (Thermo Scientific, Waltham, MA, USA) and RNA Nano-Chips in Agilent 2100 Bioanalyzer (Agilent technologies Inc. Santa Clara, CA, USA) respectively. Then, 2 µg RNA were reverse transcribed using the High Capacity cDNA Reverse Transcription Kit (Applied Biosystems, Carlsbad, CA). The resultant cDNAs were diluted 1:2 with nuclease-free water before qRT-PCR analysis.

Target genes and quantitative reverse transcription PCR

Gene expression responses were evaluated by quantitative reverse transcription-PCR (qRT-PCR). Primers were designed according to MIQE guidelines with the aid of Geneious software (version 9.0) for amplifying mRNA from 14 single genes, (see supplementary information **Table S3**) including 2 selected internal control genes (housekeeping genes, HKGs) submitted to stability validation by NormFinder and GeNorm software (Andersen et al., 2004; Vandesompele et al., 2002). Standard curves using 10-fold dilution series of pooled cDNA were

developed to calculate the PCR amplification efficiency (E) $E = 10^{(1/slope) - 1 \times 100}$ and the regression coefficient (R^2) of each primer pair.

The cDNAs were amplified by qRT-PCR on an Applied Biosystems ABI 7500 Fast real-time cycling platform. The reactions were carried out in duplicate in a final volume of 20 µl, containing 10 µl PowerUp SYBR Green Master Mix (Applied Biosystems, United States), 2 µl of diluted cDNA, 0.8 µl of 5 µM reverse and forward primers (final concentration of 200 nM), and 6.4 µl of nuclease-free water. The thermocycling protocol consisted in 95°C for 10 min for hot-start polymerase activation, followed by 40 cycles of denaturation at 95°C for 15 s, annealing at 60°C for 1 min, and a melting curve stage as the default setting from 60°C to 95°C. The melting curve analysis was performed after each amplification to confirm the product specificity. These conditions were used for all primer pairs. Duplicated samples were analyzed for three biological experiments. The gene expression ratios were calculated using the ΔΔCT method after data normalization considering the expression level of the two HKGs *GyrA* and *RpoD.*

Phenotypic analysis by scanning electron microscopy (SEM) and transmission electron microscopy (TEM)

Growing cells were recovered in the exponential phase. Bacteria incubated with or without the polyphenolic fractions were washed three times with PBS by centrifuging at 6000 x g for 10 min at 4ºC. Sample processing for scanning electron microscopy (SEM) and transmission electron microscopy (TEM) were performed at IBIS laboratory of Molecular Imaging and Microscopy, Laval University (Québec, QC, Canada). For SEM analysis, the *Akk*-cells were fixed in 2.5% glutaraldehyde in cacodylate buffer (0.1M pH 7.3) for 30 min and washed three times with cacodylate buffer (0.1M pH 7.3) for 10 min. Subsequently, the cells were treated with 1% osmium tetroxide (OsO_4) in cacodylate buffer (0.1M, pH 7.3) for 90 min and then, washed as described above. After dehydration in an ethanol series (a stepwise increase from 30%, through 50%, 70%, 95%, and finally to 100%), the cells were transferred into a solution of hexamethyldisilazane. The dried specimens were coated with a thin layer of metal gold-palladium by the use of a sputter coater. The SEM images were obtained with JSM-6360LV scanning electron microscope (JEOL) (Tokyo, Japon).

For the TEM analysis aimed to detect the formation of capsular exopolysaccharides by *A. muciniphila*, the PBS-washed *Akk*-cells were suspended in the 2.5% glutaraldehyde fixative solution containing 0.15% ruthenium red in cacodylate buffer (0.1M, pH 7.3). The *Akk*-cells suspensions were incubated at 4ºC for 2h, and subsequently centrifuged at 7,500 x g for 10 min. The cells were resuspended in cacodylate buffer containing 0.05% of ruthenium red and then, added polycationic ferritin (1 mg/mL). After 30 min of incubation at room temperature, the reaction was stopped by the addition of 10X volumes of cacodylate buffer with 0.05% of ruthenium red. The cells were washed three times in the same buffer, and the pellets were microencapsulated in 3% agarose (w/v). The agar-solidified samples were treated for 2 hours with 1% osmium tetroxide in cacodylate buffer containing 0.05% ruthenium red. Once washed three times, the samples were submitted to sequential dehydration with acetone (30, 50, 70, 95, 100, 100%) containing 0.05% ruthenium red. The samples were then embedded in propylene oxide twice for 30 min and later in a propylene oxide: Epon resin mixture (1 :1). The samples were held in the Epon resin solution for 3-4 hours. To allow the polymerization of the resin, the samples were incubated at 37ºC for 24h and then, placed at 60ºC for 72h. Ultra-thin sections samples were finally examined under a transmission electron microscope JEOL, JEM-1230 (Tokyo, Japon) at 80 Kv coupled to a Gatan XP1000 camera (software Gatan digital micrograph).

Quantification and statistical analysis

Statistical analysis

The results are expressed as the mean ± standard error of the mean (SEM) of three independent experiments. Statistical analysis was carried out using Graph Pad Prism 7 software (GraphPad Software, Inc., La Jolla, CA). One-way ANOVA and Benjamini, Krieger and Yekutieli test corrections were applied to analyze the real-time qPCR gene expression data. Genes were reported as fold change compared to control assays (BHI-Muc) and were considered as differentially expressed when corrected p-values (*q*-value) were denoted as follows unless otherwise indicated: p* < 0.05; ** p< 0.01; *** p< 0.001. **** p<0.0001. Statistical tests used are indicated in each figure legend.

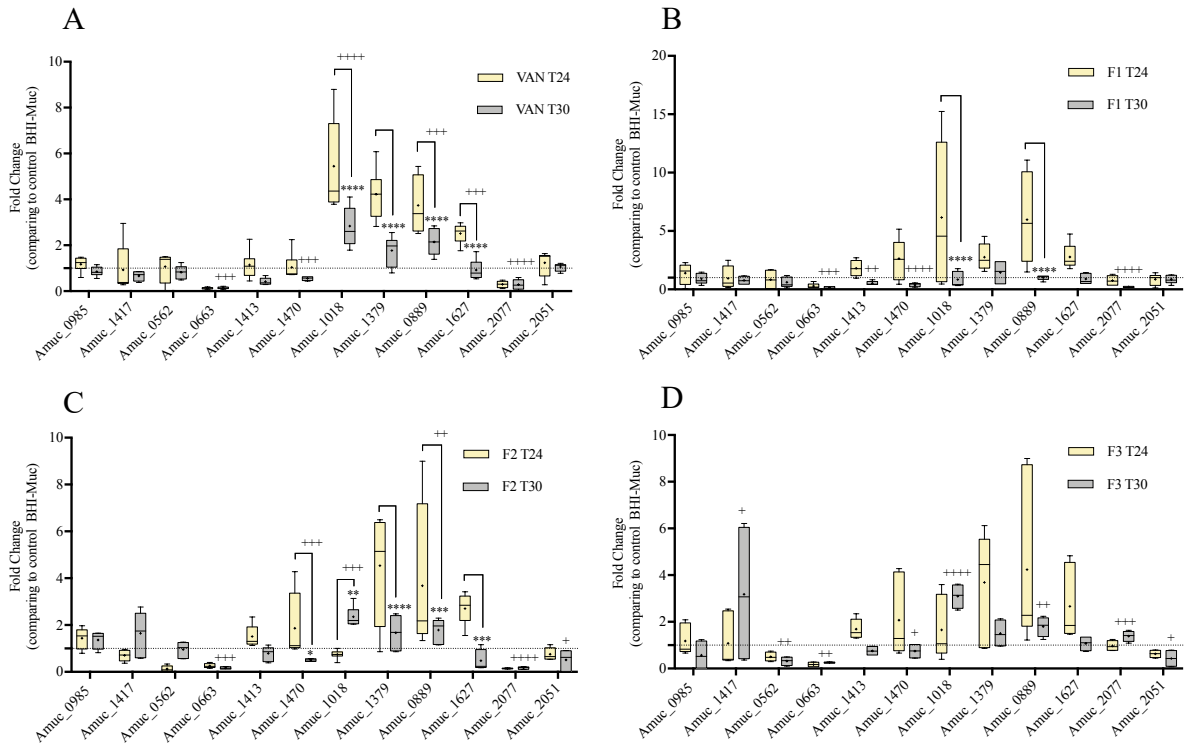

Figure 1. Time-course genetic profile of Akkermansia muciniphila growth in presence of vancomycin and polyphenolic fractions.

The fold change of gene expressions relative to BHI-Muc grown cells (control dotted line normalized to 1.0) in the presence of (A) vancomycin (VAN), (B) Flavonoid A-rich fraction (F1), (C) Flavonoid B-rich fraction (F2), (D) Flavonoid C-rich fraction (F3) were evaluated at 24h (exponential phase) and 30h (end of exponential phase) of *A. muciniphila* growth. Boxes are the interquartile range; median values are plotted as bands and mean values are represented by the mark "+" within the boxes. Two-way ANOVA with Benjamini test for multiple comparison corrections were performed to compare the entire genetic profile between samples at 24h and 30h from the same treatment. Ordinary one-way ANOVA with Benjamini multiple comparison corrections were performed to compare treatments against the BHI-Muc control treated-cells at 30h. *$p < 0.05$, **$p < 0.01$, ***$p < 0.005$, ****$p<0.0001$ are time-course differentially expressed genes within samples, and + $p < 0.05$, ++ $p < 0.01$, +++ $p < 0.005$, ++++ $p<0.0001$ are significant compared to BHI-Muc control Akk-cells.

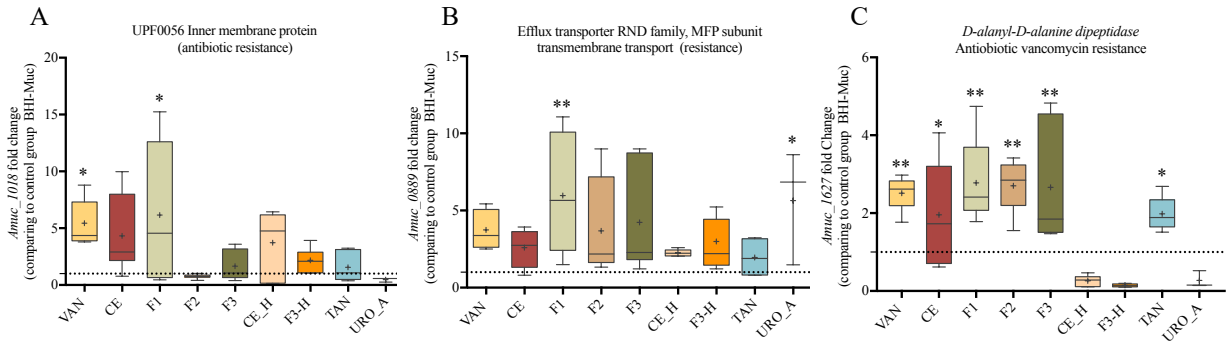

Figure 2. Akkermansia muciniphila displays antibiotic-related molecular defense mechanisms to polyphenolic fractions.

The fold change of gene expression of UPF0056 inner membrane protein (A), efflux transporter RND family (B), and the D-alanyl-D-alanine dipeptidase (C) determined by RT-qPCR were normalized with the level of GyrA and RpoD expression and were calculated relative to the expression of *Akk*-cells grown in the BHI-Muc control broth (dotted line normalized to 1.0). Boxes are the interquartile range; median values are plotted as bands and mean values are represented by the mark "+" within the boxes. Ordinary one-way ANOVA with Benjamini test for multiple comparison corrections were performed, *$p < 0.05$, **$p < 0.01$, ***$p < 0.005$, ****$p<0.0001$ compared to control.

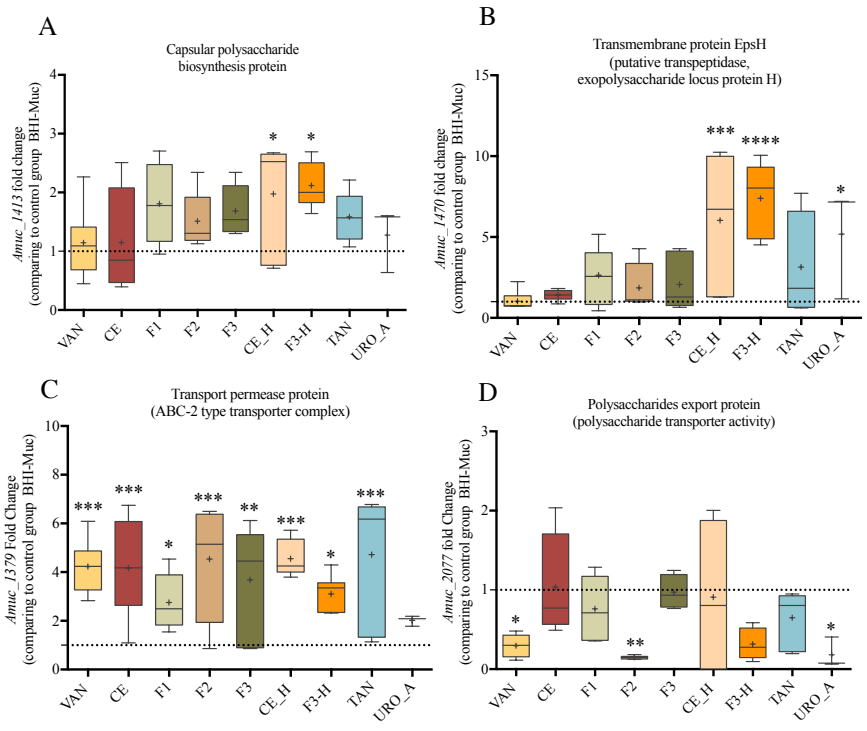

Figure 3. Relative upregulation of genes coding for capsular exopolysaccharide biosynthesis and membrane transporters related to exopolysaccharides secretion in Akkermansia muciniphila.

(A) The fold change of gene expression of capsular polysaccharide biosynthesis protein Amuc_1413, (B) exopolysaccharide locus protein H Amuc_1470, (C) ABC-2 type transporter complex Amuc_1379 and (D) polysaccharide export protein Amuc_2077 were analyzed by RT-qPCR normalized to HKGs *GyrA* and *RpoD* expression and compared to the expression of *Akk*-cells grown in the BHI-Muc control broth (dotted line normalized to 1.0). Boxes are the interquartile range; median values are plotted as bands and mean values are represented by the mark "+" within the boxes. Ordinary one-way ANOVA with Benjamini test for multiple comparison corrections were performed, *$p < 0.05$, **$p < 0.01$, ***$p < 0.005$, ****$p<0.0001$ compared to control.

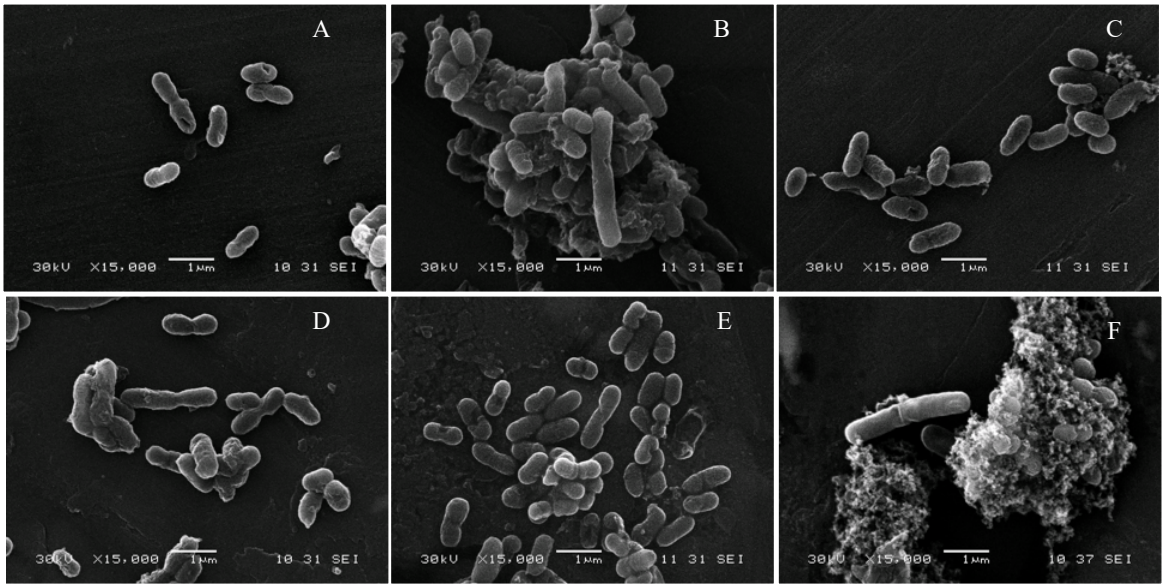

Figure 4. Representative Scanning electron micrographs showing the cellular morphology and surface state of Akkermansia muciniphila exposed to vancomycin and polyphenolic fractions.

Representative SEM images of *Akk*-cells grown in (A) BHI-Muc control, (B) Vancomycin VAN, (C) Cranberry extract CE, (D) F1, (E) F2 and (E) F3.

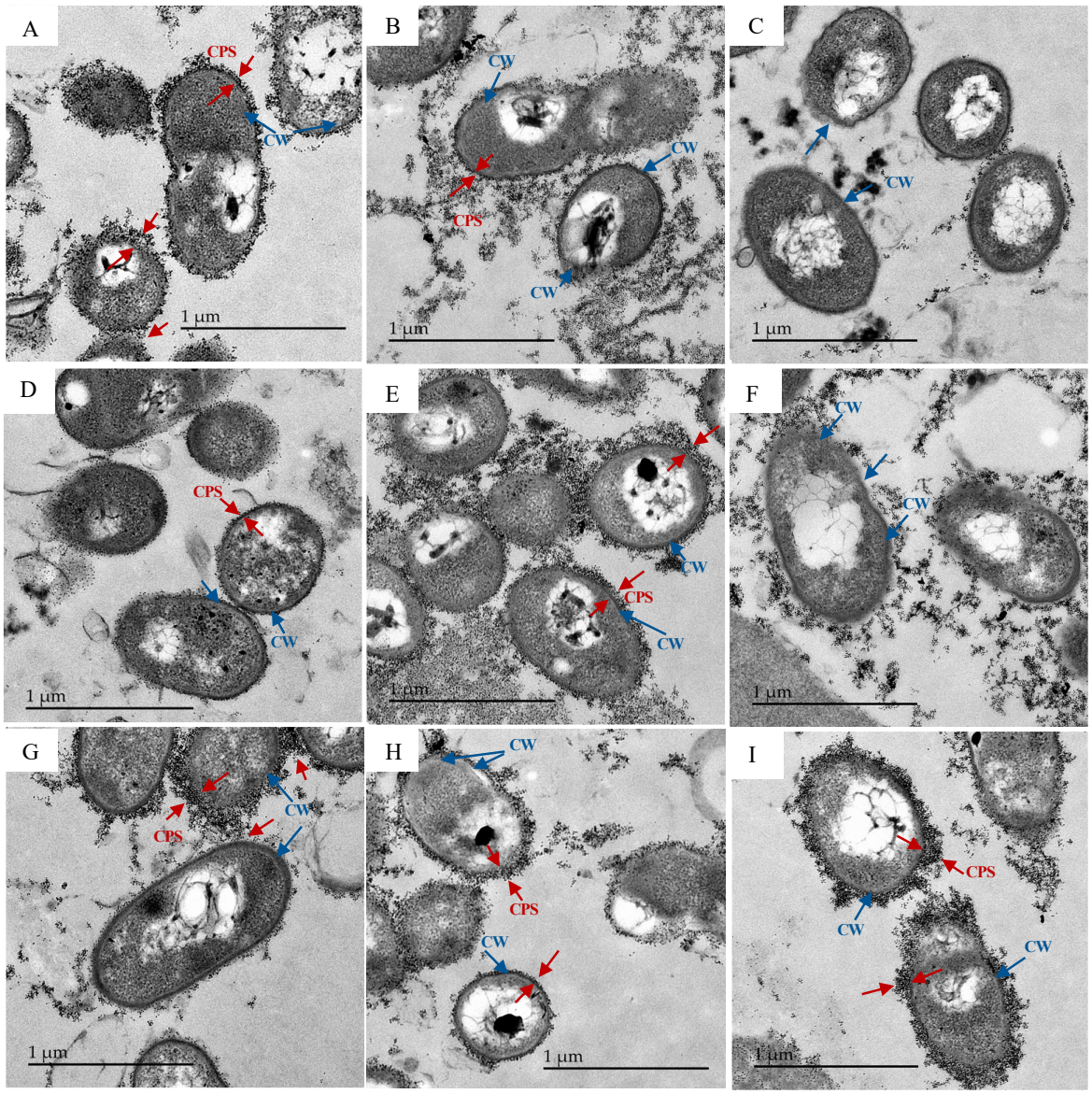

Figure 5. Transmission electron microscopy (TEM) analysis of Akkermansia muciniphila stained with ruthenium red demonstrates the exopolysaccharides capsule.

Representative micrographs show the formation of surface capsular polysaccharide for *Akk*-cells grown in (A) BHI-Muc control broth, supplemented either with (B) Vancomycin VAN, (C) Cranberry extract CE, (D) F1, (E) F2, (F) F3, (G) High concentration of cranberry extract CE-H, (H) High concentration of F3, F3-H and (I) Urolithin A, Uro-A. TEM revealed that the *Akk*-cells grown in BHI-Muc was surrounded by a thick polysaccharides capsule (51.0 ± 3.2 nm) (CPS, red arrows) and a defined double cell wall (CW, blue arrows). The thickness of the VAN-grown *Akk*-cells is partially reduced (25.7 ± 4.3 nm) and their CW seems to be slightly affected. The CE-grown *Akk*-cells showed a marked impact in the formation and adherence of CPS to the cell surface (15.3 ± 1.9 nm). The F1-grown *Akk*-cells

presented a scattered and less thick CPS (23.7 ± 4.3 nm). The F2 fraction could restore the CPS phenotype (63.0 ± 2.6 nm). The F3 affected the adherence and density of the CPS in *Akk*-cells (25.3 ± 4.7 nm), as well as, the CW was partially disturbed. The CE-H showed no affection at the CW level, the CPS thickness was 86.7 ± 11.2 nm. The high concentration of F3-H appears also to contribute in the density and adherence of the CPS, presenting a thickness of 67 ± 5.6 nm. The microbial metabolite Uro-A presented a significant density of CPS layer with 108.7 ± 8.0 nm, appearing compact around the cell. The scale bar represents 1 μm.

Supplementary information

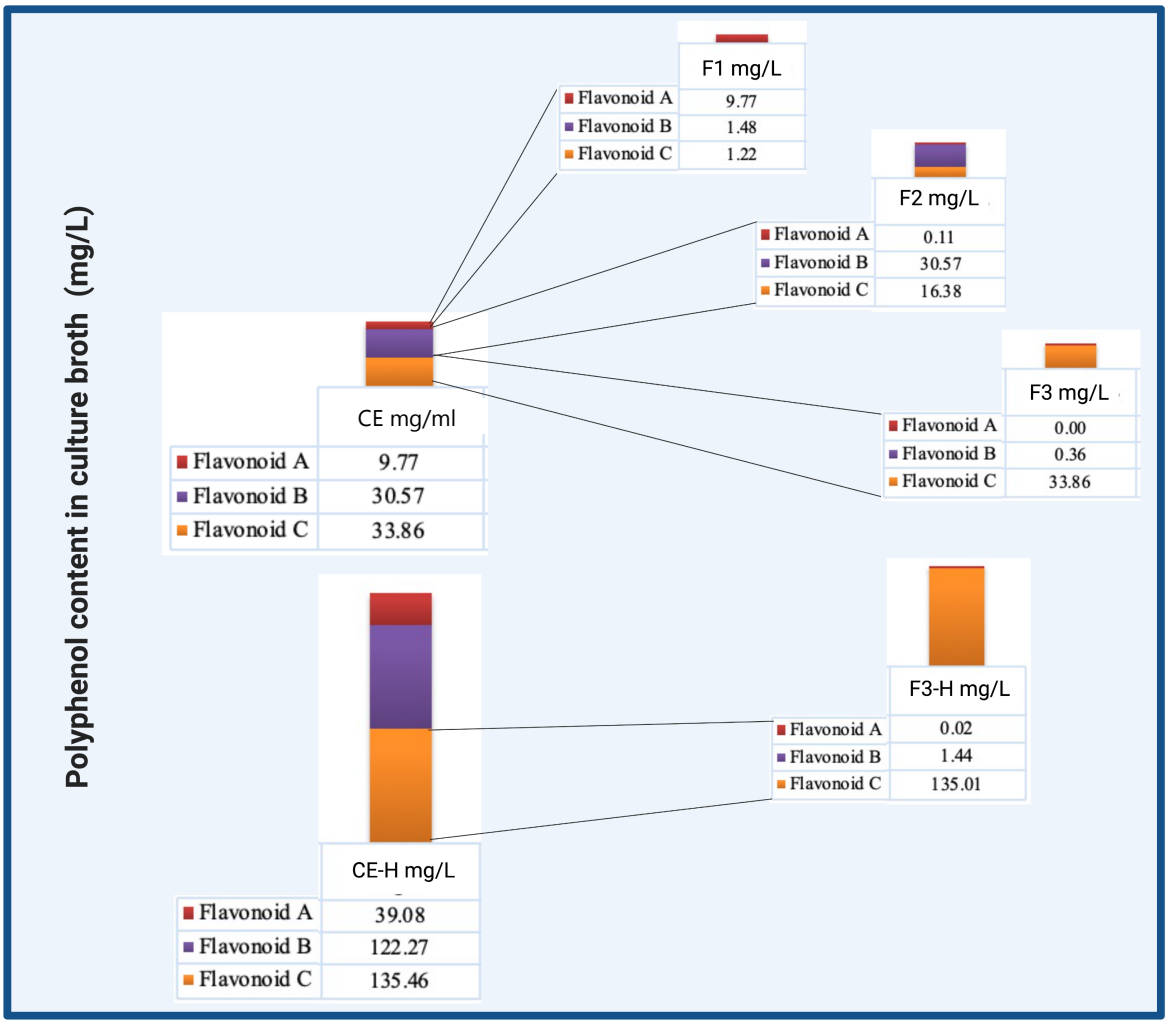

Figure S1. Polyphenolic content provided by the extracts and fractions to the culture broth.

Akkermansia muciniphila was grown in BHI-Muc broth supplemented either with 600 mg/L of total cranberry extract (CE), cranberry polyphenolic fractions riches in flavonoid A (F1, 221 mg/L), Flavonoid B (F2, 381 mg/L), Flavonoid C (F3, 115 mg/L), a higher concentration of cranberry extract (CE-H, 2400 mg/L) and a higher concentration of flavonoid C (F3-H 460 mg/L). The concentrations of flavonoids varied according to the extract or specific polyphenolic fractions and their amount added to the culture broth.

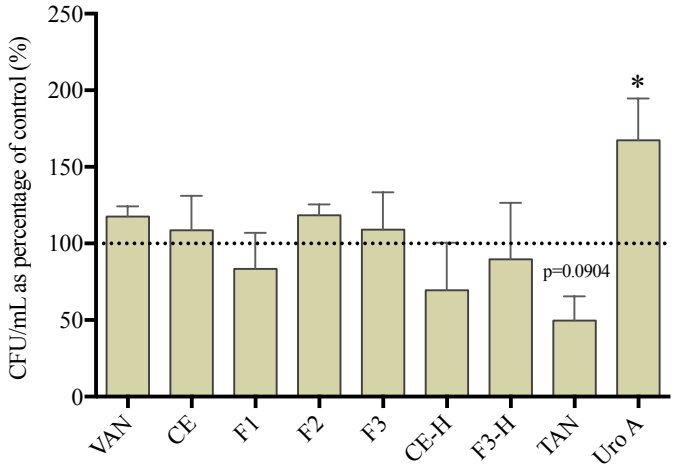

Figure S2. Cellular viability of Akkermansia muciniphila was unaffected by the presence of polyphenolic extracts and stimulated by urolithin A.

Akk-cells were grown in BHI-Muc broth supplemented either with 6 mg/L of vancomycin (VAN) as reference of antimicrobial agent , 600 mg/L of total cranberry extract (CE), cranberry polyphenolic fractions riches in flavonoid A (F1 221 mg/L), flavonoid B (F2, 381 mg/L), flavonoid C (F3, 115 mg/L), a higher concentration of CE (CE-H, 2400 mg/L), a higher concentration of flavonoid C (F3-H, 460 mg/L), a tannins-rich extract (TAN 143 mg/L) and the microbial metabolite urolithin A (Uro-A, 6.85 mg/L). Results are expressed as the number of colony forming unities per milliliter of culture broth (CFU/mL) in percentage normalized to controls (BHI-Muc control broth, considered to represent 100%, dotted line). Graphs are represented as mean ± SEM of three independent experiments, each broth assay performed at least in triplicate. ANOVA *$p < 0.05$, **$p < 0.01$, ***$p < 0.005$, ****$p<0.0001$ compared to control.

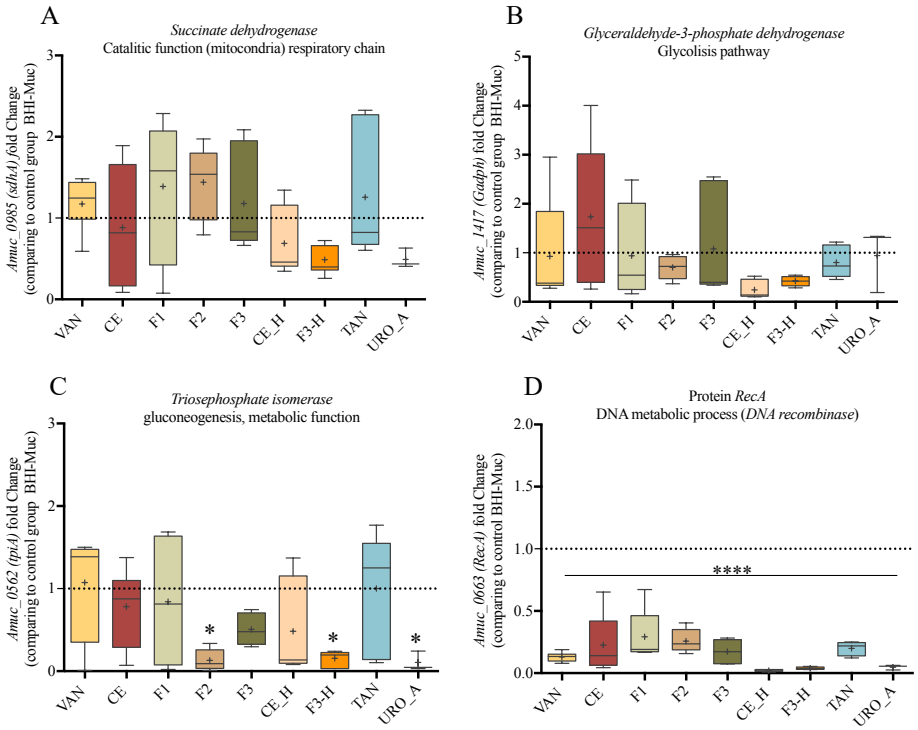

Figure S3. Akkermansia muciniphila exhibit down-regulations of genes coding for metabolic process under polyphenolic fractions.

The fold change of gene expression of Succinate dehydrogenase Amuc_0985 (A), glyseraldehyde-3-phosphate dehydrogenase *Gapdh* Amuc_1417 (B), triophosphate isomerase *tpiA* Amuc_0562 (C) and protein *RecA* Amuc_2077 (D) were analyzed by RT-qPCR normalized to HKGs *GyrA* and *RpoD* and compared to the expression of *Akk*-cells grown in the BHI-Muc control broth (dotted line normalized to 1.0). Boxes are the interquartile range; median values are plotted as bands and mean values are represented by the mark "+" within the boxes. Ordinary one-way ANOVA with Benjamini test for multiple comparison corrections were performed, *$p < 0.05$, **$p < 0.01$, ***$p < 0.005$, ****$p<0.0001$ compared to control.

Table S1. Phenolic characterization of cranberry extract

Phenolic content (mg/100 g dry weight)	
Polyphenol type	**Whole Cranberry extract (CE)**
Total phenolic content (%)	**31.33% ± 1.01**
Anthocyanins	**1628.2 ± 5.8**
Cyanidin 3-galactoside	35.5 ± 1.8
Cyanidin 3-glucoside	602.8 ± 1.8
Cyanidin 3-arabinoside	403.6 ± 1.0
Peonidin 3-galactoside	108.3 ± 1.8
Peonidin 3-glucoside	460.5 ± 1.9
Peonidin 3-arabinoside	17.6 ± 2.2
Proanthocyanins	**10738.9 ± 100.8**
Monomers	998.5 ± 5.6
Dimers	2528.8 ± 28.9
Trimers	1567.5 ± 17.1
Tetramers	958.0 ± 2.3
Pentamers	433.4 ± 1.8
Hexamers	295.4 ± 7.0
Heptamers	89.7 ± 2.0
Octamers	68.7 ± 2.4
Nonamers	64.5 ± 1.0
Decamers	33.7 ± 3.1
Polymers >10	3700.8 ± 29.6
Flavonols, flavan-3-nols and phenolic acids	**4964.5**
Catechin	63.5 ± 5.3
Epicatechin	429.5 ± 12.8
Gallic acid	1.0 ± 0.3
Protocatechuic acid	275.3 ± 7.5
P-coumaric acid	1189.8 ± 49.4
Caffeic acid	139.4 ± 4.1
Ferulic acid	23.9 ± 4.9
3-caffeoylquinic acid	0.2 ± 0.1
4-caffeoylquinic acid	21.9 ± 1.8
5-caffeoylquinic acid	524.2 ± 6.8
Quercetine	831.3 ± 31.9
Quercetine-glucoside	629.7 ± 18.1
Quercetine-galactoside	ND
Quercetine-rhamnoside	376.4 ± 5.1
Quercetine-xyloside	378.8 ± 13.0
Quercetine-arabinoside	79.6 ± 7.8
Rutin	ND

Results are expressed as mean of triplicate ± SD. ND, not detected.

Table S2. Proanthocyanins content of TAN-active extract

Polyphenols content (mg/100 g)	
Total proanthocyanins content (%)	**58.44% ± 0.01**
Monomers	241.43± 33.23
Dimers	9562.88 ± 28,9
Trimers	44668.02 ± 102.21
Tetramers	935.83 ± 43.57
Pentamers	463.46 ± 6.06
Hexamers	ND
Heptamers	ND
Octamers	ND
Nonamers	ND
Decamers	ND
Polymers >10	2571.44 ± 42.72

Results are expressed as mean of triplicate ± SD. ND, not detected.

Table S3. Primer sequences and their respective PCR efficiencies used in the present study

Gene	Sequences	Protein Cluster name	Slope	R^2	PCR Efficiency (E, %)	Exponent	Log E
Amuc_1286 Forward	GGGAAGTGGTGGACGGTATC	DNA chain gyrase *(GyrA)*	-3.50	0.9985	93.15	0.286	1.97
Amuc_1286 Reverse	CGGTGCGGAAGTAGTTGTCA						
Amuc_1626 Forward	GCACGGAAGAAGAGGACGAA	RNA Polymerase, sigma D *(rpoD)*, RNA polymerase sigma factor *SigA*	-3.52	0.9989	92.51	0.284	1.97
Amuc_1626 Reverse	TCACGGGTAAGCAGGGAAAC						
Amuc_0985 Forward	CCACATGATGAGGCCCAGTT	Succinate dehydrogenase or fumarate reductase, flavoprotein subunit *(sdhA)*	-3.63	0.9983	88.43	0.275	1.95
Amuc_0985 Reverse	TTACCTGACGACCACCAAGC						
Amuc_1417 Forward	AGAAGTAAACGCCGCCATGA	Glyceraldehyde-3-phosphate dehydrogenase *(Gadph)*	-3.46	0.9995	94.73	0.289	1.98
Amuc_1417 Reverse	AAGCCGGAGTCAAAGATGCA						
Amuc_0562 Forward	CCCTTCACCACCATTCCCTC	Triophosphate isomerase *(tpiA)*	-3.67	0.9994	87.41	0.273	1.94
Amuc_0562 Reverse	TGGCATCCGTTTCTCCGAAA						
Amuc_0663 Forward	GCGCCTTGGAGACAACGT	Protein *RecA* (DNA recombinase)	-3.47	0.9995	93.99	0.288	1.97
Amuc_0663 Reverse	GAGCGCGGTCAATCAGAAG						
Amuc_1413 Forward	GGCTGACTTCCTACCTGCTG	Capsular exopolysaccharide family	-3.49	0.9995	93.53	0.287	1.97
Amuc_1413 Reverse	GAAGGGTCAAAGGGAGTGGG						
Amuc_1470 Forward	TTGAAGGCATCCCAGTGTCC	Eight transmembrane protein *EpsH* (Exosortase Eps related)	-3.57	0.9999	90.68	0.280	1.96
Amuc_1470 Reverse	GGCTTCAAATCATCGCGACG						
Amuc_1018 Forward	AGGGTTCGTCTTTTCCGTCC	UPF0056 inner membrane protein (antibiotic resistance)	-3.52	1.0000	92.46	0.284	1.97
Amuc_1018 Reverse	ACGGGAGCTTGTATTTGCGT						
Amuc_1379 Forward	AATGAGCTGGAGAGATGCGG	Transport permease protein	-3.56	0.9994	91.00	0.281	1.96
Amuc_1379 Reverse	CTGGAAGGCACGGGAATCTT						
Amuc_0889 Forward	TGCCGGAAGTGTCTGTCATG	Efflux transporter, RND family, MFP subunit	-3.54	0.9997	91.58	0.282	1.96
Amuc_0889 Reverse	CGTCTGCCCTTCCTGATAGC						
Amuc_1627 Forward	GGTGTGGCTGTGGATGTTTC	D-alanyl-D-alanine dipeptidase	-3.55	0.9987	91.20	0.281	1.96
Amuc_1627 Reverse	GGAGTCTGTGGTGGAACTGG						
Amuc_2077 Forward	TGCCTCCGTCAATGTTCAGA	Polysaccharide export protein	-3.53	0.9942	92.07	0.283	1.96
Amuc_2077 Reverse	GGTTCCGTTGGTTTCCCTGA						
Amuc_2051 Forward	GCCAACATGCCTACGGATCT	Glutamate dehydrogenase	-3.71	0.9962	86.06	0.270	1.93
Amuc_2051 Reverse	GGTCTTCAGCTTGTGGTCCA						

GENERAL DISCUSSION AND CONCLUSION

The aims of the present thesis were to evaluate the prebiotic potential of polyphenols in modulating the gut microbiota and especially prompting the growth of *A. muciniphila,* and to study whether and how this bacterium might adapt to polyphenols. First, we proposed to study the prebiotic effects of polyphenol-rich cranberry and blueberry whole fruit powders and those of their fibrous fractions on the gut microbiota composition and functions in a murine model of diet-induced obesity. We focused on the role of both berry constituents to inhibit pathobionts associated to gut dysbiosis and host metabolic disturbances, and to selectively favour health-promoting symbionts, especially *A. muciniphila*. Second, we proceeded to identify which phenolic category was responsible for the observed *A. muciniphila* bloom, and reduce obesity associated metabolic and intestinal disorders. The approach consisted in administrating to mice a whole wild blueberry extract and three phenolic sub-fractions, constituted mainly by anthocyanidins, oligomeric and polymeric PACs at the same proportion as encountered in the total extract. In this model, we particularly investigated the histological morphology and mucin profile of colon tissues, as mechanisms by which, these compounds might restore the ecological niche of *A. muciniphila* in the context of obesity. Finally, we cultured *Akkermansia* in a mucin-enriched medium supplemented either with a cranberry whole extract, one of its three phenolic sub-fractions, or a phenolic microbial metabolite. The goal was to evaluate whether these polyphenols might affect the *Akkemansia* growth and elucidate whether, in turn, this bacterium expresses molecular mechanisms of defence and adaptation to polyphenols, which could explain the bloom observed in the whole microbiota. This *in vitro* model was useful to understand the interaction between *A. muciniphila* and distinct polyphenolic fractions and explain whether these compounds might elicit a particular pattern in this bacterium related to its probiotic potential in the host.

Effects of berry constituents in reducing obesity-associated markers in HFHS-diet induced obese mice

It is now clear that a number of metabolic disorders like obesity and T2D are associated with gut microbiota dysbiosis, including a reduced bacterial diversity, reduced gene richness

and functionality, loss of beneficial symbionts and increase of pathobionts, leading to intestinal epithelium damage and inflammation (Cheng et al., 2018a; Cotillard et al., 2013; Ley et al., 2006; Ravussin et al., 2012; Thingholm et al., 2019). Therefore, the stimulation of beneficial microbes, which has been shown to actively contribute to attenuating obesity and intestinal dysbiosis, constitute feasible therapeutic approach to prevent this disorder. Using a murine model of diet-induced obesity, we demonstrated that the phenolic compounds were responsible for the prebiotic-like effects on *A. muciniphila*, since such an effect was not significantly triggered by the fibrous fractions from the berries. In addition, symbionts associated to lean mice gut microbiota, were also promoted by the berry polyphenol-rich powders, including *Eggerthellaceae, Coriobacteriales, D. newyorkensis*, and *Angelakisella.* Furthermore, the analysis of the gut microbiome unveiled that beyond the taxonomic composition and microbial diversity, the gene richness and functions of the gut microbiota are, in a large part, determining the physiological outcomes in the host.

In the first animal model, blueberry as did cranberry polyphenol-rich powder attenuated gut pathobionts, but it was not reflected in the mouse phenotype, notably the BW loss. Here, the relative proportion of opportunistic pathogens found correlated to the consumption of the HFHS-diet, were inhibited by cranberry polyphenols, and by its fibrous fractions; these findings were reflected in a lower BW and a lower hepatic TG level in obese mice (see **Figure 1**). Particularly, we noticed that, albeit both polyphenol-rich berry powders inhibited opportunistic genera such as *Ruminiclostridium, Romboutsia* and *Oscillibacter* in HFHS-fed mice, cranberry inhibited the proportion of *Butyricicoccus, Anaerotruncus, Anaerovax, Turicibacter, Staphylococcus* and *Lactococcus*. Constrained distance-based redundancy analysis of the microbial functions showed that the mice fed the polyphenols-rich blueberry powder, as well as its fibrous fraction, presented a similar functional structure than the untreated HFHS-fed mice (**Figure 1**). By analyzing the FRI, we demonstrated that polyphenol-rich cranberry powder (rich in PACs), in addition to stimulating health-promoting bacteria, including *A. muciniphila,* significantly shifted the predicted functional profile away from that of untreated obese mice. These outcomes indicate that the inhibition of pathobionts and the functional traits of specific gut bacterial species were crucial in the progress of obesity. This last observation was also supported by a recent study which demonstrated that despite significant differences were found within the taxonomic structure

of the gut microbiota of obese individuals from different geographic origins, similar metabolic disturbances were consistently observed among them (Medina et al., 2019). In the present thesis the gut metagenome was predicted from the 16S rRNA gene sequencing, and of course, was relevant to elucidate the role of polyphenols on the gut microbiota and its functional contribution to the host health.

Very interesting, *A. muciniphila* was distinctly stimulated by both polyphenol-rich berry powders and PACs oligomer-rich polyphenolic fraction. This bacterium is a well-known biomarker of a healthy microbiome in humans and animals and considered a keystone against the development of obesity and other metabolic and inflammatory disorders (Derrien et al., 2017; Everard et al., 2013; Roopchand et al., 2015a). A variety of dietary polyphenols have demonstrated selective prebiotic effects on this unique gut representative species (Anhê et al., 2014; Collins et al., 2016a; Etxeberria et al., 2015; Henning et al., 2017; Kuhn et al., 2018; Li et al., 2015a; Masumoto et al., 2016; Pan et al., 2017; Roopchand et al., 2015b; Zhang et al., 2017b). Tannins and particularly the proanthocyanins appear to be the type of polyphenols responsible for the stimulation of this bacterium. The administration of A-type proanthocyanin-rich cranberry extract (Anhê et al., 2014), B-type proanthocyanins-rich grape extract (Kuhn et al., 2018; Roopchand et al., 2015a), ellagitannins-rich pomegranate extract (Li et al., 2015a), and apple oligomeric and polymeric proanthocyanins (Masumoto et al., 2016) have been shown to significantly increase the proportion of *A. muciniphila* in both humans and animals. We especially identified in a second animal model that the PACs enriched fractions were involved in the bloom of *A. muciniphila,* providing a favourable ecological niche to this bacterium, and responsible for the cardiometabolic benefits of the whole polyphenolic extract. The polymeric PACs improved the glucose homoeostasis in obese mice.

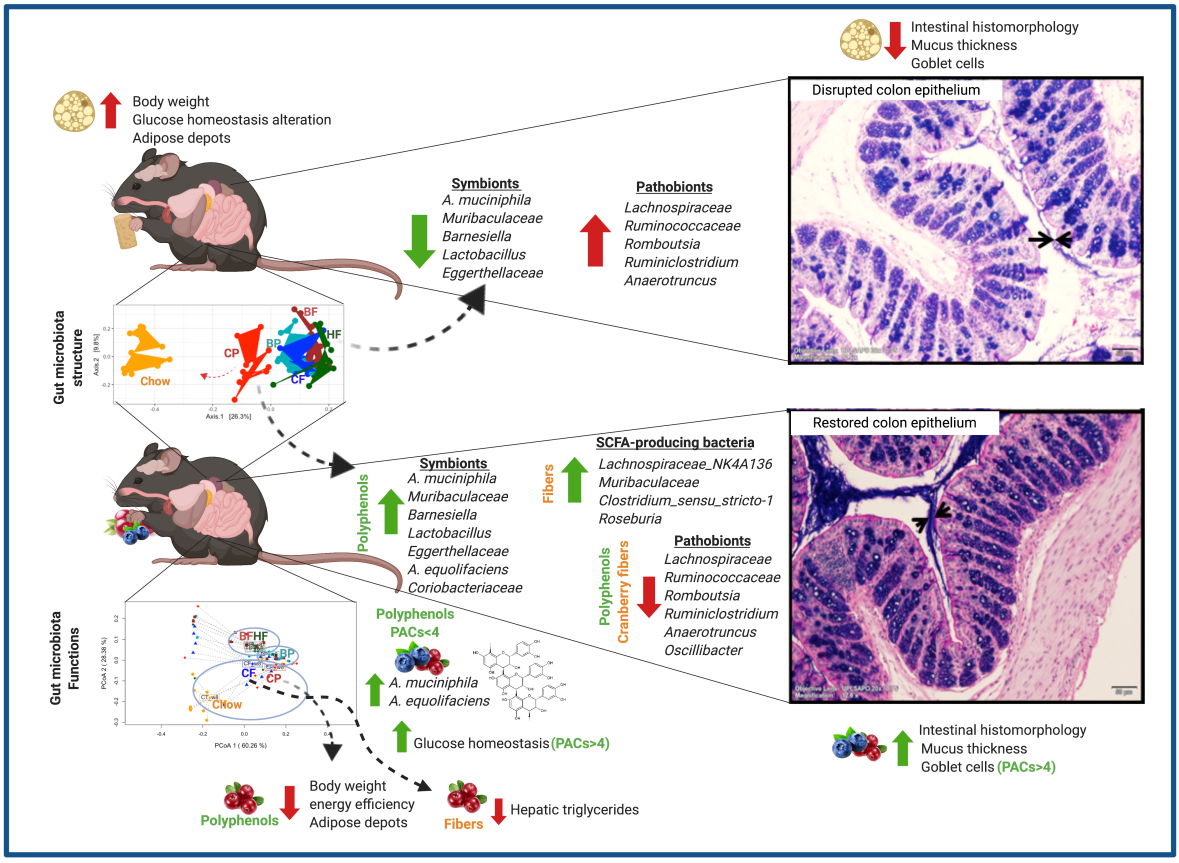

Figure 1. Prebiotic potential of berry polyphenols and fibres and their impact in preventing HFHS-diet induced obesity in mice.

Eight-weeks dietary supplementation with polyphenol-rich cranberry (CP) and blueberry (BP) powders distinctly shaped the gut microbiota structure of obese mice. Both polyphenol-rich berry powders inhibited HFHS-diet induced pathobionts associated to obesity and favoured symbiotic bacteria. The fibre-rich cranberry (CF) and blueberry (BF) fractions stimulated short-chain fatty acids (SCFA)-producing bacteria; contrary to the BF, only the CF additionally inhibited pathobionts. The gut microbial functions were positively influenced by the polyphenol-rich CP and CF in obese mice. Those changes were reflected in a reduced energy efficiency, reduced body weight and adipose tissue depot in mice fed the CP-diet, and in a reduced hepatic triglycerides level in mice fed the CF-diet. Within the blueberry whole extract, the polyphenolic fractions rich in oligomeric and polymeric proanthocyanidins (PACs<4 and PACs>4 respectively) significantly contributed to attenuating obesity-related alteration. Particularly, the fraction rich in oligomeric PACs<4 selectively prompted *A muciniphila* and *A. equolifaciens* in obese mice. The polymeric PACs>4 rich fraction improved the glucose metabolism and restored the *A. muciniphila* ecological niche by stimulating the mucin-secreting goblet cells in colonic tissues of obese mice.

Gut dysbiosis provokes impaired intestinal barrier function, decrease thickness of the mucus layer covering the gut epithelium, promote inflammation and stimulate systemic immune system (Everard et al., 2013; Kim et al., 2012; Liu et al., 2017; Mastrodonato et al., 2014; Schneeberger et al., 2015b). Through the histo-morphological analysis of colon tissues,

we demonstrated the detrimental effects of a HFHS-diet in the inner mucus layer and mucin-secreting GC. The results from the animal experiments demonstrate that the dietary supplementation with polyphenolic extracts improves the colonic mucus thickness in obese mice. Particularly, blueberry polymeric PACs significantly induced a higher number of mucin-secreting GC. In other studies, PACs-rich extracts and other phenolics also increase the thickness of the mucus layer by increasing the number of mucin-secreting goblet cells and both the synthesis of secretory and membrane bounded mucins (Pierre et al., 2013; Zhang et al., 2017b). We suggest that *A. muciniphila,* which is affected by a disrupted colonic mucus layer provoked by metabolic and inflammatory diseases (Png et al., 2010), can recolonize the gut by both the augmentation of mucin and suppression of competing opportunistic bacteria occupying its normal ecological niche.

In the present work, PAS/AB staining allowed us to observe significant changes in the proportion of different type of mucin-filled GC, in particular, neutral, acid and a combination of both, in the context of obesity. The PAS is specific to α-glycol-rich neutral mucins and the AB to acidic mucins, including sulfated or sialylated type mucins (Sharma and Schumacher, 1995). We specifically wanted to determine if this latter type of mucins could be indicators of the quality of the mucus and their susceptibility to the degradation by residing microbiota. Accordingly, sulfomucins and sialomucins (acid or mixed PAS/AB mucins) are more resistant to bacterial sialidases (Tarabova et al., 2016). Importantly, a trend to increase the acidic-mixed mucin in obese mice fed the blueberry polyphenolic fractions was remarked, suggesting that polyphenols might modulate the proportion of sulfated type or sialylated mucins; albeit, further analysis are needed. Particularly, the mucin glycosylation pattern, primarily, an increased glycan sulfation has been shown to play a protective role (Tobisawa et al., 2010). Recently, a positive correlation of *A. muciniphila* with higher proportion of sulfated mucin have been observed in patients showing attenuated inflammation and improved ulcerative colitis (Earley et al., 2019). Using HID-AB stain to quantify the percentage of sulfation in histological specimens of the colon in the three cohorts, the profiles indicated that the inflamed mucosa in acute UC was associated with a significant lower percentage of sulfomucin. Multiple linear regression analysis revealed the percentage of sulphation as a marker of *A. muciniphila* abundance (Earley et al., 2019).

Polyphenols enriched diets favor taxonomic biomarkers attenuating gut dysbiosis and obesity

Although to completely decipher a specific profile of a disrupted gut microbiome (dysbiosis) and its association with the etiology of diseases is as burgeoning area to be further exploited, promising findings have led to discriminate microbial biomarkers in a disease or eubiotic state. A high F/B ratio has been proposed as a marker of gut dysbiosis in obesity and other metabolic diseases (Koliada et al., 2017; Turnbaugh et al., 2008; Turnbaugh et al., 2006). However, this ratio has resulted an invalid indicator, being inconsistent throughout several studies (Walters et al., 2014; Zhang et al., 2012; Zhang et al., 2010). In the present thesis, the phenolic treatments in mice showed to significantly change the proportion of microbial members relative to the control counterparts, but this fact was mainly reflected at a finer taxonomic level, rather than in the proportion of the *Firmicutes/Bacteroidetes* phyla. Thus, specific bacteria species and the weight of their metabolic functions on attenuating obesity-associated alterations, appear to be more pertinent. In chapter I and II, unassigned genera belonging to *Ruminococcaceae* and *Lachnospiraceae* were characteristic of the gut microbiota of HFHS-diet induced obese mice as compared to Chow-fed mice, and they were inhibited by polyphenols supplementation, consistent with other studies (Cheng et al., 2018a; Tu et al., 2018; Ushiroda et al., 2019). The significant reduction of the relative proportion of those taxa by polyphenol enriched diets, appears to be related to the improvement of obesity phenotype. For instance, positive correlations were found between *Ruminococcaceae* (i.e *Ruminiclostrium*), *Lachnospiraceae* and BW gain in mice. On the contrary, inverse correlations were found between *Lactobacillus* spp., *Muribaculaceae*, *Clostridium_sensu_stricto_1* and *Eggerthellaceae* not only with BW (**Figure S1**), but with adipose mass depots, energy efficiency, and liver TG; while positive effects were observed in increasing caecum weight and colonic mucus thickness.

Noteworthy, *A. muciniphila* was a characteristic microbial biomarker of the gut microbiota of mice fed the polyphenols-rich berry diets and has generally been shown to be involved in improving host metabolic and inflammatory alterations (Everard et al., 2013; Plovier et al., 2017). *Adlercreutzia equolifaciens* was another species triggered upon polyphenols intake, which might contribute to host health by its polyphenol-degrading

capabilities, generating bioactive phenolic metabolites (Alakomi et al., 2007; Saha et al., 2016; Takagaki and and Bulletin, 2015). Our results are consistent with those reported by Ushiroda et al. (2019), who using C57BL/6N HFD-induced obese mice, demonstrated that EGCG significantly lowered the abundance of the genera *Ruminococcus, Lachnospiraceae*, and *Anaerotruncus*, and prompted higher abundance of the genera *Adlercreutzia* and *Akkermansia.* In this study*,* EGCG inhibited the BW gain and the hepatic triglyceride content induced by the HFD*,* and the *A. muciniphila* increase was associated with improvement in bile acid dysregulation. Likewise, Tu et al. (2018), using C57BL/6J mice fed an obesogenic diet, demonstrated the inhibitory effects of a black raspberries phenolic extract on 10 bacterial genera from the phylum *Firmicutes*, including *Ruminococcus,* and the stimulatory effect on *A. muciniphila,* which was increased 157-fold. Furthermore, the *Ruminococcus* genera and the *Clostridia* class*,* were inhibited in Winstar rats supplemented with grape seed proanthocyanidin extract for 8-days (Casanova-Martí et al., 2017). Additionally, we highlighted for the first time the capacity of polyphenol-rich cranberry powder to stimulate the bloom of the species *Dubosiella newyorkensis* (*Erysipelotrichaceae*), a potential new marker of eubiosis which was recently suggested to have probiotic and anti-obesity potential (Cox and Blaser, 2018).

Microbial enterotype-like clusters correlate to the intake of polyphenols and fibres

Enterotypes represent optimized cluster of microbial community composition with high connection to the dietary habits of the host (Costea et al. 2018). Using CCA-ordinations, the mouse gut microbiome showed a clear stratification, differentiating the HFHS, carbohydrates-rich Chow-fed mice, and the berry polyphenols or fibres fed mice. Those clusters were featured by specific bacterial taxa (see **Figure 2**). We showed that *Lachnospiraceae* and *Ruminococcaceae* were distinct taxonomic markers of the HFHS-fed mice gut microbiota and predictive metagenome, which were highly correlated with the obesity-associated phenotype, as was previously reported by Nakayama et al. (2017). Throught distance-based redundancy analysis, these authors also identified a positive correlation between the fat intake and the fecal abundance of *Ruminococcaceae* and *Lachnospiraceae* families, in children with westernized dietary habits. Particularly, the

western-diet drove the children microbiota towards the fat-associated *Bacteroidaceae* community (denoted as BB-type enterotype), which includes the genera *Lachnospira*, *Ruminococcus* and *Bacteroides,* whilst the lean children enterotype was characterized by *Prevotella* genus (Nakayama et al., 2017). In the present thesis, the enterotype-clustering approach led to establish the species-specific response to dietary polyphenols and how that contributed to greater improvements in obesity phenotype, notably the BW gain. The gut microbiota of lean mice fed the polysaccharide-rich Chow-diet was characterized by *Muribaculaceae* (previously classified as *S24-7*), which family belongs to carbohydrate-degrading specialists, characterizing a healthy mouse microbiome. The taxa of *Eggerthellaceae, Lactobacillus* and *Lachnospiraceae_NKA136_group* were features of the gut microbiota of both the mice fed polysaccharide-rich Chow-diet and those fed polyphenol-rich cranberry diet. Remarkably, *D. newyorkensis, Coriobacteriales* and *Akkermansia* were confirmed to positively correlate with the intake of polyphenol-rich cranberry powder and with a lower BW gain in diet-induced obese mice. These findings agree with the anti-obesity potential of *A. muciniphila* and *D. newyorkensis* demonstrated in previous studies (Anhê et al., 2014; Cox and Blaser, 2018). We failed to detect taxonomic markers correlated to the supplementation of a HFHS-diet with berry fibres; notably, mice fed the blueberry fibrous fraction presented a similar taxonomic composition of the gut microbiota to that observed in obese mice. However, it is worthy to note that three enterotypes were identified in the mice gut microbiota by using the clustering approach of partitioning around medoids (PAM) followed by Arumugam et al. (2011) and Costea et al.(2018); notably the *Bacteroidetes/Muribaculaceae* (ET-P), *Prevotella/Akkermansiaceae* (ET-P) and *Firmicutes-Ruminococcus* (ET-F) enterotypes. Here, we demonstrated that the HFHS-fed mice and those supplemented with berry fibrous fractions were linked to the *Firmicutes-Ruminococcus* enterotype, while lean mice fed the Chow-diet were categorized within the *Bacteroidetes/Muribaculaceae* and *Prevotella/Akkermansiaceae* enterotypes. Interestingly, mice fed the polyphenol-rich cranberry powder were strongly confined to the *Prevotella/Akkermansiaceae* enterotype, underlining the role of cranberry polyphenols in driving the obesity-associated microbiota to a healthier functional enterotype (de Moraes et al., 2017).

Moreover, using the MaAslin model as complementary tool, we determined which type of diet (HFHS-supplemented with polyphenol-rich berry powders, or fibre-rich fractions) were influencing the gut microbiome structure of obese mice. Overall, we established: 1) the link between the bloom of *Coriobacteriaceae* and *Eggerthellaceae* with the presence of polyphenols; 2) the cranberry fibres effect in increasing the abundance of the polyphenols-degrading families *Coriobacteraiceae* and *Eggerthellaceae*, emphasizing the strong interaction between non-extractible polyphenols with fibres; 3) the selective prebiotic effect of polyphenol-rich berry powders on *A. muciniphila*; and 4) the inverse correlations amongst bacterial obesity-associated pathobionts and the consumption of polyphenol-rich cranberry powder.

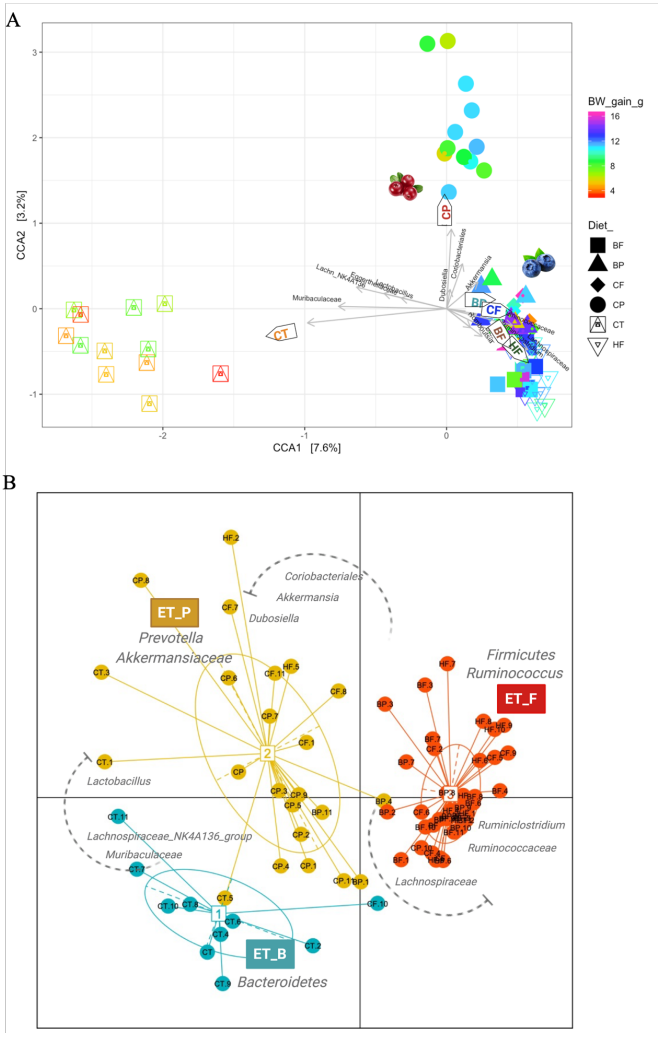

Figure 2. The dietary berry supplementation causes a distinct enterotype-like clustering.

A) Ordination of Canonical Correspondence Analysis (CCA) showing the connection between diet type and taxonomic biomarkers in mice gut microbiota. The arrows indicate the taxonomic markers discriminating the different groups. Lean mice fed a carbohydrate-rich Chow diet (CT) clustered to the left of the CCA; *Muribaculaceae* was the main taxonomic feature of this gut microbiota. Obese mice fed a high-fat high-sucrose diet (HF) clustered in the bottom right side of the CCA plot. *Ruminococcaceae, Romboutsia, Ruminiclostridium*, and *Lachnospiraceae* characterized this microbiota of obese mice. Mice fed HFHS-diet supplemented with polyphenol-rich whole cranberry powder (CP) were positioned in the upper right space of the CCA, showing lower body weight (BW) gain as compared to obese untreated mice; *Dubosiella newyorkensis, Coriobacteriaceae* and *Akkermansia muciniphila* characterized this microbiota. *Eggerthellaceae, Lactobacillus* and *Lachnospiraceae_NKA136* characterized both CT and CP-fed mice. Mice fed the HFHS-diet supplemented with polyphenol-rich whole blueberry powder (BP) and cranberry fibre fraction (CF) clustered in the mid-right side of the CCA. *Ruminococcaceae* was a taxonomic feature of CF-fed mice. *A. muciniphila* was characteristic of BP-fed mice gut microbiota and shared the same space as the CP-fed mice. Mice fed HFHS-supplemented with blueberry fibres (BF) shared the same space as the HF-group. *Romboutsia, Ruminiclostridium* were the main characteristics of BF gut microbiota. The colour of the symbols from each group represents the changes in mouse body weight gain in grams (denoted as BW_gain_g in the figure legend) after 8-week of intervention. B) Ordination on Jensen-Shannon distance metrics shows the enterotype clustering of mice gut microbiota (coloured ellipses) as determined by PAM methods used by Arumugam et al., (2011) and Costea et al., (2018), with dots representing abundance distributions of bacterial genera from each mouse and numbered white rectangles marking the centre of each enterotype. Three enterotypes were identified: 1) *Bacteroidetess* denoted as ET_B; 2) *Prevotella/Akkermansiaceae* denoted as ET_P; and 2) *Firmicutes/Ruminococcus* denoted as ET_F. Bacterial taxa that are principally responsible for the separation of mice enterotypes and correlated to the diets are listed. Diet-type codes follow that in graph A. Mice fed the CT-diet were categorized within the ET_B and ET_P; mice fed the CP-diet moslty fell into the ET_P cluster, while the mice fed the HFHS-diet, and the fibre-rich fractions were principally encompassed by the ET_F.

What about the berry fibres as prebiotics?

Non-digestible fibres are fermented in the colon into SCFAs essential to provide energy to colonocytes and to the maintain a regular immune response (Donohoe et al., 2011; Yan and Ajuwon, 2017). The dietary fibres are known to stimulate probiotics like *Lactobacillus* and *Bifidobacterium* (Bindels et al., 2015; Vulevic et al., 2013; Walton et al., 2012). In our experiments, the genus of *Bifidobacterium* was undetected in the mouse gut microbiota, but other beneficial bacteria were modulated by the berry fibre fractions. As a matter of fact, the family *Muribaculaceae,* considered a healthy biomarker of the mouse indigenous gut microbiota (Cao et al., 2019), as well as *Lactobacillus, Lachnospinaceae_NK4A136_*group and *Clostridium_sensu_stricto_1* with butyrate-producing abilities were stimulated by fibres. Nonetheless, the unfavourable metabolic outcome that was observed in the obese mice fed the blueberry fibre-rich fraction, led to question the desirable effect of stimulating the SCFA-producing bacteria in a condition of obesity-associated dysbiosis, without inhibiting the HFHS-diet increased pathobionts, which are detrimental for the host metabolic status. Specifically, dietary supplementation with blueberry fibrous fraction in dysbiotic obese mice, did not significantly affect the core microbiota and did not alter the proportion of pathobionts

associated with the obesity phenotype. In this case, it is possible that the positive effect of SCFA-producing bacteria was not strong enough to compensate for the diet-induced metabolic alterations. On the contrary, the cranberry fibre-rich fraction, which contained significant amount of non-extractible PACs, was more effective in reducing the relative abundance of *Ruminococcaceae* (i.e. *Ruminiclostridium*, *Oscillibacter,* and *Anaerotruncus*) and in lowering the TG level in obese mice than the blueberry fibres which had less residual polyphenols. Thus, non-extractible polyphenols interacting with fibres were shown to restore and/or promote the colonization of carbohydrates-degrading bacteria while inhibiting the above opportunistic genera. Additionally, the cranberry pectic polysaccharides have been shown to exert antimicrobial action against pathogens (Hotchkiss et al., 2015; Sun et al., 2015), a feature that has not yet been demonstrated for blueberry cell wall polysaccharides. In summary, the pleiotropic action of polyphenols and their association with fibres, either free or bound, is a promising therapeutic dietary strategy to counteract obesity, emphasizing the role of the antimicrobial action of both cranberry constituents against opportunistic bacteria.

Are the antimicrobial properties of phenolics important for attenuating HFHS-diet induced obesity?

Antibiotics, while not always specific, are generally addressed to inhibit gut pathogens, which open space to the colonization of symbionts and health beneficial microbes; in some cases antibiotics are considered reliable therapy for dysbiosis-associated diseases (Hansen et al., 2012; Ianiro et al., 2016; Ray and Aich, 2019; Rodrigues et al., 2017). The best example illustrating the microbiota manipulation by antibiotics, is the inhibition of *Firmicutes* phylum (Gram-positive bacteria) and the promoting effect on *Verrucomicrobia* (*A. muciniphila,* Gram-negative) by Vancomycin (Ray and Aich, 2019). Vancomycin is a glycopeptide antibiotic that kills bacterial cells by inhibiting cell wall peptidoglycan biosynthesis, thus affecting mostly Gram-positive bacteria (Ge et al., 1999). By using Th2 (BALB/c) and Th1-(C57BL/6) mice models, Ray and Aich (2019) showed that the vancomycin treatment, whilst reducing *Firmicutes* and *Bacteroides* and increasing *Proteobacteria* until day 4, increased the phylum *Verrucomicrobia* from day 5 of intervention. Importantly, the increased *Akkermansia* proportion was linked to a decreased inflammation and improved glucose

homoeostasis in the host. The authors remarked that albeit vancomycin treatment initially increased pathogenic *Proteobacteria*, subsequent doses of the antibiotic prompted *A. muciniphila* in the gut, providing significant health-related benefits. Importantly, inducing *A. muciniphila* by vancomycin treatment in early life was also demonstrated to reduce the risk of developing diabetes in NOD mice (Hansen et al., 2012). Our results showed that polyphenols, like antibiotics, inhibit opportunistic pathogens correlated to obesity. In the chapters I and II, we demonstrated that members of the *Rumicococcaceae* and *Lachnospiraceae* families are consistently encountered in the HFHS-diet fed mice. These findings agree with those of previous studies which showed that those pathobionts were increasing the risk and persistence of metabolic and intestinal diseases in mice and humans. For instance, *Ruminococcaceae* (i.e. *Anaerotruncus, Oscillospira,* and *Ruminococcus*) genera have been associated with aberrant colonic crypts in HFD-fed mice treated with azoxymethane (Zeng et al., 2018) and found co-exclusive with *Akkermansiaceae* in IBD (i.e *A. muciniphila*) (Png et al., 2010). *Lachnospiraceae bacterium* and members of *Ruminococcaceae* were also abundant in obese subjects (Liu et al., 2017). Additionally, members of *Lachnospiraceae* family are prevalent in IBD subjects and have been associated with high LDL cholesterol levels (Backhed et al., 2007; Beaumont et al., 2016; Fu et al., 2015; Turnbaugh et al., 2006). Noteworthy, the administration of polyphenols-rich extract and berry powders prevented the overgrowth of *Ruminococcus, Ruminiclostridium*, and *Lachnospiraceae* (*Firmicutes* phylum) and significantly prompted *A. muciniphila* among other resilient/tolerant beneficial members of the gut microbiota, such as *Lactobacillus*, *A. equolifaciens*, and *Eggerthellaceae.* Our findings concur with the observations that changes in the proportion of the phyla *Firmicutes* and *Bacteroidetes* decreased bacterial energy metabolism induced by polyphenols (Masumoto et al., 2016; Xue et al., 2016). A reduced abundance of *Clostridium*, *Lachnospiraceae* and *Ruminococcus* genera belonging to the phylum *Firmicutes*, but the increase of *Faecalibacterium* and *Lactobacillus* species have been induced by polyphenols (Casanova-Martí et al., 2018; Cheng et al., 2018b; Song et al., 2015; Tzounis et al., 2011). Furthermore, the *Bacteroides* and *Prevotella* genera belonging to the phylum *Bacteroidetes* are also triggered by polyphenols (Attri and Goel, 2018).

Polyphenols, in addition to cause cell membrane damage like vancomycin does (Lacombe et al., 2013e), have the ability to decrease bacterial virulence (Shah et al., 2008), cause

quorum sensing disruption (Maisuria et al., 2016b), decrease nutrient accessibility (i.e. by chelating iron, interacting with proteins), and alter bacterial metabolism (Lacombe et al., 2010b; Rempe et al., 2017; Xue et al., 2016). These antimicrobial mechanisms may be involved in the growth inhibition of different gut opportunistic bacteria from the phylum *Firmicutes*, resulting in an increase of probiotics and polyphenols-tolerant symbiotic bacteria. Our results sustain this working hypothesis based on the fact that polyphenol induced inhibition of pathobionts, thereby improving gut dysbiosis and metabolic alterations. We observed an over-representation of gut microbiota functions accounting for antimicrobial protection and xenobiotic metabolisms by using both Tax4Fun2 and PICRUSt bioinformatic tools in the two animal models studied (chapter I, berry powders and chapter II, polyphenolic fractions). Notably, microbial functional pathways, such as biosynthesis of secondary metabolites, butanoate metabolism, benzoate degradation, drug resistance to antimicrobial, ABC transporters, membrane transporters, and bacterial motility proteins were significantly increased in mice fed the polyphenols-rich diets as compared to control counterparts. These findings are coherent with the role of phenolics as antimicrobials, in modulating the bacteria activity, resistance mechanisms to antimicrobials or membrane protection strategies (see **Figure 3**). Other authors have reported that gut bacteria growing in presence of polyphenol supplemented medium, modulate ABC-type and multidrug transporters, genes involved in cell wall synthesis, xenobiotic rejection and DNA synthesis and repair (Firrman et al., 2018; Firrman et al., 2016a).

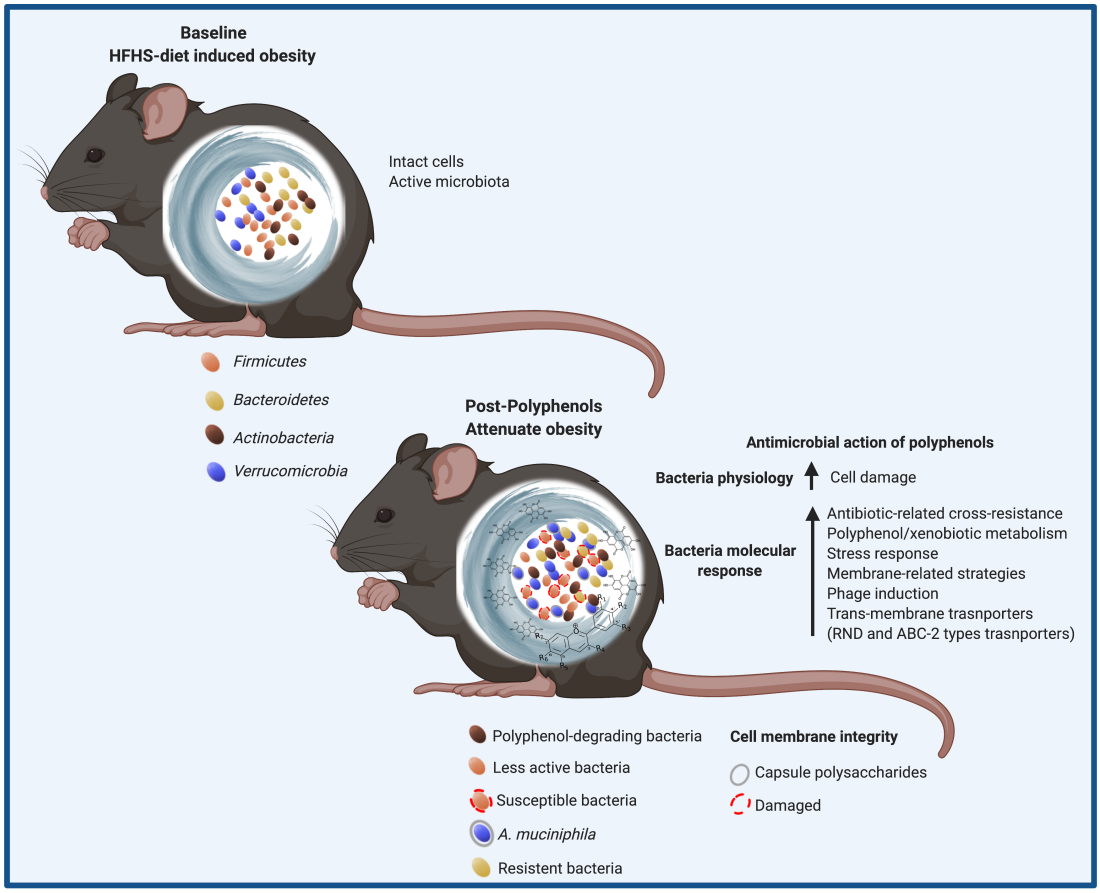

Figure 3. Impact of polyphenols on bacterial community-wide gene expression: insights from A. muciniphila in vitro model.

The HFHS-diet induces higher proportion of *Firmicutes* reported to be more metabolically active in obesity, and lower the proportion of symbionts, such a *Verrucomicrobia (A. muciniphila).* The antimicrobial action of polyphenols influences microbial physiology and triggers expression of multi-drugs resistance and metabolism genes. Polyphenols, acting as antibiotics, target cell wall biosynthesis, provoke cell wall damage and modify the structure of the active microbiota found in obesity. Bacteria possessing the genetic degrading machinery might modify the polyphenols efficacy and their impact on the cells. Members of *Actinobacteria* phylum (i.e. *Coriobacteriaceae* and *Eggerthellaceae*) are capable of metabolizing polyphenols. Members of *Firmicutes* phylum are susceptible to polyphenols intake in mice. *A. muciniphila* appears resistant to polyphenolic fractions rich in anthocyanins, PACs oligomers and polymers. Molecular tools including genes coding for RND and ABC-2 type transporters, antibiotic-resistance, production of capsule polysaccharides, change of peptidoglycan structure and energy management are involved in *A. muciniphila* resilience upon polyphenols.

The prebiotic-like effect of polyphenols implies species-specific enzymatic and molecular adaptation to phenolics

The bacterial adaptation to phenolic antimicrobial activity, as well as, the enzymatic capability to degrade polyphenols by probiotic bacteria might explain their bloom or their

supression in the colon. Berry polyphenols were shown to decrease bacterial pathogens (e.g. *Escherichia coli* O157: H7 and *Listeria monocytogenes*) and stimulate the colonization of probiotic *Lactobacillus rhamnosus* (Lacombe et al., 2013c; Lacombe et al., 2012; Puupponen-Pimiä et al., 2005). Strains of *Lactobacillus* such as *L. plantarum*, *L. casei* and *L. acidophilus* have been shown thrive in presence of polyphenols because of their ability to metabolize tannins and grow in presence of polyphenolic extracts enriched media (Hervert-Hernández et al., 2009; Reverón et al., 2013; Tabasco et al., 2011). Similarly, the increased relative proportion of *Bacteroides* spp. species by polyphenols is attributed to their bacterial catabolism (Attri and Goel, 2018). In the present work, we noticed a significant increase of the proportion of *Eggerthellaceae* and *Coriobacteriaceae* families (i.e. *A. equolifaciens*) by polyphenol-rich berry powders and polyphenolic fractions in obese mice. *Coriobacteriaceae* and *Eggerthellaceae* families have the unique capacity to break down polyphenols and can thus use them as a trophic factor for growth. Among the species belonging to these families, *Gordonibacter* spp., *Eggerthella lenta* and *Adlercreutzia equolifaciens* have been identified as polyphenols-converting gut bacteria (Braune and Blaut, 2016). These species are known to catalyze ellagitannins and flavan-3-ols, and have the capacity to cleave the C-ring of all (epi)catechin stereoisomers and other derivatives (Takagaki and and Bulletin, 2015).

Microbial phenolic metabolites, as their native compounds, might exert antioxidant, antiproliferative, and anti-inflammatory activities (Alakomi et al., 2007; Saha et al., 2016). Especially, a number of polyphenol-degrading bacteria have been shown to potentiate the bioactivity of parent polyphenols. This is the case of diaizin producing equol, lignans producing enterolactones, xanthohumol producing 8-prenyl naringenin, and ellagitannins metabolized to urolithins (Espin et al., 2017). Authors also believe that PACs can be potentiated by bacteria to produce active isomers of valerolactones. The bioavailability and potential bioactivities of valerolactones are very topical and the focus of the current research (Mele et al., 2017; Mena et al., 2019). Indeed, valerolactone isomers were recently shown to reduce monocyte adhesion to vascular endothelium with potentialities in prevention of atherosclerosis (Lee et al., 2017). Obviously, changes in microbiota functions would have repercussions in producing or degrading certain metabolites that have marked effects in the well-being of the host. Studies have found that xenobiotic metabolism, particularly linked to

polyphenols by the gut microbiota is associated with reduced inflammation, promoting gut health in context of obesity (Fang et al., 2018; Fernandez-Millan et al., 2014).

Can *Akkermansia muciniphila* degrade polyphenols?

Bacteria may exhibit inducible machinery adapted to either degrade polyphenols or to manage cell-protection mechanisms that must be activated by the polyphenol presence. In this thesis, the selective prebiotic effect of polyphenols on *A. muciniphila* were in part, confirmed by the restoration of its ecological niche *in vivo*. In parallel, the genetic and phenotypic analyses of *A. muciniphila* grown statically in presence of different classes of polyphenols led us to uncover specific mechanisms by which *A. muciniphila* metabolically and physiologically adapt to the polyphenolic fractions *in vitro* (discussed below). This bacterium has the molecular capacity to maintain growth in presence of the molecules in monoculture condition and is resilient after polyphenols intake within a microbial community. However, to our knowledge, the enzymatic potential of *A. muciniphila* to break down these compounds has not been investigated. To shed light on this, we screened the sequenced *Akkermansia's* genome *in-silico* in search for genes involved in the degradation of polyphenols. Surprisingly, we found out that *A. muciniphila* (ATCC BAA-835) harbors two genes linked to flavonol quercetin degradation: a cupin domain-containing protein encoded by Amuc_0801 (NCBI Reference Sequence: WP_012419849.1) and γ- carboxymuconolactone decarboxylase encoded by Amuc_1806 (NCBI Reference Sequence: WP_081429203.1). The *in-silico* analysis of the conserved domains (CD) and protein architecture of those gene sequences, led to identify potential matches and similarities against deposited sequences of enzymes quercetinases in the NCBI resources (Conserved domain search service). Interestingly, the CD-analysis showed a significant hit (1.79e-19 < E-value < 0.01,) of γ-carboxymuconolactone decarboxylase with Cupin domain protein related to quercetin dioxygenase (*QdoI*, COG1917). The quercetinases have been mostly described in plant-associated fungi, however, they have also been described in the bacterial species *Bacillus subtilis* (Fetzner, 2012; Schaab et al., 2006). The cupin-containing protein with activity of quercetinase *(VdQase)* and the *QdoI* are dioxygenases with a cupin fold that are able to cleave two C-C bonds from the heterocyclic ring of flavonol quercetin (Fetzner, 2012; Hadrami et al., 2015).

Fecal microbiota has demonstrated the production of the metabolites of quercetin including 3-(3,4-dihydroxyphenyl) propionic acid, 3,4-dihydroxyphenylacetic acid, 3,4-dihydroxybenzoic acid (i.e., protocatechuic acid), and phenylacetic acid (Peng et al., 2017; Serra et al., 2012), with a potential role in the improvement of an impaired glucose metabolism (Carrasco-Pozo et al., 2015). Importantly, recent published study reported that the administration of quercetin to obese Wistar rats favoured *A. muciniphila* fecal abundance, concomittantly with the prevention of body weight gain and reduced serum insulin level (Etxeberria et al., 2015). Altogether, these findings along with the *in-silico* analysis presented in this thesis suggest that *A. muciniphila* might thrive on dietary quercetin owing to the presence of quercetinases and favour the increase of this bacterium in the host gut. However, in depth studies are required to confirm this proposition.

Apart from the putative enzymatic ability of *A. muciniphila* to degrade quercetin, studies have suggested that this bacterium could degrade hydrolyzable tannins, such as ellagitannins (Henning et al., 2017; Li et al., 2015a). This fact stems from the correlation of this bacterium with the presence of the microbial metabolite Urolithin-A, and the *in vivo* and *in vitro* stimulation of *A. muciniphila* by pomegranate extract. This is a very interesting suggestion that will necessitate further research. In the present thesis, we examined the *A. muciniphila* physiological response to the presence of Urolithin-A and evaluated the degradation of this molecule in the culture medium. Noteworthy, we did not observe significant changes in the concentration of urolithin-A in the *Akkermansia's* growing medium, indicating that *A. muciniphila* does not degrade this metabolite upon 24h of incubation as presented in the **Figure S2**. On the contrary, this phenolic metabolite typically induced molecular responses in *A. muciniphila*, which is later discussed.

Polyphenols induce antimicrobial adaptation mechanisms linked to cell membrane transporters in *A. muciniphila*

In the chapter III of the present thesis, changes in the cell morphology and genetic expression involving defence mechanisms to antibiotics were evaluated in *Akkermansia* grown with cranberry extract or its polyphenolic fractions rich in anthocyanidins, oligomeric and polymeric PACs. Antibiotics targeting the cell wall synthesis (i.e. vancomycin and β-

lactams), induce resistance mechanisms in bacteria by altering the hydrophobic properties of the membrane or by changing the activity of porins or efflux pumps (Fernandez and Hancock, 2012). Polyphenols appear to elicit analogous mechanisms in *A. muciniphila* as does vancomycin. Initially, we decided to grow *Akkermansia* in a vancomycin supplemented medium, since some reports demonstrated that this antibiotic exerted a prebiotic-like effects on *A. muciniphila* in humans and rodents (Hansen et al., 2012; Ray and Aich, 2019). Interestingly, the expression of the inner membrane protein (Amuc_1018), the RND membrane transporter (Amuc_0889), and of course, the vancomycin resistance gene *VanX* (Amuc_1627) were up-regulated in vancomycin-treated *Akkermansia* cells as compared to control culture (see **Figure 3**). Interestingly, *A. muciniphila* also up-regulate the *VanX* gene (conferring resistance to vancomycin) in presence of the polyphenolic fractions. This mechanism is used by bacteria to change the cell wall peptidoglycan structure (Lessard and Walsh, 1999). In parallel to the induction of the *VanX* gene responsible for a putative modification of the bacterial cell-wall peptidoglycan structure, we observed an alteration of the usual shape of the bacteria and a typical cell elongation of *Akkermansia* (see **Figure S3**); this finding is a well-known defence and resistance response to antibiotics in Gram-negative bacteria (Otero et al., 2017). Additionally, *A. muciniphila* made use of membrane transporters to detoxify the presence of polyphenols in the growing environment. For instance, the anthocyanins rich fraction, only provoked slight wrinkled surface on *Akkermansia* cells, and triggered the expression of the efflux transporter RND family (Amuc_0889) and the UPF0056 inner membrane protein associated to antibiotic resistance, whereas it lowered the expression of *tpiA* and *RecA*, involved in glucose metabolism and protection against oxidative damage and other environmental stresses, respectively. These observations signify that polyphenols can affect bacteria through both oxidative damage and disruption of the cell envelope. In line with this, a proteomic analysis of *L. plantarum* challenged with tannic acid showed that it modulates metabolic capacity to save energy and expresses proteins involved in oxidative stress defence and cell wall biogenesis (Curiel et al., 2011), even though, this strain has been demonstrated to degrade tannins and being promoted by polyphenols (Filannino et al., 2018; Fritsch et al., 2016; Jiménez et al., 2013; Tabasco et al., 2011). Consistent with the property of polyphenols to affect the bacteria cell wall (Lacombe et al.,

2013b), we demonstrated that *A. muciniphila,* regulates genes playing a key role in the peptidoglycan biosynthesis in response to phenolics as does the probiotic *L. plantarum*.

The RND superfamily is not only capable to expel a wide range of substrates, but it can also intervene in bacteria adaptation to the environment (Alvarez-Ortega et al., 2013). For instance, rhizosphere microbiota significantly exploits different efflux pumps to support bacterial plant colonization (Burse et al., 2004; Hernandez-Mendoza et al., 2007; Palumbo et al., 1998; Pletzer and Weingart, 2014). In plant ecosystems, polyphenols have been identified to act as effectors of RND efflux pumps. The multifarious functions of membrane transporters in environmental ecosystems are beyond the scope of the present thesis, but this exemplifies the potential role of RND transporters for effective gut colonization by *A. muciniphila*. Importantly, *A. muciniphila* growth was unaffected by the presence of polyphenolic fractions; conversely, the presence of the metabolite Urolithin A stimulated its growth by 167%. Indeed, it has been reported a strong correlation between a higher proportion of *A. muciniphila* with the presence of urolithin A (Garcia-Villalba et al., 2017; Tomás-Barberán et al., 2017). The up-regulation by 5.7-fold of the gene coding for the RND transporter (Amuc_0889) was crucial to sustain a higher *Akkermansia* growth in Uro-A supplemented medium as compared to control. Remarkably, RND-type transporters have been shown to be essential for Gram-negative bacteria to resist host-derived substrates, such as bile salts, and consequently, growth and survive in the intestinal tract (Piddock, 2006). It is also worthy to note that urolithins exert antimicrobial and anti-quorum sensing activities, for example, by inhibiting N-acyl homoserine lactones (AHL), a QS signal molecule involved in cell population density and biofilm formation (Gimenez-Bastida et al., 2012; Mendez-Vilas et al., 2011). Urolithins A and B have been shown to alter the expression levels of genes critically involved in the synthesis of lactones and swimming motility of the enteropathogen *Yersinia enterocolitica* (Mendez-Vilas et al., 2011). These results suggest that dietary derived polyphenols metabolites (i.e. urolithin A), as demonstrated for their precursor ellagitannins, may exert antimicrobial effects in the colon and suppress the colonization of opportunistic bacteria, contributing to an eubiotic microbiota in the gut. In the present thesis, we could demonstrate that *A. muciniphila* also has the capacity to adapt to urolithin A by producing CPS and employing membrane-based transporters.

Polyphenols induce the expression of capsule polysaccharides and exopolysaccharides by *A. muciniphila*

In addition to induce antibiotic-related genes to confer cross-resistance, polyphenols may induce the expression of genes to cope with the physical attack to the cell wall or could act on mechanisms to regulate cell physiology in *A. muciniphila.* The chain length (DP), the type of polyphenols and the dose or concentration showed to have a crucial role in the modulation of those antimicrobial protection mechanisms in bacteria. The *in vitro* assays on *A. muciniphila* confirmed that PACs were influencing most of the putative transpeptidase exopolysaccharide locus protein *H* and the capsular polysaccharide biosynthesis protein. We could demonstrate that within the whole cranberry extract, the polymeric PACs were significantly inducing the secretion of slime polysaccharides and the formation of a CPS, and such an effect was confirmed by molecular and morphological analyses in *A. muciniphila.* By doubling the concentration of the whole cranberry extract (CE-H) and its fraction rich in polymeric PACs (F3-H), we observed that *A. muciniphila* increased by 6.0 and 7.4-fold the expression of *Eps-H*, respectively, and by 2-fold the CPS for both extracts. The secretion of CPS/EPS products is often addressed as a mechanism to keep the outer membrane from being penetrated by antibiotics, but also to allow the bacteria to grow and save energy under somewhat unfavourable condition in the gut (Moradali and Rehm, 2020). The administration of *A. muciniphila* grown under mucin-depleted conditions was shown to be effective in reducing obesity and improving intestinal barrier integrity of obese mice (Shin et al., 2019). In this study, an outer membrane protein (Amuc_1100) was elicited in *A. muciniphila* by the absence of mucin, and found to provide a probiotic role against obesity (Plovier et al., 2017; Shin et al., 2019). However, the capacity of *Akkermansia* to produce CPS/EPS structures, as well as their glycobiological content is an underexplored area of research. The polysaccharide capsules and exopolysaccharides of this bacterium, which were demonstrated to be influenced by polyphenolic fractions, might contain distinctive component sugars, and elicit physiological pathways, positive for host health. Multiple mechanisms exist for CPS/EPS synthesis, being well studied in *E. coli* systems (Bliss and Silver, 1996; Willis and Whitfield, 2013). For instance, the Wza and Wzy-dependent mechanism, which implies glycosyltransferases action to assembly oligosaccharides units in the cytoplasm. These

oligosaccharides are subsequently polymerized into longer chains on the cell surface (gram-positive bacteria) or the periplasm, and then exported to the cell surface (gram-negative bacteria) (Cuthbertson et al., 2009). Another mechanism employed by Gram-negative bacteria is the ABC transporter–dependent synthesis, where the entire glycan chain is polymerized in the cytoplasm face of the inner membrane; the completed molecule is then exported by the ABC transporter (Cuthbertson et al., 2010). A third mechanism is the synthase-dependent system, where a single protein serves as both a polymerase and an exporter, but the details of the export process are unknown. Synthases are processive glycosyltransferases involved in the formation of important biological molecules, including bacterial cellulose, hyaluronan, and poly-β-D-N-acetylglucosamine (GlcNAc) (Cuthbertson et al., 2010).

A. muciniphila encodes multiple gene clusters that enable it to produce larger amount of CPS/EPS. We identified, through *in silico* analysis, a gene set coding for capsular polysaccharide biosynthesis and polysaccharide transmembrane transporter activity and outer membrane and EPS production genes, which are listed in the **Table 1**. In the present thesis, we demonstrated that when *A. muciniphila* is cultured on a mucin-based medium containing cranberry polyphenolic fractions or polyphenols' microbial metabolite Urolithin A, the expression of a capsular polysaccharide biosynthetic protein (Amuc_1413), transmembrane protein H linked to the synthesis of exopolysaccharide *EpsH* (Exosortase, Amuc_1470), and a transmembrane transport protein (ABC-type permease, Amuc_1379) are significantly stimulated. The formation of CPS and the secretion of EPS were confirmed by Transmission electronic microscopy (TEM) observations after ruthenium red staining of *A. muciniphila* cells. We hypothesize that as the outer membrane protein Amuc_1100, glycopolysaccharide-rich microbial product, herein demonstrated to be produced from the selective pressure by polyphenols, might also trigger favourable immune and metabolic response counteracting obesity. The increase in *A. muciniphila* EPS and CPS by cranberry polyphenols might contribute to human health by positively affecting the composition of gut microbiota, by maintaining the integrity of epithelial mucosa and preserving intestinal homoeostasis. Due to their physicochemical properties, namely their film forming capacity and their rheology (viscosity, gelation, etc.), the secreted polysaccharides might improve the integrity of the mucosal barrier by increasing the thickness of the mucus layer, and decreasing

the susceptibility to colonization by pathogens. Likewise, both capsular (CPS) and free polysaccharides (EPS) of members of gut microbota have long been shown to play a major role in modulating the immune response. Examples of immunomodulatory polysaccharides, are those from the Gram-positive probiotics *Bifidobacterium breve* and *Lactobacillus plantarum* (Fanning et al., 2012; Zhou et al., 2019), and the Gram-negative symbionts *B. thetaiotaomicron* and *B. fragilis* (Martens et al., 2009; Porter et al., 2017). CPS molecules induce Tregs in the intestine and suppress inflammation, but also support the adaptation of probiotics to the intestinal microenvironment (Neff et al., 2016; Porter et al., 2017). The plethora of polysaccharides and glycans that these bacterial species supply to the intestinal milieu might be fermentable substrates for various intestinal bacteria (Lammerts van Bueren et al., 2015). Therefore, glycan-mediated symbioses may also occur between *A. muciniphila* and other microbial members of the human intestinal ecosystem.

Table 1. *Genes set coding for capsular (CPS) and free polysaccharides (EPS) biosynthesis in A. muciniphila genome*

Gene symbol	Protein cluster name	Accession number	Conserved domains (CD)
Amuc_1413	Capsular polysaccharide biosynthesis protein	WP_012420451.1	Bacterial tyrosine (BY)-kinase Exopolysaccharide transport protein family 187735905
Amuc_1414	Polysaccharide export protein	WP_012420452.1	Wza superfamily 187735906
Amuc_1470	Eight transmembrane protein *EpsH* Exosortase/archaeosortase family protein	WP_012420507.1	Exosortase_*EpsH*, PEP-CTERM anchor motif. Locus associated with biosynthesis of the exopolysaccharide methanol-an. 187735961
Amuc_2077	Polysaccharide export protein	WP_012421100.1	Wza superfamily Polysaccharide biosynthesis/export protein 187736555
Amuc_2078	Capsular exopolysaccharide family	WP_012421101.1	Bacterial tyrosine (BY)-kinase tyrosine-protein kinase Wzc 187736556
Amuc_2098	Acyltransferase 3	WP_012421121.1	Peptidoglycan/LPS O-acetylase *OafA/YrhL* 187736576
Amuc_1379	ABC-2 type Transport permease protein	WP_012420418.1	Capsular polysaccharide export systems in gram-negative bacteria 187735872

The use of cranberry polyphenolic fractions or urolithin-A for the production, isolation and glyco-characterization of *Akkermansia*'s polysaccharides, for the prevention or treatment of metabolic diseases, is patentable. Promising ongoing experiments is being conducted to substantiate the discovery claim. The characterization of these molecules which may have many advantages over prebiotic compounds modulating the intestinal microbiota (postbiotics), would open new avenues for the prevention and treatment of metabolic and inflammatory bowel diseases.

Concluding remarks

The present thesis provides a better understanding on the contribution of berry polyphenols and fibres in promoting bacteria that can restore a quantitative deficiency induced in a context of obesity (chapter I). The advance in bioinformatic technics and recently available statistical packages have allowed a more in-depth and detailed characterization of the gut microbiome, providing not only information on the taxonomic composition, but also inferring specific alterations on the functional profile of the gut microbiota. The use of Tax4Fun2, PICRUSt and multivariate MaAslin model, were useful to establish relevant correlations between the predicted functional changes of the gut microbiota with the impact that it may trigger in the host phenotypes. In addition, multivariate correlations led to connect the presence of polyphenols and fibres as berry constituents, with the relative abundance of a particular phylotype. The prediction of functional capabilities of the gut microbiota by bioinformatic tools, could enable the detection of metagenome variation in obesity and the preventive role of polyphenol-rich diets. However, the accurate characterization of microbial functional pathways involved in the attenuation of metabolic disorders, require further studies by other methods such as transcriptomics and proteomics, useful for microbiome-based precision therapies.

We demonstrated that depending of their nature, the polyphenols distinctly modulate the gut microbiota (Chapter II). First, the PACs-rich fractions were contributing the most to a significant bloom of *A. muciniphila* and enhanced its ecological niche by increasing mucus thickness and GC number in obese mice. Second, the polymeric PACs-rich fraction triggered stronger antimicrobial adaptation in *A. muciniphila*, encompassing mechanisms of cell-wall

protection and physiological metabolism (chapter III). Importantly, this is the first study, uncovering molecularly and morphologically, the capacity of *A. muciniphila* to produce CPS and EPS upon the exposure to PACs and urolithin A. Both bacterial by-products might fall into the concept of post-biotics (Cuevas-Sierra et al., 2019), since increasing evidences are pointing *A. muciniphila* membrane components as potential probiotic. Altogether, both animal model and *in vitro* approaches underline the antimicrobial properties of polyphenols to hamper HFHS-diet induced pathobionts associated to obesity, and to promote *A. muciniphila* with promising probiotic traits.

FUTURE WORK

In addition to metabolic benefits, polyphenols and symbiotic bacteria provide the host with several functions that promote innate and adaptive immune response, protect against inflammation and control pathogen colonization. For instance, balance between Th17 cells and Treg cells in the intestinal lamina propria is influenced by the intestinal microbiota (Fitzgibbon and Mills, 2020). Thus, the host immune response should be considered in future work on the effect of polyphenols on the host and its effect microbiota homeostasis. From the results obtained in the present thesis, many questions remain to be investigated: Can the polyphenols trigger specific immune response and anti-inflammatory markers in the intestinal epithelium? How are the goblet cells affected by the presence of polyphenols? Can the polyphenol-induced CPS/EPS in *Akkermansia* sense changes in the host immune system to attenuate dysbiosis-associated diseases? Can polyphenols differently elicit CPS assembly and profile in *Akkermansia*? Might the ability to express CPS/EPS and RND family confer to *Akkermansia* benefits to longer gut persistence? In the current work, important genes were identified to play a role in maintaining, even improving, the growth of *A. muciniphila* under polyphenols-enriched media. A deletion of those loci in *A. muciniphila*, the subsequent mono-colonization of mice with those strains, and the dietary supplementation with phenolics would be a pertinent approach to provide answers the above questions. This symbiont could also be genetically engineered to express glyco-polysaccharides molecules with probiotic and immunomodulatory benefits to the host. The induction of probiotic traits in *A. muciniphila* by polyphenols-enriched diets could be considered for a further stratification and personalized health care in certain host condition.

Additionally, performing an extensive analysis of the proteome or transcriptome will yield insights on the activity of *A. muciniphila* in the microbiome. This would contribute to better understand how this bacterium might metabolically adapt in dysbiosis and symbiosis with other members of the gut microbiota and how it might respond to polyphenols presence while interacting with the whole gut microbial community or with a simplified human microbiota consortium (SIHUMI).

Supplementary information

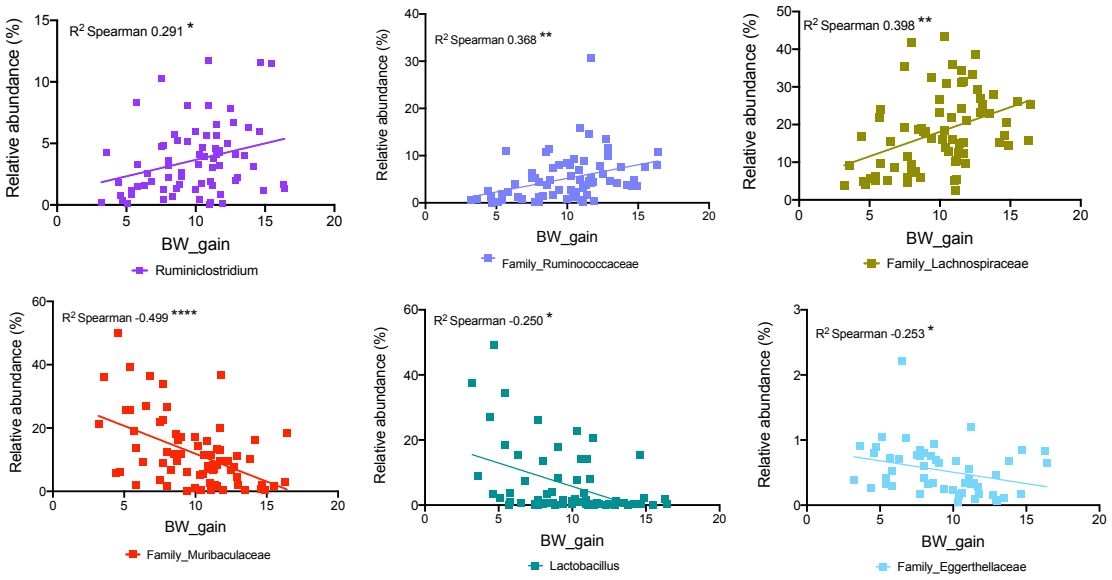

Figure S1. Representative microbial markers associated with the body weight in mice.

Each panel displays a correlation plot between different taxa with BW changes. Each point in a plot represents the values of the linear combinations for a sample pair in the correlation. The line represents the linear regression of the points displayed on the plot. Spearman correlation R2 scores are indicated in the graphs. Asterisks indicate bacterial taxa for which the association was significant, *p<0.05, **p<0.01, ***p<0.001, ****p<0.0001.

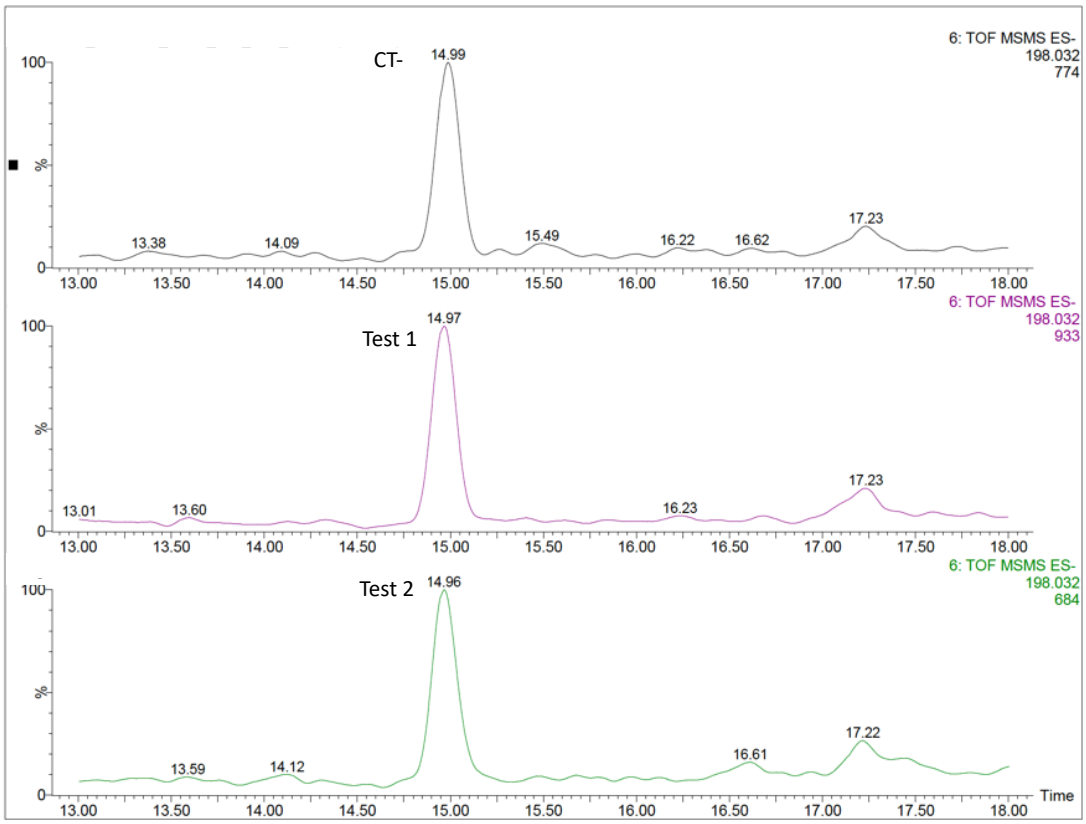

Figure S2. Akkermansia muciniphila does not metabolize the microbial phenolic metabolite Urolithin A.

Akkermansia muciniphila was grown in a mucin-based culture media enriched with urolithin A. The chromatograms of samples analyzed by UPLC-QToF are illustrating the pick of Urolithin A in the negative control (CT, retention time 14.99, 2.1 mg/L), and two independent *A. muciniphila* cultures, Test 1 (retention time 14.97, 2.8 mg/L) and Test 2 (retention time 14.96. 1.8 mg/L) after 24h of incubation in anoxic condition. Those findings indicate no apparent degradation of urolithin A.

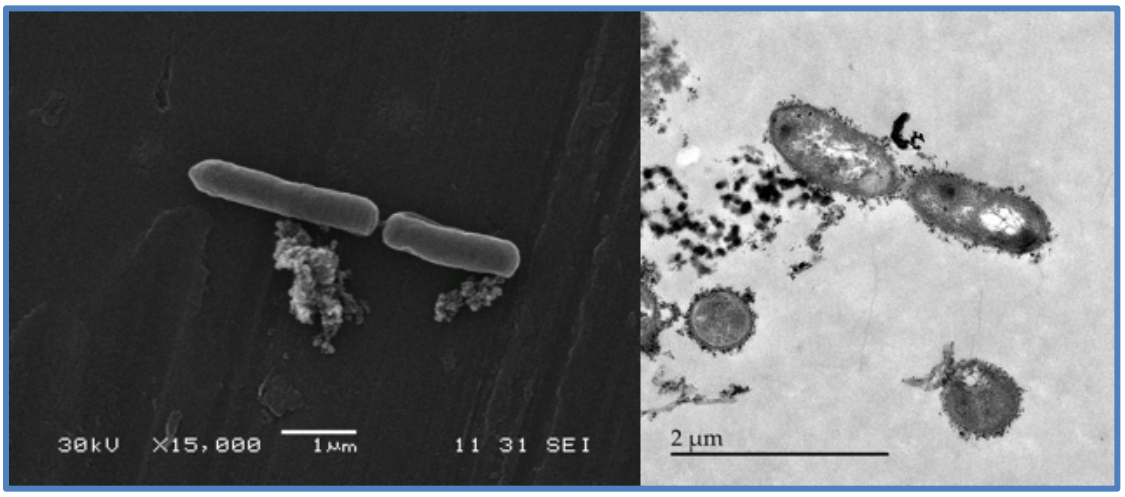

Figure S3. Cellular elongation in Akkermansia muciniphila cells submitted to grown under cranberry polyphenolic fraction.

SEM and TEM images of *A. muciniphila* grown under polymeric PACs rich fraction from cranberry polyphenolic extract. As the Vancomycin, PACs induced elongation size in *A. muciniphila,* but the cells were particularly surrounded by a CPS under polyphenols enriched media.

BIBLIOGRAPHY

Adam, C.L., Williams, P.A., Dalby, M.J., Garden, K., Thomson, L.M., Richardson, A.J., Gratz, S.W., and Ross, A.W. (2014). Different types of soluble fermentable dietary fibre decrease food intake, body weight gain and adiposity in young adult male rats. Nutrition & Metabolism. 11(1), 36. DOI: 10.1186/1743-7075-11-36.

Adewunmi, Y., Namjilsuren, S., Walker, W.D., Amato, D.N., Amato, D.V., Mavrodi, O.V., Patton, D.L., and Mavrodi, D.V. (2020). Antimicrobial activity of, and cellular pathways targeted by, p-Anisaldehyde and epigallocatechin gallate in the opportunistic human pathogen *Pseudomonas aeruginosa*. Appl Environ Microbiol. 86(4). Published online 2019/12/08 DOI: 10.1128/AEM.02482-19.

Agriculture., A.R.S.U.S.D.o., 2018. USDA Database for the proanthocyanidin content of selectedfFoods., V.2.1 Nutrient Data Laboratory, Beltsville Human Nutrition Research Center.

Ahn, J., Sinha, R., Pei, Z., Dominianni, C., Wu, J., Shi, J., Goedert, J.J., Hayes, R.B., and Yang, L. (2013). Human gut microbiome and risk for colorectal cancer. J Natl Cancer Inst. 105(24), 1907-1911. Published online 2013/12/10 DOI: 10.1093/jnci/djt300.

Alakomi, H.-L., Puupponen-Pimiä, R., Aura, A.-M., Helander, I.M., Nohynek, L., Oksman-Caldentey, K.-M., and Saarela, M. (2007). Weakening of *Salmonella* with selected microbial metabolites of berry-derived phenolic compounds and organic Acids. J Agr Food Chem. 55(10), 3905-3912. DOI: 10.1021/jf070190y.

Alam, M.A., Subhan, N., Hossain, H., Hossain, M., Reza, H.M., Rahman, M.M., and Ullah, M.O. (2016). Hydroxycinnamic acid derivatives: a potential class of natural compounds for the management of lipid metabolism and obesity. Nutr Metab (Lond). 13, 27. Published online 2016/04/14 DOI: 10.1186/s12986-016-0080-3.

Alam, M.T., Amos, G.C.A., Murphy, A.R.J., Murch, S., Wellington, E.M.H., and Arasaradnam, R.P. (2020). Microbial imbalance in inflammatory bowel disease patients at different taxonomic levels. Gut Pathog. 12, 1. Published online 2020/01/09 DOI: 10.1186/s13099-019-0341-6.

Almeida, A., Mitchell, A.L., Tarkowska, A., and Finn, R.D. (2018). Benchmarking taxonomic assignments based on 16S rRNA gene profiling of the microbiota from commonly sampled environments. Gigascience. 7(5). Published online 2018/05/16 DOI: 10.1093/gigascience/giy054.

Alvarez-Ortega, C., Olivares, J., and Martínez, J.L. (2013). RND multidrug efflux pumps: what are they good for? Frontiers in Microbiology. 4, 7. DOI: 10.3389/fmicb.2013.00007.

Amir, A., McDonald, D., Navas-Molina, J.A., Kopylova, E., Morton, J.T., Xu, Z.Z., Kightley, E.P., Thompson, L.R., Hyde, E.R., Gonzalez, A., et al. (2017). Deblur rapidly resolves single-nucleotide community sequence patterns. mSystems. 2(2), e00191-00116. DOI: 10.1128/msystems.00191-16 PMID - 28289731.

Anhê, F.F., Roy, D., Pilon, G., Dudonné, S., Matamoros, S., Varin, T.V., Garofalo, C., Moine, Q., Desjardins, Y., Levy, E., et al. (2014). A polyphenol-rich cranberry extract protects from diet-induced obesity, insulin resistance and intestinal inflammation in association with increased *Akkermansia* spp. population in the gut microbiota of mice. Gut. 64(6). DOI: 10.1136/gutjnl-2014-307142.

Ansaldo, E., Slayden, L.C., Ching, K.L., Koch, M.A., Wolf, N.K., Plichta, D.R., Brown, E.M., Graham, D.B., Xavier, R.J., Moon, J.J., et al. (2019). *Akkermansia muciniphila* induces intestinal adaptive immune responses during homeostasis. Science. 364(6446), 1179-1184. Published online 2019/06/22 DOI: 10.1126/science.aaw7479.

Arumugam, M., Raes, J., Pelletier, E., Le Paslier, D., Yamada, T., Mende, D.R., Fernandes, G.R., Tap, J., Bruls, T., Batto, J.M., et al. (2011). Enterotypes of the human gut microbiome. Nature. 473(7346), 174-180. Published online 2011/04/22 DOI: 10.1038/nature09944.

Attri, S., and Goel, G. (2018). Influence of polyphenol rich seabuckthorn berries juice on release of polyphenols and colonic microbiota on exposure to simulated human digestion model. Food Res Int. 111, 314-323. DOI: 10.1016/j.foodres.2018.05.045.

Auclair, S., Silberberg, M., Gueux, E., Morand, C., Mazur, A., Milenkovic, D., and Scalbert, A. (2008). Apple polyphenols and fibers attenuate atherosclerosis in apolipoprotein E-deficient mice. J Agric Food Chem. 56(14), 5558-5563. Published online 2008/06/19 DOI: 10.1021/jf800419s.

Backhed, F., Ley, R.E., Sonnenburg, J.L., Peterson, D.A., and Gordon, J.I. (2005). Host-bacterial mutualism in the human intestine. Science. 307(5717), 1915-1920. Published online 2005/03/26 DOI: 10.1126/science.1104816.

Backhed, F., Manchester, J.K., Semenkovich, C.F., and Gordon, J.I. (2007). Mechanisms underlying the resistance to diet-induced obesity in germ-free mice. Proc Natl Acad Sci U S A. 104(3), 979-984. Published online 2007/01/11 DOI: 10.1073/pnas.0605374104.

Bansil, R., and Turner, B.S. (2006). Mucin structure, aggregation, physiological functions and biomedical applications. Curr Opin Colloid In. 11(2-3), 164-170. DOI: 10.1016/j.cocis.2005.11.001.

Bazzocco, S., Mattila, I., Guyot, S., Renard, C., and Aura, A.-M. (2008). Factors affecting the conversion of apple polyphenols to phenolic acids and fruit matrix to short-chain fatty acids by human faecal microbiota in vitro. European journal of nutrition. 47(8), 442-452. DOI: 10.1007/s00394-008-0747-2.

Beals, E.W. (1984). Advances in ecological research. Adv Ecol Res. 14, 1-55. DOI: 10.1016/s0065-2504(08)60168-3.

Beaumont, M., Goodrich, J.K., Jackson, M.A., Yet, I., Davenport, E.R., Vieira-Silva, S., Debelius, J., Pallister, T., Mangino, M., Raes, J., et al. (2016). Heritable components of the human fecal microbiome are associated with visceral fat. Genome Biol. 17(1), 189. Published online 2016/09/27 DOI: 10.1186/s13059-016-1052-7.

Bektas, A., Schurman, S.H., Sen, R., and Ferrucci, L. (2018). Aging, inflammation and the environment. Exp Gerontol. 105, 10-18. Published online 2017/12/25 DOI: 10.1016/j.exger.2017.12.015.

Biagi, E., Franceschi, C., Rampelli, S., Severgnini, M., Ostan, R., Turroni, S., Consolandi, C., Quercia, S., Scurti, M., Monti, D., et al. (2016). Gut microbiota and extreme longevity. Curr Biol. 26(11), 1480-1485. Published online 2016/05/18 DOI: 10.1016/j.cub.2016.04.016.

Bindels, L.B., Delzenne, N.M., Cani, P.D., and Walter, J. (2015). Towards a more comprehensive concept for prebiotics. Nat Rev Gastroenterol Hepatol. 12(5), 303-310. Published online 2015/04/01 DOI: 10.1038/nrgastro.2015.47.

Blaker, K., M., and Olmstead, J., W. (2015). Cell wall composition of the skin and flesh tissue of crisp and standard texture southern highbush blueberry genotypes. J Berry Res. 5(1), 9-15. DOI: 10.3233/jbr-140085.

Blanco, P., Hernando-Amado, S., Reales-Calderon, J., Corona, F., Lira, F., Alcalde-Rico, M., Bernardini, A., Sanchez, M., and Martinez, J. (2016). Bacterial multidrug efflux pumps: Much more than antibiotic resistance determinants. Microorganisms. 4(1), 14. DOI: 10.3390/microorganisms4010014.

Bliss, J.M., and Silver, R.P. (1996). Coating the surface: a model for expression of capsular polysialic acid in *Escherichia coli* K1. Mol Microbiol. 21(2), 221-231. Published online 1996/07/01 DOI: 10.1046/j.1365-2958.1996.6461357.x.

Bodogai, M., O'Connell, J., Kim, K., Kim, Y., Moritoh, K., Chen, C., Gusev, F., Vaughan, K., Shulzhenko, N., Mattison, J.A., et al. (2018). Commensal bacteria contribute to insulin resistance in aging by activating innate B1a cells. Sci Transl Med. 10(467). Published online 2018/11/16 DOI: 10.1126/scitranslmed.aat4271.

Borges, G., Degeneve, A., Mullen, W., and Crozier, A. (2010). Identification of flavonoid and phenolic antioxidants in black currants, blueberries, raspberries, red currants, and cranberries. J Agric Food Chem. 58(7), 3901-3909. Published online 2009/12/17 DOI: 10.1021/jf902263n.

Boto-Ordóñez, M., Urpi-Sarda, M., Queipo-Ortuño, M., Tulipani, S., Tinahones, F.J., and Andres-Lacueva, C. (2014). High levels of Bifidobacteria are associated with increased levels of anthocyanin microbial metabolites: a randomized clinical trial. Food & Function. 5(8), 1932-1938. DOI: 10.1039/c4fo00029c.

Braune, A., and Blaut, M. (2016). Bacterial species involved in the conversion of dietary flavonoids in the human gut. Gut Microbes. 7(3), 216-234. DOI: 10.1080/19490976.2016.1158395.

Burse, A., Weingart, H., and Ullrich, M.S. (2004). NorM, an *Erwinia amylovora* multidrug efflux pump involved in in vitro competition with other epiphytic bacteria. Appl Environ Microbiol. 70(2), 693-703. Published online 2004/02/10 DOI: 10.1128/aem.70.2.693-703.2004.

Callahan, B.J., McMurdie, P.J., and Holmes, S.P. (2017). Exact sequence variants should replace operational taxonomic units in marker-gene data analysis. ISME J. 11(12), 2639-2643. Published online 2017/07/22 DOI: 10.1038/ismej.2017.119.

Callahan, B.J., McMurdie, P.J., Rosen, M.J., Han, A.W., Johnson, A.A., and Holmes, S.P. (2016). DADA2: High-resolution sample inference from Illumina amplicon data. Nature Methods. 13(7). DOI: 10.1038/nmeth.3869.

Canfora, E.E., Jocken, J.W., and Blaak, E.E. (2015). Short-chain fatty acids in control of body weight and insulin sensitivity. Nat Rev Endocrinol. 11(10), 577-591. Published online 2015/08/12 DOI: 10.1038/nrendo.2015.128.

Cao, W., Chin, Y., Chen, X., Mi, Y., Xue, C., Wang, Y., and Tang, Q. (2019). The role of gut microbiota in the resistance to obesity in mice fed a high fat diet. Int J Food Sci Nutr. 1-11. Published online 2019/11/28 DOI: 10.1080/09637486.2019.1686608.

Caputo, A., Dubourg, G., Croce, O., Gupta, S., Robert, C., Papazian, L., Rolain, J.M., and Raoult, D. (2015). Whole-genome assembly of *Akkermansia muciniphila* sequenced directly from human stool. Biology Direct. 10:5.

Cardona, F., Andrés-Lacueva, C., and Tulipani, S. (2013). Benefits of polyphenols on gut microbiota and implications in human health. The Journal of nutritional.

Carrasco-Pozo, C., Gotteland, M., Castillo, R.L., and Chen, C. (2015). 3,4-dihydroxyphenylacetic acid, a microbiota-derived metabolite of quercetin, protects against pancreatic β-cells dysfunction induced by high cholesterol. Experimental Cell Research. 334(2), 270-282. DOI: 10.1016/j.yexcr.2015.03.021.

Casanova-Martí, À., Serrano, J., Blay, T.M., Terra, X., Ardévol, A., and Pinent, M. (2017). Acute selective bioactivity of grape seed proanthocyanidins on enteroendocrine secretions in the gastrointestinal tract. Food & Nutrition Research. 61(1), 1321347. DOI: 10.1080/16546628.2017.1321347.

Casanova-Martí, À., Serrano, J., Portune, K.J., Sanz, Y., Blay, T.M., Terra, X., Ardévol, A., and Pinent, M. (2018). Grape seed proanthocyanidins influence gut microbiota and enteroendocrine secretions in female rats. Food & Function. 9(3), 1672-1682. DOI: 10.1039/c7fo02028g.

Celik, E.E., Gokmen, V., and Skibsted, L.H. (2015). Synergism between soluble and dietary fiber bound antioxidants. J Agric Food Chem. 63(8), 2338-2343. Published online 2015/02/19 DOI: 10.1021/acs.jafc.5b00009.

Chang, C.J., Lin, T.L., Tsai, Y.L., Wu, T.R., Lai, W.F., Lu, C.C., and Lai, H.C. (2019). Next generation probiotics in disease amelioration. J Food Drug Anal. 27(3), 615-622. Published online 2019/07/22 DOI: 10.1016/j.jfda.2018.12.011.

Chassard, C., Delmas, E., Robert, C., and Bernalier-Donadille, A. (2010). The cellulose-degrading microbial community of the human gut varies according to the presence or absence of methanogens. FEMS Microbiol Ecol. 74(1), 205-213. Published online 2010/07/29 DOI: 10.1111/j.1574-6941.2010.00941.x.

Cheng, M., Zhang, X., Zhu, J., Cheng, L., Cao, J., Wu, Z., Weng, P., and Zheng, X. (2018). A metagenomics approach to the intestinal microbiome structure and function in high fat diet-induced obesity mice fed with oolong tea polyphenols. Food & Function. 9(2), 1079-1087. DOI: 10.1039/C7FO01570D.

Cheng, Z., Wang, Y., and Li, B. (2018). Illumina MiSeq reveals the influence of blueberry malvidin-3-galactoside on fecal microbial community structure and metabolizes of liver cancer mice. Peerj Prepr. 6, e27429v27422. DOI: 10.7287/peerj.preprints.27429v2.

Chia, L., Hornung, B.V.H., Aalvink, S., Schaap, P.J., de Vos, W.M., Knol, J., and Belzer, C. (2018). Deciphering the trophic interaction between *Akkermansia muciniphila* and the butyrogenic gut commensal *Anaerostipes caccae* using a metatranscriptomic approach. Antonie van Leeuwenhoek. 111(6), 859-873. DOI: 10.1007/s10482-018-1040-x.

Christensen, H., Andersson, A.J., Jørgensen, S.L., and Vogt, J.K. (2018). Learning Materials in Biosciences. 135-161. DOI: 10.1007/978-3-319-99280-8_8.

Ciocan, D., Rebours, V., Voican, C.S., Wrzosek, L., Puchois, V., Cassard, A.M., and Perlemuter, G. (2018). Characterization of intestinal microbiota in alcoholic patients with and without alcoholic hepatitis or chronic alcoholic pancreatitis. Sci Rep. 8(1), 4822. Published online 2018/03/21 DOI: 10.1038/s41598-018-23146-3.

Clifford, M.N. (2004). Diet-derived phenols in plasma and tissues and their implications for health. Planta Medica. 70(12), 1103-1114. DOI: 10.1055/s-2004-835835.

Coleman, C.M., Auker, K.M., Killday, K.B., Azadi, P., Black, I., and Ferreira, D. (2019). Arabinoxyloglucan oligosaccharides may contribute to the antiadhesive properties of porcine urine after cranberry consumption. J Nat Prod. 82(3), 589-605. Published online 2019/03/16 DOI: 10.1021/acs.jnatprod.8b01043.

Collado, M.C., Derrien, M., Isolauri, E., de Vos, W.M., and Salminen, S. (2007). Intestinal integrity and *Akkermansia muciniphila*, a mucin-degrading member of the intestinal microbiota present in infants, adults, and the elderly. Appl Environ Microbiol. 73(23), 7767-7770. Published online 2007/10/16 DOI: 10.1128/AEM.01477-07.

Collins, B., Hoffman, J., Martinez, K., Grace, M., Lila, M., Cockrell, C., Nadimpalli, A., Chang, E., Chuang, C.-C., Zhong, W., et al. (2016). A polyphenol-rich fraction obtained from table grapes decreases adiposity, insulin resistance and markers of inflammation and impacts gut microbiota in high-fat-fed mice. J Nutritional Biochem. 31, 150-165. DOI: 10.1016/j.jnutbio.2015.12.021.

Collins, K.H., Paul, H.A., Hart, D.A., Reimer, R.A., Smith, I.C., Rios, J.L., Seerattan, R.A., and Herzog, W. (2016). A high-fat high-sucrose diet rapidly alters muscle integrity, inflammation and gut microbiota in Male Rats. Sci Rep. 6, 37278. Published online 2016/11/18 DOI: 10.1038/srep37278.

Coman, V., and Vodnar, D.C. (2020). Hydroxycinnamic acids and human health: recent advances. J Sci Food Agric. 100(2), 483-499. Published online 2019/09/01 DOI: 10.1002/jsfa.10010.

Corfield, A.P. (2018). The Interaction of the gut microbiota with the mucus barrier in health and disease in human. Microorganisms. 6(3). Published online 2018/08/04 DOI: 10.3390/microorganisms6030078.

Costabile, A., Klinder, A., Fava, F., Napolitano, A., Fogliano, V., Leonard, C., Gibson, G.R., and Tuohy, K.M. (2008). Whole-grain wheat breakfast cereal has a prebiotic effect on the human gut microbiota: a double-blind, placebo-controlled, crossover study. Br J Nutr. 99(1), 110-120. Published online 2007/09/01 DOI: 10.1017/S0007114507793923.

Costea, P.I., Hildebrand, F., Arumugam, M., Backhed, F., Blaser, M.J., Bushman, F.D., de Vos, W.M., Ehrlich, S.D., Fraser, C.M., Hattori, M., et al. (2018). Enterotypes in the landscape of gut microbial community composition. Nat Microbiol. 3(1), 8-16. Published online 2017/12/20 DOI: 10.1038/s41564-017-0072-8.

Côté, J., Caillet, S., Doyon, G., Dussault, D., Sylvain, J.F., and Lacroix, M. (2011). Antimicrobial effect of cranberry juice and extracts. Food Control. 22(8), 1413-1418. DOI: 10.1016/j.foodcont.2011.02.024.

Cotillard, A., Kennedy, S.P., Kong, L.C., Prifti, E., Pons, N., Le Chatelier, E., Almeida, M., Quinquis, B., Levenez, F., Galleron, N., et al. (2013). Dietary intervention impact on gut microbial gene richness. Nature. 500(7464), 585-588. Published online 2013/08/30 DOI: 10.1038/nature12480.

Cox, L.M., and Blaser, M., 2018. Probiotic compositions for improving metabolism and immunity, in: N.Y. University (Ed.) Justia Patents, A61K 35/741 (20060101); A61K 45/06 (20060101) ed. New York University, New York , NY (US).

Cuevas-Sierra, A., Ramos-Lopez, O., Riezu-Boj, J.I., Milagro, F.I., and Martinez, J.A. (2019). Diet, gut microbiota, and obesity: Links with host genetics and epigenetics and potential applications. Adv Nutr. 10(suppl_1), S17-S30. Published online 2019/02/06 DOI: 10.1093/advances/nmy078.

Cummings, J.H., Wiggins, H.S., Jenkins, D.J., Houston, H., Jivraj, T., Drasar, B.S., and Hill, M.J. (1978). Influence of diets high and low in animal fat on bowel habit, gastrointestinal transit time, fecal microflora, bile acid, and fat excretion. J Clin Invest. 61(4), 953-963. Published online 1978/04/01 DOI: 10.1172/JCI109020.

Curiel, J.A., Rodríguez, H., De la Rivas, B., Anglade, O., Baraige, F., Zagorec, M., Champomier-Vergès, M., Muñoz, R., and de Felipe, F. (2011). Response of a *Lactobacillus plantarum* human isolate to tannic acid

challenge assessed by proteomic analyses. Molecular nutrition & Food research 55, 1454-1465. DOI: 10.1002/mnfr.201000621.

Cuthbertson, L., Kos, V., and Whitfield, C. (2010). ABC Transporters involved in export of cell surface glycoconjugates. Microbiology and Molecular Biology Reviews. 74(3), 341-362. DOI: 10.1128/MMBR.00009-10.

Cuthbertson, L., Mainprize, I.L., Naismith, J.H., and Whitfield, C. (2009). Pivotal roles of the outer membrane polysaccharide export and polysaccharide copolymerase protein families in export of extracellular polysaccharides in gram-negative bacteria. Microbiol Mol Biol Rev. 73(1), 155-177. Published online 2009/03/05 DOI: 10.1128/MMBR.00024-08.

Dalby, M.J., Ross, A.W., Walker, A.W., and Morgan, P.J. (2017). Dietary uncoupling of gut microbiota and energy harvesting from obesity and glucose tolerance in mice. Cell Rep. 21(6), 1521-1533. Published online 2017/11/09 DOI: 10.1016/j.celrep.2017.10.056.

Dao, M.C., Everard, A., Aron-Wisnewsky, J., Sokolovska, N., Prifti, E., Verger, E.O., Kayser, B.D., Levenez, F., Chilloux, J., Hoyles, L., et al. (2016). *Akkermansia muciniphila* and improved metabolic health during a dietary intervention in obesity: relationship with gut microbiome richness and ecology. Gut. 65(3), 426-436. Published online 2015/06/24 DOI: 10.1136/gutjnl-2014-308778.

Das, Q., Lepp, D., Yin, X., Ross, K., McCallum, J.L., Warriner, K., Marcone, M.F., and Diarra, M.S. (2019). Transcriptional profiling of *Salmonella* enterica serovar Enteritidis exposed to ethanolic extract of organic cranberry pomace. PLoS One. 14(7), e0219163. Published online 2019/07/04 DOI: 10.1371/journal.pone.0219163.

Dauchet, L., Amouyel, P., and Dallongeville, J. (2009). Fruits, vegetables and coronary heart disease. Nat Rev Cardiol. 6(9), 599-608. Published online 2009/08/05 DOI: 10.1038/nrcardio.2009.131.

David, L.A., Maurice, C.F., Carmody, R.N., Gootenberg, D.B., Button, J.E., Wolfe, B.E., Ling, A.V., Devlin, A.S., Varma, Y., Fischbach, M.A., et al. (2014). Diet rapidly and reproducibly alters the human gut microbiome. Nature. 505(7484), 559-563. Published online 2013/12/18 DOI: 10.1038/nature12820.

de la Cuesta-Zuluaga, J., Corrales-Agudelo, V., Velasquez-Mejia, E.P., Carmona, J.A., Abad, J.M., and Escobar, J.S. (2018). Gut microbiota is associated with obesity and cardiometabolic disease in a population in the midst of Westernization. Sci Rep. 8(1), 11356. Published online 2018/07/29 DOI: 10.1038/s41598-018-29687-x.

de La Serre, C.B., Ellis, C.L., Lee, J., Hartman, A.L., Rutledge, J.C., and Raybould, H.E. (2010). Propensity to high-fat diet-induced obesity in rats is associated with changes in the gut microbiota and gut inflammation. Am J Physiol Gastrointest Liver Physiol. 299(2), G440-448. Published online 2010/05/29 DOI: 10.1152/ajpgi.00098.2010.

de Las Rivas, B., Rodriguez, H., Anguita, J., and Munoz, R. (2019). Bacterial tannases: classification and biochemical properties. Appl Microbiol Biotechnol. 103(2), 603-623. Published online 2018/11/22 DOI: 10.1007/s00253-018-9519-y.

Delmar, J.A., Su, C.C., and Yu, E.W. (2014). Bacterial multidrug efflux transporters. Annu Rev Biophys. 43, 93-117. Published online 2014/04/08 DOI: 10.1146/annurev-biophys-051013-022855.

Delzenne, N.M., Cani, P.D., Everard, A., Neyrinck, A.M., and Bindels, L.B. (2015). Gut microorganisms as promising targets for the management of type 2 diabetes. Diabetologia. 58(10), 2206-2217. Published online 2015/08/01 DOI: 10.1007/s00125-015-3712-7.

de Moraes, A.C., Fernandes, G.R., da Silva, I.T., Almeida-Pititto, B., Gomes, E.P., Pereira, A.D., and Ferreira, S.R. (2017). Enterotype May Drive the Dietary-Associated Cardiometabolic Risk Factors. Front Cell Infect Microbiol. 7, 47. Published online 2017/03/11 DOI: 10.3389/fcimb.2017.00047.

Denev, P., Ciz, M., Kratchanova, M., and Blazheva, D. (2019). Black chokeberry (*Aronia melanocarpa*) polyphenols reveal different antioxidant, antimicrobial and neutrophil-modulating activities. Food Chem. 284, 108-117. Published online 2019/02/13 DOI: 10.1016/j.foodchem.2019.01.108.

Deplancke, B., and Gaskins, R.H. (2001). Microbial modulation of innate defense: goblet cells and the intestinal mucus layer. Am J Clin Nutrition. 73(6). DOI: 10.1093/ajcn/73.6.1131S.

Derrien, M., Baarlen, P., Hooiveld, G., Norin, E., Müller, M., and de Vos, W.M. (2011). Modulation of mucosal immune response, tolerance, and proliferation in mice colonized by the mucin-degrader *Akkermansia muciniphila*. Frontiers in Microbiology. 2, 166. DOI: 10.3389/fmicb.2011.00166.

Derrien, M., Belzer, C., and de Vos, W.M. (2017). *Akkermansia muciniphila* and its role in regulating host functions. Microbial pathogenesis. 106, 171-181. DOI: 10.1016/j.micpath.2016.02.005.

Derrien, M., Collado, M.C., Ben-Amor, K., Salminen, S., and de Vos, W.M. (2008). The Mucin degrader *Akkermansia muciniphila* is an abundant resident of the human intestinal tract. Appl Environ Microbiol. 74(5), 1646-1648. Published online 2007/12/18 DOI: 10.1128/AEM.01226-07.

Derrien, M., Vaughan, E.E., Plugge, C.M., and de Vos, W.M. (2004). *Akkermansia muciniphila* gen. nov., sp. nov., a human intestinal mucin-degrading bacterium. International Journal of Systematic and Evolutionary Microbiology. 54(5), 1469-1476. DOI: 10.1099/ijs.0.02873-0.

DeSantis, T.Z., Hugenholtz, P., Larsen, N., Rojas, M., Brodie, E.L., Keller, K., Huber, T., Dalevi, D., Hu, P., and Andersen, G.L. (2006). Greengenes, a chimera-checked 16S rRNA gene database and workbench compatible with ARB. Applied and Environmental Microbiology. 72(7), 5069-5072. DOI: 10.1128/aem.03006-05.

Dewulf, E.M., Cani, P.D., Claus, S.P., Fuentes, S., Puylaert, P.G., Neyrinck, A.M., Bindels, L.B., de Vos, W.M., Gibson, G.R., Thissen, J.P., et al. (2013). Insight into the prebiotic concept: lessons from an exploratory, double blind intervention study with inulin-type fructans in obese women. Gut. 62(8), 1112-1121. Published online 2012/11/09 DOI: 10.1136/gutjnl-2012-303304.

Dharmani, P., Srivastava, V., Kissoon-Singh, V., and Chadee, K. (2009). Role of intestinal mucins in innate host defense mechanisms against pathogens. J Innate Immun. 1(2), 123-135. Published online 2009/01/01 DOI: 10.1159/000163037.

Dolara, P., Luceri, C., De Filippo, C., Femia, A.P., Giovannelli, L., Caderni, G., Cecchini, C., Silvi, S., Orpianesi, C., and Cresci, A. (2005). Red wine polyphenols influence carcinogenesis, intestinal microflora, oxidative damage and gene expression profiles of colonic mucosa in F344 rats. Mutat Res. 591(1-2), 237-246. Published online 2005/11/19 DOI: 10.1016/j.mrfmmm.2005.04.022.

Dominguez-Bello, M.G., Costello, E.K., Contreras, M., Magris, M., Hidalgo, G., Fierer, N., and Knight, R. (2010). Delivery mode shapes the acquisition and structure of the initial microbiota across multiple body habitats in newborns. Proc Natl Acad Sci U S A. 107(26), 11971-11975. Published online 2010/06/23 DOI: 10.1073/pnas.1002601107.

Donohoe, D.R., Garge, N., Zhang, X., Sun, W., O'Connell, T.M., Bunger, M.K., and Bultman, S.J. (2011). The microbiome and butyrate regulate energy metabolism and autophagy in the mammalian colon. Cell Metab. 13(5), 517-526. Published online 2011/05/03 DOI: 10.1016/j.cmet.2011.02.018.

Doré, J., and Corthier, G. (2010). The human intestinal microbiota. Gastroentérologie Clinique Et Biologique. 34, S7-S15. DOI: 10.1016/s0399-8320(10)70015-4 PMID - 20889008.

Douglas, G.M., Maffei, V.J., Zaneveld, J., Yurgel, S.N., Brown, J.R., Taylor, C.M., Huttenhower, C., and Langille, M.G.I. (2019). PICRUSt2: An improved and extensible approach for metagenome inference. Biorxiv. 672295. DOI: 10.1101/672295.

Dreher, M.L. (2017). Dietary fiber in health and disease. 41-66. DOI: 10.1007/978-3-319-50557-2_3.

Dubourg, G., Lagier, J.-C., Armougom, F., Robert, C., Audoly, G., Papazian, L., and Raoult, D. (2013). High-level colonisation of the human gut by *Verrucomicrobia* following broad-spectrum antibiotic treatment. International Journal of Antimicrobial Agents. 41(2), 149-155. DOI: 10.1016/j.ijantimicag.2012.10.012.

Dudonné, S., Dubé, P., Anhê, F., Pilon, G., Marette, A., Lemire, M., Harris, C., Dewailly, E., and Desjardins, Y. (2015). Comprehensive analysis of phenolic compounds and abscisic acid profiles of twelve native Canadian berries. Journal of Food Composition and Analysis. 44, 214-224. DOI: 10.1016/j.jfca.2015.09.003.

Duncan, S.H., Russell, W.R., Quartieri, A., Rossi, M., Parkhill, J., Walker, A.W., and Flint, H.J. (2016). Wheat bran promotes enrichment within the human colonic microbiota of butyrate-producing bacteria that release ferulic acid. Environ Microbiol. 18(7), 2214-2225. Published online 2015/12/05 DOI: 10.1111/1462-2920.13158.

Durazzo, A., Lucarini, M., Souto, E.B., Cicala, C., Caiazzo, E., Izzo, A.A., Novellino, E., and Santini, A. (2019). Polyphenols: A concise overview on the chemistry, occurrence, and human health. Phytother Res. 33(9), 2221-2243. Published online 2019/07/31 DOI: 10.1002/ptr.6419.

Duynhoven, J.v., Vaughan, E.E., Jacobs, D.M., Kemperman, R.A., Velzen, E.J.J.v., Gross, G., Roger, L.C., Possemiers, S., Smilde, A.K., Dore, J., et al. (2010). Metabolic fate of polyphenols in the human superorganism. Proc National Acad Sci. 108(Supplement_1), 4531-4538. DOI: 10.1073/pnas.1000098107 PMID - 20615997.

Earley, H., Lennon, G., Balfe, A., Coffey, J.C., Winter, D.C., and O'Connell, P.R. (2019). The abundance of *Akkermansia muciniphila* and its relationship with sulphated colonic mucins in health and ulcerative colitis. Sci Rep. 9(1), 15683. Published online 2019/11/02 DOI: 10.1038/s41598-019-51878-3.

Eckburg, P.B., Bik, E.M., Bernstein, C.N., Purdom, E., Dethlefsen, L., Sargent, M., Gill, S.R., Nelson, K.E., and Relman, D.A. (2005). Diversity of the human intestinal microbial flora. Science. 308(5728), 1635-1638. Published online 2005/04/16 DOI: 10.1126/science.1110591.

Edgar, R.C. (2016). UNOISE2: improved error-correction for Illumina 16S and ITS amplicon sequencing. Biorxiv. 081257. DOI: 10.1101/081257.

Edgar, R.C. (2017). Accuracy of microbial community diversity estimated by closed- and open-reference OTUs. PeerJ. 5, e3889. Published online 2017/10/12 DOI: 10.7717/peerj.3889.

El Kaoutari, A., Armougom, F., Gordon, J.I., Raoult, D., and Henrissat, B. (2013). The abundance and variety of carbohydrate-active enzymes in the human gut microbiota. Nat Rev Microbiol. 11(7), 497-504. Published online 2013/06/12 DOI: 10.1038/nrmicro3050.

Ellekilde, M., Krych, L., Hansen, C.H., Hufeldt, M.R., Dahl, K., Hansen, L.H., Sorensen, S.J., Vogensen, F.K., Nielsen, D.S., and Hansen, A.K. (2014). Characterization of the gut microbiota in leptin deficient obese mice - Correlation to inflammatory and diabetic parameters. Res Vet Sci. 96(2), 241-250. Published online 2014/02/22 DOI: 10.1016/j.rvsc.2014.01.007.

Engels, C., Knodler, M., Zhao, Y.Y., Carle, R., Ganzle, M.G., and Schieber, A. (2009). Antimicrobial activity of gallotannins isolated from mango (Mangifera indica L.) kernels. J Agric Food Chem. 57(17), 7712-7718. Published online 2009/08/07 DOI: 10.1021/jf901621m.

Espin, J.C., Gonzalez-Sarrias, A., and Tomas-Barberan, F.A. (2017). The gut microbiota: A key factor in the therapeutic effects of (poly)phenols. Biochem Pharmacol. 139, 82-93. Published online 2017/05/10 DOI: 10.1016/j.bcp.2017.04.033.

Esposito, D., Chen, A., Grace, M.H., Komarnytsky, S., and Lila, M. (2014). Inhibitory effects of wild blueberry anthocyanins and other flavonoids on biomarkers of acute and chronic inflammation in vitro. J Agr Food Chem. 62(29), 7022-7028. DOI: 10.1021/jf4051599.

Etxeberria, U., Arias, N., Boqué, N., Macarulla, M.T., Portillo, M.P., Martínez, J.A., and Milagro, F.I. (2015). Reshaping faecal gut microbiota composition by the intake of trans-resveratrol and quercetin in high-fat sucrose diet-fed rats. J Nutritional Biochem. 26(6), 651-660. DOI: 10.1016/j.jnutbio.2015.01.002.

Everard, A., Belzer, C., Geurts, L., Ouwerkerk, J.P., Druart, C., Bindels, L.B., Guiot, Y., Derrien, M., Muccioli, G.G., Delzenne, N.M., et al. (2013). Cross-talk between *Akkermansia muciniphila* and intestinal epithelium controls diet-induced obesity. Proc National Acad Sci. 110(22), 9066-9071. DOI: 10.1073/pnas.1219451110.

Everard, A., Lazarevic, V., Derrien, M., Girard, M., Muccioli, G.G., Neyrinck, A.M., Possemiers, S., Van Holle, A., Francois, P., de Vos, W.M., et al. (2011). Responses of gut microbiota and glucose and lipid metabolism to

prebiotics in genetic obese and diet-induced leptin-resistant mice. Diabetes. 60(11), 2775-2786. Published online 2011/09/22 DOI: 10.2337/db11-0227.

Faith, J.J., Guruge, J.L., Charbonneau, M., Subramanian, S., Seedorf, H., Goodman, A.L., Clemente, J.C., Knight, R., Heath, A.C., Leibel, R.L., et al. (2013). The long-term stability of the human gut microbiota. Science. 341(6141), 1237439. Published online 2013/07/06 DOI: 10.1126/science.1237439.

Falony, G., Calmeyn, T., Leroy, F., and De Vuyst, L. (2009). Coculture fermentations of *Bifidobacterium* species and *Bacteroides thetaiotaomicron* reveal a mechanistic insight into the prebiotic effect of inulin-type fructans. Appl Environ Microbiol. 75(8), 2312-2319. Published online 2009/03/03 DOI: 10.1128/AEM.02649-08.

Fang, C., Kim, H., Barnes, R.C., Talcott, S.T., and Mertens-Talcott, S.U. (2018). Obesity-associated diseases biomarkers are differently modulated in lean and obese individuals and inversely correlated to plasma polyphenolic metabolites after 6 weeks of mango (*Mangifera indica* L.) consumption. Mol Nutr Food Res. e1800129. Published online 2018/05/26 DOI: 10.1002/mnfr.201800129.

Fanning, S., Hall, L.J., Cronin, M., Zomer, A., MacSharry, J., Goulding, D., Motherway, M.O., Shanahan, F., Nally, K., Dougan, G., et al. (2012). Bifidobacterial surface-exopolysaccharide facilitates commensal-host interaction through immune modulation and pathogen protection. Proc Natl Acad Sci U S A. 109(6), 2108-2113. Published online 2012/02/07 DOI: 10.1073/pnas.1115621109.

Feliciano, R.P., Meudt, J.J., Shanmuganayagam, D., Krueger, C.G., and Reed, J.D. (2014). Ratio of "A-type" to "B-type" proanthocyanidin interflavan bonds affects extra-intestinal pathogenic *Escherichia coli i*nvasion of gut epithelial cells. J Agric Food Chem. 62(18), 3919-3925. Published online 2013/11/13 DOI: 10.1021/jf403839a.

Fernandez, L., and Hancock, R.E. (2012). Adaptive and mutational resistance: role of porins and efflux pumps in drug resistance. Clin Microbiol Rev. 25(4), 661-681. Published online 2012/10/05 DOI: 10.1128/CMR.00043-12.

Fernandez-Millan, E., Ramos, S., Alvarez, C., Bravo, L., Goya, L., and Martin, M.A. (2014). Microbial phenolic metabolites improve glucose-stimulated insulin secretion and protect pancreatic beta cells against tert-butyl hydroperoxide-induced toxicity via ERKs and PKC pathways. Food Chem Toxicol. 66, 245-253. Published online 2014/02/05 DOI: 10.1016/j.fct.2014.01.044.

Ferrer, M., Ruiz, A., Lanza, F., Haange, S.B., Oberbach, A., Till, H., Bargiela, R., Campoy, C., Segura, M.T., Richter, M., et al. (2013). Microbiota from the distal guts of lean and obese adolescents exhibit partial functional redundancy besides clear differences in community structure. Environ Microbiol. 15(1), 211-226. Published online 2012/08/16 DOI: 10.1111/j.1462-2920.2012.02845.x.

Fetzner, S. (2012). Ring-Cleaving Dioxygenases with a Cupin Fold. Applied and Environmental Microbiology. 78(8), 2505-2514. DOI: 10.1128/aem.07651-11.

Filannino, P., Di Cagno, R., and Gobbetti, M. (2018). Metabolic and functional paths of lactic acid bacteria in plant foods: get out of the labyrinth. Curr Opin Biotechnol. 49, 64-72. Published online 2017/08/23 DOI: 10.1016/j.copbio.2017.07.016.

Firrman, J., Liu, L., Argoty, G.A., Zhang, L., Tomasula, P., Wang, M., Pontious, S., Kobori, M., and Xiao, W. (2018). Analysis of temporal changes in growth and gene expression for commensal gut microbes in response to the polyphenol Naringenin. Microbiol Insights. 11, 1178636118775100. Published online 2018/07/18 DOI: 10.1177/1178636118775100.

Firrman, J., Liu, L., Zhang, L., Arango Argoty, G., Wang, M., Tomasula, P., Kobori, M., Pontious, S., and Xiao, W. (2016). The effect of quercetin on genetic expression of the commensal gut microbes *Bifidobacterium catenulatum, Enterococcus caccae* and *Ruminococcus gauvreauii.* Anaerobe. 42, 130-141. Published online 2016/11/05 DOI: 10.1016/j.anaerobe.2016.10.004.

Fitzgibbon, G., and Mills, K.H.G. (2020). The microbiota and immune-mediated diseases: Opportunities for therapeutic intervention. Eur J Immunol. 50(3), 326-337. Published online 2020/01/29 DOI: 10.1002/eji.201948322.

Fritsch, C., Heinrich, V., Vogel, R.F., and Toelstede, S. (2016). Phenolic acid degradation potential and growth behavior of lactic acid bacteria in sunflower substrates. Food Microbiol. 57, 178-186. Published online 2016/04/08 DOI: 10.1016/j.fm.2016.03.003.

Fu, J., Bonder, M.J., Cenit, M.C., Tigchelaar, E.F., Maatman, A., Dekens, J.A., Brandsma, E., Marczynska, J., Imhann, F., Weersma, R.K., et al. (2015). The gut microbiome contributes to a substantial proportion of the variation in blood lipids. Circ Res. 117(9), 817-824. Published online 2015/09/12 DOI: 10.1161/CIRCRESAHA.115.306807.

Garcia-Mazcorro, J.F., Lage, N.N., Mertens-Talcott, S., Talcott, S., Chew, B., Dowd, S.E., Kawas, J.R., and Noratto, G.D. (2018). Effect of dark sweet cherry powder consumption on the gut microbiota, short-chain fatty acids, and biomarkers of gut health in obese *db/db* mice. PeerJ. 6, e4195. Published online 2018/01/10 DOI: 10.7717/peerj.4195.

Garcia-Villalba, R., Vissenaekens, H., Pitart, J., Romo-Vaquero, M., Espín, J., Grootaert, C., Selma, M.V., Raes, K., Smagghe, G., Possemiers, S., et al. (2017). The Gastrointestinal Simulation Model TWIN-SHIME® shows differences between human Urolithin-metabotypes in gut microbiota composition, pomegranate polyphenol metabolism, and transport along the intestinal tract. J Agr Food Chem. 65(27), 5480-5493. DOI: 10.1021/acs.jafc.7b02049.

Ge, M., Chen, Z., Onishi, H.R., Kohler, J., Silver, L.L., Kerns, R., Fukuzawa, S., Thompson, C., and Kahne, D. (1999). Vancomycin derivatives that inhibit peptidoglycan biosynthesis without binding D-Ala-D-Ala. Science. 284(5413), 507-511. Published online 1999/04/16 DOI: 10.1126/science.284.5413.507.

Gibson, G.R., Hutkins, R., Sanders, M., Prescott, S.L., Reimer, R.A., Salminen, S.J., Scott, K., Stanton, C., Swanson, K.S., Cani, P.D., et al. (2017). Expert consensus document: The international scientific association for probiotics and prebiotics (ISAPP) consensus statement on the definition and scope of prebiotics. Nature Reviews Gastroenterology & Hepatology. 14(8), 491-502. DOI: 10.1038/nrgastro.2017.75.

Gill, S.R., Pop, M., Deboy, R.T., Eckburg, P.B., Turnbaugh, P.J., Samuel, B.S., Gordon, J.I., Relman, D.A., Fraser-Liggett, C.M., and Nelson, K.E. (2006). Metagenomic analysis of the human distal gut microbiome. Science. 312(5778), 1355-1359. Published online 2006/06/03 DOI: 10.1126/science.1124234.

Gimenez-Bastida, J.A., Truchado, P., Larrosa, M., Espin, J.C., Tomas-Barberan, F.A., Allende, A., and Garcia-Conesa, M.T. (2012). Urolithins, ellagitannin metabolites produced by colon microbiota, inhibit Quorum Sensing in *Yersinia enterocolitica*: Phenotypic response and associated molecular changes. Food Chem. 132(3), 1465-1474. Published online 2012/06/01 DOI: 10.1016/j.foodchem.2011.12.003.

Gómez-Gallego, C., Pohl, S., Salminen, S., Vos, D.W.M., and Kneifel, W. (2016). *Akkermansia muciniphila*: a novel functional microbe with probiotic properties. Beneficial microbes. 7(4), 571-584. DOI: 10.3920/bm2016.0009.

Gonzalez-Sarrias, A., Romo-Vaquero, M., Garcia-Villalba, R., Cortes-Martin, A., Selma, M.V., and Espin, J.C. (2018). The Endotoxemia marker lipopolysaccharide-binding protein is reduced in overweight-obese subjects consuming pomegranate extract by modulating the gut microbiota: A randomized clinical trial. Mol Nutr Food Res. 62(11), e1800160. Published online 2018/04/18 DOI: 10.1002/mnfr.201800160.

Graham, C., Mullen, A., and Whelan, K. (2015). Obesity and the gastrointestinal microbiota: a review of associations and mechanisms. Nutr Rev. 73(6), 376-385. Published online 2015/05/27 DOI: 10.1093/nutrit/nuv004.

Greenacre, M. (2017). Ordination with any dissimilarity measure: a weighted Euclidean solution. Ecology. 98(9), 2293-2300. Published online 2017/06/22 DOI: 10.1002/ecy.1937.

Gregori, D., French, M., Gallipoli, S., Lorenzoni, G., and Ghidina, M. (2019). Global, regional, and national levels of fruit and vegetable consumption from the ROUND (World Map of Consumption of Fruit and Vegetables and Nutrient Deficits) Project (P18-067-19). Curr Dev Nutrition. 3(Suppl 1). DOI: 10.1093/cdn/nzz039.p18-067-19 PMID - 31224034.

Greig, C.J., Alper, A., Goodman, A.L., and Cowles, R.A. (2018). Mucosal homeostasis is altered in the ileum of gnotobiotic mice. J Surg Res. 231, 331-337. Published online 2018/10/04 DOI: 10.1016/j.jss.2018.05.055.

Guo, X., Li, S., Zhang, J., Wu, F., Li, X., Wu, D., Zhang, M., Ou, Z., Jie, Z., Yan, Q., et al. (2017). Genome sequencing of 39 *Akkermansia muciniphila* isolates reveals its population structure, genomic and functional diverisity, and global distribution in mammalian gut microbiotas. BMC Genomics. 18(1), 800. DOI: 10.1186/s12864-017-4195-3.

Guo, X., Tresserra-Rimbau, A., Estruch, R., Martinez-Gonzalez, M.A., Medina-Remon, A., Fito, M., Corella, D., Salas-Salvado, J., Portillo, M.P., Moreno, J.J., et al. (2017). Polyphenol levels are inversely correlated with body weight and obesity in an elderly population after 5 years of follow up (The randomised PREDIMED Study). Nutrients. 9(5). Published online 2017/05/04 DOI: 10.3390/nu9050452.

Guo, X., Zhang, J., Wu, F., Zhang, M., Yi, M., and Peng, Y. (2016). Different subtype strains of *Akkermansia muciniphila* abundantly colonize in southern China. J Appl Microbiol. 120(2), 452-459. Published online 2015/12/17 DOI: 10.1111/jam.13022.

Gurung, M., Li, Z., You, H., Rodrigues, R., Jump, D.B., Morgun, A., and Shulzhenko, N. (2020). Role of gut microbiota in type 2 diabetes pathophysiology. EBioMedicine. 51, 102590. Published online 2020/01/07 DOI: 10.1016/j.ebiom.2019.11.051.

Hadrami, A., Islam, M., Adam, L.R., and Daayf, F. (2015). A cupin domain-containing protein with a quercetinase activity (VdQase) regulates *Verticillium dahliae*'s pathogenicity and contributes to counteracting host defenses. Frontiers in Plant Science. 6, 440. DOI: 10.3389/fpls.2015.00440.

Haft, D.H., Paulsen, I.T., Ward, N., and Selengut, J.D. (2006). Exopolysaccharide-associated protein sorting in environmental organisms: the PEP-CTERM/EpsH system. Application of a novel phylogenetic profiling heuristic. BMC Biol. 4, 29. Published online 2006/08/26 DOI: 10.1186/1741-7007-4-29.

Hanninen, A., Toivonen, R., Poysti, S., Belzer, C., Plovier, H., Ouwerkerk, J.P., Emani, R., Cani, P.D., and De Vos, W.M. (2018). *Akkermansia muciniphila* induces gut microbiota remodelling and controls islet autoimmunity in NOD mice. Gut. 67(8), 1445-1453. Published online 2017/12/23 DOI: 10.1136/gutjnl-2017-314508.

Hansen, C.H.F., Krych, L., Nielsen, D.S., and Diabetologia, V.-F.K. (2012). Early life treatment with vancomycin propagates *Akkermansia muciniphila* and reduces diabetes incidence in the NOD mouse. Diabetologia. 55, 2285-2294. DOI: 10.1007/s00125-012-2564-7.

Heinritz, S.N., Weiss, E., Eklund, M., Aumiller, T., Louis, S., Rings, A., Messner, S., Camarinha-Silva, A., Seifert, J., Bischoff, S.C., et al. (2016). Intestinal microbiota and microbial metabolites are changed in a pig model fed a high-fat/low-fiber or a low-fat/high-fiber diet. PLoS One. 11(4), e0154329. Published online 2016/04/23 DOI: 10.1371/journal.pone.0154329.

Henderson, G., Yilmaz, P., Kumar, S., Forster, R.J., Kelly, W.J., Leahy, S.C., Guan, L.L., and Janssen, P.H. (2019). Improved taxonomic assignment of rumen bacterial 16S rRNA sequences using a revised SILVA taxonomic framework. PeerJ. 7, e6496. Published online 2019/03/14 DOI: 10.7717/peerj.6496.

Henning, S.M., Summanen, P.H., Lee, R.-P., Yang, J., Finegold, S.M., Heber, D., and Li, Z. (2017). Pomegranate ellagitannins stimulate the growth of *Akkermansia muciniphila* in vivo. Anaerobe. 43, 56-60. DOI: 10.1016/j.anaerobe.2016.12.003.

Hernandez-Mendoza, A., Nava, N., Santana, O., Abreu-Goodger, C., Tovar, A., and Quinto, C. (2007). Diminished redundancy of outer membrane factor proteins in rhizobiales: a *nodT* homolog is essential for free-living *Rhizobium etli*. J Mol Microbiol Biotechnol. 13(1-3), 22-34. Published online 2007/08/19 DOI: 10.1159/000103594.

Herren, C.M., and McMahon, K.D. (2017). Cohesion: a method for quantifying the connectivity of microbial communities. ISME J. 11(11), 2426-2438. Published online 2017/07/22 DOI: 10.1038/ismej.2017.91.

Hersoug, L.G., Moller, P., and Loft, S. (2016). Gut microbiota-derived lipopolysaccharide uptake and trafficking to adipose tissue: implications for inflammation and obesity. Obes Rev. 17(4), 297-312. Published online 2015/12/30 DOI: 10.1111/obr.12370.

Hervert-Hernández, D., and Goñi, I. (2011). Dietary polyphenols and human gut microbiota: a Review. Food Reviews International. 27(2), 154-169. DOI: 10.1080/87559129.2010.535233.

Hervert-Hernández, D., Pintado, C., Rotger, R., and Goñi, I. (2009). Stimulatory role of grape pomace polyphenols on *Lactobacillus acidophilus* growth. International Journal of Food Microbiology. 136(1), 119-122. DOI: 10.1016/j.ijfoodmicro.2009.09.016.

Heyman-Lindén, L., Kotowska, D., Sand, E., Bjursell, M., Plaza, M., Turner, C., Holm, C., Fåk, F., and Berger, K. (2016). Lingonberries alter the gut microbiota and prevent low-grade inflammation in high-fat diet fed mice. Food & nutrition research. DOI: 10.3402/fnr.v60.29993.

Hidalgo, M., Oruna-Concha, J.M., Kolida, S., Walton, G.E., Kallithraka, S., Spencer, J.P.E., Gibson, G.R., and de Pascual-Teresa, S. (2012). Metabolism of anthocyanins by human gut microflora and their influence on gut bacterial growth. J Agr Food Chem. 60(15), 3882-3890. DOI: 10.1021/jf3002153.

Holscher, H.D. (2017). Dietary fiber and prebiotics and the gastrointestinal microbiota. Gut Microbes. 8(2), 172-184. Published online 2017/02/07 DOI: 10.1080/19490976.2017.1290756.

Hong, P.Y., Croix, J.A., Greenberg, E., Gaskins, H.R., and Mackie, R.I. (2011). Pyrosequencing-based analysis of the mucosal microbiota in healthy individuals reveals ubiquitous bacterial groups and micro-heterogeneity. PLoS One. 6(9), e25042. Published online 2011/10/04 DOI: 10.1371/journal.pone.0025042.

Hooda, S., Boler, B.M., Serao, M.C., Brulc, J.M., Staeger, M.A., Boileau, T.W., Dowd, S.E., Fahey, G.C., Jr., and Swanson, K.S. (2012). 454 pyrosequencing reveals a shift in fecal microbiota of healthy adult men consuming polydextrose or soluble corn fiber. J Nutr. 142(7), 1259-1265. Published online 2012/06/01 DOI: 10.3945/jn.112.158766.

Hotchkiss, A.T., Nuñez, A., Strahan, G.D., Chau, H.K., White, A.K., Marais, J.P.J., Hom, K., Vakkalanka, M.S., Di, R., Yam, K.L., et al. (2015). Cranberry xyloglucan structure and inhibition of *Escherichia coli* adhesion to epithelial cells. J Agr Food Chem. 63(23), 5622-5633. DOI: 10.1021/acs.jafc.5b00730.

Hou, Y.P., He, Q.Q., Ouyang, H.M., Peng, H.S., Wang, Q., Li, J., Lv, X.F., Zheng, Y.N., Li, S.C., Liu, H.L., et al. (2017). Human gut microbiota associated with obesity in chinese children and adolescents. Biomed Res Int. 2017, 7585989. Published online 2017/12/08 DOI: 10.1155/2017/7585989.

Howell, A.B., Reed, J.D., Krueger, C.G., Winterbottom, R., Cunningham, D.G., and Leahy, M. (2005). A-type cranberry proanthocyanidins and uropathogenic bacterial anti-adhesion activity. Phytochemistry. 66(18), 2281-2291. Published online 2005/08/02 DOI: 10.1016/j.phytochem.2005.05.022.

Hsieh, S., Porter, N.T., Donermeyer, D.L., Horvath, S., Strout, G., Saunders, B.T., Zhang, N., Zinselmeyer, B., Martens, E.C., Stappenbeck, T.S., et al. (2020). Polysaccharide capsules equip the human symbiont *Bacteroides thetaiotaomicron* to modulate immune responses to a dominant antigen in the intestine. J Immunol. 204(4), 1035-1046. Published online 2020/01/05 DOI: 10.4049/jimmunol.1901206.

Huang, B., Long, J., Liao, H., Liu, L., Li, J., Zhang, J., Li, Y., Wang, X., and Yang, R. (2019). Characteristics of bacterial community and function in paddy soil profile around antimony mine and its response to antimony and arsenic contamination. Int J Environ Res Public Health. 16(24). Published online 2019/12/11 DOI: 10.3390/ijerph16244883.

Huang, W., Zhu, Y., Li, C., Sui, Z., and Min, W. (2016). Effect of blueberry anthocyanins Malvidin and glycosides on the antioxidant properties in endothelial cells. Oxid Med Cell Longev. 2016, 1591803. Published online 2016/04/02 DOI: 10.1155/2016/1591803.

Ianiro, G., Tilg, H., and Gasbarrini, A. (2016). Antibiotics as deep modulators of gut microbiota: between good and evil. Gut. 65(11), 1906-1915. Published online 2016/08/18 DOI: 10.1136/gutjnl-2016-312297.

Jakobek, L., and Matić, P. (2018). Non-covalent dietary fiber - polyphenol interactions and their influence on polyphenol bioaccessibility. Trends in Food Science & Technology. 83(The Journal of Nutrition 132 2002), 235-247. DOI: 10.1016/j.tifs.2018.11.024.

James, S.L., Christophersen, C.T., Bird, A.R., Conlon, M.A., Rosella, O., Gibson, P.R., and Muir, J.G. (2015). Abnormal fibre usage in UC in remission. Gut. 64(4), 562-570. Published online 2014/07/20 DOI: 10.1136/gutjnl-2014-307198.

Jiao, X., Wang, Y., Lin, Y., Lang, Y., Li, E., Zhang, X., Zhang, Q., Feng, Y., Meng, X., and Li, B. (2019). Blueberry polyphenols extract as a potential prebiotic with anti-obesity effects on C57BL/6 J mice by modulating the gut microbiota. J Nutritional Biochem. 64, 88-100. DOI: 10.1016/j.jnutbio.2018.07.008.

Jiménez, N., Curiel, J., Reverón, I., Rivas, B., and Muñoz, R. (2013). Uncovering the *Lactobacillus plantarum* WCFS1 gallate decarboxylase involved in tannin degradation. Applied and environmental microbiology. 79(14), 4253-4263. DOI: 10.1128/AEM.00840-13.

Johansson, M.E., Gustafsson, J.K., Sjoberg, K.E., Petersson, J., Holm, L., Sjovall, H., and Hansson, G.C. (2010). Bacteria penetrate the inner mucus layer before inflammation in the dextran sulfate colitis model. PLoS One. 5(8), e12238. Published online 2010/09/02 DOI: 10.1371/journal.pone.0012238.

Johansson, M.E., Jakobsson, H.E., Holmen-Larsson, J., Schutte, A., Ermund, A., Rodriguez-Pineiro, A.M., Arike, L., Wising, C., Svensson, F., Backhed, F., et al. (2015). Normalization of host intestinal mucus layers requires long-term microbial colonization. Cell Host Microbe. 18(5), 582-592. Published online 2015/11/04 DOI: 10.1016/j.chom.2015.10.007.

Johansson, M.E., Larsson, J.M., and Hansson, G.C. (2011). The two mucus layers of colon are organized by the MUC2 mucin, whereas the outer layer is a legislator of host-microbial interactions. Proc Natl Acad Sci U S A. 108 Suppl 1, 4659-4665. Published online 2010/07/10 DOI: 10.1073/pnas.1006451107.

Johansson, M.E., Phillipson, M., Petersson, J., Velcich, A., Holm, L., and Hansson, G.C. (2008). The inner of the two Muc2 mucin-dependent mucus layers in colon is devoid of bacteria. Proc Natl Acad Sci U S A. 105(39), 15064-15069. Published online 2008/09/23 DOI: 10.1073/pnas.0803124105.

Joo, H.S., Fu, C.I., and Otto, M. (2016). Bacterial strategies of resistance to antimicrobial peptides. Philos Trans R Soc Lond B Biol Sci. 371(1695). Published online 2016/05/11 DOI: 10.1098/rstb.2015.0292.

Joshi, S.S., Howell, A.B., and D'Souza, D.H. (2014). *Cronobacter sakazakii* reduction by blueberry proanthocyanidins. Food Microbiol. 39, 127-131. Published online 2014/01/07 DOI: 10.1016/j.fm.2013.11.002.

Jun, S.R., Robeson, M.S., Hauser, L.J., Schadt, C.W., and Gorin, A.A. (2015). PanFP: pangenome-based functional profiles for microbial communities. BMC Res Notes. 8, 479. Published online 2015/09/28 DOI: 10.1186/s13104-015-1462-8.

Karlsson, C.L., Onnerfalt, J., Xu, J., Molin, G., Ahrne, S., and Thorngren-Jerneck, K. (2012). The microbiota of the gut in preschool children with normal and excessive body weight. Obesity (Silver Spring). 20(11), 2257-2261. Published online 2012/05/02 DOI: 10.1038/oby.2012.110.

Kawabata, K., Yoshioka, Y., and Terao, J. (2019). Role of intestinal microbiota in the bioavailability and physiological functions of dietary polyphenols. Molecules. 24(2). Published online 2019/01/24 DOI: 10.3390/molecules24020370.

Ke, X., Walker, A., Haange, S.B., Lagkouvardos, I., Liu, Y., Schmitt-Kopplin, P., von Bergen, M., Jehmlich, N., He, X., Clavel, T., et al. (2019). Synbiotic-driven improvement of metabolic disturbances is associated with changes in the gut microbiome in diet-induced obese mice. Mol Metab. 22, 96-109. Published online 2019/02/23 DOI: 10.1016/j.molmet.2019.01.012.

Kemperman, R.A., Gross, G., Mondot, S., Possemiers, S., Marzorati, M., Wiele, T.V.d., Doré, J., and Vaughan, E.E. (2013). Impact of polyphenols from black tea and red wine/grape juice on a gut model microbiome. Food Res Int. 53(2), 659-669. DOI: 10.1016/j.foodres.2013.01.034.

Kim, J.H., An, H.J., Garrido, D., German, J.B., Lebrilla, C.B., and Mills, D.A. (2013). Proteomic analysis of *Bifidobacterium longum* subsp. *infantis* reveals the metabolic insight on consumption of prebiotics and host glycans. PLoS One. 8(2), e57535. Published online 2013/03/08 DOI: 10.1371/journal.pone.0057535.

Kim, K.A., Gu, W., Lee, I.A., Joh, E.H., and Kim, D.H. (2012). High fat diet-induced gut microbiota exacerbates inflammation and obesity in mice via the TLR4 signaling pathway. PLoS One. 7(10), e47713. Published online 2012/10/24 DOI: 10.1371/journal.pone.0047713.

Kim, Y., Choi, Y., Ham, H., Jeong, H.-S., and Lee, J. (2013). Protective effects of oligomeric and polymeric procyanidin fractions from defatted grape seeds on tert-butyl hydroperoxide-induced oxidative damage in HepG2 cells. Food Chemistry. 137(1-4), 136-141. DOI: 10.1016/j.foodchem.2012.10.006.

Koh, A., De Vadder, F., Kovatcheva-Datchary, P., and Backhed, F. (2016). From dietary fiber to host Physiology: short-chain fatty acids as key bacterial metabolites. Cell. 165(6), 1332-1345. Published online 2016/06/04 DOI: 10.1016/j.cell.2016.05.041.

Koh, H. (2018). An adaptive microbiome alpha-diversity-based association analysis method. Sci Rep. 8(1), 18026. Published online 2018/12/24 DOI: 10.1038/s41598-018-36355-7.

Koliada, A., Syzenko, G., Moseiko, V., Budovska, L., Puchkov, K., Perederiy, V., Gavalko, Y., Dorofeyev, A., Romanenko, M., Tkach, S., et al. (2017). Association between body mass index and *Firmicutes/Bacteroidetes* ratio in an adult Ukrainian population. BMC Microbiology. 17(1), 120. DOI: 10.1186/s12866-017-1027-1.

Korpela, K., Salonen, A., Virta, L.J., Kekkonen, R.A., Forslund, K., Bork, P., and de Vos, W.M. (2016). Intestinal microbiome is related to lifetime antibiotic use in Finnish pre-school children. Nat Commun. 7, 10410. Published online 2016/01/27 DOI: 10.1038/ncomms10410.

Kostic, A.D., Gevers, D., Siljander, H., Vatanen, T., Hyotylainen, T., Hamalainen, A.M., Peet, A., Tillmann, V., Poho, P., Mattila, I., et al. (2015). The dynamics of the human infant gut microbiome in development and in progression toward type 1 diabetes. Cell Host Microbe. 17(2), 260-273. Published online 2015/02/11 DOI: 10.1016/j.chom.2015.01.001.

Krause, D.O., Smith, W.J.M., Brooker, J.D., and McSweeney, C.S. (2005). Tolerance mechanisms of streptococci to hydrolysable and condensed tannins. Animal feed science and Technology. 121, 59-75.

Kuhn, P., Kalariya, H.M., Poulev, A., Ribnicky, D.M., Jaja-Chimedza, A., Roopchand, D.E., and Raskin, I. (2018). Grape polyphenols reduce gut-localized reactive oxygen species associated with the development of metabolic syndrome in mice. PLOS ONE. 13(10). DOI: 10.1371/journal.pone.0198716.

Lacombe, A., Li, R.W., Klimis-Zacas, D., Kristo, A.S., Tadepalli, S., Krauss, E., Young, R., and Wu, V.C. (2013a). Lowbush wild blueberries have the potential to modify gut microbiota and xenobiotic metabolism in the rat colon. PLoS One. 8(6), e67497. Published online 2013/07/11 DOI: 10.1371/journal.pone.0067497.

Lacombe, A., McGivney, C., Tadepalli, S., Sun, X., and Wu, V.C.H. (2013). The effect of American cranberry (*Vaccinium macrocarpon*) constituents on the growth inhibition, membrane integrity, and injury of *Escherichia coli* O157: H7 and *Listeria monocytogenes* in comparison to *Lactobacillus rhamnosus*. Food microbiology. 34(2), 352-359.

Lacombe, A., Tadepalli, S., A., H.-C., and Wu, C.H. (2013b). Phytochemicals in lowbush wild blueberry inactivate *Escherichia coli* O157:H7 by damaging its cell membrane. Foodborne pathogens and disease 10, 9. DOI: 10.1089/fpd.2013.1504.

Lacombe, A., Wu, V.C., Tyler, S., and Edwards, K. (2010a). Antimicrobial action of the American cranberry constituents; phenolics, anthocyanins, and organic acids, against *Escherichia coli* O157:H7. Int J Food Microbiol. 139(1-2), 102-107. Published online 2010/02/16 DOI: 10.1016/j.ijfoodmicro.2010.01.035.

Lacombe, A., and Wu, V.C.H. (2017). The potential of berries to serve as selective inhibitors of pathogens and promoters of beneficial microorganisms. Food Quality and Safety. 1(1), 3-12. DOI: 10.1093/fqs/fyx001.

Lacombe, A., Wu, V.C.H., Tyler, S., and journal of food, E.K. (2010b). Antimicrobial action of the American cranberry constituents; phenolics, anthocyanins, and organic acids, against *Escherichia coli* O157: H7. International journal of Food Microbiology 139, 102-107. DOI: doi:10.1016/j.ijfoodmicro.2010.01.035.

Lacombe, A., Wu, V.C.H., White, J., Tadepalli, S., and Andre, E.E. (2012). The antimicrobial properties of the lowbush blueberry *(Vaccinium angustifolium)* fractional components against foodborne pathogens and the conservation of probiotic *Lactobacillus rhamnosus*. Food microbiology. 30, 124-131. DOI: doi:10.1016/j.fm.2011.10.006.

Lammerts van Bueren, A., Saraf, A., Martens, E.C., and Dijkhuizen, L. (2015). Differential metabolism of exopolysaccharides from probiotic Lactobacilli by the human gut symbiont *Bacteroides thetaiotaomicron*. Appl Environ Microbiol. 81(12), 3973-3983. Published online 2015/04/05 DOI: 10.1128/AEM.00149-15.

Langille, M.G., Zaneveld, J., Caporaso, J.G., McDonald, D., Knights, D., Reyes, J.A., Clemente, J.C., Burkepile, D.E., Vega Thurber, R.L., Knight, R., et al. (2013). Predictive functional profiling of microbial

communities using 16S rRNA marker gene sequences. Nat Biotechnol. 31(9), 814-821. Published online 2013/08/27 DOI: 10.1038/nbt.2676.

Larsen, N., Bussolo de Souza, C., Krych, L., Barbosa Cahu, T., Wiese, M., Kot, W., Hansen, K.M., Blennow, A., Venema, K., and Jespersen, L. (2019). Potential of pectins to beneficially modulate the gut microbiota depends on their structural properties. Front Microbiol. 10, 223. Published online 2019/03/05 DOI: 10.3389/fmicb.2019.00223.

Larsson, J.M., Karlsson, H., Crespo, J.G., Johansson, M.E., Eklund, L., Sjovall, H., and Hansson, G.C. (2011). Altered O-glycosylation profile of MUC2 mucin occurs in active ulcerative colitis and is associated with increased inflammation. Inflamm Bowel Disease. 17(11), 2299-2307. Published online 2011/02/04 DOI: 10.1002/ibd.21625.

Lavelle, A., Lennon, G., O'Sullivan, O., Docherty, N., Balfe, A., Maguire, A., Mulcahy, H.E., Doherty, G., O'Donoghue, D., Hyland, J., et al. (2015). Spatial variation of the colonic microbiota in patients with ulcerative colitis and control volunteers. Gut. 64(10), 1553-1561. Published online 2015/01/18 DOI: 10.1136/gutjnl-2014-307873.

Laville, E., Perrier, J., Bejar, N., Maresca, M., Esque, J., Tauzin, A.S., Bouhajja, E., Leclerc, M., Drula, E., Henrissat, B., et al. (2019). Investigating host microbiota relationships through functional metagenomics. Front Microbiol. 10, 1286. Published online 2019/07/06 DOI: 10.3389/fmicb.2019.01286.

Le Chatelier, E., Nielsen, T., Qin, J., Prifti, E., Hildebrand, F., Falony, G., Almeida, M., Arumugam, M., Batto, J.M., Kennedy, S., et al. (2013). Richness of human gut microbiome correlates with metabolic markers. Nature. 500(7464), 541-546. Published online 2013/08/30 DOI: 10.1038/nature12506.

Leal-Diaz, A.M., Noriega, L.G., Torre-Villalvazo, I., Torres, N., Aleman-Escondrillas, G., Lopez-Romero, P., Sanchez-Tapia, M., Aguilar-Lopez, M., Furuzawa-Carballeda, J., Velazquez-Villegas, L.A., et al. (2016). Aguamiel concentrate from Agave salmiana and its extracted saponins attenuated obesity and hepatic steatosis and increased *Akkermansia muciniphila* in C57BL6 mice. Sci Rep. 6, 34242. Published online 2016/09/30 DOI: 10.1038/srep34242.

Lecerf, J.M., Depeint, F., Clerc, E., Dugenet, Y., Niamba, C.N., Rhazi, L., Cayzeele, A., Abdelnour, G., Jaruga, A., Younes, H., et al. (2012). Xylo-oligosaccharide (XOS) in combination with inulin modulates both the intestinal environment and immune status in healthy subjects, while XOS alone only shows prebiotic properties. Br J Nutr. 108(10), 1847-1858. Published online 2012/01/24 DOI: 10.1017/S0007114511007252.

Lee, C.C., Kim, J., Kim, J., Oh, Y., Han, S., Park, J., Lee, K., and Lee, C. (2017). 5-(3′,4′-Dihydroxyphenyl-γ-valerolactone), a major microbial metabolite of proanthocyanidin, attenuates THP-1 monocyte-endothelial adhesion. International Journal of Molecular Sciences. 18(7), 1363. DOI: 10.3390/ijms18071363.

Lee, S., Keirsey, K.I., Kirkland, R., Grunewald, Z.I., Fischer, J.G., and de Serre, C.B. (2018). Blueberry supplementation influences the gut microbiota, inflammation, and insulin resistance in high-fat-diet-fed rats. J Nutrition. 148(2), 209-219. DOI: 10.1093/jn/nxx027.

Lessard, I.A.D., and Walsh, C.T. (1999). VanX, a bacterial d-alanyl-d-alanine dipeptidase: Resistance, immunity, or survival function? Proc National Acad Sci. 96(20), 11028-11032. DOI: 10.1073/pnas.96.20.11028.

Ley, R.E., Hamady, M., Lozupone, C., Turnbaugh, P.J., Ramey, R.R., Bircher, J.S., Schlegel, M.L., Tucker, T.A., Schrenzel, M.D., Knight, R., et al. (2008). Evolution of mammals and their gut microbes. Science. 320(5883), 1647-1651. Published online 2008/05/24 DOI: 10.1126/science.1155725.

Ley, R.E., Peterson, D.A., and Gordon, J.I. (2006). Ecological and evolutionary forces shaping microbial diversity in the human intestine. Cell. 124(4), 837-848. Published online 2006/02/25 DOI: 10.1016/j.cell.2006.02.017.

Li, D., Li, B., Ma, Y., Sun, X., Lin, Y., and Meng, X. (2017). Polyphenols, anthocyanins, and flavonoids contents and the antioxidant capacity of various cultivars of highbush and half-high blueberries. Journal of Food Composition and Analysis. 62, 84-93. DOI: 10.1016/j.jfca.2017.03.006.

Li, J., Lin, S., Vanhoutte, P.M., Woo, C.W., and Xu, A. (2016). *Akkermansia Muciniphila* protects against atherosclerosis by preventing metabolic endotoxemia-induced inflammation in Apoe-/- Mice. Circulation. 133(24), 2434-2446. Published online 2016/05/05 DOI: 10.1161/CIRCULATIONAHA.115.019645.

Li, Z., Henning, S.M., Lee, R.-P., Lu, Q.-Y., Summanen, P.H., Thames, G., Corbett, K., Downes, J., Tseng, C.-H., Finegold, S.M., et al. (2015). Pomegranate extract induces ellagitannin metabolite formation and changes stool microbiota in healthy volunteers. Food & Function. 6(8), 2487-2495. DOI: 10.1039/C5FO00669D.

Liang, C., Tseng, H.C., Chen, H.M., Wang, W.C., Chiu, C.M., Chang, J.Y., Lu, K.Y., Weng, S.L., Chang, T.H., Chang, C.H., et al. (2017). Diversity and enterotype in gut bacterial community of adults in Taiwan. BMC Genomics. 18(Suppl 1), 932. Published online 2017/02/16 DOI: 10.1186/s12864-016-3261-6.

Licht, T.R., Hansen, M., Bergstrom, A., Poulsen, M., Krath, B.N., Markowski, J., Dragsted, L.O., and Wilcks, A. (2010). Effects of apples and specific apple components on the cecal environment of conventional rats: role of apple pectin. BMC Microbiol. 10, 13. Published online 2010/01/22 DOI: 10.1186/1471-2180-10-13.

Liquori, G.E., Mastrodonato, M., Mentino, D., Scillitani, G., Desantis, S., Portincasa, P., and Ferri, D. (2012). In situ characterization of O-linked glycans of Muc2 in mouse colon. Acta Histochem. 114(7), 723-732. Published online 2012/01/21 DOI: 10.1016/j.acthis.2011.12.009.

Liston, S.D., Mann, E., and Whitfield, C. (2017). Glycolipid substrates for ABC transporters required for the assembly of bacterial cell-envelope and cell-surface glycoconjugates. Biochim Biophys Acta Mol Cell Biol Lipids. 1862(11), 1394-1403. Published online 2016/10/31 DOI: 10.1016/j.bbalip.2016.10.008.

Liu, R., Hong, J., Xu, X., Feng, Q., Zhang, D., Gu, Y., Shi, J., Zhao, S., Liu, W., Wang, X., et al. (2017). Gut microbiome and serum metabolome alterations in obesity and after weight-loss intervention. Nat Med. 23(7), 859-868. Published online 2017/06/20 DOI: 10.1038/nm.4358.

Liu, W., Zhang, R., Shu, R., Yu, J., Li, H., Long, H., Jin, S., Li, S., Hu, Q., Yao, F., et al. (2020). Study of the relationship between microbiome and colorectal cancer susceptibility using 16S rRNA sequencing. Biomed Res Int. 2020, 1-17. DOI: 10.1155/2020/7828392.

Lozupone, C.A., Stombaugh, J.I., Gordon, J.I., Jansson, J.K., and Knight, R. (2012). Diversity, stability and resilience of the human gut microbiota. Nature. 489(7415), 220-230. Published online 2012/09/14 DOI: 10.1038/nature11550.

Lu, P., Burger-van Paassen, N., van der Sluis, M., Witte-Bouma, J., Kerckaert, J.P., van Goudoever, J.B., Van Seuningen, I., and Renes, I.B. (2011). Colonic gene expression patterns of mucin Muc2 knockout mice reveal various phases in colitis development. Inflamm Bowel Dis. 17(10), 2047-2057. Published online 2011/09/13 DOI: 10.1002/ibd.21592.

Ludwig, W., Schleifer, K.-H., and Whitman, W.B. (2009). Systematic Bacteriology. 1-13. DOI: 10.1007/978-0-387-68489-5_1.

Lukovac, S., Belzer, C., Pellis, L., Keijser, B.J., de Vos, W.M., Montijn, R.C., and Roeselers, G. (2014). Differential modulation by *Akkermansia muciniphila* and *Faecalibacterium prausnitzii* of host peripheral lipid metabolism and histone acetylation in mouse gut organoids. mBio. 5(4). Published online 2014/08/15 DOI: 10.1128/mBio.01438-14.

Lydon, K.A., and Lipp, E.K. (2018). Taxonomic annotation errors incorrectly assign the family *Pseudoalteromonadaceae* to the order *Vibrionales* in Greengenes: implications for microbial community assessments. PeerJ. 6, e5248. Published online 2018/07/19 DOI: 10.7717/peerj.5248.

Ma, G., and Chen, Y. (2020). Polyphenol supplementation benefits human health via gut microbiota: A systematic review via meta-analysis. J Funct Food. 66, 103829. DOI: 10.1016/j.jff.2020.103829.

Maisuria, V.B., Los Santos, Y.L., Tufenkji, N., and Deziel, E. (2016). Cranberry-derived proanthocyanidins impair virulence and inhibit quorum sensing of *Pseudomonas aeruginosa*. Sci Rep. 6, 30169. Published online 2016/08/10 DOI: 10.1038/srep30169.

Marin, L., Miguelez, E.M., Villar, C.J., and Lombo, F. (2015). Bioavailability of dietary polyphenols and gut microbiota metabolism: antimicrobial properties. Biomed Res Int. 2015, 905215. Published online 2015/03/25 DOI: 10.1155/2015/905215.

Martens, E.C., Chiang, H.C., and Gordon, J.I. (2008). Mucosal glycan foraging enhances fitness and transmission of a saccharolytic human gut bacterial symbiont. Cell Host Microbe. 4(5), 447-457. Published online 2008/11/11 DOI: 10.1016/j.chom.2008.09.007.

Martens, E.C., Roth, R., Heuser, J.E., and Gordon, J.I. (2009). Coordinate regulation of glycan degradation and polysaccharide capsule biosynthesis by a prominent human gut symbiont. J Biol Chem. 284(27), 18445-18457. Published online 2009/05/01 DOI: 10.1074/jbc.M109.008094.

Mastrodonato, M., Mentino, D., Portincasa, P., Calamita, G., Liquori, G.E., and Ferri, D. (2014). High-fat diet alters the oligosaccharide chains of colon mucins in mice. Histochem Cell Biol. 142(4), 449-459. Published online 2014/04/29 DOI: 10.1007/s00418-014-1221-2.

Masumoto, S., Terao, A., Yamamoto, Y., Mukai, T., Miura, T., and Shoji, T. (2016). Non-absorbable apple procyanidins prevent obesity associated with gut microbial and metabolomic changes. Sci Rep-uk. 6(1), 31208. DOI: 10.1038/srep31208.

Mateos-Martin, M.L., Perez-Jimenez, J., Fuguet, E., and Torres, J.L. (2012). Non-extractable proanthocyanidins from grapes are a source of bioavailable (epi)catechin and derived metabolites in rats. Br J Nutr. 108(2), 290-297. Published online 2011/12/07 DOI: 10.1017/S0007114511005678.

Maurice, C.F., Haiser, H.J., and Turnbaugh, P.J. (2013). Xenobiotics shape the physiology and gene expression of the active human gut microbiome. Cell. 152(1-2), 39-50. Published online 2013/01/22 DOI: 10.1016/j.cell.2012.10.052.

McDougall, C.J., Wong, R., Scudera, P., Lesser, M., and DeCosse, J.J. (1993). Colonic mucosal pH in humans. Dig Dis Sci. 38(3), 542-545. Published online 1993/03/01 DOI: 10.1007/bf01316512.

McGuckin, M.A., Lindén, S.K., Sutton, P., and Florin, T.H. (2011). Mucin dynamics and enteric pathogens. Nature reviews. Microbiology. 9(4), 265-278. DOI: 10.1038/nrmicro2538 PMID - 21407243.

Medina, D.A., Li, T., Thomson, P., Artacho, A., Perez-Brocal, V., and Moya, A. (2019). Cross-regional view of functional and taxonomic microbiota composition in obesity and post-obesity treatment shows country specific microbial contribution. Front Microbiol. 10, 2346. Published online 2019/11/05 DOI: 10.3389/fmicb.2019.02346.

Mele, L., Carobbio, S., Brindani, N., Curti, C., Rodriguez-Cuenca, S., Bidault, G., Mena, P., Zanotti, I., Vacca, M., Vidal-Puig, A., et al. (2017). Phenyl-gamma-valerolactones, flavan-3-ol colonic metabolites, protect brown adipocytes from oxidative stress without affecting their differentiation or function. Mol Nutr Food Res. 61(9). Published online 2017/03/10 DOI: 10.1002/mnfr.201700074.

Mena, P., Bresciani, L., Brindani, N., Ludwig, I.A., Pereira-Caro, G., Angelino, D., Llorach, R., Calani, L., Brighenti, F., Clifford, M.N., et al. (2019). Phenyl-gamma-valerolactones and phenylvaleric acids, the main colonic metabolites of flavan-3-ols: synthesis, analysis, bioavailability, and bioactivity. Nat Prod Rep. 36(5), 714-752. Published online 2018/11/24 DOI: 10.1039/c8np00062j.

Mendez-Vilas, A., Giménez, J.A., Truchado, P., Larrosa, M., Espín, J.C., Tomás-Barberán, F., García-Conesa, M.T., and Allende, A. (2011). Urolithins, metabolites hroduced by human colonic microflora, act as quorum sensing inhibitors of *Yersinia enterocolitica* Affecting its Gene Expression. 202-206. DOI: 10.1142/9789814354868_0039.

Modi, S.R., Collins, J.J., and Relman, D.A. (2014). Antibiotics and the gut microbiota. Journal of Clinical Investigation. 124(10), 4212-4218. DOI: 10.1172/jci72333.

Moradali, M.F., and Rehm, B.H.A. (2020). Bacterial biopolymers: from pathogenesis to advanced materials. Nat Rev Microbiol. Published online 2020/01/30 DOI: 10.1038/s41579-019-0313-3.

Moran, A.P., Gupta, A., and Joshi, L. (2011). Sweet-talk: role of host glycosylation in bacterial pathogenesis of the gastrointestinal tract. Gut. 60(10), 1412-1425. Published online 2011/01/14 DOI: 10.1136/gut.2010.212704.

Moreno-Indias, I., Sanchez-Alcoholado, L., Perez-Martinez, P., Andres-Lacueva, C., Cardona, F., Tinahones, F., and Queipo-Ortuno, M.I. (2016). Red wine polyphenols modulate fecal microbiota and reduce markers of

the metabolic syndrome in obese patients. Food Funct. 7(4), 1775-1787. Published online 2015/11/26 DOI: 10.1039/c5fo00886g.

Morgan, X.C., Tickle, T.L., Sokol, H., Gevers, D., Devaney, K.L., Ward, D.V., Reyes, J.A., Shah, S.A., LeLeiko, N., Snapper, S.B., et al. (2012). Dysfunction of the intestinal microbiome in inflammatory bowel disease and treatment. Genome Biol. 13(9), R79. Published online 2012/09/28 DOI: 10.1186/gb-2012-13-9-r79.

Moya, A., and Ferrer, M. (2016). Functional Redundancy-Induced Stability of Gut Microbiota Subjected to Disturbance. Trends Microbiol. 24(5), 402-413. Published online 2016/03/22 DOI: 10.1016/j.tim.2016.02.002.

Muegge, B.D., Kuczynski, J., Knights, D., Clemente, J.C., Gonzalez, A., Fontana, L., Henrissat, B., Knight, R., and Gordon, J.I. (2011). Diet drives convergence in gut microbiome functions across mammalian phylogeny and within humans. Science. 332(6032), 970-974. Published online 2011/05/21 DOI: 10.1126/science.1198719.

Nakayama, J., Yamamoto, A., Palermo-Conde, L.A., Higashi, K., Sonomoto, K., Tan, J., and Lee, Y.K. (2017). Impact of westernized diet on gut microbiota in children on Leyte Island. Front Microbiol. 8, 197. Published online 2017/03/07 DOI: 10.3389/fmicb.2017.00197.

Narayan, N.R., Weinmaier, T., Laserna-Mendieta, E.J., Claesson, M.J., Shanahan, F., Dabbagh, K., Iwai, S., and DeSantis, T.Z. (2020). Piphillin predicts metagenomic composition and dynamics from DADA2-corrected 16S rDNA sequences. BMC Genomics. 21(1), 56. DOI: 10.1186/s12864-019-6427-1 PMID - 31952477.

Nearing, J.T., Douglas, G.M., Comeau, A.M., and Langille, M.G.I. (2018). Denoising the Denoisers: an independent evaluation of microbiome sequence error-correction approaches. PeerJ. 6, e5364. Published online 2018/08/21 DOI: 10.7717/peerj.5364.

Neff, C.P., Rhodes, M.E., Arnolds, K.L., Collins, C.B., Donnelly, J., Nusbacher, N., Jedlicka, P., Schneider, J.M., McCarter, M.D., Shaffer, M., et al. (2016). Diverse intestinal bacteria contain putative zwitterionic capsular polysaccharides with anti-inflammatory properties. Cell Host Microbe. 20(4), 535-547. Published online 2016/10/04 DOI: 10.1016/j.chom.2016.09.002.

Neto, C.C. (2007). Cranberry and blueberry: evidence for protective effects against cancer and vascular diseases. Mol Nutr Food Res. 51(6), 652-664. Published online 2007/05/30 DOI: 10.1002/mnfr.200600279.

Neto, C.C., Krueger, C.G., Lamoureaux, T.L., Kondo, M., Vaisberg, A.J., Hurta, R.A.R., Curtis, S., Matchett, M.D., Yeung, H., Sweeney, M.I., et al. (2005). MALDI-TOF MS characterization of proanthocyanidins from cranberry fruit (*Vaccinium macrocarpon*) that inhibit tumor cell growth and matrix metalloproteinase expressionin vitro. J Sci Food Agr. 86(1), 18-25. DOI: 10.1002/jsfa.2347.

Nie, Y., and Stürzenbaum, S.R. (2019). Proanthocyanidins of natural origin: molecular mechanisms and implications for lipid disorder and aging-associated diseases. Advances in Nutrition. 10(3), 464-478. DOI: 10.1093/advances/nmy118.

Nile, S.H., and Park, S.W. (2014). Edible berries: Bioactive components and their effect on human health. Nutrition. 30(2), 134-144. DOI: 10.1016/j.nut.2013.04.007 PMID - 24012283.

O'Rourke, A., Beyhan, S., Choi, Y., Morales, P., Chan, A.P., Espinoza, J.L., Dupont, C.L., Meyer, K.J., Spoering, A., Lewis, K., et al. (2020). Mechanism-of-action classification of antibiotics by global transcriptome profiling. Antimicrob Agents Chemother. Published online 2020/01/08 DOI: 10.1128/AAC.01207-19.

Ogura, K., Ogura, M., Shoji, T., Sato, Y., Tahara, Y., Yamano, G., Sato, H., Sugizaki, K., Fujita, N., Tatsuoka, H., et al. (2016). Oral administration of apple procyanidins ameliorates insulin resistance via suppression of pro-inflammatory cytokines expression in liver of diabetic *ob/ob* mice. J Agr Food Chem. 64(46), 8857-8865. DOI: 10.1021/acs.jafc.6b03424.

Otero, F., Gosalvez, J., Bou, G., and Fernandez, J.L. (2017). Simple and fast detection of resistance to antibiotic inhibitors of protein synthesis in gram-negative pathogens through evaluation of mitomycin C-induced cell elongation. Microb Drug Resist. 23(8), 973-981. Published online 2017/05/04 DOI: 10.1089/mdr.2017.0028.

Ottman, N., Davids, M., Suarez-Diez, M., Boeren, S., Schaap, P.J., Martins Dos Santos, V.A.P., Smidt, H., Belzer, C., and de Vos, W.M. (2017). Genome-scale model and omics analysis of metabolic capacities of

Akkermansia muciniphila reveal a preferential mucin-degrading lifestyle. Appl Environ Microbiol. 83(18). Published online 2017/07/09 DOI: 10.1128/AEM.01014-17.

Ottman, N., Reunanen, J., Meijerink, M., Pietilä, T.E., Kainulainen, V., Klievink, J., Huuskonen, L., Aalvink, S., Skurnik, M., Boeren, S., et al. (2017). Pili-like proteins of *Akkermansia muciniphila* modulate host immune responses and gut barrier function. PLOS ONE. 12(3). DOI: 10.1371/journal.pone.0173004.

Ouwerkerk, J.P., de Vos, W.M., and Belzer, C. (2013). Glycobiome: bacteria and mucus at the epithelial interface. Best Pract Res Clin Gastroenterol. 27(1), 25-38. Published online 2013/06/19 DOI: 10.1016/j.bpg.2013.03.001.

Ouwerkerk, J.P., van der Ark, K.C.H., Davids, M., Claassens, N.J., Finestra, T., de Vos, W.M., and Belzer, C. (2016). Adaptation of *Akkermansia muciniphila* to the oxic-anoxic interface of the mucus layer. Applied and Environmental Microbiology. 82(23), 6983-6993. DOI: 10.1128/AEM.01641-16.

Palumbo, J.D., Kado, C.I., and Phillips, D.A. (1998). An isoflavonoid-inducible efflux pump in agrobacterium tumefaciens is involved in competitive colonization of roots. Journal of Bacteriology. 180(12), 3107-3113. DOI: 10.1128/jb.180.12.3107-3113.1998.

Pamer, E.G. (2016). Resurrecting the intestinal microbiota to combat antibiotic-resistant pathogens. Science. 352(6285), 535-538. Published online 2016/04/30 DOI: 10.1126/science.aad9382.

Pan, P., Lam, V., Salzman, N., Huang, Y.-W., Yu, J., Zhang, J., and Wang, L.-S. (2017). Black raspberries and their anthocyanin and fiber fractions alter the composition and diversity of gut microbiota in F-344 Rats. Nutrition and Cancer. 1-9. DOI: 10.1080/01635581.2017.1340491.

Papa, E., Docktor, M., Smillie, C., Weber, S., Preheim, S.P., Gevers, D., Giannoukos, G., Ciulla, D., Tabbaa, D., Ingram, J., et al. (2012). Non-invasive mapping of the gastrointestinal microbiota identifies children with inflammatory bowel disease. PLoS One. 7(6), e39242. Published online 2012/07/07 DOI: 10.1371/journal.pone.0039242.

Peng, X., Zhang, Z., Zhang, N., Liu, L., Li, S., and Wei, H. (2017). In vitro catabolism of quercetin by human fecal bacteria and the antioxidant capacity of its catabolites. Food & Nutrition Research. 58(1), 23406. DOI: 10.3402/fnr.v58.23406.

Piddock, L.J. (2006). Multidrug-resistance efflux pumps - not just for resistance. Nat Rev Microbiol. 4(8), 629-636. Published online 2006/07/18 DOI: 10.1038/nrmicro1464.

Pierre, J.F., Heneghan, A.F., Feliciano, R.P., Shanmuganayagam, D., Roenneburg, D.A., Krueger, C.G., Reed, J.D., and Kudsk, K.A. (2013). Cranberry proanthocyanidins improve the gut mucous layer morphology and function in mice receiving elemental enteral nutrition. Journal of Parenteral and Enteral Nutrition. 37(3), 401-409. DOI: 10.1177/0148607112463076.

Pletzer, D., and Weingart, H. (2014). Characterization and regulation of the resistance-nodulation-cell division-type multidrug efflux pumps *MdtABC* and *MdtUVW* from the fire blight pathogen *Erwinia amylovora*. BMC Microbiol. 14, 185. Published online 2014/07/12 DOI: 10.1186/1471-2180-14-185.

Plovier, H., Everard, A., Druart, C., Depommier, C., Van Hul, M., Geurts, L., Chilloux, J., Ottman, N., Duparc, T., Lichtenstein, L., et al. (2017). A purified membrane protein from *Akkermansia muciniphila* or the pasteurized bacterium improves metabolism in obese and diabetic mice. Nat Med. 23(1), 107-113. Published online 2016/11/29 DOI: 10.1038/nm.4236.

Png, C.W., Linden, S.K., Gilshenan, K.S., Zoetendal, E.G., McSweeney, C.S., Sly, L.I., McGuckin, M.A., and Florin, T.H. (2010). Mucolytic bacteria with increased prevalence in IBD mucosa augment in vitro utilization of mucin by other bacteria. Am J Gastroenterol. 105(11), 2420-2428. Published online 2010/07/22 DOI: 10.1038/ajg.2010.281.

Porter, N.T., Canales, P., Peterson, D.A., and Martens, E.C. (2017). A subset of polysaccharide capsules in the human symbiont *Bacteroides thetaiotaomicron* promote increased competitive fitness in the mouse gut. Cell Host & Microbe. 22(4), 494. DOI: 10.1016/j.chom.2017.08.020.

Porter, N.T., Luis, A.S., and Martens, E.C. (2018). *Bacteroides thetaiotaomicron*. Trends Microbiol. 26(11), 966-967. Published online 2018/09/09 DOI: 10.1016/j.tim.2018.08.005.

Prior, R.L., Lazarus, S.A., Cao, G., Muccitelli, H., and Hammerstone, J.F. (2001). Identification of procyanidins and anthocyanins in blueberries and cranberries (*Vaccinium* spp.) using high-performance liquid chromatography/mass spectrometry. J Agr Food Chem. 49(3), 1270-1276. DOI: 10.1021/jf001211q.

Puupponen-Pimiä, R., Nohynek, L., Hartmann-Schmidlin, S., Kähkönen, M., Heinonen, M., Määttä-Riihinen, K., and Oksman-Caldentey, K.M. (2005). Berry phenolics selectively inhibit the growth of intestinal pathogens. Journal of Applied Microbiology. 98(4), 991-1000. DOI: 10.1111/j.1365-2672.2005.02547.x.

Quast, C., Pruesse, E., Yilmaz, P., Gerken, J., Schweer, T., Yarza, P., Peplies, J., and Glöckner, F. (2013). The SILVA ribosomal RNA gene database project: improved data processing and web-based tools. Nucleic Acids Research. 41(D1). DOI: 10.1093/nar/gks1219.

Ranjan, R., Rani, A., Finn, P.W., and Perkins, D.L. (2018). Multiomic strategies reveal diversity and important functional aspects of human gut microbiome. Biomed Res Int. 2018, 6074918. Published online 2018/12/26 DOI: 10.1155/2018/6074918.

Raouf, A.H., Tsai, H.H., Parker, N., Hoffman, J., Walker, R.J., and Rhodes, J.M. (1992). Sulphation of colonic and rectal mucin in inflammatory bowel disease: reduced sulphation of rectal mucus in ulcerative colitis. Clin Sci (Lond). 83(5), 623-626. Published online 1992/11/01 DOI: 10.1042/cs0830623.

Ravi, A., Halstead, F.D., Bamford, A., Casey, A., Thomson, N.M., van Schaik, W., Snelson, C., Goulden, R., Foster-Nyarko, E., Savva, G.M., et al. (2019). Loss of microbial diversity and pathogen domination of the gut microbiota in critically ill patients. Microb Genom. 5(9). Published online 2019/09/19 DOI: 10.1099/mgen.0.000293.

Ravussin, Y., Koren, O., Spor, A., LeDuc, C., Gutman, R., Stombaugh, J., Knight, R., Ley, R.E., and Leibel, R.L. (2012). Responses of gut microbiota to diet composition and weight loss in lean and obese mice. Obesity (Silver Spring). 20(4), 738-747. Published online 2011/05/20 DOI: 10.1038/oby.2011.111.

Ray, P., and Aich, P. (2019). Effects of gut microbiota perturbation on Th1- and Th2-biased mice following treatment with Vancomycin. Biorxiv. 516898. DOI: 10.1101/516898.

Reid, D.T., Eller, L.K., Nettleton, J.E., and Reimer, R.A. (2016). Postnatal prebiotic fibre intake mitigates some detrimental metabolic outcomes of early overnutrition in rats. Eur J Nutr. 55(8), 2399-2409. Published online 2015/09/27 DOI: 10.1007/s00394-015-1047-2.

Rempe, C.S., Burris, K.P., Lenaghan, S.C., and Stewart, N.C. (2017). The potential of systems biology to discover antibacterial mechanisms of plant phenolics. Frontiers in Microbiology. 8, 422. DOI: 10.3389/fmicb.2017.00422.

Reunanen, J., Kainulainen, V., Huuskonen, L., Ottman, N., Belzer, C., Huhtinen, H., de Vos, W.M., and Satokari, R. (2015). *Akkermansia muciniphila* adheres to enterocytes and strengthens the integrity of the epithelial cell layer. Appl Environ Microbiol. 81(11), 3655-3662. Published online 2015/03/22 DOI: 10.1128/AEM.04050-14.

Reveron, I., de las Rivas, B., Matesanz, R., Munoz, R., and Lopez de Felipe, F. (2015). Molecular adaptation of *Lactobacillus plantarum* WCFS1 to gallic acid revealed by genome-scale transcriptomic signature and physiological analysis. Microb Cell Fact. 14, 160. Published online 2015/10/11 DOI: 10.1186/s12934-015-0345-y.

Reveron, I., Plaza-Vinuesa, L., Franch, M., de Las Rivas, B., Munoz, R., and Lopez de Felipe, F. (2018). Transcriptome-based analysis in *Lactobacillus plantarum* WCFS1 reveals new insights into resveratrol effects at system level. Mol Nutr Food Res. 62(9), e1700992. Published online 2018/03/25 DOI: 10.1002/mnfr.201700992.

Reverón, I., Rodríguez, H., Campos, G., Curiel, J., Ascaso, C., Carrascosa, A.V., Prieto, A., de las Rivas, B., Muñoz, R., and de Felipe, F. (2013). Tannic acid-dependent modulation of selected *Lactobacillus plantarum* traits linked to gastrointestinal survival. PLoS ONE. 8(6). DOI: 10.1371/journal.pone.0066473.

Ring, C., Klopfleisch, R., Dahlke, K., Basic, M., Bleich, A., and Blaut, M. (2019). *Akkermansia muciniphila* strain ATCC BAA-835 does not promote short-term intestinal inflammation in gnotobiotic interleukin-10-deficient mice. Gut Microbes. 10(2), 188-203. Published online 2018/09/27 DOI: 10.1080/19490976.2018.1511663.

Robbe, C., Capon, C., Coddeville, B., and Michalski, J.C. (2004). Structural diversity and specific distribution of O-glycans in normal human mucins along the intestinal tract. Biochem J. 384(Pt 2), 307-316. Published online 2004/09/14 DOI: 10.1042/BJ20040605.

Robert, C.l., and Bernalier-Donadille, A. (2003). The cellulolytic microflora of the human colon: evidence of microcrystalline cellulose-degrading bacteria in methane-excreting subjects. FEMS Microbiology Ecology. 46(1), 81-89. DOI: 10.1016/s0168-6496(03)00207-1 PMID - 19719585.

Rodrigues, R.R., Greer, R.L., Dong, X., KN, D.S., Gurung, M., Wu, J.Y., Morgun, A., and Shulzhenko, N. (2017). Antibiotic-induced alterations in gut microbiota are associated with changes in glucose metabolism in healthy mice. Front Microbiol. 8, 2306. Published online 2017/12/08 DOI: 10.3389/fmicb.2017.02306.

Rodríguez-Daza, M.-C., Daoust, L., Boutkrabt, L., Pilon, G., Varin, T., Dudonné, S., Levy, É., Marette, A., Roy, D., and Desjardins, Y. (2020). Wild blueberry proanthocyanidins shape distinct gut microbiota profile and influence glucose homeostasis and intestinal phenotypes in high-fat high-sucrose fed mice. Sci Rep-uk. 10(1), 2217. DOI: 10.1038/s41598-020-58863-1.

Rodriguez-Pineiro, A.M., Bergstrom, J.H., Ermund, A., Gustafsson, J.K., Schutte, A., Johansson, M.E., and Hansson, G.C. (2013). Studies of mucus in mouse stomach, small intestine, and colon. II. Gastrointestinal mucus proteome reveals Muc2 and Muc5ac accompanied by a set of core proteins. Am J Physiol Gastrointest Liver Physiol. 305(5), G348-356. Published online 2013/07/09 DOI: 10.1152/ajpgi.00047.2013.

Roopchand, D.E., Carmody, R.N., Kuhn, P., Moskal, K., Rojas-Silva, P., Turnbaugh, P.J., and Raskin, I. (2015). Dietary polyphenols promote growth of the gut bacterium *Akkermansia muciniphila* and attenuate high-fat diet–induced metabolic syndrome. Diabetes. 64(8), 2847-2858. DOI: 10.2337/db14-1916.

Ruas-Madiedo, P., Gueimonde, M., Fernandez-Garcia, M., de los Reyes-Gavilan, C.G., and Margolles, A. (2008). Mucin degradation by *Bifidobacterium* strains isolated from the human intestinal microbiota. Appl Environ Microbiol. 74(6), 1936-1940. Published online 2008/01/29 DOI: 10.1128/AEM.02509-07.

Russell, W.R., Gratz, S.W., Duncan, S.H., Holtrop, G., Ince, J., Scobbie, L., Duncan, G., Johnstone, A.M., Lobley, G.E., Wallace, R.J., et al. (2011). High-protein, reduced-carbohydrate weight-loss diets promote metabolite profiles likely to be detrimental to colonic health. Am J Clin Nutr. 93(5), 1062-1072. Published online 2011/03/11 DOI: 10.3945/ajcn.110.002188.

Saha, P., Yeoh, B., Singh, R., Chandrasekar, B., Vemula, P., Haribabu, B., Vijay-Kumar, M., and Jala, V.R. (2016). Gut microbiota conversion of dietary ellagic acid into bioactive phytoceutical Urolithin A inhibits heme peroxidases. PLOS ONE. 11(6). DOI: 10.1371/journal.pone.0156811.

Schaab, M.R., Barney, B.M., and Francisco, W.A. (2006). Kinetic and spectroscopic studies on the quercetin 2,3-dioxygenase from *Bacillus subtilis*. Biochemistry. 45(3), 1009-1016. DOI: 10.1021/bi051571c.

Scher, J.U., Ubeda, C., Artacho, A., Attur, M., Isaac, S., Reddy, S.M., Marmon, S., Neimann, A., Brusca, S., Patel, T., et al. (2015). Decreased bacterial diversity characterizes the altered gut microbiota in patients with psoriatic arthritis, resembling dysbiosis in inflammatory bowel disease. Arthritis Rheumatol. 67(1), 128-139. Published online 2014/10/17 DOI: 10.1002/art.38892.

Schneeberger, M., Everard, A., Gómez-Valadés, A.G., Matamoros, S., Ramírez, S., Delzenne, N.M., Gomis, R., Claret, M., and Cani, P.D. (2015). *Akkermansia muciniphila* inversely correlates with the onset of inflammation, altered adipose tissue metabolism and metabolic disorders during obesity in mice. Sci Rep-uk. 5(1), 16643. DOI: 10.1038/srep16643 PMID - 26563823.

Schroeder, B.O., Birchenough, G.M.H., Stahlman, M., Arike, L., Johansson, M.E.V., Hansson, G.C., and Backhed, F. (2018). Bifidobacteria or fiber protects against diet-induced microbiota-mediated colonic mucus deterioration. Cell Host Microbe. 23(1), 27-40 e27. Published online 2017/12/26 DOI: 10.1016/j.chom.2017.11.004.

Serra, A., Macià, A., Romero, M.-P., Reguant, J., Ortega, N., and Motilva, M.-J. (2012). Metabolic pathways of the colonic metabolism of flavonoids (flavonols, flavones and flavanones) and phenolic acids. Food Chemistry. 130(2), 383-393. DOI: 10.1016/j.foodchem.2011.07.055.

Serrano, J., Puupponen-Pimia, R., Dauer, A., Aura, A.M., and Saura-Calixto, F. (2009). Tannins: current knowledge of food sources, intake, bioavailability and biological effects. Mol Nutr Food Res. 53 Suppl 2, S310-329. Published online 2009/05/14 DOI: 10.1002/mnfr.200900039.

Shah, S., Stapleton, P.D., and Taylor, P.W. (2008). The polyphenol (−)-epicatechin gallate disrupts the secretion of virulence-related proteins by *Staphylococcus aureus*. Letters in Applied Microbiology. 46(2), 181-185. DOI: 10.1111/j.1472-765x.2007.02296.x.

Shan, K., Qu, H., Zhou, K., Wang, L., Zhu, C., Chen, H., Gu, Z., Cui, J., Fu, G., Li, J., et al. (2019). Distinct gut microbiota induced by different fat-to-sugar-ratio high-energy diets share similar pro-obesity genetic and metabolite profiles in prediabetic mice. mSystems. 4(5). Published online 2019/10/09 DOI: 10.1128/mSystems.00219-19.

Shankar, V., Agans, R., and Paliy, O. (2017). Advantages of phylogenetic distance based constrained ordination analyses for the examination of microbial communities. Sci Rep. 7(1), 6481. Published online 2017/07/27 DOI: 10.1038/s41598-017-06693-z.

Sharma, R., and Schumacher, U. (1995). Morphometric analysis of intestinal mucins under different dietary conditions and gut flora in rats. Dig Dis Sci. 40(12), 2532-2539. Published online 1995/12/01 DOI: 10.1007/bf02220438.

Sheflin, A.M., Melby, C.L., Carbonero, F., and Weir, T.L. (2017). Linking dietary patterns with gut microbial composition and function. Gut Microbes. 8(2), 113-129. Published online 2016/12/15 DOI: 10.1080/19490976.2016.1270809.

Shen, X., Sun, X., Xie, Q., Liu, H., Zhao, Y., Pan, Y., Hwang, C.-A., and Wu, V.C.H. (2014). Antimicrobial effect of blueberry (*Vaccinium corymbosum* L.) extracts against the growth of *Listeria monocytogenes* and *Salmonella Enteritidis*. Food Control. 35(1), 159-165. DOI: 10.1016/j.foodcont.2013.06.040.

Sheng, L., Jena, P.K., Liu, H.X., Hu, Y., Nagar, N., Bronner, D.N., Settles, M.L., Baumler, A.J., and Wan, Y.Y. (2018). Obesity treatment by epigallocatechin-3-gallate-regulated bile acid signaling and its enriched *Akkermansia muciniphila*. FASEB J. fj201800370R. Published online 2018/06/09 DOI: 10.1096/fj.201800370R.

Shin, J., Noh, J.-R., Chang, D.-H., Kim, Y.-H., Kim, M., Lee, E., Cho, S., Ku, B., Rhee, M.-S., Kim, B.-C., et al. (2019). Elucidation of *Akkermansia muciniphila* probiotic traits driven by mucin depletion. Frontiers in Microbiology. 10, 1137. DOI: 10.3389/fmicb.2019.01137.

Shin, N.-R., Lee, J.-C., Lee, H.-Y., Kim, M.-S., Whon, T., Lee, M.-S., and Bae, J.-W. (2014). An increase in the *Akkermansia* spp. population induced by metformin treatment improves glucose homeostasis in diet-induced obese mice. Gut. 63(5), 727. DOI: 10.1136/gutjnl-2012-303839.

Shin, N.R., Whon, T.W., and Bae, J.W. (2015). Proteobacteria: microbial signature of dysbiosis in gut microbiota. Trends Biotechnol. 33(9), 496-503. Published online 2015/07/27 DOI: 10.1016/j.tibtech.2015.06.011.

Shinohara, K., Ohashi, Y., Kawasumi, K., Terada, A., and Fujisawa, T. (2010). Effect of apple intake on fecal microbiota and metabolites in humans. Anaerobe. 16(5), 510-515. Published online 2010/03/23 DOI: 10.1016/j.anaerobe.2010.03.005.

Siezen, R.J., and Kleerebezem, M. (2011). The human gut microbiome: are we our enterotypes? Microb Biotechnol. 4(5), 550-553. Published online 2011/08/19 DOI: 10.1111/j.1751-7915.2011.00290.x.

Silver, R.P., Prior, K., Nsahlai, C., and Wright, L.F. (2001). ABC transporters and the export of capsular polysaccharides from Gram-negative bacteria. Res Microbiol. 152(3-4), 357-364. DOI: 10.1016/s0923-2508(01)01207-4 PMID - 11421283.

Singla, R.K., Dubey, A.K., Garg, A., Sharma, R.K., Fiorino, M., Ameen, S.M., Haddad, M.A., and Al-Hiary, M. (2019). Natural polyphenols: Chemical classification, definition of classes, subcategories, and structures. J AOAC Int. 102(5), 1397-1400. Published online 2019/06/16 DOI: 10.5740/jaoacint.19-0133.

Skrovankova, S., Sumczynski, D., Mlcek, J., Jurikova, T., and Sochor, J. (2015). Bioactive compounds and antioxidant activity in different types of berries. International Journal of Molecular Sciences. 16(10), 24673-24706. DOI: 10.3390/ijms161024673.

Slavin, J. (2013). Fiber and prebiotics: mechanisms and health benefits. Nutrients. 5(4), 1417-1435. Published online 2013/04/24 DOI: 10.3390/nu5041417.

Smith, A.H., Zoetendal, E., and Mackie, R.I. (2005). Bacterial mechanisms to overcome inhibitory effects of dietary tannins. Microb Ecol. 50(2), 197-205. Published online 2005/10/14 DOI: 10.1007/s00248-004-0180-x.

Sommer, F., Adam, N., Johansson, M.E., Xia, L., Hansson, G.C., and Backhed, F. (2014). Altered mucus glycosylation in core 1 O-glycan-deficient mice affects microbiota composition and intestinal architecture. PLoS One. 9(1), e85254. Published online 2014/01/15 DOI: 10.1371/journal.pone.0085254.

Song, M.-y., Wang, J.-h., Eom, T., and Kim, H. (2015). *Schisandra chinensis* fruit modulates the gut microbiota composition in association with metabolic markers in obese women: a randomized, double-blind placebo-controlled study. Nutrition Research. 35(8), 655-663. DOI: 10.1016/j.nutres.2015.05.001.

Song, Y., Wen, L., Sun, J., Bai, W., Jiao, R., Hu, Y., Peng, X., He, Y., and Ou, S. (2016). Cytoprotective mechanism of ferulic acid against high glucose-induced oxidative stress in cardiomyocytes and hepatocytes. Food Nutr Res. 60, 30323. Published online 2016/02/13 DOI: 10.3402/fnr.v60.30323.

Sonnenburg, E.D., Smits, S.A., Tikhonov, M., Higginbottom, S.K., Wingreen, N.S., and Sonnenburg, J.L. (2016). Diet-induced extinctions in the gut microbiota compound over generations. Nature. 529(7585), 212-215. Published online 2016/01/15 DOI: 10.1038/nature16504.

Sonnenburg, E.D., and Sonnenburg, J.L. (2014). Starving our microbial self: the deleterious consequences of a diet deficient in microbiota-accessible carbohydrates. Cell Metab. 20(5), 779-786. Published online 2014/08/27 DOI: 10.1016/j.cmet.2014.07.003.

Stoupi, S., Williamson, G., Viton, F., Barron, D., King, L.J., Brown, J.E., and Clifford, M.N. (2010). In vivo bioavailability, absorption, excretion, and pharmacokinetics of [14C]procyanidin B2 in male rats. Drug Metab Dispos. 38(2), 287-291. Published online 2009/11/17 DOI: 10.1124/dmd.109.030304.

Stubbendieck, R.M., and Straight, P.D. (2017). Linearmycins activate a two-component signaling system involved in bacterial competition and biofilm morphology. Journal of Bacteriology. 199(18), 17. DOI: 10.1128/JB.00186-17.

Sun, J., Marais, J., Khoo, C., LaPlante, K., Vejborg, R.M., Givskov, M., Tolker-Nielsen, T., Seeram, N.P., and Rowley, D.C. (2015). Cranberry (*Vaccinium macrocarpon*) oligosaccharides decrease biofilm formation by uropathogenic *Escherichia coli*. J Funct Food. 17(Planta 216 3 2003), 235-242. DOI: 10.1016/j.jff.2015.05.016.

Swidsinski, A., Dorffel, Y., Loening-Baucke, V., Theissig, F., Ruckert, J.C., Ismail, M., Rau, W.A., Gaschler, D., Weizenegger, M., Kuhn, S., et al. (2011). Acute appendicitis is characterised by local invasion with *Fusobacterium nucleatum/necrophorum*. Gut. 60(1), 34-40. Published online 2009/11/21 DOI: 10.1136/gut.2009.191320.

Swidsinski, A., Sydora, B.C., Doerffel, Y., Loening-Baucke, V., Vaneechoutte, M., Lupicki, M., Scholze, J., Lochs, H., and Dieleman, L.A. (2007). Viscosity gradient within the mucus layer determines the mucosal barrier function and the spatial organization of the intestinal microbiota. Inflamm Bowel Dis. 13(8), 963-970. Published online 2007/04/25 DOI: 10.1002/ibd.20163.

Tabasco, R., Sánchez-Patán, F., Monagas, M., Bartolomé, B., Moreno-Arribas, V.M., Peláez, C., and Requena, T. (2011). Effect of grape polyphenols on lactic acid bacteria and bifidobacteria growth: Resistance and metabolism. Food Microbiology. 28(7), 1345-1352. DOI: 10.1016/j.fm.2011.06.005.

Tailford, L.E., Owen, C.D., Walshaw, J., Crost, E.H., Hardy-Goddard, J., Le Gall, G., de Vos, W.M., Taylor, G.L., and Juge, N. (2015). Discovery of intramolecular trans-sialidases in human gut microbiota suggests novel mechanisms of mucosal adaptation. Nat Commun. 6, 7624. Published online 2015/07/15 DOI: 10.1038/ncomms8624.

Takagaki, A., and and Bulletin, N.-F. (2015). Bioconversion of (−)-epicatechin,(+)-epicatechin,(−)-catechin, and (+)-catechin by (−)-epigallocatechin-metabolizing bacteria. Biological and Pharmaceutical Bulletin. DOI: 10.1248/bpb.b14-00813.

Tamura, T., Ozawa, M., Tanaka, N., Arai, S., and Mura, K. (2016). *Bacillus cereus* response to a proanthocyanidin trimer, a transcriptional and functional analysis. Current Microbiology. 73(1), 115-123. DOI: 10.1007/s00284-016-1032-x.

Tarabova, L., Makova, Z., Piesova, E., Szaboova, R., and Faixova, Z. (2016). Intestinal mucus layer and mucins (a review). Folia Veterinaria. 60(1), 21-25. DOI: 10.1515/fv-2016-0003.

Theodoratou, E., Campbell, H., Ventham, N.T., Kolarich, D., Pucic-Bakovic, M., Zoldos, V., Fernandes, D., Pemberton, I.K., Rudan, I., Kennedy, N.A., et al. (2014). The role of glycosylation in IBD. Nat Rev Gastroenterol Hepatol. 11(10), 588-600. Published online 2014/06/11 DOI: 10.1038/nrgastro.2014.78.

Thingholm, L.B., Ruhlemann, M.C., Koch, M., Fuqua, B., Laucke, G., Boehm, R., Bang, C., Franzosa, E.A., Hubenthal, M., Rahnavard, A., et al. (2019). Obese individuals with and without type 2 diabetes show different gut microbial functional capacity and composition. Cell Host Microbe. 26(2), 252-264 e210. Published online 2019/08/11 DOI: 10.1016/j.chom.2019.07.004.

Tobisawa, Y., Imai, Y., Fukuda, M., and Kawashima, H. (2010). Sulfation of colonic mucins by N-acetylglucosamine 6-O-sulfotransferase-2 and its protective function in experimental colitis in mice. J Biol Chem. 285(9), 6750-6760. Published online 2009/12/19 DOI: 10.1074/jbc.M109.067082.

Tomás-Barberán, F.A., González-Sarrías, A., García-Villalba, R., Núñez-Sánchez, M.A., Selma, M.V., García-Conesa, M.T., and Espín, J. (2017). Urolithins, the rescue of "old" metabolites to understand a "new" concept: Metabotypes as a nexus among phenolic metabolism, microbiota dysbiosis, and host health status. Molecular Nutrition & Food Research. 61(1), 1500901. DOI: 10.1002/mnfr.201500901.

Tu, P., Bian, X., Chi, L., Gao, B., Ru, H., Knobloch, T.J., Weghorst, C.M., and Lu, K. (2018). Characterization of the functional changes in mouse gut microbiome associated with increased *Akkermansia muciniphila* population modulated by dietary black raspberries. ACS Omega. 3(9), 10927-10937. Published online 2018/10/06 DOI: 10.1021/acsomega.8b00064.

Turnbaugh, P.J., Bäckhed, F., Fulton, L., and Gordon, J.I. (2008). Diet-induced obesity is linked to marked but reversible alterations in the mouse distal gut microbiome. Cell Host & Microbe. 3(4), 213-223. DOI: 10.1016/j.chom.2008.02.015.

Turnbaugh, P.J., Hamady, M., Yatsunenko, T., Cantarel, B.L., Duncan, A., Ley, R.E., Sogin, M.L., Jones, W.J., Roe, B.A., Affourtit, J.P., et al. (2009). A core gut microbiome in obese and lean twins. Nature. 457(7228), 480-484. Published online 2008/12/02 DOI: 10.1038/nature07540.

Turnbaugh, P.J., Ley, R.E., Hamady, M., Fraser-Liggett, C.M., Knight, R., and Gordon, J.I. (2007). The human microbiome project. Nature. 449(7164), 804-810. Published online 2007/10/19 DOI: 10.1038/nature06244.

Turnbaugh, P.J., Ley, R.E., Mahowald, M.A., Magrini, V., Mardis, E.R., and Gordon, J.I. (2006). An obesity-associated gut microbiome with increased capacity for energy harvest. Nature. 444(7122), 1027. DOI: 10.1038/nature05414.

Tzounis, X., Rodriguez-Mateos, A., Vulevic, J., Gibson, G.R., Kwik-Uribe, C., and Spencer, J.P.E. (2011). Prebiotic evaluation of cocoa-derived flavanols in healthy humans by using a randomized, controlled, double-blind, crossover intervention study. Am J Clin Nutrition. 93(1), 62-72. DOI: 10.3945/ajcn.110.000075.

Ulrey, R.K., Barksdale, S.M., Zhou, W., and van Hoek, M.L. (2014). Cranberry proanthocyanidins have anti-biofilm properties against *Pseudomonas aeruginosa.* BMC Complement Altern Med. 14, 499. Published online 2014/12/17 DOI: 10.1186/1472-6882-14-499.

Ushiroda, C., Naito, Y., Takagi, T., Uchiyama, K., Mizushima, K., Higashimura, Y., Yasukawa, Z., Okubo, T., Inoue, R., Honda, A., et al. (2019). Green tea polyphenol (epigallocatechin-3-gallate) improves gut dysbiosis and serum bile acids dysregulation in high-fat diet-fed mice. J Clin Biochem Nutr. 65(1), 34-46. DOI: 10.3164/jcbn.18-116 PMID - 31379412.

Vadekeetil, A., Alexandar, V., Chhibber, S., and Harjai, K. (2016). Adjuvant effect of cranberry proanthocyanidin active fraction on antivirulent property of ciprofloxacin against *Pseudomonas aeruginosa*. Microb Pathog. 90, 98-103. Published online 2015/12/02 DOI: 10.1016/j.micpath.2015.11.024.

Van den Abbeele, P., Gerard, P., Rabot, S., Bruneau, A., El Aidy, S., Derrien, M., Kleerebezem, M., Zoetendal, E.G., Smidt, H., Verstraete, W., et al. (2011). Arabinoxylans and inulin differentially modulate the mucosal and luminal gut microbiota and mucin-degradation in humanized rats. Environ Microbiol. 13(10), 2667-2680. Published online 2011/09/03 DOI: 10.1111/j.1462-2920.2011.02533.x.

van der Lugt, B., van Beek, A.A., Aalvink, S., Meijer, B., Sovran, B., Vermeij, W.P., Brandt, R.M.C., de Vos, W.M., Savelkoul, H.F.J., Steegenga, W.T., et al. (2019). *Akkermansia muciniphila* ameliorates the age-related decline in colonic mucus thickness and attenuates immune activation in accelerated aging Ercc1 (-/Delta7) mice. Immun Ageing. 16, 6. Published online 2019/03/23 DOI: 10.1186/s12979-019-0145-z.

Van der Sluis, M., De Koning, B.A., De Bruijn, A.C., Velcich, A., Meijerink, J.P., Van Goudoever, J.B., Buller, H.A., Dekker, J., Van Seuningen, I., Renes, I.B., et al. (2006). Muc2-deficient mice spontaneously develop colitis, indicating that MUC2 is critical for colonic protection. Gastroenterology. 131(1), 117-129. Published online 2006/07/13 DOI: 10.1053/j.gastro.2006.04.020.

van der Waaij, L.A., Harmsen, H.J., Madjipour, M., Kroese, F.G., Zwiers, M., van Dullemen, H.M., de Boer, N.K., Welling, G.W., and Jansen, P.L. (2005). Bacterial population analysis of human colon and terminal ileum biopsies with 16S rRNA-based fluorescent probes: commensal bacteria live in suspension and have no direct contact with epithelial cells. Inflamm Bowel Dis. 11(10), 865-871. Published online 2005/09/29 DOI: 10.1097/01.mib.0000179212.80778.d3.

Van Herreweghen, F., Van den Abbeele, P., De Mulder, T., De Weirdt, R., Geirnaert, A., Hernandez-Sanabria, E., Vilchez-Vargas, R., Jauregui, R., Pieper, D.H., Belzer, C., et al. (2017). In vitro colonisation of the distal colon by *Akkermansia muciniphila* is largely mucin and pH dependent. Benef Microbes. 8(1), 81-96. Published online 2016/11/09 DOI: 10.3920/BM2016.0013.

van Passel, M.W., Kant, R., Zoetendal, E.G., Plugge, C.M., Derrien, M., Malfatti, S.A., Chain, P.S., Woyke, T., Palva, A., de Vos, W.M., et al. (2011). The genome of *Akkermansia muciniphila,* a dedicated intestinal mucin degrader, and its use in exploring intestinal metagenomes. PLoS One. 6(3), e16876. Published online 2011/03/11 DOI: 10.1371/journal.pone.0016876.

Vandeputte, D., Falony, G., Vieira-Silva, S., Wang, J., Sailer, M., Theis, S., Verbeke, K., and Raes, J. (2017). Prebiotic inulin-type fructans induce specific changes in the human gut microbiota. Gut. 66(11), 1968-1974. Published online 2017/02/19 DOI: 10.1136/gutjnl-2016-313271.

Vendrame, S., Guglielmetti, S., Riso, P., Arioli, S., Klimis-Zacas, D., and Porrini, M. (2011). Six-week consumption of a wild blueberry powder drink increases bifidobacteria in the human gut. J Agr Food Chem. 59(24), 12815-12820. DOI: 10.1021/jf2028686.

Verberkmoes, N.C., Russell, A.L., Shah, M., Godzik, A., Rosenquist, M., Halfvarson, J., Lefsrud, M.G., Apajalahti, J., Tysk, C., Hettich, R.L., et al. (2009). Shotgun metaproteomics of the human distal gut microbiota. ISME J. 3(2), 179-189. Published online 2008/10/31 DOI: 10.1038/ismej.2008.108.

Vicente, A.R., Ortugno, C., Rosli, H., Powell, A.L., Greve, L.C., and Labavitch, J.M. (2007). Temporal sequence of cell wall disassembly events in developing fruits. 2. Analysis of blueberry (Vaccinium species). J Agric Food Chem. 55(10), 4125-4130. Published online 2007/04/13 DOI: 10.1021/jf063548j.

Vulevic, J., Juric, A., Tzortzis, G., and Gibson, G.R. (2013). A mixture of trans-galactooligosaccharides reduces markers of metabolic syndrome and modulates the fecal microbiota and immune function of overweight adults. J Nutr. 143(3), 324-331. Published online 2013/01/11 DOI: 10.3945/jn.112.166132.

Wagg, C., Schlaeppi, K., Banerjee, S., Kuramae, E.E., and van der Heijden, M.G.A. (2019). Fungal-bacterial diversity and microbiome complexity predict ecosystem functioning. Nat Commun. 10(1), 4841. Published online 2019/10/28 DOI: 10.1038/s41467-019-12798-y.

Walker, A.W., Sanderson, J.D., Churcher, C., Parkes, G.C., Hudspith, B.N., Rayment, N., Brostoff, J., Parkhill, J., Dougan, G., and Petrovska, L. (2011). High-throughput clone library analysis of the mucosa-associated microbiota reveals dysbiosis and differences between inflamed and non-inflamed regions of the intestine in

inflammatory bowel disease. BMC Microbiol. 11, 7. Published online 2011/01/12 DOI: 10.1186/1471-2180-11-7.

Walsh, C. (2020). Antibiotics. 68-100. DOI: 10.1128/9781555819316.ch4.

Walters, W.A., Xu, Z., and Knight, R. (2014). Meta-analyses of human gut microbes associated with obesity and IBD. FEBS Letters. 588(22), 4223-4233. DOI: 10.1016/j.febslet.2014.09.039.

Walton, G.E., van den Heuvel, E.G., Kosters, M.H., Rastall, R.A., Tuohy, K.M., and Gibson, G.R. (2012). A randomised crossover study investigating the effects of galacto-oligosaccharides on the faecal microbiota in men and women over 50 years of age. Br J Nutr. 107(10), 1466-1475. Published online 2011/09/14 DOI: 10.1017/S0007114511004697.

Wang, L., Wu, Y., Zhuang, L., Chen, X., Min, H., Song, S., Liang, Q., Li, A.D., and Gao, Q. (2019). Puerarin prevents high-fat diet-induced obesity by enriching *Akkermansia muciniphila* in the gut microbiota of mice. PLoS One. 14(6), e0218490. Published online 2019/06/25 DOI: 10.1371/journal.pone.0218490.

Wang, M., Ahrne, S., Jeppsson, B., and Molin, G. (2005). Comparison of bacterial diversity along the human intestinal tract by direct cloning and sequencing of 16S rRNA genes. FEMS Microbiol Ecol. 54(2), 219-231. Published online 2005/12/08 DOI: 10.1016/j.femsec.2005.03.012.

Wang, Q., Garrity, G.M., Tiedje, J.M., and Cole, J.R. (2007). Naïve bayesian classifier for rapid assignment of rRNA sequences into the new bacterial taxonomy. Applied and Environmental Microbiology. 73(16), 5261-5267. DOI: 10.1128/aem.00062-07.

Wang, Y., Ames, N.P., Tun, H.M., Tosh, S.M., Jones, P.J., and Khafipour, E. (2016). High molecular weight barley beta-glucan alters gut microbiota toward reduced cardiovascular disease risk. Front Microbiol. 7, 129. Published online 2016/02/24 DOI: 10.3389/fmicb.2016.00129.

Wegorzewska, M.M., Glowacki, R.W.P., Hsieh, S.A., Donermeyer, D.L., Hickey, C.A., Horvath, S.C., Martens, E.C., Stappenbeck, T.S., and Allen, P.M. (2019). Diet modulates colonic T cell responses by regulating the expression of a *Bacteroides thetaiotaomicron* antigen. Sci Immunol. 4(32). Published online 2019/02/10 DOI: 10.1126/sciimmunol.aau9079.

Wemheuer, F., Taylor, J.A., Daniel, R., Johnston, E., Meinicke, P., Thomas, T., and Wemheuer, B. (2018). Tax4Fun2: a R-based tool for the rapid prediction of habitat-specific functional profiles and functional redundancy based on 16S rRNA gene marker gene sequences. Biorxiv. 490037. DOI: 10.1101/490037.

White, B.L., Howard, L.R., and Prior, R.L. (2010). Proximate and polyphenolic characterization of cranberry pomace. J Agric Food Chem. 58(7), 4030-4036. Published online 2009/12/22 DOI: 10.1021/jf902829g.

Willis, L.M., and Whitfield, C. (2013). Structure, biosynthesis, and function of bacterial capsular polysaccharides synthesized by ABC transporter-dependent pathways. Carbohydrate Research. 378, 35-44. DOI: 10.1016/j.carres.2013.05.007.

Wojnicz, D., Tichaczek-Goska, D., Korzekwa, K., Kicia, M., and Hendrich, A.B. (2016). Study of the impact of cranberry extract on the virulence factors and biofilm formation by *Enterococcus faecalis* strains isolated from urinary tract infections. Int J Food Sci Nutr. 67(8), 1005-1016. Published online 2016/07/28 DOI: 10.1080/09637486.2016.1211996.

Wrzosek, L., Miquel, S., Noordine, M.L., Bouet, S., Joncquel Chevalier-Curt, M., Robert, V., Philippe, C., Bridonneau, C., Cherbuy, C., Robbe-Masselot, C., et al. (2013). *Bacteroides thetaiotaomicron* and *Faecalibacterium prausnitzii* influence the production of mucus glycans and the development of goblet cells in the colonic epithelium of a gnotobiotic model rodent. BMC Biol. 11, 61. Published online 2013/05/23 DOI: 10.1186/1741-7007-11-61.

Wu, G.D., Chen, J., Hoffmann, C., Bittinger, K., Chen, Y.Y., Keilbaugh, S.A., Bewtra, M., Knights, D., Walters, W.A., Knight, R., et al. (2011). Linking long-term dietary patterns with gut microbial enterotypes. Science. 334(6052), 105-108. Published online 2011/09/03 DOI: 10.1126/science.1208344.

Wu, H., Esteve, E., Tremaroli, V., Khan, M.T., Caesar, R., Manneras-Holm, L., Stahlman, M., Olsson, L.M., Serino, M., Planas-Felix, M., et al. (2017). Metformin alters the gut microbiome of individuals with treatment-

naive type 2 diabetes, contributing to the therapeutic effects of the drug. Nat Med. 23(7), 850-858. Published online 2017/05/23 DOI: 10.1038/nm.4345.

Wu, V.C., Qiu, X., de los Reyes, B.G., Lin, C.S., and Pan, Y. (2009). Application of cranberry concentrate (*Vaccinium macrocarpon*) to control *Escherichia coli* O157:H7 in ground beef and its antimicrobial mechanism related to the downregulated *slp, hdeA* and *cfa*. Food Microbiol. 26(1), 32-38. Published online 2008/11/26 DOI: 10.1016/j.fm.2008.07.014.

Wu, V.C.H., Qiu, X., Bushway, A., and Harper, L. (2008). Antibacterial effects of American cranberry (*Vaccinium macrocarpo*n) concentrate on foodborne pathogens. LWT-Food Science and Technology.

Xie, Y., Yang, W., Tang, F., Chen, X., and Ren, L. (2014). Antibacterial activities of flavonoids: Structure-activity relationship and mechanism. Current Medicinal Chemistry. 22(1), 132-149. DOI: 10.2174/09298673216661409161134 43.

Xue, B., Xie, J., Huang, J., Chen, L., Gao, L., Ou, S., Wang, Y., and Peng, X. (2016). Plant polyphenols alter a pathway of energy metabolism by inhibiting fecal *Bacteroidetes* and *Firmicutes* in vitro. Food & Function. 7(3), 1501-1507. DOI: 10.1039/c5fo01438g.

Yan, H., and Ajuwon, K.M. (2017). Butyrate modifies intestinal barrier function in IPEC-J2 cells through a selective upregulation of tight junction proteins and activation of the *Akt* signaling pathway. PLoS One. 12(6), e0179586. Published online 2017/06/28 DOI: 10.1371/journal.pone.0179586.

Yassour, M., Lim, M.Y., Yun, H.S., Tickle, T.L., Sung, J., Song, Y.M., Lee, K., Franzosa, E.A., Morgan, X.C., Gevers, D., et al. (2016). Sub-clinical detection of gut microbial biomarkers of obesity and type 2 diabetes. Genome Med. 8(1), 17. Published online 2016/02/18 DOI: 10.1186/s13073-016-0271-6.

Yi, W., Akoh, C.C., Fischer, J., and Krewer, G. (2006). Absorption of anthocyanins from blueberry extracts by caco-2 human intestinal cell monolayers. J Agric Food Chem. 54(15), 5651-5658. Published online 2006/07/20 DOI: 10.1021/jf0531959.

Yoshizaki, T., Ishihara, J., Kotemori, A., Yamamoto, J., Kokubo, Y., Saito, I., Yatsuya, H., Yamagishi, K., Sawada, N., Iwasaki, M., et al. (2020). Association of vegetable, fruit, and okinawan vegetable consumption with incident stroke and coronary heart disease. J Epidemiol. 30(1), 37-45. Published online 2019/01/16 DOI: 10.2188/jea.JE20180130.

Zeng, H., Ishaq, S.L., Liu, Z., and Bukowski, M.R. (2018). Colonic aberrant crypt formation accompanies an increase of opportunistic pathogenic bacteria in C57BL/6 mice fed a high-fat diet. J Nutr Biochem. 54, 18-27. Published online 2017/12/11 DOI: 10.1016/j.jnutbio.2017.11.001.

Zhang, C., Zhang, M., Pang, X., Zhao, Y., Wang, L., and Zhao, L. (2012). Structural resilience of the gut microbiota in adult mice under high-fat dietary perturbations. ISME J. 6(10), 1848-1857. Published online 2012/04/13 DOI: 10.1038/ismej.2012.27.

Zhang, C., Zhang, M., Wang, S., Han, R., Cao, Y., Hua, W., Mao, Y., Zhang, X., Pang, X., Wei, C., et al. (2010). Interactions between gut microbiota, host genetics and diet relevant to development of metabolic syndromes in mice. ISME J. 4(2), 232-241. Published online 2009/10/30 DOI: 10.1038/ismej.2009.112.

Zhang, Z., Geng, J., Tang, X., Fan, H., Xu, J., Wen, X., Ma, Z.S., and Shi, P. (2014). Spatial heterogeneity and co-occurrence patterns of human mucosal-associated intestinal microbiota. ISME J. 8(4), 881-893. Published online 2013/10/18 DOI: 10.1038/ismej.2013.185.

Zhang, Z., Wu, X., Cao, S., Cromie, M., Shen, Y., Feng, Y., Yang, H., and Li, L. (2017). Chlorogenic acid ameliorates experimental colitis by promoting growth of *Akkermansia* in mice. Nutrients. 9(7), 677. DOI: 10.3390/nu9070677.

Zhang, Z., Wu, X., Cao, S., Wang, L., Wang, D., Yang, H., Feng, Y., Wang, S., and Li, L. (2016). Caffeic acid ameliorates colitis in association with increased *Akkermansia* population in the gut microbiota of mice. Oncotarget. 7(22), 31790-31799. DOI: 10.18632/oncotarget.9306 PMID - 27177331.

Zhao, Z., Egashira, Y., and Sanada, H. (2003). Digestion and absorption of ferulic acid sugar esters in rat gastrointestinal tract. J Agric Food Chem. 51(18), 5534-5539. Published online 2003/08/21 DOI: 10.1021/jf034455u.

Zhernakova, A., Kurilshikov, A., Bonder, M., Tigchelaar, E.F., Schirmer, M., Vatanen, T., Mujagic, Z., Vila, A., Falony, G., Vieira-Silva, S., et al. (2016). Population-based metagenomics analysis reveals markers for gut microbiome composition and diversity. Science. 352(6285), 565-569. DOI: 10.1126/science.aad3369.

Zhou, X., Zhang, K., Qi, W., Zhou, Y., Hong, T., Xiong, T., Xie, M., and Nie, S. (2019). Exopolysaccharides from *Lactobacillus plantarum* NCU116 enhances colonic mucosal homeostasis by controlling epithelial cell differentiation and *c-Jun/Muc2* signaling. J Agric Food Chem. 67(35), 9831-9839. Published online 2019/08/14 DOI: 10.1021/acs.jafc.9b03939.

Zhou, Z.Y., Ren, L.W., Zhan, P., Yang, H.Y., Chai, D.D., and Yu, Z.W. (2016). Metformin exerts glucose-lowering action in high-fat fed mice via attenuating endotoxemia and enhancing insulin signaling. Acta Pharmacol Sin. 37(8), 1063-1075. Published online 2016/05/18 DOI: 10.1038/aps.2016.21.

Zhu, B., Wang, X., and Li, L. (2010). Human gut microbiome: the second genome of human body. Protein Cell. 1(8), 718-725. Published online 2011/01/05 DOI: 10.1007/s13238-010-0093-z.

Zoetendal, E.G., Smith, A.H., A., S.-M., and Mackie, R.I. (2008). The *BaeSR* two-component regulatory system mediates resistance to condensed tannins in *Escherichia coli*. Applied and Environmental Microbiology. 535-539. DOI: 10.1128/AEM.02271-07.

Zou, J., Chassaing, B., Singh, V., Pellizzon, M., Ricci, M., Fythe, M.D., Kumar, M.V., and Gewirtz, A.T. (2018). Fiber-mediated nourishment of gut microbiota protects against diet-induced obesity by restoring IL-22-mediated colonic health. Cell Host Microbe. 23(1), 41-53 e44. Published online 2017/12/26 DOI: 10.1016/j.chom.2017.11.003.